

**Hydrogeological conceptualisation of a tropical river catchment
in a crystalline basement area and transfer into a numerical
groundwater flow model
- Case study for the Upper Ouémé catchment in Benin -**

Dissertation
zur
Erlangung des Doktorgrades (Dr. rer. nat.)
der
Mathematisch–Naturwissenschaftlichen Fakultät
der
Rheinischen Friedrich–Wilhelms–Universität Bonn

vorgelegt von
Tobias El-Fahem
aus
Celle

Bonn, Januar 2008

Angefertigt mit Genehmigung der Mathematisch-Naturwissenschaftlichen
Fakultät der Rheinischen Friedrich-Wilhelms-Universität Bonn

1. Referent: Prof. Dr. B. Reichert

2. Referent: Prof. Dr. B. Dieckrüger

Tag der Promotion: 18.07.2008

Diese Dissertation ist auf dem Hochschulschriftenserver der ULB Bonn
http://hss.ulb.uni-bonn.de/diss_online elektronisch publiziert.

Ich versichere an Eides statt, dass ich
diese Arbeit selbstständig ausgeführt
habe und keine außer den angegebenen
Hilfsmitteln verwendet habe.

(Tobias El-Fahem)

Bonn, Juli 2008

Abstract

The scope of this PhD thesis was the hydrogeological conceptualisation of the Upper Ouémé river catchment in Benin. The study area exceeds 14'500 km² and is underlain by a crystalline basement. At this setting the typical sequence of aquifers - a regolith aquifer at the top and a fractured bedrock aquifer at the bottom – is encountered, which is found in basement areas all over Africa and elsewhere in the world. The chosen regional approach revealed important information about the hydrochemistry and hydrogeology of this catchment.

Based on the regional conceptual model a numerical groundwater flow model was designed. The numerical model was used to estimate the impact of climate change on the regional groundwater resources.

This study was realised within the framework of the German interdisciplinary research project IMPETUS (English translation: “integrated approach to the efficient management of scarce water resources in West Africa”), which is jointly managed by the German universities of Bonn and Cologne. Since the year 2000 the Upper Ouémé catchment was the principal target for investigations into the relevant processes of the regional water cycle. A first study from 2000 to 2003 (FASS 2004) focused on the hydrogeology of a small local catchment (~30 km²).

In the course of this thesis five field campaigns were underdone from the year 2004 to 2006. In the beginning of 2004 a groundwater monitoring net was installed based on 12 automatic data loggers. Manual piezometric measurements and the sampling of groundwater and surface water were realised for each campaign throughout the whole study area. Water samples were analysed for major ions, for a choice of heavy metals and for their composition by deuterium, oxygen-18 and tritium. The numerical model was performed with FEFLOW[®].

The hydraulic and hydrochemical characteristics were described for the regolith aquifer and the bedrock aquifer. The regolith aquifer plays the role of the groundwater stock with low conductivity while the fractures of the bedrock may conduct water relatively fast towards extraction points. Flow in fractures of the bedrock depends on the connectivity of the fracture network which might be of local to subregional importance.

Stable isotopes in combination with hydrochemistry proved that recharge occurs on catchment scale and exclusively by precipitation. Influx of groundwater from distant areas along dominant structures like the Kandi fault or from the Atacora mountain chain is excluded. The analysis of tritium in groundwater from different depths revealed the interesting fact of the strongly rising groundwater ages. Bedrock groundwater may possibly be much older than 50 years.

Equilibrium phases of the silicate weathering products kaolinite and montmorillonite showed that the deeper part of the regolith aquifer and the bedrock aquifer feature either stagnant or less mobile groundwater while the shallow aquifer level is influenced by seasonal groundwater table fluctuations. The hydrochemical data characterised this zone by the progressive change of the hydrochemical facies of recently infiltrated rainwater on its flow path into deeper parts of the aquifers. Surprisingly it was found out that seasonal influences on groundwater hydrochemistry are minor, mainly because they affect only the groundwater levels close to the surface.

The transfer of the hydrogeological features of the Upper Ouémé catchment into a regional numerical model demanded a strong simplification. Groundwater tables are a reprint of the general surface morphology. Pumping or other types of groundwater extraction would have only very local impact on the available groundwater resources.

It was possible to integrate IMPETUS scenario data into the groundwater model. As a result it was shown that the impact of climate change on the groundwater resources until the year 2025 under the given conditions will be negligible due to the little share of precipitation needed for recharge and the low water needs for domestic use.

Reason for concern is the groundwater quality on water points in the vicinity of settlements because of contamination by human activities as shown for the village of Dogué. Nitrate concentrations achieved in many places already alerting levels. Health risks from fluoride or heavy metals were excluded for the Upper Ouémé area.

Kurzfassung

In der vorliegenden Dissertationsarbeit wird ein hydrogeologisches Konzeptmodell für das Flusseinzugsgebiet des Oberen Ouémés in Benin entworfen. Das Untersuchungsgebiet liegt auf einem kristallinen Sockelgebiet und zeigt die dafür typische Abfolge des Regolithaquifers im Hangenden und eines Kluftaquifers im Liegenden. Diese Sequenz ist typisch für Kristallingebiete in ganz Afrika aber auch auf anderen Kontinenten. Es wurde ein regionaler Ansatz verwendet, der wichtige Erkenntnisse über Hydrochemie und Hydrogeologie des 14'500 km² großen Flusseinzugsgebiets lieferte.

Basierend auf dem regionalen Konzept wurde ein numerisches Grundwasserströmungsmodell entworfen. Dieses Modell wurde verwandt, um den Einfluss des Klimawandels auf die regionalen Grundwasserressourcen zu bestimmen.

Diese Studie wurde im Rahmen des Forschungsprojekts IMPETUS (Integratives Managementprojekt für den effizienten und tragfähigen Umgangs mit Süßwasser) angefertigt. IMPETUS ist ein Gemeinschaftsprojekt der Universitäten Bonn und Köln, welches durch das Bundesministerium für Bildung und Forschung (BMBF; Fördernummer. 07 GWK 02) und das Ministerium für Wissenschaft und Forschung des Landes Nordrhein-Westfalens (MWF; Fördernummer: 223-21200200) finanziert wird. Ziel ist die Entwicklung eines Decision Support Systems für die Wasserbewirtschaftung in Benin. Das Einzugsgebiet des Oberen Ouémés ist das Hauptuntersuchungsgebiet zur Erfassung der relevanten Prozesse im regionalen Wasserkreislauf. Eine erste Studie von 2000 bis 2003 von FASS (2004) konzentrierte sich auf die Hydrogeologie eines kleinen, lokalen Einzugsgebiets (~30 km²).

In den Jahren 2004 bis 2006 wurden fünf Geländekampagne durchgeführt, um ausreichend Daten für die vorliegende Studie zu erheben. Jede Kampagne fand entweder am Ende einer Regenzeit oder aber am Ende einer Trockenzeit statt. Zu Beginn 2004 wurde mittels 12 automatischer Grundwasserstandsmessgeräten ein Beobachtungsnetz aufgebaut. Die Grundwasserstände wurden täglich registriert und regelmäßig ausgelesen. Zusätzlich wurden bei jeder Kampagne im gesamten Arbeitsgebiet manuelle Grundwasserstandsmessungen und Grund- wie Oberflächenwasserbeprobungen durchgeführt. Die Wasserproben wurden auf die wichtigsten Ionen, einer Auswahl an Schwermetallen, sowie auf den Gehalt an Deuterium, Sauerstoff-18 und Tritium hin analysiert. Das numerische Modell wurde mit FEFLOW[®] erstellt.

Der Regolith- und der Kluftaquifer wurden hydrochemisch und hydrogeologisch charakterisiert. Das Grundwasserströmungsfeld im Regolith passt sich der allgemeinen Geländeform an. Die Strömungsbewegungen finden dabei vornehmlich in Untereinzugsgebieten in Richtung der jeweiligen, lokalen Vorfluter statt. Der Regolithaquifer ist ein wichtiger Grundwasserspeicher, allerdings mit geringer Leitfähigkeit. Der Kluftaquifer kann Wasser zwar schnell leiten hat aber nur ein geringes Speichervermögen. Das Kluftströmungsfeld hängt vor allem von der hydraulischen Vernetzung der Klüfte ab.

Die Auswertung der stabilen Isotopenzusammensetzung in Verbindung mit den hydrochemischen Analysen wies eine Grundwasserneubildung im Einzugsgebiet ausschließlich durch Niederschläge nach. Ein unterirdischer Zufluss aus entfernten

Gebieten, z.B. entlang prominenter Strukturen wie die Kandi-Störung oder aus dem Vorland des Atakora-Gebirges, konnte ausgeschlossen werden. Außerdem konnte gezeigt werden, dass einer Veränderung der Grundwasserchemie durch einsickerndes, durch Verdampfung aufkonzentriertes, Oberflächenwasser keine Bedeutung zukommt.

Die Anwendung der Tritium-Methode an Grundwasserproben aus verschiedenen Tiefenbereichen deckte ein deutlich ansteigendes Grundwasseralter mit zunehmender Tiefe auf. Das Grundwasser im Kluftaquifer ist möglicherweise sehr viel älter als 50 Jahre.

Diese Beobachtung stimmt mit der Interpretation der Grundwasserchemie überein. Die Gleichgewichtsverteilung der silikatischen Verwitterungsphasen Kaolinit und Montmorillonit machen deutlich, dass im tieferen Teil des Regolithaquifers und des Kluftaquifers eine nur langsame bis stagnierende Grundwasserströmung auftritt. Die Grundwasserstandsbeobachtung mittels der automatischen Piezometer stellt klar, dass wichtige Grundwasserbewegungen nur im flachen Aquiferbereich bis in etwa 10 m Tiefe stattfinden. Die hydrochemischen Daten beschreiben den fortschreitenden chemischen Wandel von infiltrierendem Regenwasser abwärts in tiefere Aquiferbereiche. Überraschenderweise konnten saisonale Einflüsse auf die Grundwasserchemie in größeren Tiefen ausgeschlossen werden. Nur in Oberflächennähe, kommt es zur Verdünnung durch Regenfälle.

Der Transfer der hydrogeologischen Merkmale des Oberen Ouémé-Einzugsgebiet in ein numerisches Modell bedurfte einer starken Vereinfachung. Die Grundwasseroberfläche zeichnet die Geländeoberfläche nach. Eine überregionale Grundwasserströmung ist nicht wahrscheinlich. Künstliche Grundwasserentnahmen werden daher nur lokal den Grundwasserspiegel beeinflussen.

Das Hauptziel der numerischen Modellierung ist daher nicht die exakte Voraussage von Grundwasserständen für spezifische Zeitpunkte im Oberen Ouémé-Einzugsgebiet, sondern ob es auf Änderungen in der Grundwasserentnahme oder -neubildung angemessen reagiert.

Es war möglich die Szenariendaten des IMPETUS-Projekts in das Modell zu integrieren. Der Klimawandel wird bis in das Jahr 2025 kaum Einfluss auf die Grundwasserverfügbarkeit im Arbeitsgebiet haben. Dies liegt darin begründet, dass für die Grundwasserneubildung nur ein geringer Anteil der Niederschläge benötigt wird. Zudem ist der öffentliche Wasserbedarf im Arbeitsgebiet sehr gering.

Für Beunruhigung sorgt hingegen die häufig schlechte Trinkwasserqualität des Grundwassers aus siedlungsnahen Brunnen und Pumpen. Ursache dafür ist die Verschmutzung durch anthropogene Einflüsse, wie es z.B. für das Dorf Dogué gezeigt wird. Nitrat erreicht vielerorts bedenkliche Konzentrationen. Gesundheitsrisiken durch Fluorid oder Schwermetalle, wie Arsen, konnten für das Obere Ouémé-Gebiet ausgeschlossen werden.

Résumé

La présente thèse de doctorat est consacrée à la conception d'un modèle de l'hydrogéologie régionale du bassin versant de la Haute Vallée de l'Ouémé au Bénin. Cette zone d'étude s'étale sur environ 14'500 km² au centre de ce pays subtropical. Elle repose sur du socle cristallin, dans un environnement géologique typique, dont les caractéristiques aquifères se retrouvent en beaucoup d'autres lieux d'Afrique ainsi que sur d'autres continents. Nous trouvons au toit, un aquifère dans les altérites – le régolite, et au mur, le réservoir à porosité de fracture des roches cristallines du socle.

Une approche régionale a révélé des informations importantes sur l'hydrochimie et l'hydrogéologie de ce bassin versant. Basé sur ce concept, un modèle numérique était créé. Il était utilisé pour évaluer l'impact du changement climatique sur les ressources en eau souterraine dans la zone d'étude.

Ce travail a été réalisé dans le cadre du projet de recherche IMPETUS (Approche intégrée pour la gestion efficiente des ressources hydriques limitées en Afrique de l'Ouest), qui réunit les Universités de Bonn et de Cologne, et financé par le BMBF (Ministère fédéral de l'Education et de la Recherche).

Une première étude hydrogéologique menée entre 2000 et 2004 (FASS 2004) a décrit d'importants processus au niveau d'un sous-bassin (~30 km²) de la zone d'étude actuelle, dont les résultats sont utilisés comme références.

La préparation de cette thèse a comporté cinq campagnes de terrain qui ont été réalisées pendant les années 2004 à 2006. En début 2004, un réseau d'observation des nappes, consistant en 12 enregistreurs automatiques, était installé dans la zone d'étude. Des mesures manuelles de la piézométrie ainsi que l'échantillonnage d'eaux souterraines et de surface ont été réalisés pour chaque campagne dans tout le bassin versant. Dans ces échantillons, ont été analysés les ions majeurs, une sélection des métaux lourds et leur composition en deutérium, oxygène-18 et tritium. Ensuite, la modélisation a été élaborée avec le logiciel FEFLOW[®].

Les caractéristiques hydrauliques et hydrochimiques des aquifères du régolite et du cristallin ont été décrites. L'importance du régolite est celui d'un réservoir, avec une basse conductivité. Les fractures du socle cristallin, au contraire, conduisent bien l'eau mais ne l'emmagasinent pas assez. L'écoulement d'eau dans le cristallin dépend de la connectivité des fractures qui, au Bénin, se comprend entre l'échelle locale et sous-régionale.

En combinaison avec les mesures hydrochimiques, les isotopes stables ont montré que la recharge des nappes s'effectue au niveau du bassin versant par des précipitations. Un afflux, ayant pour l'origine les structures dominantes comme la faille de Kandi ou la chaîne de l'Atacora, pouvait être exclu. Les teneurs de tritium ont démontré l'accroissement de l'âge en fonction de la profondeur. L'eau contenue dans le cristallin a probablement beaucoup plus que 50 ans.

Les phases d'équilibre de kaolinite et montmorillonite indiquaient un milieu stagnant des eaux souterraines dans les niveaux profonds du régolite et de l'aquifère cristallin. C'est la zone de la nappe phréatique jusqu'à une profondeur de 10 m qui est mobile sous l'influence des fluctuations saisonnières. Il était observé que le changement saisonnier n'a que peu d'influence sur la chimie des eaux souterraines profondes.

Le transfert dans un modèle numérique requiert une simplification du modèle conceptuel régional. Ainsi, la nappe phréatique reflète la morphologie du terrain et la zone d'influence d'une extraction éventuelle de l'eau souterraine ne concerne que l'échelle locale.

Il a été possible d'intégrer les données des scénarios d'IMPETUS dans le modèle numérique. Les résultats montrent que l'influence du changement climatique sur les ressources en eau souterraine est négligeable sous des conditions discutées jusqu'à l'année 2025.

Finalement, les niveaux de contamination des eaux souterraines aux points d'eau proches des agglomérations humaines, par exemple le village Dogué, sont inquiétants. La concentration de nitrate atteint des taux alarmants en de nombreux points d'eau. En revanche, dans la Haute Vallée de l'Ouémé, les teneurs en fluor et en métaux lourds ne causent pas des risques pour la santé.

Acknowledgements

There are so many people I ought to thank for their assistance and encouragement that I will certainly miss to name them all.

First, I would like to thank my supervisor, Barbara Reichert of the Geological Institute of the University of Bonn, for invaluable inspirations and her tolerance. I would also like to thank Bernd Diekkrüger for his willingness to be my co-supervisor. Our discussions and his questions helped me to go forward with the modelling.

I am very grateful to Michael Sarvan and Lars Bohnenkämper, two diploma students, for their assistance during the long and exhaustive field campaigns. Thanks for the great time we had together in the field.

I'm very thankful to the staff of the DGEau Cotonou and the people of the SEau Parakou and Djougou for sharing their experience and data with me. Without their engagement this thesis would not have been possible. Thanks to Thomas de Beyer (IGIP-GTZ) and Conrad Thombansen (GTZ) for providing me lots of information about the structure of Benin's water program. I would like to thank Christophe Zunino (DANIDA) who explained me the technical issues about water supply from bedrock aquifers. Thanks of course to Christophe Peugeot and Luc Séguis (both IRD) from whom I could learn a lot about the hydrology in the study area.

I am grateful to all the people of the IMPETUS projects with whom I had the pleasure to work during the last years. Some must be mentioned here. My predecessor Thorsten Fass prepared the field for me and provided with his thesis very useful information and data about the study area. Simone Giertz, Claudia Hiepe und Gero Steup of subproject A2 for important discussions. Michael Christoph was a most helpful project manager. The project coordinators Elisabeth van den Akker and Andreas Preu and their outstanding secretary Conforte Mensah for their never ending support in all issues concerning the work in Benin.

The critical comments of my fellow geologists Sébastien Cappy and Stephan Klose helped to greatly improve the quality of this work.

Thanks to the technical staff of the Geological Institute of Bonn, Bettina Schulte-van Berkum, Camilla Kurth, Dirk Handwerk, Sven Berkau and Horst Wörmann, for their support in hydrochemical analysis and truly technical issues. The geological and hydrogeological maps were scanned in Germany with the kindly permission and support of the urban planning section of the Bonner Stadthaus. Student assistant Helge Hinkelmann (Geological Institute Bonn) digitised all maps in meticulous work. His work is highly regarded.

And last but not least I wish to thank all of the people in Benin who worked with us. Their tolerance, goodness and helpfulness are unforgettable. Finally, I have to admit that it was a wonderful possibility to experience this part of West Africa and to learn about its problems, its people and culture.

This work was supported by the Federal German Ministry of Education and Research (BMBF) under grant No. 07 GWK 02 and by the Ministry of Science and Research (MWF) of the federal state of Northrhine-Westfalia under grant No. 223-21200200.

Table of Contents

Abstract	ii
Kurzfassung	iv
Résumé	vi
Acknowledgements	viii
Table of Contents	ix
List of Figures	xi
List of Tables	xvi
List of Equations	xviii
Annex (on CD)	xviii
Abbreviations	xx
1. Introduction	1
1.1 General overview.....	1
1.2 Motivation and objective of the study	3
1.3 State of research on the fractured basement of Benin.....	4
2. Materials and methods	7
2.1 Mapping and imagery	7
2.1.1 Geological and hydrogeological map	7
2.1.2 Digital elevation model and satellite images	8
2.2 Borehole data base (Base des données intégrées – BDI)	10
2.3 Piezometry.....	11
2.4 Sampling campaigns and sampling procedure	15
2.4.1 Field campaigns	15
2.4.2 Physico-chemical parameters	17
2.4.3 Hydrochemical parameters	17
2.5 Environmental isotope analysis	19
2.5.1 Deuterium and oxygen-18.....	19
2.5.2 Tritium	21
2.5.3 Sampling and Analysis.....	22
2.6 Regionalisation through geostatistical methods.....	23
2.7 Groundwater flow model.....	24
2.7.1 General concepts of numerical modelling.....	24
2.7.2 Modelling standards of FEFLOW®	26
3. Case study: The Upper Ouémé river catchment	28
3.1 Overall geography	28
3.2 Water policy	29
3.3 Climate.....	30
3.4 Geomorphology and hydrography	33
3.5 Vegetation.....	38
3.6 Geology	40
3.6.1 Regional Geology.....	40
3.6.2 Geology of the study area	45
3.6.3 Regolith formation	47
3.7 Hydrogeology.....	51
3.7.1 Bedrock aquifer	51
3.7.2 Regolith aquifer	55
4. Piezometry	58
4.1 Data logger time series.....	58
4.2 Regionalisation of piezometric data	68

Table of Contents

5. Hydrochemistry	73
5.1 Physico-chemical characteristics.....	73
5.1.1 Temperature.....	73
5.1.2 pH.....	73
5.1.3 Electrical conductivity.....	75
5.1.4 Redox potential.....	77
5.1.5 Oxygen.....	79
5.2 Hydrochemical parameters.....	80
5.2.1 Distinction of hydrochemical groups.....	80
5.2.2 Hydrochemical characteristics of the groundwater in the HVO.....	83
5.2.3 Discussion of group 3 – the southern province.....	87
5.3 Seasonal variations.....	91
5.4 Groundwater quality.....	98
5.4.1 Physico-chemical quality.....	98
5.4.2 Fluoride.....	98
5.4.2.1 Geological sources.....	98
5.4.2.2 Fluoride in the study area.....	99
5.4.3 Nitrate and Nitrite.....	100
5.4.3.1 Nitrogen compounds in the environment.....	100
5.4.3.2 Nitrate in the study area.....	101
5.4.4 Heavy metals.....	104
5.4.5 Sodium adsorption ratio (SAR).....	105
6. Environmental isotopes	107
6.1 Stable isotopes in precipitation and surface water.....	107
6.2 Stable isotopes in Groundwater.....	108
6.3 Tritium data from the HVO.....	110
6.4 Tritium age determination of groundwater in the HVO.....	111
7. Conceptual hydrogeological model	115
8. Groundwater flow model	118
8.1 Objectives of the model.....	118
8.2 Model geometry.....	118
8.3 Boundary Conditions.....	119
8.4 Hydraulic parameters.....	122
8.5 Integration of scenario information.....	123
8.5.1 Climate scenarios.....	123
8.5.2 Socio-economic scenarios.....	124
8.5.3 Recharge.....	124
8.5.4 Water use.....	126
8.6 Stationary model.....	129
8.7 Transient models.....	132
8.7.1 Scenario model A1B.....	132
8.7.2 Scenario model B1.....	134
8.7.3 Model comparison.....	136
8.8 Uncertainties and constraints.....	138
9. Conclusions	140
10. Recommendations and outlook	142
References	143

List of Figures

Fig. 1.1: *Situation of the IMPETUS project areas in West Africa (modified from IMPETUS 2003; World geographical projection, WGS 84). Project area A: Ouémé river catchment; Project area B: Wadi Drâa.1*

Fig. 1.2: *Precipitation variability in West Africa for the period June – September 1950–2002 (from IMPETUS 2003).2*

Fig. 1.3: *Fields of investigation of the IMPETUS subprojects and their interaction (IMPETUS 2003).3*

Fig. 2.1: *Distribution of all geological map sheets covering Benin (Projection: UTM, Zone 31P, WGS 84). For reference: Latin numbers represent the sheet's name.7*

Fig. 2.2: *Coverage of Benin by hydrogeological maps (Projection: UTM, Zone 31P, WGS 84). For reference: Latin numbers represent the sheet's name.8*

Fig. 2.3: *Coverage of Benin by Landsat imagery. The coverage of the HVO area demands a mosaic of Landsat scenes 192/53 and 192/54. (from JUDEX 2003).9*

Fig. 2.4: *Locations of the installed divers in and around the HVO (Projection: UTM, Zone 31P, WGS 84).11*

Fig. 2.5: *Installation of the automatic data loggers in observation wells (photo a) and footpumps (photo b) with authorisation by the villagers and in cooperation with the technical staff of the beninese water ministry.12*

Fig. 2.6: *Distribution of the sampling locations in the HVO (Projection: UTM, Zone 31P, WGS 84). For the corresponding abbreviations see Annex 1.16*

Fig. 2.7: *Examples of the relationship between $\delta^2\text{H}$ and $\delta^{18}\text{O}$ in meteoric water, evaporating water and water in interactions with rock (taken from COOK and HERCZEG 2000).20*

Fig. 2.8: *Slope of the radioactive decay curve of Tritium (from KENDALL and MCDONNELL 1998).21*

Fig. 2.9: *Some types of elements, based on the finite difference concept and the finite element concept (from ANDERSON and WOESSNER 1994).25*

Fig. 2.10: *The typical triangular element e. Each node is labelled (i, j, m) counter-clockwise and has its own x, y-coordinates marked by the specific footnote (modified from WANG and ANDERSON 1982).25*

Fig. 3.1: *Overview Benin – Extension of the Ouémé catchment and location of the Upper Ouémé catchment (modified from IMPETUS map pool; Projection: UTM, Zone 31P, WGS 84).29*

Fig. 3.2: *Climate chart of Parakou. Data from 1961 to 2005 (with the permission of M. Gosset, IRD 2007). Long-term average amount of precipitation: 1147 mm. Average temperature: 27.1 °C. Black solid line = maximum temperatures; black dashed line = minimum temperatures.31*

Fig. 3.3: *1- During the boreal winter less intense solar rays reach West Africa. This causes a weak thermal contrast. While the ocean is heated by relatively hot currents humidifying the air above the ocean, the continent suffers under the dry Harmattan. 2- In June the sun heats up the continent while a cold ocean current hits the coast. The heated air above the continent mounts and draws in colder and humid air from the sea. This is the beginning of the monsoon. 3- One month later the condensation of the vapour, caused by the first rainfalls, liberates considerable amounts of energy. Thus the air gets heated up and rises. Meanwhile the soil is cooling. Storms occur and form squall lines of considerable length (modified from JUBELIN 2006).31*

Fig. 3.4: *Rainfall distribution modelled for different decades. Yearly precipitation in the HVO varies from 1100 to 1300 mm/a. The North is in general slightly drier than the South (taken from M. Diederich, IMPETUS 2006).32*

Table of Contents

Fig. 3.5:	Comparison of historical precipitation measurements with observations in 2006 for the two gauging stations (ASECNA) at Parakou and Djougou. The measured daily precipitation is accumulated over the year. Data ranges from 1950 to 2006 (with permission of M. Gosset, IRD 2007).	33
Fig. 3.6:	Perspective view on the DEM of the HVO. Z-level is 20 times exaggerated (horizontal scale 1:10.000; vertical scale 1:500). The morphologic valleys contain seasonal rivers. (Projection: UTM, Zone 31P, WGS 84). Cross sections A-A' and B-B' are traced by black lines and are represented in Fig. 3.7.	34
Fig. 3.7:	Cross sections A-A' and B-B,' as shown in Fig. 3.6. The z-level is 50 times exaggerated.	34
Fig. 3.8:	Inselberg of Wari-Marou (620 m asl) at UTM 407864/1013209.	35
Fig. 3.9:	Schematic transect of a bas-fond to show the distribution of dominant clay minerals. B.H. = Borehole (taken from MCFARLANE 1987a).	35
Fig. 3.10:	Riverbed of the Ouémé in the northern half of the HVO during the dry season (UTM 407864/1013209).	36
Fig. 3.11:	Hydrographic net of the rivers in the HVO catchment. The striking of the Kandi fault has a strong impact on the course of rivers in the East of the HVO. (Projection: UTM, Zone 31P, WGS 84).	37
Fig. 3.12:	a) The water course is controlled by fractures ("en baionette"). b) Sinuosity depends on morphological features and not on fractures (from CEFIGRE 1990).	38
Fig. 3.13:	NDVI of Landsat images for the HVO area (period: October 2000). White reflection signifies dense vegetation.	39
Fig. 3.14:	A tamarinde tree in the Atacora mountain area. If a second tree is found, there might be high probability to track a fracture along the connecting between the two trees.	40
Fig. 3.15:	Generalised and simplified map of the main part of the eastern domain of the Pan African of West Africa. Younger igneous rocks are not shown (Geographic projection, WGS 1984; modified from WRIGHT et al. 1985).	42
Fig. 3.16:	Schematic cross section (not to scale) to illustrate a possible plate tectonic interpretation for the southern part of the eastern Pan African domain in West Africa (from WRIGHT et al. 1985).	43
Fig. 3.17:	Generalised map to show the extent of correlation between the Precambrian Tuareg shield of the Hoggar and the eastern Pan African domain in the southern part of West Africa (not to scale, from WRIGHT et al. 1985).	44
Fig. 3.18:	Kinematics of thrusting and wrench faulting in the Pan-African and Brazilian belts of Ghana, Togo and Benin and North eastern Brazil. Legend: 1 = Mesozoic-Cenozoic; 2 = West African craton covered by the Volta Basin; 3 = Pan-African and Brasiliano belts, 4 = external nappes (1), intermediate nappes (2), internal nappes (3); 5 = thermobarometric studies: sampling location in the external nappes (A, B), in the intermediate nappes (C, D) and in the internal nappes (E); 6 = thrust; 7 = dextral transcurrent shear zone; 8 = direction of nappe transport (modified from BRITO NEVES et al. 2001).	44
Fig. 3.19:	Geological map of the Upper Ouémé catchment. Modified after OBEMINES 1984, 1990 and 1990a (Projection: UTM, Zone 31P, WGS 84). Settlements were chosen for reference.	46
Fig. 3.20:	Conceptual hydrogeological model of the crystalline basement aquifers in Africa (modified from CHILTON and FOSTER 1993).	47
Fig. 3.21:	Weathering under different constellations of fractures (from ENGALENC 1978).	48
Fig. 3.22:	A saprolite profile outcropping at an eroded river valley next to the Okpara barrage. Sites A, B and C are less than 10 m distant from each another (East of Parakou; UTM 470614/1026203).	50

Fig. 3.23:	<i>Pisolith at the Okpara dam. Pisolitic iron grains can be identified on the close-up on the right (East of Parakou; UTM 470614/1026203).</i>	50
Fig. 3.24:	<i>Percentual distribution of the depth (in a 5 m interval) of encountered water inflow into borewells in the crystalline area of Benin (Data from SOGREAH and SCET 1999).</i>	52
Fig. 3.25:	<i>Distribution of lognormal kf values in the bedrock aquifer and the limits of the kf zones achieved from the BDI data (Projection: UTM, Zone 31P, WGS 84).</i>	53
Fig. 3.26:	<i>The theoretical relative distribution of recharge, interflow and runoff in the centre and the periphery of bas-fonds (dambos) and at the interfluves (from McFarlane 1987a). The occurrence of smectitic deposits is marked by the black layer.</i>	57
Fig. 4.1:	<i>Groundwater head time series of the HVO data loggers. The data sets are filtered. Only the measurements at 5 am are shown.</i>	59
Fig. 4.2:	<i>Groundwater head time series of the HVO data loggers (continued). The data sets are filtered. Only the measurements at 5 am are shown.</i>	60
Fig. 4.3:	<i>The enlarged view on the groundwater hydrograph of HVO-3 (unfiltered) for two different dates in 2004. The view at the top shows the daily fluctuations of the groundwater table in the dry season, the screenshot at the bottom respectively the rainy season.</i>	61
Fig. 4.4:	<i>Comparison of rainfall, runoff and groundwater levels at Bétérou (HVO-9) for the year 2004. The data set is filtered for 5:00 am measurements only.</i>	62
Fig. 4.5:	<i>Comparison of rainfall, runoff and groundwater levels at Tchétou (HVO-9 for the year 2004). The data set is filtered for 5:00 am measurements only.</i>	63
Fig. 4.6:	<i>Comparison of rainfall, runoff and groundwater levels at Dogué (HVO-12) for the year 2004. The data set is filtered for 5:00 am measurements only.</i>	63
Fig. 4.7:	<i>Average trend equation XT for the 6 data logger time series with an approved statistical relevance.</i>	67
Fig. 4.8:	<i>Regional distribution of all manual and automatic piezometric measurements realised in the vicinity of the study area (Projection: UTM, Zone 31P, WGS 84).</i>	69
Fig. 4.9:	<i>The groundwater levels during the rainy season are generally higher as in the dry season 2004 (Projection: UTM, Zone 31P, WGS 84).</i>	70
Fig. 4.10:	<i>Distribution of the groundwater differences in 2005 (Projection: UTM, Zone 31P, WGS 84).</i>	70
Fig. 4.11:	<i>Exemplary interpolation of manually made groundwater measurements. The data was interpolated and then subtracted from the DEM.</i>	71
Fig. 4.12:	<i>Difference between the two dry seasons of the years 2004 and 2005 (Projection: UTM, Zone 31P, WGS 84).</i>	72
Fig. 5.1:	<i>Determination of correlation between air and water temperature.</i>	73
Fig. 5.2:	<i>pH data of boreholes (a) and dug wells (b) presented respectively in histograms.</i>	74
Fig. 5.3:	<i>Plot of pH and bicarbonate from all sample campaigns. Curves show the pH-bicarbonate relationship for partial pressures of CO₂ in the atmosphere (10^{-3.5}) and for the soil zone (2 examples: 10^{-1.5} and 10^{-2.0}).</i>	75
Fig. 5.4:	<i>EC data of boreholes (a) and dug wells (b) presented respectively in histograms.</i>	75
Fig. 5.5:	<i>Regionalised EC data for the (a) bedrock aquifer and for the (b) regolith aquifer (Projection: UTM, Zone 31P, WGS 84).</i>	76
Fig. 5.6:	<i>Kriging of EC measurements made on borewells after completion of the drilling phase (Source: BDI) (Projection: UTM, Zone 31P, WGS 84).</i>	77
Fig. 5.7:	<i>The oxygen content plotted against the redox potential.</i>	78
Fig. 5.8:	<i>Redox potential and pe range encountered in natural systems at near-neutral pH (modified from SIGG 1999).</i>	78
Fig. 5.9:	<i>Rang distribution in percent of all electric conductivity measurements for dug wells and borewells made in the field during the period of 2004 to 2006.</i>	80

Table of Contents

Fig. 5.10:	The distribution of all hydrochemical groups in the study area (Projection: UTM, Zone 31P, WGS 84).	81
Fig. 5.11:	Whisker-Box-Plot for the electric conductivity measured from dug wells and borewells.	83
Fig. 5.12:	Piper plot of all three hydrochemical groups in the HVO.	84
Fig. 5.13:	Schoeller diagram of the median group composition.	85
Fig. 5.14:	Change of the aluminium concentration in relation to pH with increasing depth (with the kind permission of Luc Séguis, IRD 2007) at Nalohou test site (UTM 347124/1077311). Site description: 3 boreholes with different filter depths at 2 m, 10 m and 20 m.	85
Fig. 5.15:	a) Plot of silicon against chloride and b) plot of silicon against calcium.	86
Fig. 5.16:	Scatter diagrams of sodium against chloride (a) and against calcium (b).	87
Fig. 5.17:	Interpolation of regolith thickness from BDI data (Projection: UTM, Zone 31P, WGS 84). Kriging was done with an exponential variogram.	88
Fig. 5.18:	The stability diagram for albite and its weathering products kaolinite and Na-Montmorillonite.	89
Fig. 5.19:	Changes in the kaolinite-montmorillonite reaction quotient for the hydrochemical groundwater groups in the HVO (modified after GARRELS 1967).	90
Fig. 5.20:	Correlation diagram of sulphate against chloride. The dashed line represents a 1:1 relationship for both constituents.	90
Fig. 5.21:	Plot of all groundwater samples (grey and black crosses) in Gibb's diagram. Samples discussed in the text are marked with black crosses. Arrows show the relative position of different samples from the same location. Circles embrace samples of the same sampling point or equal habits. The wells with strong precipitation signature are found in Tab. 5.8.	91
Fig. 5.22:	Hydrochemical facies of different points in the HVO represented in Schoeller diagrams. The diagrams combine the seasonal samples from all points within the vicinity of a village (with exception of the village of Dogué, because of visibility). The villages are in alphabetical order.	94
Fig. 5.23:	(continued) Hydrochemical facies of different points in the HVO represented in Schoeller diagrams. The diagrams combine the seasonal samples from all points within the vicinity of a village (with exception of the village of Dogué, because of visibility). The villages are in alphabetical order.	95
Fig. 5.24:	(continued) Hydrochemical facies of different points in the HVO represented in Schoeller diagrams. The diagrams combine the seasonal samples from all points within the vicinity of a village (with exception of the village of Dogué, because of visibility). The villages are in alphabetical order.	96
Fig. 5.25:	(continued) Hydrochemical facies of different points in the HVO represented in Schoeller diagrams. The diagrams combine the seasonal samples from all points within the vicinity of a village (with exception of the village of Dogué, because of visibility). The villages are in alphabetical order.	97
Fig. 5.26:	Stability phases of nitrogen compounds in a pe/pH diagram (N-O-H system). The samples are plotted for each season respectively.	101
Fig. 5.27:	Correlation of chloride against nitrate (after BARRETT et al. 2000).	102
Fig. 5.28:	Nitrogen and oxygen isotopes of nitrate in groundwater samples from the Collines department in Benin, rainy season 2003 (taken from CRANE 2006). The source composition is from ROCK and MAYER (2002). The trend line has a slope of ~0.5, indicative of behaviour consistent with denitrification. All 11 samples were taken from open dug wells.	102

Fig. 5.29:	<i>Evolution of nitrate concentrations in groundwater from W-BDOG-1 and W-BDOG-2 in Dogué from 2001 – 2006. Data from 2001 to 2002 was collected by FASS (2004). No field campaign in 2003.</i>	103
Fig. 5.30:	<i>Groundwater classification for the HVO for all sampled seasons. Grey triangles = dug wells; black crosses = borewells.</i>	106
Fig. 6.1:	<i>a) Comparison of GNIP data (Kano-Nigeria = light grey x / Niamey-Niger = grey +) with the HVO rainfall data (black rhombus). The global meteoric water line (GMWL as gray dashed line) is calculated by Craig's notation (Eq. 6.1). b) Groundwater analyses (grey +) are shown in relation to the GMWL. Analyses from surface waters (grey x) are grouped around an evaporation line (light gray dashed line).</i>	107
Fig. 6.2:	<i>left) Dry season 2004: Isotope relationships for groundwater samples from wells (circles=regolith) and pumps (triangles=bedrock). right) Rainy season 2004: Isotope relationships for groundwater samples from wells (circles=regolith) and pumps (triangles=bedrock). The letters (a) to (h) signify a choice of samples from the same locations.</i>	108
Fig. 6.3:	<i>left) Comparison of groundwater samples from the dry season 2002 (black x, FASS 2004) and from the dry season 2004 (grey +). right) Comparison of groundwater samples from the rainy season 2002 (black x, FASS 2004) and from the rainy season 2004 (grey +).</i>	109
Fig. 6.4:	<i>D-excess measured from precipitation samples at the village of Dogué in the years 2002 and 2004. In 2003 no sampling took place. Horizontal lines = dry season; vertical lines = rainy season.</i>	109
Fig. 6.5:	<i>Seasonal fluctuations of TU in precipitation measured at different stations of the GNIP database (IAEA/WMO 2001) with an enlarged view for the years 1970 to 2000.</i>	110
Fig. 6.6:	<i>a) Distribution of tritium in relation to the sample depth. b) Drawdown of the groundwater level in fractures causes seepage from the regolith aquifer above and thus mixture of younger with older water.</i>	112
Fig. 7.1:	<i>Conceptual model of the regional hydrogeology (modified from DANIEL et al. 1997; not scaled; vertically exaggerated). Effective recharge takes place at tophill – discharge downhill. The groundwater table (blue) is set in the regolith. Groundwater in the saturated zone flows towards local morphological depressions. Flow in the bedrock is limited to the fracture zones.</i>	115
Fig. 7.2:	<i>Nalohou test site, Ara catchment (UTM 347124/1077311): Measurements from three boreholes of different filter depths (upper screen depth: 2 m, 10 m and 20 m; screen length: 1 m respectively). Boreholes positioned on the crest, the slope and the valley. Left – Observation of the groundwater table. Right – Measurements of the electric conductivity. Raw data received with the kind permission of L. Séguis, IRD (2007).</i>	116
Fig. 8.1:	<i>Presentation of the model area in a 3D sketch. Three layers, with a plane surface but a dip from the North to the South, represent the regional geology.</i>	119
Fig. 8.2:	<i>Distribution of the boundary conditions in the model area for the 3rd layer (bedrock). For the regolith layer the distribution is the same, but without the well boundaries (Projection: UTM, Zone 31P, WGS 84).</i>	120
Fig. 8.3:	<i>Case A - Accordance of the hydrological and hydrogeological watershed. Case B – Shift of the hydrogeological watershed due to fracture connectivity.</i>	121
Fig. 8.4:	<i>The placement of the well conditions at the bottom of the third model layer is based on the assumed filter position in drill holes. Extracted water leaves the model without any redistribution. Therefore the mesh nodes of concern in the 1st and 2nd layer are described as well conditions with 0 m³/d extraction. The nodes set</i>	

Table of Contents

	<i>vertically above one to another will act numerically as a connected tube. Extracted water will be equilibrated by inflow from the other layers.</i>	121
Fig. 8.5:	<i>Average yearly recharge (unweighted) from all HRUs for each scenario A1B and B1 with trend (dashed lines) and trend equation (original recharge data from GIERTZ 2004).</i>	124
Fig. 8.6:	<i>Effective recharge towards the groundwater table; calculated input data for the model scenarios A1B and B1. Recharge is limited to the months of the rainy season. The model starts in the beginning of the year 2002 in the middle of the dry season. Scenario A1B shows constant recharge while B1 is characterised by a decreasing recharge.</i>	125
Fig. 8.7:	<i>Projection of the demographic development in the HVO until 2025 for the three IMPETUS scenarios (data from U. SINGER, IMPETUS subproject A5).</i>	126
Fig. 8.8:	<i>Position of the remaining 66 villages after aggregation of the census data set from INSAE (2003). Each village presents a well condition in the model mesh (Projection: UTM, Zone 31P, WGS 84).</i>	127
Fig. 8.9:	<i>Groundwater contours of the HVO model area from the stationary model with 44 mm/a recharge. Groundwater flow heads generally towards the closely lying river system. Black circles show joints of rivers with a strong drawdown motivated by numerical reasons (see text).</i>	129
Fig. 8.10:	<i>Standard deviation of model solutions for different recharge cases. The area between the 22 and 55 mm/a represents equally reasonable model solutions.</i>	132
Fig. 8.11:	<i>Groundwater contours of the HVO model area from the from the final time step of the A1B scenario model. Groundwater flow heads generally towards the closely lying river system. Especially around the village of Tourou (see arrow) groundwater drawdown can be observed.</i>	133
Fig. 8.12:	<i>Groundwater table differences between the final time step of model A1B and the initial conditions from the stationary model. Positive values indicate the drawdown of the groundwater table in the A1B model in relation to the initial conditions.</i>	134
Fig. 8.13:	<i>Groundwater contours of the HVO model area from the from the final time step of the B1 scenario model. Groundwater flow heads generally towards the closely lying river system. Especially around the village of Tourou (see arrow) groundwater drawdown can be observed.</i>	135
Fig. 8.14:	<i>Groundwater table differences between the final time step of model B1 and the initial conditions from the stationary model. Positive values indicate the drawdown of the groundwater table in the B1 model in relation to the initial conditions.</i>	136
Fig. 8.15:	<i>Groundwater level differences between the final time steps of model A1B and model B1. Positive values indicate the drawdown of the groundwater table in the A1B model in relation to the initial conditions.</i>	137
Fig. 8.16:	<i>Drawdown at the pumping well of Tourou (black line) and the consumption by its population (blue line). The seasonal fluctuations of water consumption can be traced by the behaviour of the modelled groundwater table.</i>	137

List of Tables

Tab. 2.1:	<i>Locations and status of the barometers. The barometers were not installed in the boreholes for reasons of space and prevention of disturbing influences.</i>	12
Tab. 2.2:	<i>Locations and status of the data loggers.</i>	14
Tab. 2.3:	<i>Electrode types used with the WTW data logger on-site during the field campaigns in the Upper Ouémé area.</i>	17
Tab. 2.4:	<i>Sample methods and materials in an overview.</i>	18
Tab. 2.5:	<i>Detection limits of analysed constituents.</i>	18

Tab. 3.1:	<i>Typical flow net pattern in West Africa taken from CEFIGRE (1990).</i>	38
Tab. 3.2:	<i>Frequency of final borehole depths for different rock types in the Upper Ouémé catchment [%]. Values of maximum percentage are drawn on grey background (Data source: BDI).</i>	51
Tab. 3.3:	<i>Mean values for transmissivity and storativity in the Collines. Average calculated from 5 pumping test interpretations (taken from BOUKARI et al. 1985).</i>	53
Tab. 3.4:	<i>General hydrogeologic characteristics of the geological units of the Upper Ouémé catchment area (modified, from DANIEL et al. 1997).</i>	54
Tab. 3.5:	<i>Thickness of the regolith in relation to the mother rock. Data is taken from the BDI.</i>	56
Tab. 3.6:	<i>Hydraulic conductivities of regolith aquifers.</i>	56
Tab. 3.7:	<i>Area of influence for pumping tests in the regolith zone (ENGALENC 1978).</i>	57
Tab. 4.1:	<i>Trend analyses of piezometric time series data.</i>	65
Tab. 4.2:	<i>Critical values of r for the HVO divers.</i>	66
Tab. 4.3:	<i>Coordinates of the IRD piezometers in the Donga catchment.</i>	67
Tab. 4.4:	<i>Number of manual piezometric measurements on wells realised in and around the study area during different seasons from 2004 to 2006.</i>	69
Tab. 4.5:	<i>Results from the grid based recharge calculation. The volume is calculated by subtracting the grids of the interpolated manual field measurements.</i>	72
Tab. 5.1:	<i>Population statistics of temperature measurements.</i>	73
Tab. 5.2:	<i>Population statistics of redox measurements in the study area for boreholes (a+c) and wells (b+d) for the dry seasons and for the rainy seasons.</i>	79
Tab. 5.3:	<i>Population statistics of oxygen measurements of boreholes (left) and wells (right).</i>	79
Tab. 5.4:	<i>Assignment of aquifers to sample groups.</i>	81
Tab. 5.5:	<i>Samples excluded from group 3 because of too high grades of contamination.</i>	82
Tab. 5.6:	<i>Samples excluded from group 2.</i>	82
Tab. 5.7:	<i>Population statistics of the hydrochemical parameters for each group (see Annex 1).</i>	83
Tab. 5.8:	<i>Names of samples under strong precipitation influence.</i>	92
Tab. 5.9:	<i>Impact of fluoride in drinking water on health (DISSANAYAKE 1991).</i>	99
Tab. 5.10:	<i>Borewells contaminated by fluoride in Benin (oral comm. L. DOVONON, DGEAU, March 2005).</i>	99
Tab. 5.11:	<i>Fluoride concentrations observed at three well during the seasons from 2004 to 2006.</i>	100
Tab. 5.12:	<i>Limits for nitrate in drinking water in international use. It should be noted that some countries may chose other limits following their own policies.</i>	100
Tab. 5.13:	<i>Average mineralisation of the two regularly sampled dug wells in Dogué.</i>	104
Tab. 5.14:	<i>Sample locations with high salinity hazard.</i>	106
Tab. 6.1:	<i>Comparison of the seasonal differences of TU-contents of groundwater samples from different sites and depths in the HVO-area.</i>	111
Tab. 6.2:	<i>Mixing ratio of recently recharged water to groundwater from the regolith and the bedrock aquifer. Results from Eq. 6.2.</i>	113
Tab. 6.3:	<i>Entry parameters into the user interface of the Boxmodel V2-3[®] (by IHW, ETH-Zurich, ZOELLMANN et al. 2001).</i>	114
Tab. 8.1:	<i>Number of nodes and elements in the model after the final refinement.</i>	119
Tab. 8.2:	<i>Hydraulic parameters as applied to the model layers.</i>	122
Tab. 8.3:	<i>Mean values of the water consumption in l/d per capita in different types of townships in the HVO as measured from 2002 to 2003 (SCHOPP 2004).</i>	126
Tab. 8.4:	<i>Distributed use of the different water sources used to satisfy the general water demand based on the observations of SCHOPP (2004).</i>	127
Tab. 8.5:	<i>Groundwater volume in the aquifers of the HVO. Minimum water content for both aquifers is assumed (low saturation level for one year). Recharge is ignored.</i>	

Table of Contents

	<i>Maximum water extraction from a population as projected for the year 2025 is added (Scenario B2).....</i>	128
Tab. 8.6:	<i>Calculation of the discharge (in mm/a) caused by pumping in the HVO area for the comparison with the regional recharge.....</i>	128
Tab. 8.7:	<i>Total water balance of the stationary model. The well flux occurs at the 3rd layer only.</i>	130
Tab. 8.8:	<i>Comparison of discharge and recharge in the HVO model related to their share of the HVO surface.</i>	130
Tab. 8.9:	<i>Stepwise variation of recharge as input for the stationary model. For each case the error on the hydraulic heads was controlled. Minimum limit for successful computing is 1E-03 in less than 12 iteration steps (FEFLOW[®] default conditions, DIERSCH 2005).</i>	131

List of Equations

Eq. 2.1	9
Eq. 2.2	18
Eq. 2.3	19
Eq. 2.4	19
Eq. 2.5	19
Eq. 2.6	19
Eq. 2.7	21
Eq. 2.8	24
Eq. 2.9	24
Eq. 4.1	64
Eq. 4.2	64
Eq. 4.3	64
Eq. 4.4	64
Eq. 4.5	64
Eq. 4.6	64
Eq. 4.7	64
Eq. 4.8	66
Eq. 5.1	74
Eq. 5.2	77
Eq. 5.3	78
Eq. 5.4	86
Eq. 5.5	87
Eq. 5.6	105
Eq. 6.1	107
Eq. 6.2	113

Annex (on CD)

Annex 1: Hydrochemistry

A-1.1_Hydrochemistry_Dry_2004.xls.....	file
A-1.2_Hydrochemistry_Rainy_2004.xls	file
A-1.3_Hydrochemistry_Dry_2005.xls.....	file
A-1.4_Hydrochemistry_Rainy_2005.xls	file
A-1.5_Hydrochemistry_Dry_2006.xls.....	file
A-1.6_Heavymetals_Rainy_2004.doc	file
A-1.7_Heavymetals_Dry_2005.doc.....	file
A-1.8_Hydrochemistry_Surfacewater.xls	file

Annex 2: Isotopes

A-2.1_Stable_isotopesfolder
A-2.2_Tritium.....folder
A-2.3_GNIP-data.....folder

Annex 3: Piezometry

A-3.1_5am_data_and_statistics.....folder
A-3.2_Barometer_Datafolder
A-3.3_Original_Diver_Datafolder

Annex 4: Borehole database

A-4.1_BDI_Original_Year_2005.mdb.....file
A-4.2_BDI_Contents.xls.....file
A-4.3_BDI_official_dictionary.docfile

Annex 5: Groundwater flow model

A-5.1_Model_Datafolder
A-5.2_Stationary_Modelsfolder
A-5.3_A1B_Scenario_Modelfolder
A-5.4_B1_Scenario_Modelfolder

Annex 5 contains for each folder readme.txt-files with instructions about the use of the data files in the numerical model.

Notation:

- Please mind that within this study on hand decimals are separated by “.”. The separation of thousands is written with a “,”.
- Symbols used in equations are explained where they appear.

Abbreviations

asl	above medium sea level	IRD	Institut de Recherche pour le Développement
BC	Boundary Conditions	LMWL	Local Meteoric Water Line
BDI	Borehole database	mm/a	mm per year
bgl	below ground level	MDG	Millenium Development Goals
BMBF	German Federal Ministry of Education and Research	MMEE	Ministère des Mines, de l'Énergie et de l'Eau (former MMEH)
BRGM	Bureau de recherches géologiques et minières	MMEH	Ministère des Mines, de l'Énergie et de l'Hydraulique (today MMEE)
DEM	Digital elevation model	PDE	Partial differential equations
DGEau	Direction Générale de l'Eau (former DGH)	PFM	Piston Flow Model
DGH	Direction Générale de l'Hydraulique (today DGEau)	REMO	Regional Model
DM	Dispersion Model	SBEE	Société béninoise de l'Eau et l'Énergie (today Société béninoise de l'Electricité et l'Énergie)
EM	Exponential Model	SEau	Service d'Eau (former SRH)
Eq.	Equation	SONEB	Société nationale des Eaux au Bénin
FD	Finite Differences	SRES	Special Report on Emission Scenarios
FE	Finite Elements	SRH	Service Régional d'Hydraulique (today SEau)
Fig.	Figure	SRTM	Shuttle Radar Topography Mission
GNIP	Global Network of Isotopes in Precipitation	Tab.	Table
GLOWA	Global change in the hydrologic cycle	TU	Tritium units
GMWL	Global Meteoric Water Line	UN	United Nations
HRU	Hydrological Response Unit	UTM	Universal Transverse Mercator
HVO	Upper Ouémé valley (French: Haute Vallée d'Ouémé)	VSMOW	Vienna Standard Mean Ocean Water
IAEA	International Atomic Energy Agency	WGS	World Geographic System
IMPETUS	Integrated approach to the efficient Management of scarce water resources in West Africa		
IPCC	Intergovernmental Panel on Climate Change		

1. Introduction

1.1 General overview

The Republic of Benin in West Africa is among the 50 less developed countries in the ranking of the UNITED NATIONS¹ (UN-OHRLLS 2004). Benin is geographically located between the Sahel in the North and the Atlantic Ocean in the South. Due to a meteorological anomaly, the Dahomey Gap (VOLLMERT et al. 2003), Benin receives less precipitation than other countries on the same latitude (e.g. Ghana, Nigeria). This makes it more vulnerable to droughts and water shortages induced by climate change.

As in many other countries of the world, the authorities of Benin become aware that resources of potable water are limited. Climatic change in combination with world's population growth, pollution of existing resources due to industrialisation and intensive agriculture are putting the water resources and respectively agriculture increasingly under stress. Worldwide efforts are underdone to prepare governments, societies and industries to that situation.

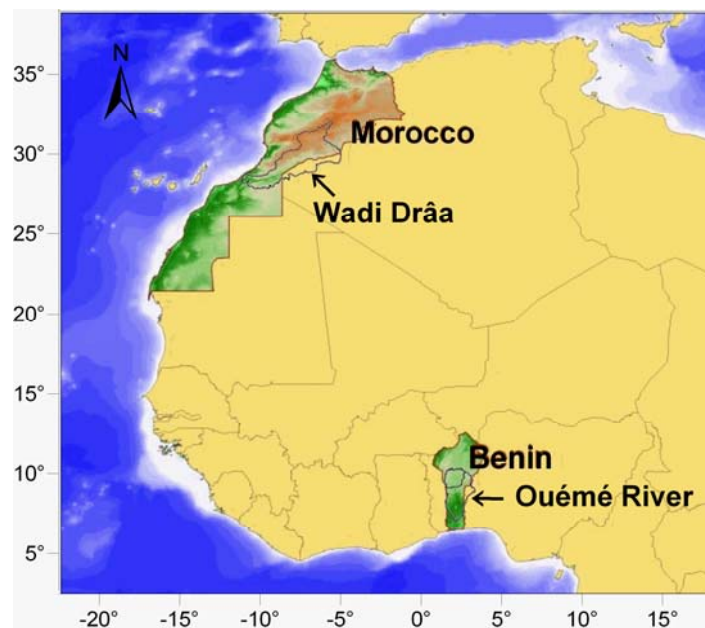


Fig. 1.1: Situation of the IMPETUS project areas in West Africa (modified from IMPETUS 2003; World geographical projection, WGS 84). Project area A: Ouémé river catchment; Project area B: Wadi Drâa.

As a contribution to this effort the German Federal Ministry of Education and Research (BMBF) has launched the program GLOWA² (Global change in the hydrologic cycle). GLOWA is a framework of 5 regionally and interdisciplinary acting projects with the aim to analyse and highlight the changes of the water cycle in different climatic zones. GLOWA projects are: Elbe, Danube, Jordan River, IMPETUS and Volta.

The IMPETUS project is an integrated approach to the efficient management of scarce water resources in West Africa hosted by the universities of Bonn and Cologne.

¹ URL: http://unstats.un.org/unsd/cdb/cdb_dict_xrxx.asp?def_code=481

² URL: <http://www.glowa.org>

1 Introduction

IMPETUS is funded by the German Federal Ministry of Education and Research (BMBF, grant No. 07 GWK 02) and the Ministry of Science and Research of the federal state of Northrhine-Westphalia (MWF, grant No. 223-21200200).

The objective of the IMPETUS West Africa project is to analyse the impact of global climate change on the water resources of the catchments of the Wadi Drâa in Morocco and of the Ouémé in Benin (see Fig. 1.1). The study areas were chosen based on the assumption that climatological processes in the northern and southern part of West Africa are related as LAMB and PEPPLER (1991) suggested.

The West African Sahel zone suffers since 1970 from extensive drought periods (BROOKS 2004). Since that time precipitation is regularly under average (see Fig. 1.2). The management of the available potable water resources in West Africa is of immense importance; not only for the Sahelian countries but for all the countries who might suffer from increasing migration, worsening economic and agricultural conditions.

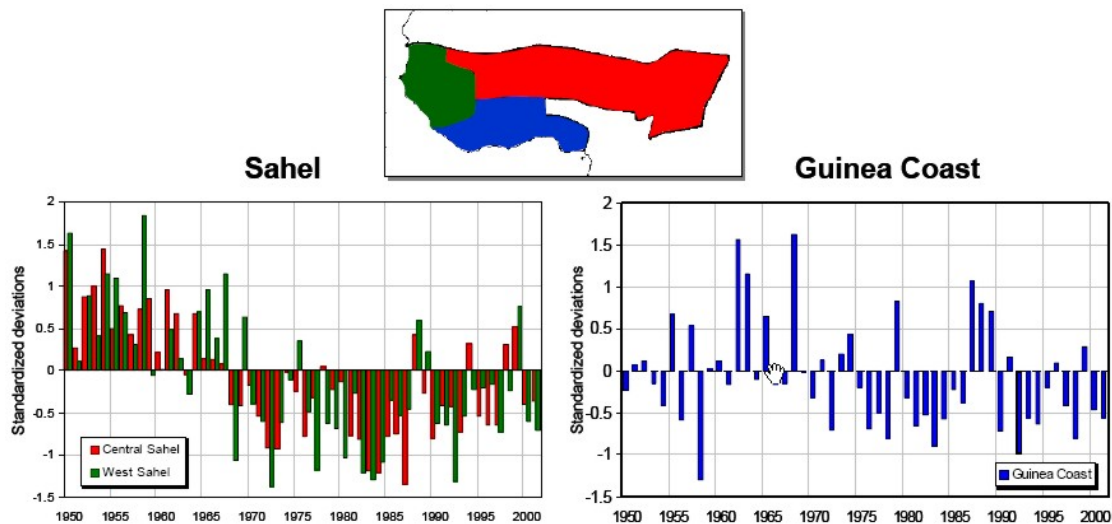


Fig. 1.2: Precipitation variability in West Africa for the period June – September 1950–2002 (from IMPETUS 2003).

The IMPETUS project is structured in subprojects (see Fig. 1.3) with differing working scales. Subproject A2 studies hydrological processes on different scales in the Upper Ouémé catchment. Subproject A2 consists of the workpackages A2-1 and A2-2 (hydrology and regional water balance), A2-3 (pedology) and A2-4 (hydrogeology). This thesis is part of the workpackage A2-4. A2 focussed during the 1st project phase from 2001 to 2003 on an interpretation of hydrological and hydrogeological processes mainly in the Aguima catchment.

The 2nd phase (2004 to 2006) regionalises the results from the 1st phase to the extent of the Upper Ouémé catchment (HVO ~14,500 km²). In the 2nd phase the application of multidisciplinary models is a principal objective.

The 3rd IMPETUS phase runs from 2006 to 2009. It mainly focusses on predictions for the whole Ouémé catchment. The socio-economic and the climate scenarios shall be integrated into the modelling process to predict changes concerning the hydrological cycle and the water resources in coming decades.

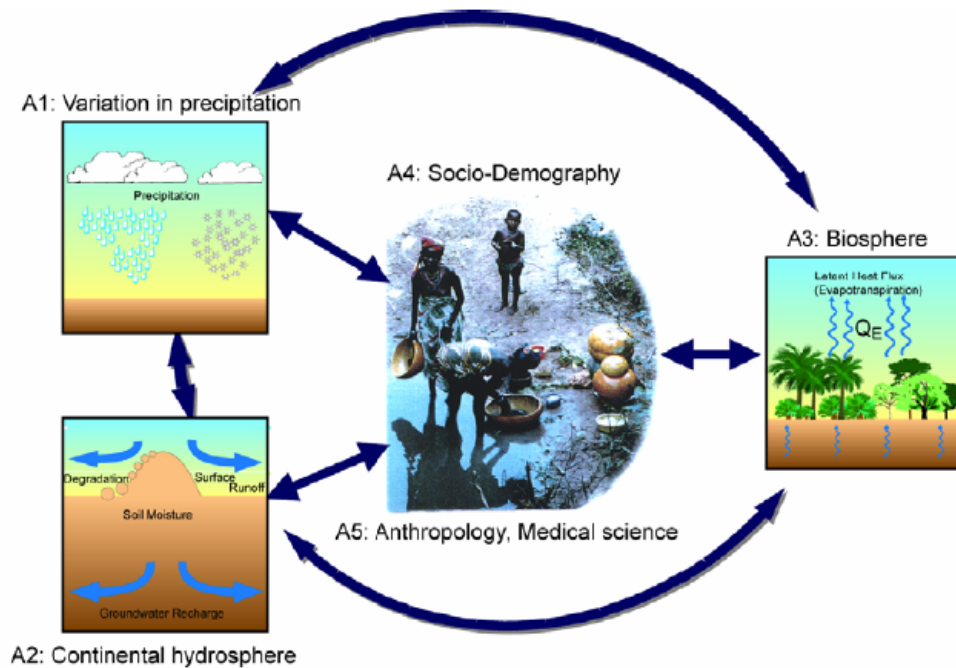


Fig. 1.3: Fields of investigation of the IMPETUS subprojects and their interaction (IMPETUS 2003).

1.2 Motivation and objective of the study

The scope of this PhD thesis was the hydrogeological conceptualisation of the Upper Ouémé river catchment in Benin (see Fig. 3.1). The study area exceeds 14,500 km² and is underlain by a crystalline basement. At this setting the typical sequence of aquifers - a regolith aquifer at the top and a fractured bedrock aquifer at the bottom - is encountered, which is found in basement areas all over Africa and elsewhere in the world. The chosen regional approach revealed important information about the hydrochemistry and hydrogeology of this catchment.

Based on the regional conceptual model a simplified numerical groundwater flow model was designed. The numerical model was used to prove the assumptions made for the conceptual model in Chapter 7 and to describe the impact of climate change on the regional groundwater resources until the year 2025. The groundwater model was developed with the finite element model FEFLOW[®] from Wasy GmbH.

In the following text it is in general referred to the Upper Ouémé basin by its French abbreviation HVO (French: "Haute Vallée d'Ouémé"). The HVO catchment is a mostly ungauged basin, which is situated entirely on old crystalline basement where two types of aquifers exist - a discontinuous fractured bedrock aquifer and a regolith aquifer.

The study integrates the local scale findings of FASS (2004) about the small Aguima subcatchment (~30 km²). Hydrochemical and environmental isotope sampling campaigns started in 2000 by FASS (2004) were regionally extended and intensified to investigate not only the regolith aquifer but as well the bedrock aquifer.

The fieldwork for this study was realised during five field trips from 2004 to 2006. During the fieldwork, 244 samples of groundwater, 10 of surface water and 11 of precipitation were collected within, as well as outside, the Upper Ouémé catchment for hydrochemical analysis. Samples for the stable isotope determination were taken at the same locations

1 Introduction

as well. Due to technical reasons only 126 samples were analysed at time of editing this thesis. Tritium was determined for 34 samples.

Twelve automatic logging devices had been installed to daily detect groundwater level fluctuations since the 1st of May 2004. These divers were regularly checked for their data; additionally manual groundwater level measurements were made in each field campaign.

The analysis of the samples for hydrochemical and isotope data form the basis for the characterisation of the different groundwater types occurring within the catchment, as well as for the determination of the major factors controlling the aquifer system. Groundwater quality was screened intensively as it is a matter of concern in the shallow phreatic aquifers in the regolith layers. Geologic information of a general nature was also collected, since the nature of the rock types and their structures have a direct influence on the groundwater regime.

The interpretation of the found data is presented in the following chapters. In the end of the thesis the overall conclusions are presented in Chapter 9. Finally recommendations are given in Chapter 10 about the future potential of hydrogeological research in the study area.

1.3 State of research on the fractured basement of Benin

In many parts of Africa groundwater is the most reliable water resource (WRIGHT 1992). Crystalline basement areas are widespread in Africa as in the world. Although they contain water bearing fractures they may not provide sufficient water resources for extensive use when its regolith cover is not thick enough to store groundwater.

The details about the hydrogeology of the West African crystalline basement are still widely unknown. Typically the biggest townships in West Africa are situated in sedimentary basins especially along the coast line. This is where most of research and technical interventions take place.

However, the Beninese strategy paper (DGH 2005) for the achievement of the United Nations millennium goals (LOEWE 2005) stipulates coverage of water supply especially for the neglected rural areas. In Benin most of these areas lay on the crystalline basement.

Though the hydrogeological research in West Africa is poorly documented important background information for both judging the renewal and managing of the resources is not available (WORLDBANK 2005). Thus, it is necessary to collect literature not only from Benin but from adjacent countries under comparable conditions.

In Benin geological (OBEMINES 1984, 1989a, 1989b, 1989c, 1989d, 1989e, 1989f, 1989g, 1989, 1995a, 1995b) and hydrogeological maps (ENGALENC 1985a, 1985b) exist which cover the whole country in a scale 1/200.000. Although this scale does not allow detailed interpretation they are the main base for any hydrogeological investigation in this area until present. Classical works on the interpretation of hydrogeology in West Africa are from ENGALENC (1978), BISCALDI (1967), BRGM-AQUATER (1986) and from CEFIGRE (1990). BOUKARI (1985) described the crystalline aquifers in the area of the city of Dassa (Central Benin). SOGREA and SCET (1997) made an overall and countrywide analysis of the well and borehole inventory in order to suggest favourable borehole sites and drilling techniques.

In the year 2000, the IMPETUS project started with hydrological and hydrogeological investigations in the HVO area. FASS (2004) gives detailed information about hydrogeology and hydrochemistry of the regolith aquifer in the Aguima catchment. Three diploma theses increase substantially the knowledge about the aquifer conditions in Benin. BAUER (2004) worked on tracer tests in the regolith zone; SARVAN (2005) prepared a regional hydrochemical characterisation of the bedrock and the regolith aquifer on multivariate statistics. BOHNENKÄMPER (2006) applied geoelectrical measurements to evaluate the morphological evolution of the regolith aquifer.

Very important input comes from the hydrologists of the IMPETUS project. GIERTZ (2004) describes the hydrological processes in a subcatchment of the HVO and modelled runoff and groundwater recharge with different applications (BORMAN 2005; GIERTZ et al. 2006). Hydrological models for HVO sub catchments are developed by the French IRD as well (VARADO 2004) and a classical hydrological work about Benin is presented by LE BARBÉ et al. (1993).

Many recent publications treat the application of geophysical techniques in detecting fractures suitable for extracting water for the rural water supply. These mainly local studies give much insight in the heterogeneity of the aquifer structures, of the regolith as well as of the bedrock aquifer. Especially from Nigeria many publications are available (e.g. ADEPELUMI et al. 2001 and 2006, EHINOLA et al. 2006, and OKEREKE 1998). Further publications come from Burkina-Faso (SAVADOGO 1997), from Zimbabwe (OWEN 2005) and from several other parts of the world (e.g. CARUTHERS and SMITH 1992).

Until today little is published about the hydrochemical characteristics of groundwater in Benin. In general the national water provider SONEB (French: "Société nationale des eaux du Bénin") samples regularly the water pumped from the aquifers and from the surface dams into their piping system. This data together with the standard analyses made from each newly drilled borehole is collected by the DGEau (French: "Direction Générale de l'Eau") in Cotonou. However, this information is still widely unpublished and is not used for a further aquifer characterisation until present.

Recent publications on hydrochemical characteristics and water quality in Benin results from a research cooperation between the University of Abomey-Calavi (Benin) and the University of Notre Dame (USA). ROOPE (2003) and CRANE (2006) worked about the general water quality in the crystalline aquifer in the Collines department in the centre of the Ouémé catchment. They worked on contaminants such as nitrate and pesticides and as well on the impact of heavy metals.

Researchers from the French IRD do very detailed hydrological work on the Donga catchment, a subcatchment of the HVO. A recent publication about hydrochemical investigations in the regolith and surface water is the thesis of KAMAGATÉ (2006). From Nigeria there is a very comprehensive interpretation of hydrochemical analyses from EDET and OKEREKE (2005).

Biological quality of water is regularly tested by the SONEB for their installations. A regional investigation in bacteriology and virology of groundwater in the HVO area is realised by the IMPETUS subproject A5. SHEKWOLO and BRISBE published in 1999 an article about bacteriology in different areas of Nigeria.

Actually there exists a close cooperation between the DGEau and the International Atomic Energy Agency (IAEA) with the objective to determine the origin and the age of

1 Introduction

the important groundwater resources in the Beninese coastal basin. Besides ZUPPI (2005) and DRAY et al. (1988) publications about environmental isotopes in Benin are scarce. However, the successful application of isotopes is described in comparable environments such as Ghana (JORGENSEN and BANOENG-YAKUBO 2001), Nigeria (e.g. LOEHNERT 1988, EDMUNDS et al. 2002 and GONI 2006). Additional publications about isotopes exist for the fractured aquifers in Uganda (e.g. TAYLOR and HOWARD 1996 and 2000).

The use of regional groundwater numerical models seems to be still in a very initial phase for most of the crystalline basement areas in sub-Saharan Africa. Although some applications of regional models are known they generally concentrate on sediment basins. For example: FAYE et al. (2001) worked out a finite element model with FEFLOW® to determine seawater intrusion in coastal aquifers of Senegal; BOUKARI et al. (1996) stated the contamination of coastal aquifers in Benin and is at present working on a finite difference model to predict their dynamics under the pumping scheme of the urban water supply for Cotonou; Roland Barthel from the German RIVERTWIN project prepared a finite difference model for the sedimentary basin of the lower Ouémé catchment in Benin (oral comm. R. BARTHEL, University of Hohenheim, 2006).

No explicit numerical models for the crystalline areas in West Africa were found. The French BRGM (French: "Bureau de recherches géologiques et minières") developed alternatively the lumped parameter model GARDENIA (THIERY 2004) which was successfully applied on local fractured aquifer systems around Ouagadougou in Burkina-Faso (FILIPPI et al. 1990).

In other countries in the world with crystalline bedrock aquifers and comparable climatic conditions the groundwater research is already quite advanced. Especially from India and Australia many interesting investigation and analysing methods are presented. Among the manifold publications from these countries some were especially useful for the here presented study. A good overview about bedrock aquifers in India and world wide is given by SINGHAL and GUPTA (1999). Hydrochemical characterisations of groundwater in bedrock and regolith aquifers are very well described by SUBHA RAO (2002) and RAJMOHAN and ELANGO (2004). Recharge processes and isotope application for the same environment are interpreted by SUKHIJA et al. (2006). TAYLOR and EGGLETON (2001) give an all-embracing description of the formation of regolith and its chemical and physical characteristics related to its morphological position and its saturation by groundwater. BUTT and ZEEGERS (1992) give as well a very conclusive insight into the characteristics on regolith deposits, more from an exploratory view but with comments on groundwater interaction.

COOK (2003) gives an overview of the demands for numerical modelling of regional fractured aquifers and thus gives emphasis to the complexity of this method in such an environment.

A very interesting documentation about a regional finite difference model comes from DANIEL et al. (1997). He modelled a regolith-fractured bedrock system with an area of around 367,800 km² in North Carolina (USA). Supported by a detailed borehole data base they made a statistical analysis of aquifer properties related to the area's morphology.

2. Materials and methods

2.1 Mapping and imagery

2.1.1 Geological and hydrogeological map

The geology of the Republic of Benin is presented by 12 geological map sheets in a scale of 1:200,000 (Fig. 2.1). A complete set of maps and their reports were given to the IMPETUS project by the DGEau. The geological maps I, II and III were ready to download from the internet-site of the University of Stuttgart-Hohenheim (HERRMANN and VENNEMANN 2000). The other maps were digitised at the Geological Institute of Bonn.

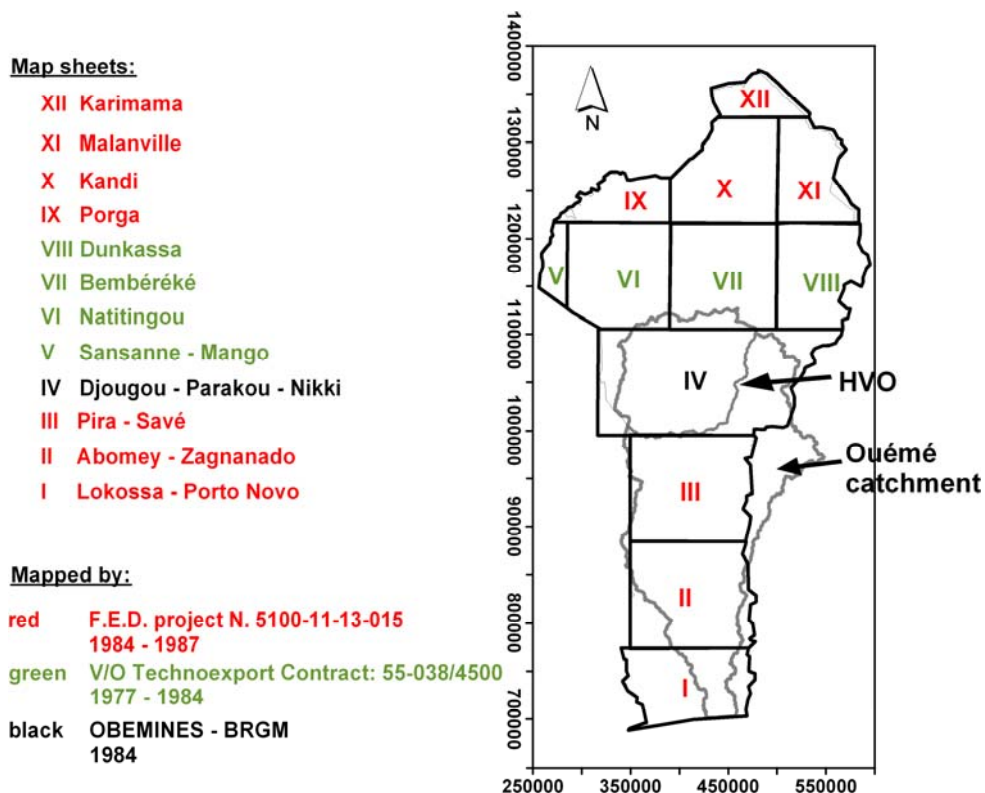


Fig. 2.1: Distribution of all geological map sheets covering Benin (Projection: UTM, Zone 31P, WGS 84). For reference: Latin numbers represent the sheet's name.

Fig. 2.1 shows that different projects worked on the geological maps with differing legends. The map sheets V to VIII are clearly denounced as “Geological and Mineral Commodity Map”. The F.E.D project emphasised the lithological character of the rocks in the mapping area as separating factor while the sheet IV shows more the structural units and the genesis of geological formations.

The HVO catchment is mainly covered by the map sheet IV (Djougou-Parakou-Nikki). Only in the North a smaller stripe belongs to the V/O Technoexport maps. A very tiny stripe in the South belongs to the F.E.D. legend. In the context of this thesis the different legends have been brought together and an integrative map for the Ouémé and for the HVO catchment has been developed.

The framework of the hydrogeological maps is more homogeneous. ENGALENC (1985a and 1985b) covered the area of Benin with two maps only (Fig. 2.2). One map

2 Materials and methods

represents the hydrogeology of the coastal sedimentary basin with a scale of 1/200.000. The other map covers the crystalline basement area and the sedimentary river basins of the North with a scale of 1/500.000. The hydrogeological units mostly respect the outline of the geological units described by the geological maps.

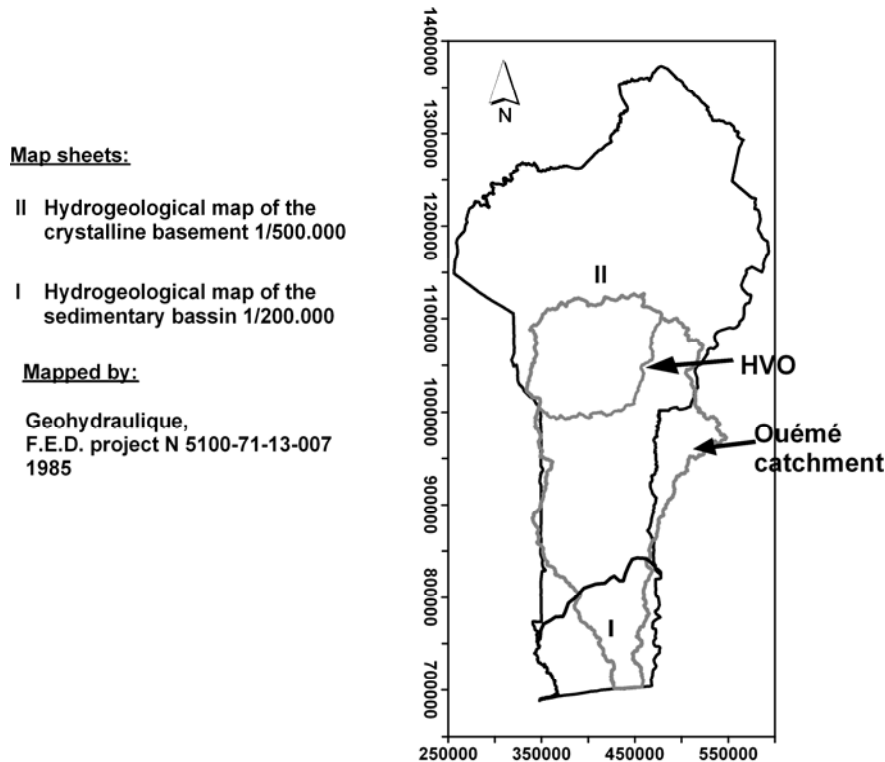


Fig. 2.2: Coverage of Benin by hydrogeological maps (Projection: UTM, Zone 31P, WGS 84). For reference: Latin numbers represent the sheet's name.

The hydrogeological maps are accompanied by a number of thematic maps (e.g. chance of success, groundwater potential, hydraulic reserves of the regolith and others).

2.1.2 Digital elevation model and satellite images

A digital elevation model (DEM) for the study area (Fig. 3.6) was derived from the C-band data of the Shuttle Radar Topography Mission (SRTM). SRTM-3 quality with a resolution of 3 arc seconds (=90 m) can be downloaded from different URLs³. The altitude is given in full meters above sea level (CZEGKA et al. 2004).

For the data poor area of Benin the SRTM DEMs are an excellent tool for interpreting the morphology and surface characteristics without the exhaustive and time consuming differential GPS elevation measurements in the field. In combination with satellite images a powerful tool is available.

Although the use of satellite imagery is highly recommended to produce fracture maps and to describe geological units in research areas (SANDER 1999) constraints exist for the HVO. A dense vegetation cover and thick regolith hide the characteristics of the crystalline basement. Especially in the rainy season the imagery is poor due to high

³ <http://edcftp.cr.usgs.gov/pub/data/srtm/>

and <http://www2.jpl.nasa.gov/srtm/cbanddataproducts.html>

standing grass and other plants. In the beginning of the dry season reflectivity of the surface is changed by field burning. Haze and clouds are other typical constraints.

The IMPETUS remote sensing subproject A3 achieved a couple of Landsat 7 ETM+ sceneries of central Benin from the USGS Radarsat International Inc⁴. The HVO area is covered by two sceneries (see Fig. 2.3).

The spectral bands can be combined to highlight the reflection characteristics of different land cover types. Mathematical operations are exercisable to combine the different bands to obtain the normalised differential vegetation index (NDVI):

$$NDVI = \frac{NIR-RED}{NIR+RED} \quad (\text{Eq. 2.1})$$

NIR = near infrared

RED = visible red



Fig. 2.3: Coverage of Benin by Landsat imagery. The coverage of the HVO area demands a mosaic of Landsat scenes 192/53 and 192/54. (from JUDEX 2003).

⁴ Url: <http://landsat.gsfc.nasa.gov>

2.2 Borehole data base (Base des données intégrées – BDI)

The DGEau is charged with the development of a national borewell inventory in form of a digital database which shall combine the information of all institutions working in Benin's water sector (BURGEAP 2004). The borewell database is called "Base de Données Intégrée" and is often referred to as **BDI**. The data is edited in 37 principal tables and some extra tables with mainly basic data. From the hydrogeological point of view the following information was achieved:

- number of borewells in the study area;
- coordinates of the borewell;
- technical description of the borewells (depth, casing, filter, ...);
- geological description of the borewells;
- pumping test data (date, length, transmissivity, ...).

The complete overview of the list entries used from each table is given in Annex 4. The continuous work with the BDI data revealed some constraints to the quality of the BDI data. They are summarised as followed:

- **Coordinates:** The screening of the coordinates of many borewells revealed in many cases either deviations or simply false locations. The cause might be errors made during typing the data into the computer (most of the original data sheets are handwritten). Another reason is that positions were already poorly measured in the field.
- **Geology:** Much confusion is given by the geological descriptions of the borehole log. The geology of close-by boreholes differs greatly. The terms granite, gneiss and migmatite are concurrently used for describing crystalline rocks. Only the shift from regolith to bedrock is in general well documented. The occurrence of saprock cannot be deduced from the BDI.
- **Pumping Tests:** The BDI does not provide the original pumping test data but only the results from computation of the transmissivity parameter. The pumping tests done in Benin are usually one-borehole tests. Thus no storage coefficient can be evaluated. The tests are step-wise conducted with changing withdrawal rates. In general 2 to 3 steps are realised each for only 1 to 2 hours (max. 6 hours). It is obvious that this procedure gives only information about the short-term productivity of fractures but not about the real transmissivity of a whole borehole section.
- **Failed boreholes:** In the fractured domain of the crystalline basement many boreholes are declared negative and are not transformed into borewells. For a statistical interpretation of hydraulic properties of certain areas or rock units it is indispensable to compare the occurrence and position of positive and negative borewells.

Data quality was proven by comparing the coordinates and their names with the existing villages in the study area. The BDI shows data for 518 boreholes within the HVO. After

the screening 358 borewell reports were used for the interpretation of geological (e.g. layer thickness) and hydrogeological (e.g. transmissivity) information.

2.3 Piezometry

In order to observe the behaviour of the groundwater table 12 automatic data loggers (diver) from Van Essen Instruments Inc. were installed in the field in the end of April 2004. The divers were placed in observation boreholes and in boreholes of footpumps distributed over all the HVO area or next to it (see the data in Tab. 2.2 and Fig. 2.4). The decision about the positions of the data loggers was taken in accordance to the local authorities (SEau Parakou, SEau Djougou and SEau Dassa). The divers were programmed to start data logging simultaneously at 2:00 am on the 1st of May 2004. The internal diver’s clock was synchronised with a portable laptop.

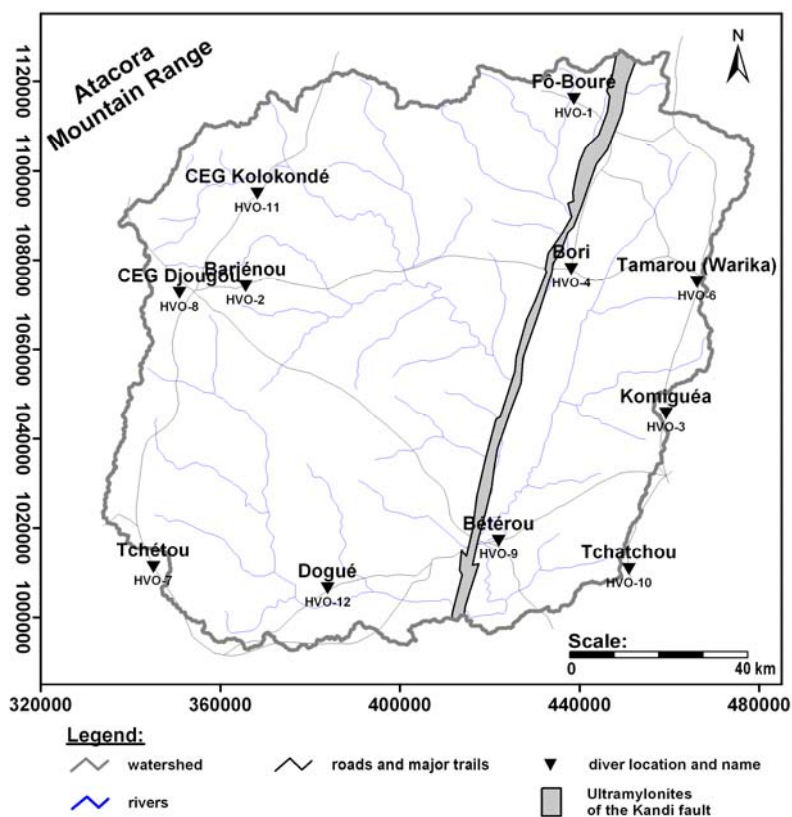


Fig. 2.4: Locations of the installed divers in and around the HVO (Projection: UTM, Zone 31P, WGS 84).

In 2004 the DGEau started a national groundwater survey on 12 boreholes either newly drilled or recovered as observation wells (SITRA.HM 2003). Four of these observation wells are located in the HVO area and were chosen for the installation of the data logger (see Fig. 2.5 a and b). At the small Dogué test site (FASS 2004) the observation GWM-3 was chosen for the installation of diver HVO-12 (x=383870/ y=1006510) (see Fig. 2.4).

The other divers were installed in footpumps in the HVO area (see Fig. 2.5 c and d). The footpumps are often called Vergnet pumps after the inventor M. Vergnet. The footpumps are technically easier to be equipped with divers but they are not found all over the HVO. Four brands of manual pumps are used in Benin: Afridev, Vergnet, India and UPM.

2 Materials and methods

Generally, only 2 types are applied. The Afridev handpump is used in case of deep boreholes (> 40 m depth). For lesser depths the Vergnet footpump is common.



a)

b)

Fig. 2.5: Installation of the automatic data loggers in observation wells (photo a) and footpumps (photo b) with authorisation by the villagers and in cooperation with the technical staff of the beninese water ministry.

The Van Essen diver measures the total pressure of the water column and the atmospheric pressure above it. Therefore it is necessary to know the exact depth of installation and it is necessary to proceed with a barometric compensation.

The atmospheric pressure is registered separately through three barometers (see. Tab. 2.1). The groundwater and the barometric time series are calibrated in the Van Essen Instruments software Logger Data Manager 3.0.4.

Tab. 2.1: Locations and status of the barometers. The barometers were not installed in the boreholes for reasons of space and prevention of disturbing influences.

Barometer	Serial N° ¹	Location	X (UTM)	Y (UTM)	Altitude [m asl]	Starting date
BM-1	56315	SRH Parakou	458756	1033700	381.26	12/04/2004
BM-2	56316	SRH Djougou	354026	1073366	443.53	19/04/2004
BM-3	56317	IMPETUS Dogué	383093	1006441	331.32	20/04/2004

¹The serial numbers are engraved on the barometer itself.

The registration interval is 3 hours what allows to register drawdown and recovery during the whole day's time. This interval was chosen as compromise between storage and energy supply what will keep the divers functional until 2008. All twelve divers were installed in borewells. The filter depth of ten borewells lies in the bedrock aquifer, one piezometer (HVO-12) penetrates the regolith aquifer only. The diver HVO-5 who was not mentioned above was installed in an observation well in Savé and is thus not relevant for the study in the HVO.

Additionally the Van Essen diver registers the water temperature. Temperature in all boreholes stays rather constant for the whole measuring period.

Most of the data time series are almost complete. Some gaps occur when the diver is torn from the borehole. This may happen during the regular inspection and repairing of footpumps. When one of the boreholes is opened the diver automatically changes its position. Any deviation from the usual hydrograph is easily seen and underlined normally by a change of temperature.

The diver at Dogué (HVO-12) was lifted by someone during the rainy season and stayed without contact to the water table.

Another influence on the water table measurements is the regular pumping at footpumps which are used for water supply in villages. Usually the women start to look for water in the early morning hours, around 6:00 am. The water table is lowered for several meters during the day and starts to recover as early as the night falls (around 7:00 pm). It is in consent with the technical advisor of the SEau Parakou C. Zunino (DANIDA) that the groundwater table at 5:00 am is fully recovered. The 5:00 am measurements are separated for the groundwater hydrographs (see Chapter 4).

The last reading of most of the divers in the field was accomplished in February 2007 (with exception of the lost data loggers HVO-7 and HVO-10; the borehole of HVO-2 was closed and not accessible by this field mission).

Tab. 2.2: Locations and status of the data loggers.

Diver ¹	Serial N ^o 2	Location	X (UTM)	Y (UTM)	Altitude ³ [m asl]	Site	Diver depth ⁴ [m bgl]	Barometer	Start	End	Status
HVO-1	44112	Fô-Bouré	438723	1116084	351.42	Piezometer	21.34	BM-2	01.05.2004	-	running
HVO-2	31358	Bariénou	365564	1074180	420.73	Footpump	19.87	BM-2	01.05.2004	-	running
HVO-3	45864	Komiguéa	459224	1045697	368.8	Piezometer	21.39	BM-1	01.05.2004	-	running
HVO-4 ⁵	45866	Bori	438147	1078043	325.73	Footpump	23.30	BM-1	17.10.2004	-	running
HVO-6	45872	Warika	466115	1075122	381.89	Footpump	21.10	BM-1	01.05.2004	-	running
HVO-7 ⁶	45873	Tchérou	345041	1011265	398.17	Footpump	24.66	BM-2	01.05.2004	22.02.2006	lost
HVO-8	45879	CEG Djoujou	350850	1072648	453.89	Footpump	27.63	BM-2	01.05.2004	-	running
HVO-9	45882	Bétérou	421959	1017223	265.86	Piezometer	27.00	BM-1	01.05.2004	-	running
HVO-10 ⁷	44096	Tchatchou	450988	1010770	348.9	Piezometer	17.40	BM-1	01.05.2004	20.04.2005	stolen
HVO-11	44105	CEG Kolokondé	368231	1094900	432.87	Footpump	25.56	BM-2	01.05.2004	-	running
HVO-12 ⁸	44111	Dogué	383870	1006510	317.08	Piezometer	7.52	BM-3	01.05.2004	29.03.2005	replaced

1 These abbreviations are used in this thesis. HVO-5 is installed in a footpump at Dassa outside the HVO.

2 The serial numbers are engraved on the diver itself.

3 The altitude was derived from the SRTM DEM.

4 The depth of installation of the diver in meters below the ground level.

5 The diver HVO-4 was first installed at Anoum (West of Djougou). Finally a more central location was found in Bori.

6-7 Both divers were either lost or stolen from their placement.

8 This data set shows a great data gap in the rainy season due to a manipulation from outsiders. The diver was later replaced into an observation well at Savé.

2.4 Sampling campaigns and sampling procedure

2.4.1 Field campaigns

Groundwater samples (in total 244) from 116 wells and 128 pumps distributed throughout the Upper Ouémé catchment were collected during 5 sampling campaigns:

- late March 2004 (end of dry season),
- end of September 2004 (end of rainy season),
- late March 2005 (end of dry season),
- late September 2005 (end of rainy season)
- beginning of March 2006 (end of dry season).

Systematically, water samples were collected at times when the dug wells and pumps are used to receive fresh groundwater, although the higher turbidity is a disadvantage. In general all water was filtered (macro and micro-filter), acidified and stored in a fridge to later be analysed in the hydrochemistry laboratory of the Geological Institute of the University of Bonn, Germany. Bicarbonate was determined by titration on-site.

In total 244 groundwater samples were taken. Many descriptive methods to treat this data amount were used to compare samples either from one season or from several seasons. Sample names were given as follows:

Sample name: D05 - W - BDOG-2
Structure: a b c d
a = Season: D = dry season
R = wet season
b = Year: years of the sampling campaign
04, 05, 06 respectively 2004, 2005, 2006
c = Type: type of the water point
W = well
F = footpump
H = handpump
P = observation borehole
d = Location: original name of the GPS-waypoint, in general an abbreviation of the location's name.

The sample locations (Fig. 2.6) are in general found in the vicinity of settlements where water points are developed for public support. The majority of the settlements are grouped along roads and trails and in general on crests. Thus the choice of samples cannot be representative for the whole of the HVO area. The concentration of the sample points along roads has a limiting factor to all interpolation procedures. Great areas remain unknown. Results from regionalisation for these data sparse areas have to be critically regarded.

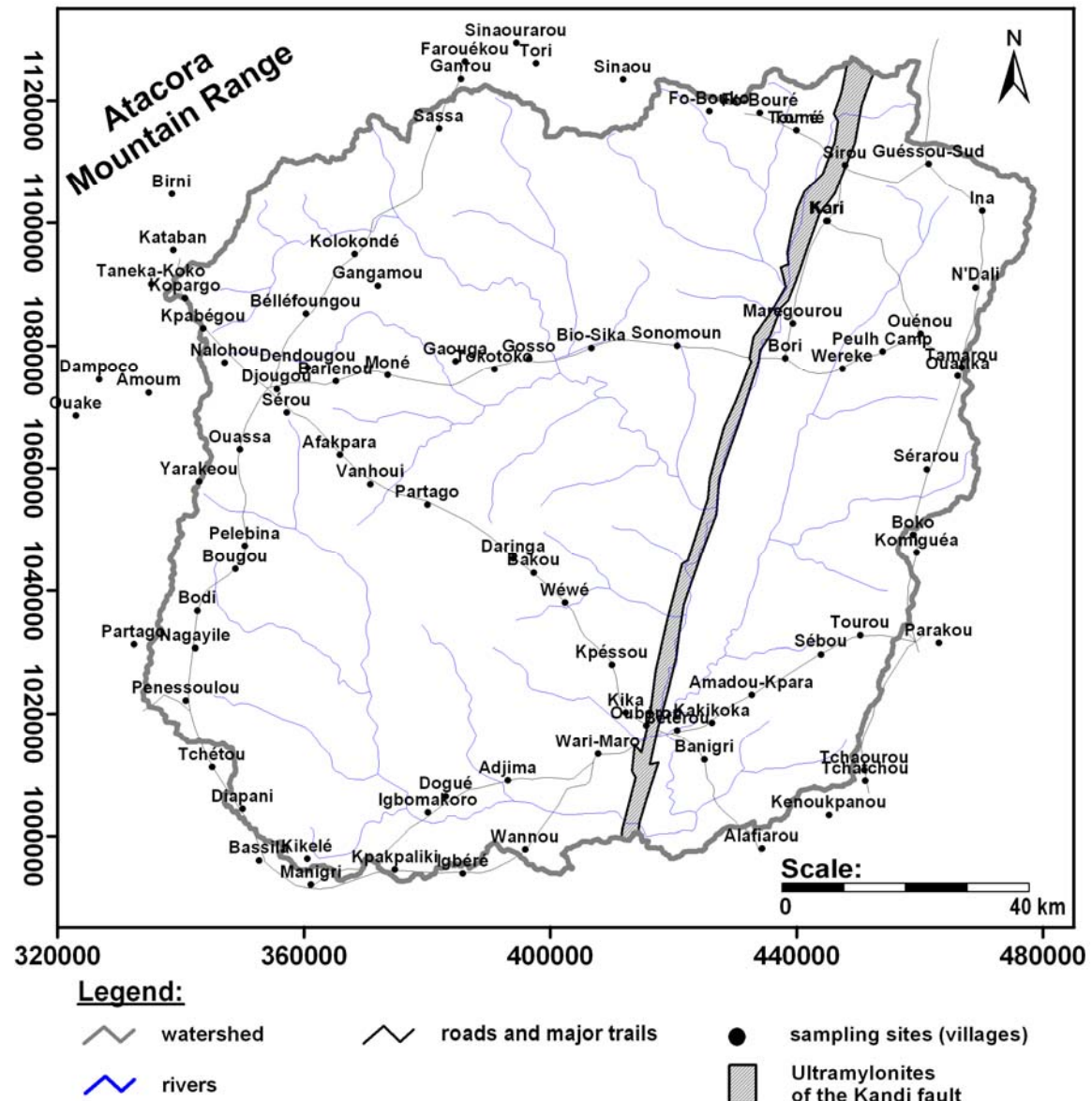


Fig. 2.6: Distribution of the sampling locations in the HVO (Projection: UTM, Zone 31P, WGS 84). For the corresponding abbreviations see Annex 1.

In addition some samples were taken for reference from surface waters (lakes and rivers) and from freshly captured precipitation. They were treated in the same way like the groundwater samples.

2.4.2 Physico-chemical parameters

Physico-chemical parameters were measured on-site for each sampling using a portable logger device of WTW (WTW Multi 350i). The data logger is equipped with different kinds of exchangeable electrodes (see Tab. 2.3).

Tab. 2.3: Electrode types used with the WTW data logger on-site during the field campaigns in the Upper Ouémé area.

Electrode	Measured parameters	Units	Error
Sentix® 41	pH	[]	± 0.01
	temperature	[°C]	
TetraCon® 325	electric conductivity	[µS/cm ²]	± 1%
	temperature	[°C]	
Sentix® ORP	redox potential	[mV]	see Chapter 5.1.4
Cellox® 325	oxygen content	[mg/l]	± 0.5%
	oxygen saturation	[%]	

The electrodes were regularly controlled and recalibrated. Each electrode has to be kept for as much time in the sampled water as is necessary to obtain stable values.

The oxygen electrode was very sensible to calibration errors and to the environmental conditions like heat and humidity. For some campaigns (rainy season 2004 and dry season 2005) the results were finally skipped because they showed illogical deviations from the general oxygen values of groundwater in this area.

2.4.3 Hydrochemical parameters

Major cations (Na⁺, K⁺, Sr²⁺, Mg²⁺ and Ca²⁺) as well as heavy metals (Fe²⁺, Mn²⁺, As²⁺, Cd²⁺, Co²⁺, Pb²⁺, Ni²⁺) were determined by atomic absorption spectroscopy, AAS. Samples were stabilised in the field by adding some drops of Suprapur (96%) HNO₃.

Samples from the first campaign 2004 were analysed with the PERKIN-ELMER (AAS 3030 B) atom absorption spectrometer, the later samplings were analysed with the AAnalyst 700 of PerkinElmer Inc.

Major anions (SO₄²⁻, Cl⁻, F⁻, NO₃⁻, NO₂⁻ and Br⁻) were analysed from not stabilised samples in a Shimadzu ion chromatograph HIC-6A.

Samples for measuring concentrations of complex ions (NH₄⁺, H₃PO₄, H₂SiO₄) were stabilised in the field by Suprapur H₂SO₄ (2-3 drops) and determined by photometric analysis with the Dr. Lange UV-VIS spectrophotometer CADAS.

Alkalinity was analysed on-site by potentiometric titration with 0.01 N HCl (TITRISOL) standardised with Na₂CO₃. Bicarbonate (HCO₃⁻) was then calculated by the equivalent of consumed acid multiplied by the atom mass.

An overview about sampling techniques and detection limits is given in Tab. 2.4 and respectively in Tab. 2.5.

2 Materials and methods

Tab. 2.4: Sample methods and materials in an overview.

Parameter	Amount	Recipient	Preparation	Method
SO ₄ ²⁻ , Cl ⁻ , F ⁻ , NO ₃ ⁻ , NO ₂ ⁻ , Br ⁻	20 ml	Polyethylene	microfiltered (0.45 µm)	IC
H ₃ PO ₄	100 ml	Polyethylene	microfiltered (0.45 µm) conserved with H ₂ SO ₄	photometry
NH ₄ ⁺ , H ₂ SiO ₄	100 ml	Polyethylene	microfiltered (0.45 µm) conserved with H ₂ SO ₄	photometry
Na ⁺ , K ⁺ , Mg ²⁺ , Ca ²⁺ , Fe ²⁺ , Mn ²⁺ , heavy metals	100 ml	Polyethylene	microfiltered (0.45 µm) conserved with HNO ₃	AAS
HCO ₃ ⁻	250 ml	Polyethylene	filtered	Titration with 0.01 N HCl

Tab. 2.5: Detection limits of analysed constituents.

Cations	Detection limit [mg/l]	Anions	Detection limit [mg/l]
Na ⁺	0.01	Cl ⁻	0.2
K ⁺	0.04	F ⁻	0.2
NH ₄ ⁺	0.1	Br ⁻	0.5
Mg ²⁺	0.002	SO ₄ ²⁻	0.5
Ca ²⁺	0.09	NO ₃ ⁻	0.5
Sr ²⁺	0.025	NO ₂ ⁻	0.5
Fe ²⁺	0.001	PO ₄ ³⁻	0.2
Mn ²⁺	0.002		

The results from the hydrochemical analyses were checked for errors and inconsistency. The most appropriate method is the calculation of the balance error of the ion charge (DVWK 1999):

$$\Delta_{\%} = \frac{\sum C_{eq} (cat.) - \sum C_{eq} (an.)}{0.5 \left[\sum C_{eq} (cat.) + \sum C_{eq} (an.) \right]} \cdot 100 \quad (\text{Eq. 2.2})$$

C_{eq} = equivalent concentration of the sum of all anions (an.) or of all cations (cat.)

HÖLTING (1996) and MATTHESS (1994) propose an acceptable error of +/- 5% for low charged water (< 2 C_{eq}) and +/- 2% for a total concentration of > 2 C_{eq} . The average concentration of groundwater in the HVO varies from 2 to 20 C_{eq} . However, the above mentioned error limits were developed for laboratory conditions in central Europe. Due to the difficult sampling and storing conditions in Benin it was agreed on acceptable error limits of +/- 15%. All samples which are not fulfilling this criterion are skipped from the data set. The distribution of error values is skewed to the right. Positive errors belong to too high cations concentrations or inversely to smaller anion concentrations. The laboratory analyses were repeated in some cases and no significant changes in the measured values were detected. The most probable source for errors is the bicarbonate titration in the field. Hence the ml-scale on the titration device is relatively coarse, errors

of +/- 1 ml may occur. The proof correction of the error balances in regard to this measuring deviation in bicarbonate often adjusted the ion balance to an acceptable level. Three not adjustable samples had to be discarded.

2.5 Environmental isotope analysis

2.5.1 Deuterium and oxygen-18

The natural occurring stable isotopes deuterium (^2H) and oxygen-18 (^{18}O) have been extensively used to examine the hydrological cycle. They are considered as ideal tracers for analysing the movement of water (MAZOR 1997). The stable isotopes provide information about recharge and discharge processes and they can be used to estimate the water exchange between aquifers or between surface water and groundwater.

The isotopic composition of water is expressed by means of an international standard with regard to its deviation from the isotopic composition of ocean water. The standard is commonly called the Vienna Standard Mean Ocean Water (VSMOW). The samples isotope relationship is notated as deviation in ‰ from the VSMOW. The values are calculated by the following two equations respectively.

$$\delta^2 H[\text{‰}] = \frac{(^2 H/H)_{\text{Sample}} - (^2 H/H)_{\text{VSMOW}}}{(^2 H/H)_{\text{VSMOW}}} \times 1000 \quad (\text{Eq. 2.3})$$

$$\delta^{18} O[\text{‰}] = \frac{(^{18} O/^{16} O)_{\text{Sample}} - (^{18} O/^{16} O)_{\text{VSMOW}}}{(^{18} O/^{16} O)_{\text{VSMOW}}} \times 1000 \quad (\text{Eq. 2.4})$$

δ = relative deviation in ‰

$\text{Ratio}_{\text{Sample}}$ = isotope content of the sample

$\text{Ratio}_{\text{VSMOW}}$ = isotope content of the Standard Mean Ocean Water

The relationship between ^2H and ^{18}O in global precipitation is called the global meteoric water line (GMWL). It is represented by the formula:

$$\delta^2 H = 8 \delta^{18} O + d \quad (\text{Eq. 2.5})$$

d = deuterium excess

By comparing worldwide precipitation data, a global mean value of it had been determined by CRAIG (1961):

$$\delta^2 H = 8 \delta^{18} O + 10 \quad (\text{Eq. 2.6})$$

The meteoric line is normally plotted in a $\delta^2\text{H} - \delta^{18}\text{O}$ diagram (Fig. 2.7), where it is used as a reference line for any subsequent analysis of groundwater samples.

Meteoric water lines derived from local sampling may show derivations from the GMWL. The shift along the deuterium-axis is called d-excess. The d-excess characterises the isotope composition of the evaporated moisture. The precipitation derived from an air mass into which the re-evaporated moisture is admixed is indicated by a large d-excess (DANSGAARD 1964). A similar effect occurs with the evaporated flux from surface waters

2 Materials and methods

(GAT et al. 1994). Isotopic depletion of air masses is as well possible by intercepting of water caught on leaves of trees, but dense forest areas are needed (oral comm. Y. TRAVIS, LHA 2005). Transpired flux of moisture does not perturb the d-value of the atmospheric moisture (SALATI et al. 1979).

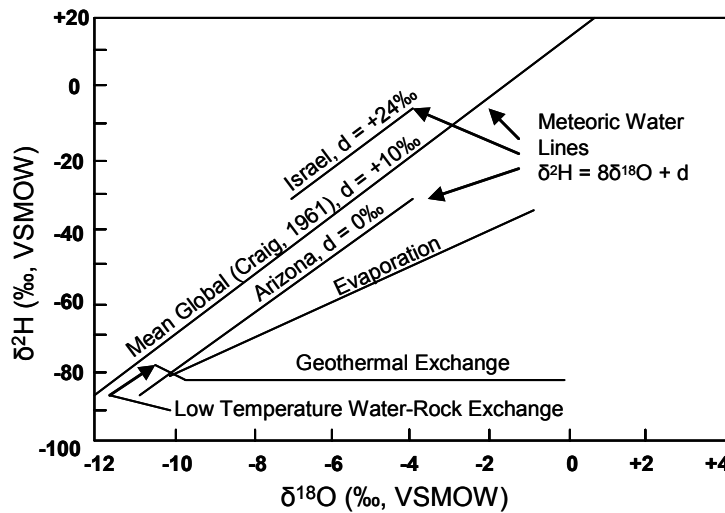


Fig. 2.7: Examples of the relationship between $\delta^2\text{H}$ and $\delta^{18}\text{O}$ in meteoric water, evaporating water and water in interactions with rock (taken from COOK and HERCZEG 2000).

$\delta^{18}\text{O}$ values are widely variable from one rainfall event to another. Mainly due to seasonal changes of ocean temperatures and air-sea interaction conditions and as well short-term events like storms. It appears that such variations vary within a range of up to $\pm 10\text{‰}$ in $\delta^{18}\text{O}$ values (GAT 1996).

Fractionation processes influence the isotope values in rain water and consequently the composition of groundwater. Fractionation results from the difference in the physical characteristics between the different weighted water isotopes. The following effects are important:

- **Temperature effect:** Temperature is the major parameter that determines the isotopic values of precipitation. By rising temperatures the precipitation becomes enriched by deuterium and oxygen-18, respectively vapour gets depleted by these stable isotopes. In regions with summer and winter precipitation the isotopic differences are represented by seasonal variations (HOEFS 1997; MAZOR 1997; COOK and HERCZEG 2000).
- **Continental effect:** The values of the isotopic ratio decrease moving away from the ocean. Travelling towards inland, water is gradually precipitated by condensation. The condensation of “heavy” water molecules is more effective. The residual air masses become gradually “lighter” in composition (MAZOR 1997; COOK and HERCZEG 2000).
- **Altitude effect:** As clouds are lifted up at orographic obstacles, the heavy isotopes are depleted and the residual precipitation gets isotopically lighter (HOEFS 1997; MAZOR 1997; COOK and HERCZEG 2000).
- **Amount effect:** Intense rainfall has a lower ^2H and ^{18}O content. Evaporation increases these contents in little rainfalls more than in big rainfall events (MAZOR 1997; COOK and HERCZEG 2000).

2.5.2 Tritium

The age of groundwater can be determined with tritium (see COOK and HERCZEG 2000; KENDALL and MCDONNELL 1998; MOSER and RAUERT 1980), which is the radioactive isotope of hydrogen. Tritium (^3H or T) has a half-life of 12.3 years (Fig. 2.8). It is created naturally by cosmic radiation. Tritium oxidizes immediately after its formation to water molecules. It is depleted from the atmosphere through precipitation. Tritium content is usually expressed in TU (tritium units). 1 TU represents a tritium concentration of $^3\text{H}/^1\text{H}=10^{-18}$ and has an activity concentration of 0.119 Bq/kg.

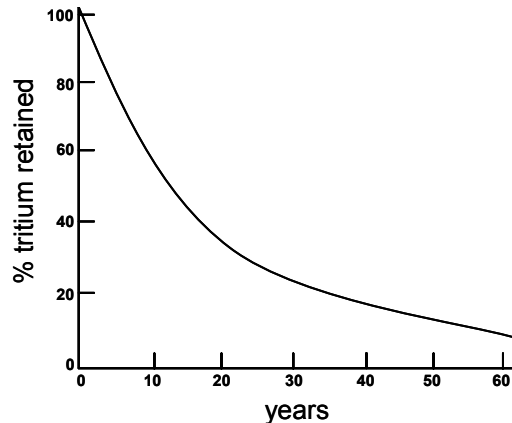


Fig. 2.8: Slope of the radioactive decay curve of Tritium (from KENDALL and MCDONNELL 1998).

Tritium values in precipitation vary because of slow atmospheric balancing. Following effects have influence on the tritium concentration in the atmosphere and thus in the precipitation (MAZOR 1997). Seasonal variations occur, with peaks in spring/summer and minimum in winter (temperate climate belt of the Northern Hemisphere). In summer the exchange of air masses in the atmosphere reaches its maximum. Tritium gets enriched above the continental troposphere and increases with distance from the oceans. Also the seasonal fluctuations are getting stronger with the distance from the oceans. In correlation to the geographic latitude the concentration of tritium tends to increase with distance from the Equator towards the poles.

Age determination is based on the measurement of the tritium concentration in the sample. The initial tritium concentration is taken from the local atmosphere. In the saturated zone, the water is separated from the atmosphere's input and the tritium content diminishes by its radioactive decay. HÖLTING (1996) proposed the comparison of the tritium concentration of the samples with the isotope content of precipitation by the following formula Eq. 2.7.

$$A = \frac{T}{\ln 2} \cdot \ln \frac{C_0}{C_{Sample}} \quad (\text{Eq. 2.7})$$

A = age

τ = half life (12.43 years)

C_0 = initial concentration

C_{Sample} = sample concentration

2 Materials and methods

The enrichment of the atmosphere by man-made tritium from nuclear bomb tests allowed using tritium to find the year of original recharge within the last 50 years. Nowadays the tritium concentration in the atmosphere and in precipitation is almost back to natural concentrations (MAZOR 1997).

2.5.3 Sampling and Analysis

All isotopes were analysed by W. Stichler from the Institute of Groundwater Ecology at the GSF in Neuherberg, Stable isotopes were sampled with 20 ml plastic bottles. Water samples were taken from dug wells and boreholes (see Annex 1). Since November 2004 rainfalls are regularly collected at three stations in the HVO area (villages of Dogué, Sérrou and Parakou). Information about stable isotope contents in precipitation in surrounding countries is taken from the GNIP data base (IAEA/WMO 2000).

Stable isotopes relationships were determined by Mass Spectrometry (MS). Deuterium analysis is done on hydrogen obtained through high-temperature reduction of water on metal or by hydrogen equilibrated with water using a Pt catalyst. Oxygene-18 analyses are done with equilibrated carbon dioxide. The precision of measurement is approximately 0.15‰ for $\delta^{18}\text{O}$ and 1‰ for $\delta^2\text{H}$ (oral comm. P. TRIMBORN, GSF 2005).

Water for tritium analysis was collected in 500 ml plastic bottles. Contact of the sampled water with air or light was avoided. Samples were taken from precipitation, lakes, rivers and groundwater from open dug wells and pumped boreholes. The analyses were done by liquid scintillation counting (LSC) method with a detection limit is 0.1 TU (FACHVERBAND FÜR STRAHLENSCHUTZ 1995).

2.6 Regionalisation through geostatistical methods

The regional interpretation of results from local field findings and sampling points demands information about the space in between the investigated zones. A couple of geostatistical methods were developed to interpolate point data (KITANIDIS 1997). The most popular estimation method is “kriging” (SCHAFMEISTER 1999), originally developed for estimations in the mining sector (AKIN and SIEMES 1988). The advantages of kriging against other interpolation methods are (after SCHAFMEISTER 1999):

- Kriging is the best linear unbiased estimator (B.L.U.E.).
- Knowledge about the spatial distribution of the variables can be applied to the choice of a suitable variogram.
- The individual spatial distribution of the measurements is respected in the interpolation net.
- The accuracy of the results is given for each estimated point.

The use of kriging and other interpolation methods is limited by the following restrictions:

- Different data sources have to be homogenised and to be processed in the same format.
- All measurements must be from the same origin, e. g. the same aquifer.
- Time dependant data, e.g. groundwater table height, should be measured in a limited period to produce a consistent picture.

The HVO shows wide areas which are not accessible for sampling, either there are no roads or there are no settlements at all. Sampling and drilling for boreholes is normally realised close to villages. As consequence wide spaces between the villages practically rest undiscovered.

Hydrochemical concentrations and hydraulic conductivities show a lognormal distribution because of the non-negativity of the original data. Before kriging the data has to be lognormalised (KITANIDIS 1997).

However, kriging tends to produce values closer to the median value of data points. Local features like sinks or peaks may thus be hidden. For each kriging procedure an experimental variogram was produced with the geostatistical software Surfer[®]. The variogram is a quantitative descriptive statistic that represents graphically the characteristics of the spatial continuity of a data set (i.e. roughness).

Different variogram models can be chosen in adaptation to the data pairs. Preferably exponential or logarithmic models were chosen in this thesis. Anisotropy of the data distribution was in general not regarded. Local anisotropy caused by local fracture zones is less important on the regional scale.

In the modelling software FEFLOW[®] regionalisation is achieved through polygons that can be designed arbitrarily or imported from other data sets. Spatial information (hydraulic parameters of geological units; recharge) or results from local measurements (e.g. pumping test) are transferred to polygon areas. The polygon value is then copied to all elemental nodes lying inside the polygon.

2.7 Groundwater flow model

2.7.1 General concepts of numerical modelling

Computer models are popular tools in groundwater management to evaluate the impact of any intervention on groundwater quantity and quality. In regard to the complex nature of subterranean flow, the first approach is to develop a conclusive conceptual model of the hydrogeological processes within the model area. The second step is the transfer of this model into a mathematical model. The mathematical description is made by partially differential equations (PDE) and auxiliary conditions (ISTOK 1989) which are solved by numerical methods. With modern microcomputers it is possible to solve these equations in convenient time.

The governing partial differential equations used in mathematical models for groundwater flow is the Laplace's equation for the saturated steady state condition (Eq. 2.8) and its derivative for the saturated transient state (Eq. 2.9):

$$\frac{\partial}{\partial x} \left(K_x \frac{\partial h}{\partial x} \right) + \frac{\partial}{\partial y} \left(K_y \frac{\partial h}{\partial y} \right) + \frac{\partial}{\partial z} \left(K_z \frac{\partial h}{\partial z} \right) = 0 \quad (\text{Eq. 2.8})$$

$$\frac{\partial}{\partial x} \left(K_x \frac{\partial h}{\partial x} \right) + \frac{\partial}{\partial y} \left(K_y \frac{\partial h}{\partial y} \right) + \frac{\partial}{\partial z} \left(K_z \frac{\partial h}{\partial z} \right) = S_s \frac{\partial h}{\partial t} \quad (\text{Eq. 2.9})$$

where,

t = time;

h = hydraulic head;

Q = volumetric flux per unit volume representing source/sink terms;

K_x, K_y, K_z = hydraulic conductivity along the x, y, z axes which are assumed to be parallel to the major axes of hydraulic conductivity;

S_s = specific storage defined as the volume of water released from storage per unit change in head per unit volume of porous material.

Laplace's equations combine Darcy's law and the continuity equation into a single second-order partial differential equation (WANG and ANDERSON 1982). In mathematical correct terms it would be necessary to write the hydraulic conductivity K with negative signs to express that the flow is directed to the bottom. However, any conceptual mathematical description of a complex natural environment is necessarily a greatly simplified description of the reality (ISTOK 1989). The auxiliary conditions mentioned above are the initial conditions and the boundary conditions (MARSAL 1989). They will be highlighted in Chapter 8.

There exist several types of numerical models. The most popular among them are the:

- Finite difference models (FD models) and,
- Finite element models (FE models).

The first visual difference among these two methods is the way to discretise the model environment (see Fig. 2.9).

The FD method applies a regular element mesh with constant cell sizes. It works best for rectangular or prismatic aquifers of uniform composition (ISTOK 1989). Its advantage is the easily understandable mathematical formulations and its solving algorithms. Especially the MODFLOW code developed by the USGS is popular and frequently applied (see e.g. CHIANG and KINZELBACH 2000; HARBAUGH et al. 2000).

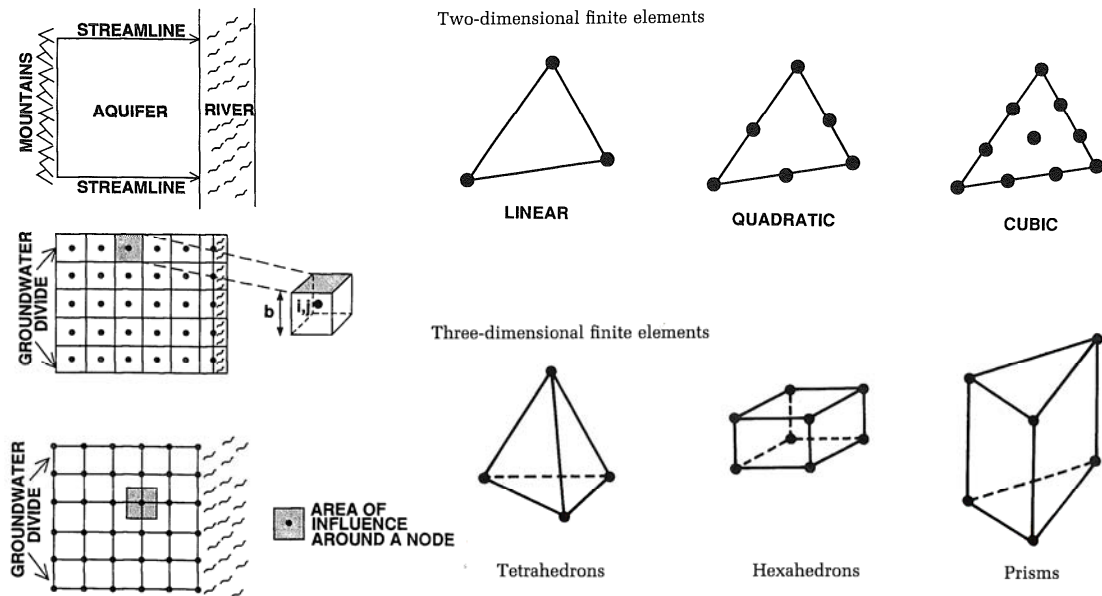


Fig. 2.9: Some types of elements, based on the finite difference concept and the finite element concept (from ANDERSON and WOESSNER 1994).

The method of finite elements is principally used in mechanical engineering. Since the late 1970s applications for groundwater modelling were developed (WANG and ANDERSON 1982). Although the FE method is based on the same basic PDEs like FD it uses other mathematical ways to solve them.

In the FE method the defined domain (solution) of a PDE is replaced by a discrete matrix of points and each ablation by a differential expression which refers to the point matrix (MARSAL 1989). The domain can be structured in partial areas of almost arbitrary size. These parts are called the *finite elements*. The shape of finite elements is mathematically flexible but most of the available software programs use the classic triangular shape (Fig. 2.10).

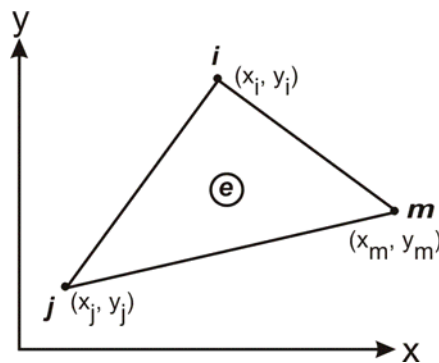


Fig. 2.10: The typical triangular element e. Each node is labelled (i, j, m) counter-clockwise and has its own x, y-coordinates marked by the specific footnote (modified from WANG and ANDERSON 1982).

2 Materials and methods

The nodes of each element are very important. Mathematically, the element nodes are the homologues of the matrix points of the FD method (MARSAL 1989).

The typical solution method for the FE method is Galerkin's method (e.g. WANG and ANDERSON 1982; ISTOK 1989). Galerkin uses the weighted residual principle to govern the PDEs for groundwater flow. It is an integral formulation which leads to a set of algebraic equations that can be solved for values in the field variable (piezometric head h and/or the concentration C for transport problems) at each node in the mesh.

First an approximate solution to the boundary or initial value problem is defined. When this approximate solution is introduced into the governing differential equation, an error the so-called residual occurs at each point in the problem domain. Then the weighted average of the residuals for each node in the finite element mesh is forced to equal zero.

Despite more complex mathematics and more computational demand the FE method offers some advantages especially for more complex models (ISTOK 1989):

1. Irregular or curved aquifer boundaries, anisotropic and heterogeneous aquifer properties and sloping soil and rock layers can easily be incorporated into the numerical model by refining the mesh and individual positioning of the elements.
2. The accuracy of solutions to groundwater flow and transport problems is very good.
3. Solutions of transport models are generally more accurate than solutions obtained by the FD method.
4. The numerical stability of equation solvers is generally better than in FD models.

2.7.2 Modelling standards of FEFLOW[®]

The regional groundwater modelling was realised with the modelling software package FEFLOW[®] 5.1 from WASY GmbH. Details about actual versions and computing capabilities can be found on the WASY homepage⁵. DIERSCH (2005) gives detailed information about all numerical methods, solvers and mathematical methods available in this software. FEFLOW[®] was chosen for different reasons:

- Due to the great size of the HVO some areas stay unknown while at other locations detailed research was made. The flexible mesh refinement due to the FE method is an advantage in this case. New field investigations (e.g. pumping tests) may deliver new information about some areas. The FE mesh can easily be modified and thus may develop together with the ongoing field research. However, practical modelling needs a number of reruns to find out optimal design variables (DIERSCH 2005).
- All spatial data can be produced externally by GIS software. The FEFLOW[®] interface accepts a great variety of data formats as input and also as output. Exchange of data is therefore easy and fast-forward.
- Besides the many features of FEFLOW[®] there is a wide choice between different equation solvers and adaptive alternative numerical solutions. Accelerated solvers allow the solution of large problems with either great number of nodes or complex structures (DIERSCH 2005).

All input data can be handled on element level. Transient and intransient data can be entered. Point data can be assigned to the mesh by geostatistical interpolation techniques such as Akima, kriging or inverse distance or simpler by polygon joining

⁵ URL: <http://www.wasy.de/english/index.html>

techniques (DIERSCH 2005). For the purpose of this thesis the direct transfer of data from GIS-shape-files on the FE nodes, the so-called joining method, was preferred. This method was applied for as many parameters as for e.g. recharge, conductivity and storage coefficient.

Topographic data was preprocessed with the geostatistical software SURFER. A variogram and a regular data grid were produced and then imported into FEFLOW[®] by a nearest neighbour function to assure that nodal elevation values are as close as possible to their real distribution.

The regional groundwater recharge is calculated externally. FEFLOW[®] does not contain a special recharge or evapotranspiration package as it is used for example in MODFLOW applications (e.g. HARBOUGH et al. 2000).

The regional model is realised in 3D with three layers. For the model saturated conditions with an unconfined and movable upper surface were selected. The automatic time-step control by the 2nd order predictor-corrector scheme “forward Adam-Bashforth” was chosen with an initial time step length of 0.001 d. Time step control was given without any further constraints. The Galerkin-based finite element method for unstructured meshes and the iterative PCG (preconditioned conjugate gradient) solver are chosen. Other convergence and error criteria are set to default.

3. Case study: The Upper Ouémé river catchment

3.1 Overall geography

The Republic of Benin is a West African country bordering the Bight of Benin between Nigeria and Togo. To the North Benin has a border with Burkina-Faso and Niger. The country extends from the North to the South almost 750 km. The width of the territory is about 110 km in the South and increases to a maximal extent of 325 km in the northern part. In total the country covers a terrestrial area of around 110,620 km².

The study area lies in the central northern part of the Republic of Benin. It is limited by the hydrological catchment borders of the Upper Ouémé valley (see Fig. 3.1). The so called HVO is more or less of orthogonal shape with a length of around 150 km in each direction. The HVO covers an area of approximately 14,500 km². The rough limits of the HVO are given in UTM coordinates (Projection: UTM, Zone N31, WGS 1984):

Upper left corner: 322912 / 985656

Lower right corner: 488925 / 1131280

Benin became a French colony in 1872. After its independence in 1960 it was first called the Republic of Dahomey and changed its name finally in 1974. During an act of restructuring in 1999 a partition in 12 departments subdivided in 77 communes was realised. Almost half of the HVO area to the West belongs to the Donga department while the other half is of the Borgou. Only a small stripe of the Atacora department covers the North of the HVO.

The population of Benin in 2007 is around 8,078,314 with an estimated birth rate of 2.674% (CIA 2007). The economy of Benin is dependent on subsistence agriculture, cotton production, and regional trade. The population density is between 10 and 150 inhabitants per km². In some regions the land is intensively cultivated, but there are also forest reserves where land use is prohibited.

Mineral resources are very limited despite some ornamental stones (BGR 2000) and an inactive gold mine at Perma in the Atacora mountain range. Other natural resources are timber and small offshore oil deposits (still unexploited).

Artificial irrigation is not applied to increase productivity (LARES 1999). CIA (2007) reported that in 2003 only 120 km² were irrigated. The central part of the Ouémé catchment around the cities of Dassa, Savé, Ouesse, Tchaourou, Savalou, Banté and Bassila attracts increasingly new settlers. The new settlers belong mainly to ethnics of northern Benin. This agricultural colonisation will have its impact on the future land use patterns (LARES 1999).

The major settlements in the study area are Parakou (200,000 inhabitants) and Djougou (50,000 inhabitants). While Parakou centre lies in the East outside the HVO, some of its peripheral townships are situated within. Djougou is an ancient caravan stop and therefore has some of the oldest settlements within the study area. The rest of the HVO is of rural character. Most of the settlements are placed along the major roads. Great areas of the HVO are apparently still not explored for new settlements, e.g. the area within the triangle Djougou-Bassila-Bétérou or the areas in between the major roads in the Northern part.

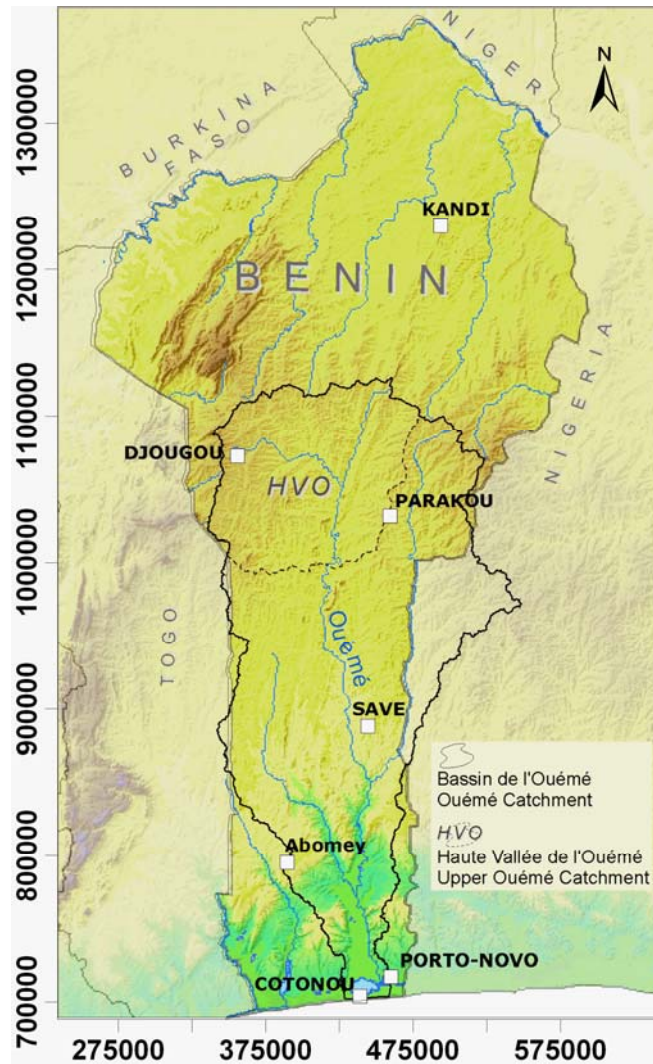


Fig. 3.1: Overview Benin – Extension of the Ouémé catchment and location of the Upper Ouémé catchment (modified from IMPETUS map pool⁶; Projection: UTM, Zone 31P, WGS 84).

3.2 Water policy

Like many other developing countries Benin is trying to adapt poverty reduction strategies and to achieve the millennium development goals (MDG⁷) until 2015 (DGH 2005).

Apart from strategies for a better access to alimentation, education and sanitation facilities, the MDGs include a program for an improved access to clean water.

The public water supply sector in Benin is divided into rural and urban water supply. Urban water supply is the domain of the national public water provider SONEB and concerns all settlements with more than 10,000 inhabitants. The DGEau is responsible for the rural water supply what means all settlements with less than the before mentioned 10,000 inhabitants.

⁶URL: http://www.impetus.uni-koeln.de/impetus.php?show=De_Pr_In

⁷ <http://www.unesco.org/bsp/eng/mdg.htm>

3 Case study: The Upper Ouémé river catchment

The Beninese government wants to improve water supply for the rural population who counts approximately 6,000,000 people (87.5% of the total population of Benin). Only 35% of them have access to potable water (DGH 2005).

In 2015 the population of Benin will have increased from 6,855,541 (in 2002) to 11,000,000 (DGH 2005). If the current conditions remain (see paragraph above), it is estimated that the rural population will reach 8.000.000 in 2015 with an increasing demand for water.

The annual production of potable water for cities by the SONEB amounts to 29,158,820 m³ in 2003 (SBEE 2003) of which 93.2% came from groundwater exploitation. The remaining 6.8% were taken from reservoirs like the storage lakes in Parakou, Djougou and Savalou. Compared with 27,830,119 m³ in 2002 this represents a growth of 4.77% (SBEE 2003). Groundwater exploitation in the rural parts of the HVO is still based on manual pumping. A typical pumped borehole in rural Africa is designed for producing 0.2 l/s to serve 250 persons within a radius 500 m (ROBINS et al. 2002).

3.3 Climate

The climate of Benin is mainly subtropical. It changes from humid in the South to semiarid in the North. The daytime temperature in the study area varies from about 20°C at the middle of the wet season to over 35°C at the peak of the dry zone. The mean annual precipitation is 1147 mm (see Fig. 3.2).

The average air humidity calculated for the period of 1960-1990 varies (respectively rainy season – dry season) between the initial values 96 to 51% and 80 to 39% in the final stage (LE BARBÉ et al. 1993). Evaporation and transpiration constitute major components of the hydrological cycle. On average they consume at least 70 to 80% of all the rainfall (BESTO 1987). In central and northern Benin one rainy season from May to September takes place due to the West African Monsoon. The start of the rain is related to the influence of the Southwest maritime air masses, which blow across the Atlantic Ocean (see Fig. 3.3). At the end of the wet season, the Harmattan, a dry and dusty wind comes from the North and pushes back the intertropical front. It affects mostly the North of Benin but may also leave the South under a thick cloak of dust. Its influence is mostly felt from December to February. The notably dry season is marked by little or no rain at all.

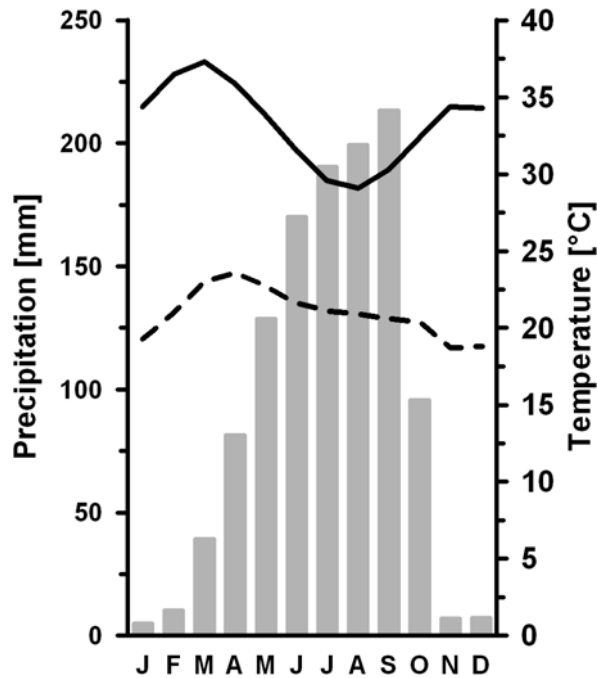


Fig. 3.2: Climate chart of Parakou. Data from 1961 to 2005 (with the permission of M. Gosset, IRD 2007). Long-term average amount of precipitation: 1147 mm. Average temperature: 27.1 °C. Black solid line = maximum temperatures; black dashed line = minimum temperatures.

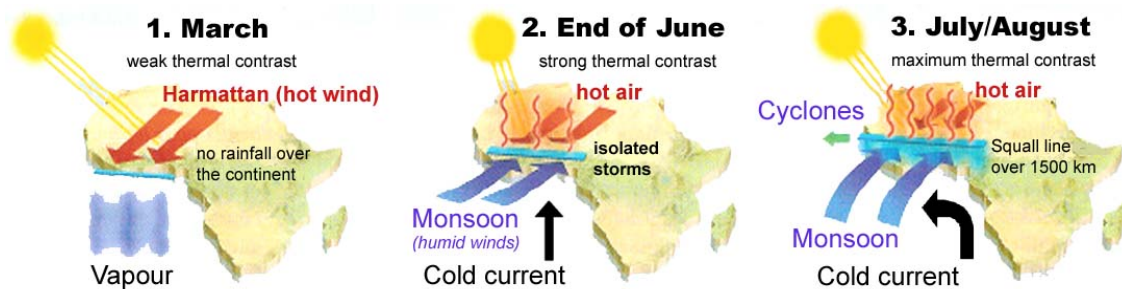


Fig. 3.3: 1- During the boreal winter less intense solar rays reach West Africa. This causes a weak thermal contrast. While the ocean is heated by relatively hot currents humidifying the air above the ocean, the continent suffers under the dry Harmattan. 2- In June the sun heats up the continent while a cold ocean current hits the coast. The heated air above the continent mounts and draws in colder and humid air from the sea. This is the beginning of the monsoon. 3- One month later the condensation of the vapour, caused by the first rainfalls, liberates considerable amounts of energy. Thus the air gets heated up and rises. Meanwhile the soil is cooling. Storms occur and form squall lines of considerable length (modified from JUBELIN 2006).

The rainfall during the wet season over the Sahel zone is the result of both the development of squall lines along the tropical convergence zone (ITCZ) and monsoon rains from the Atlantic Ocean (FONTES et al. 1993). The monsoon rains are typically warm and generated at low altitudes. In the present climate they are restricted to latitudes below 10°N. The content of heavier isotopes of such rains is relatively high. North of the Monsoon zone rainfall occurs when humid air masses, associated with the monsoon, rise over dense, dry Saharan air masses along the ITCZ.

3 Case study: The Upper Ouémé river catchment

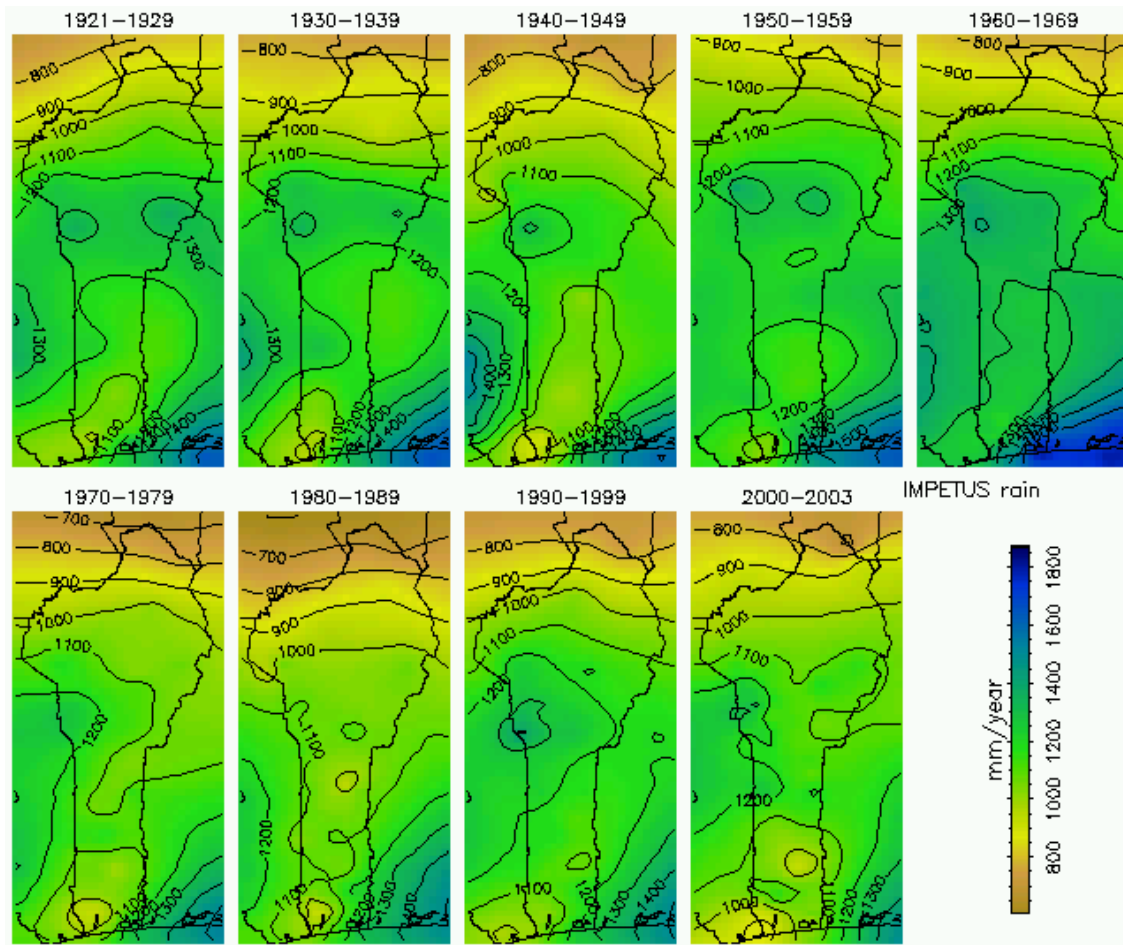


Fig. 3.4: Rainfall distribution modelled for different decades. Yearly precipitation in the HVO varies from 1100 to 1300 mm/a. The North is in general slightly drier than the South (taken from M. Diederich, IMPETUS 2006).

As stated in Chapter 1, West Africa suffers an extended drought period since the 1970s. From Fig. 3.4 it can be seen that the 1200 mm isohyet was found in the North of the HVO until the 1960s. Since then the 1200 isohyet has retreated to the Southwest. The observation of precipitations at Parakou and Djougou reveals their constantly declining amount (Fig. 3.5).

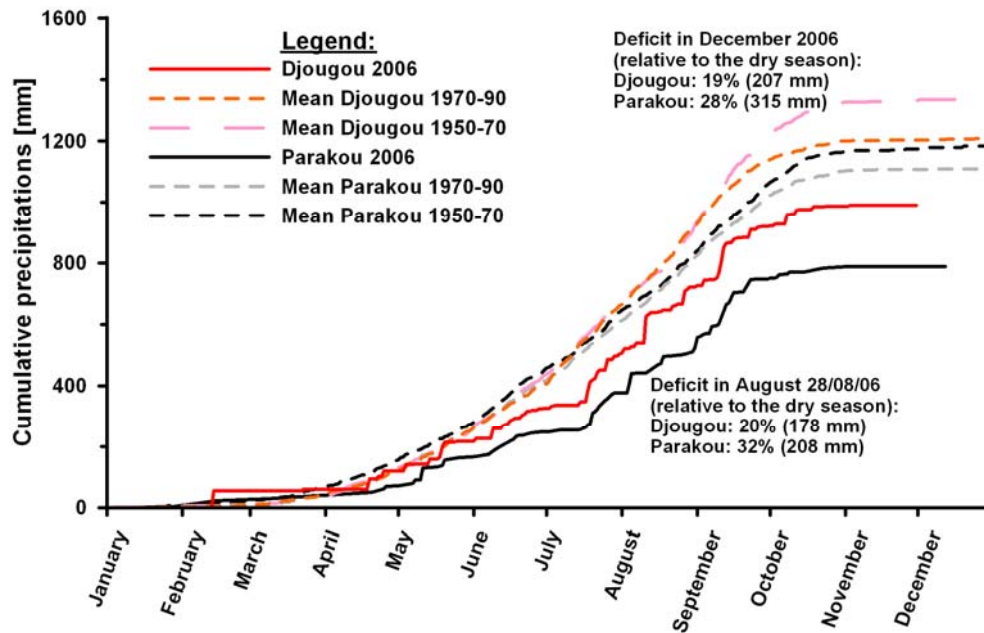


Fig. 3.5: Comparison of historical precipitation measurements with observations in 2006 for the two gauging stations (ASECNA) at Parakou and Djougou. The measured daily precipitation is accumulated over the year. Data ranges from 1950 to 2006 (with permission of M. Gosset, IRD 2007).

3.4 Geomorphology and hydrography

The study area is a peneplain with a gently undulating surface. The general elevation within the HVO ranges from around 250 to 500 m asl (Fig. 3.6). Slopes dip with 1-10%. The ground level rises towards the Atacora mountain chain in the Northwest of the study area. The highest peak within the Atacora attains 658 m (Mont Sokbaro). In the area around Djougou and the northwestern part of the HVO the ground level is about 400-500 m asl.

The view on the 50 times exaggerated elevations in both cross-sections in Fig. 3.7 shows that the detailed surface elevations are negligible compared to the horizontal extent of the HVO. Numerous subvalleys form subcatchments with local flow characteristics but the distance between the local water sheds is too small to allow any detailed hydrogeological description for each of these catchments.

The highest point in the study area is an inselberg SW of Bétérou, next to the village of Wari-Marou (620 m, Fig. 3.8). Inselbergs are “*prominent steep-sided hills of solid rock, rising abruptly from a plain of low relief*” (WHITTOW 1984). In the study area they are formed by intrusive igneous rock bodies which are harder than the surrounding material and thus resisted erosion. In the HVO they may rise up to 300 m over the surface elevation.

Surface runoff may result in considerable weathering pockets around the inselberg. These pockets are filled with deposits of coarse and fine debris and may bear interesting water resources (MCFARLANE et al. 1992b and BARKER and HERBERT 1992).

3 Case study: The Upper Ouémé river catchment

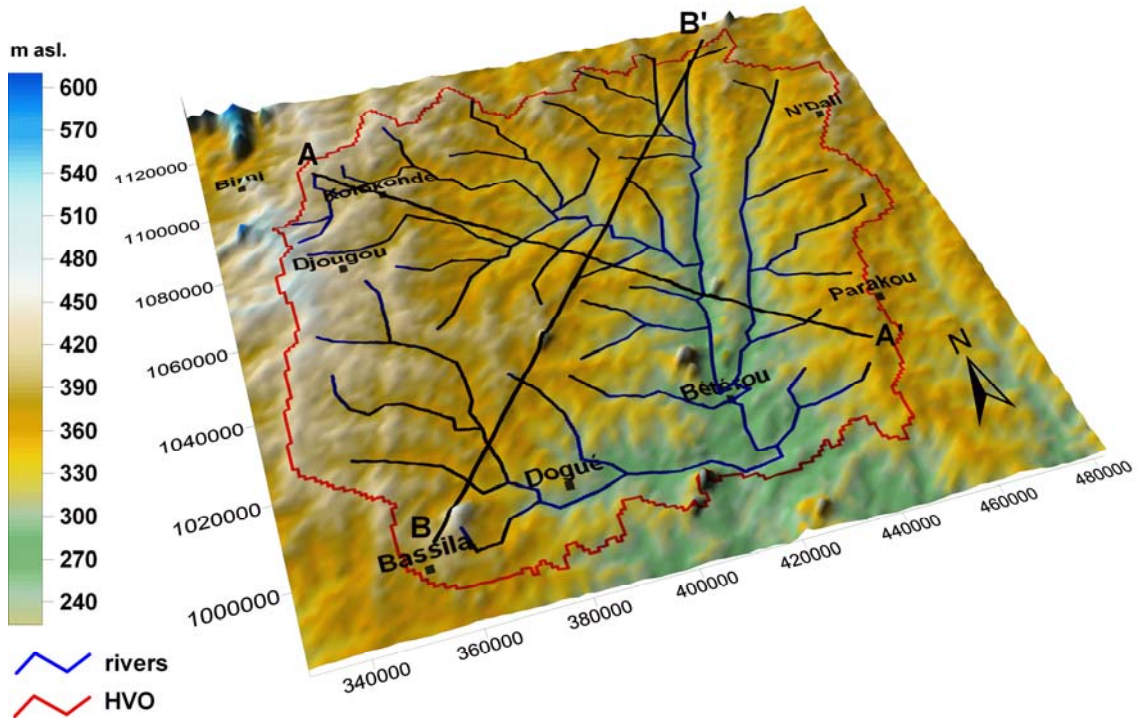


Fig. 3.6: Perspective view on the DEM of the HVO. Z-level is 20 times exaggerated (horizontal scale 1:10.000; vertical scale 1:500). The morphologic valleys contain seasonal rivers. (Projection: UTM, Zone 31P, WGS 84). Cross sections A-A' and B-B' are traced by black lines are represented in Fig. 3.7.

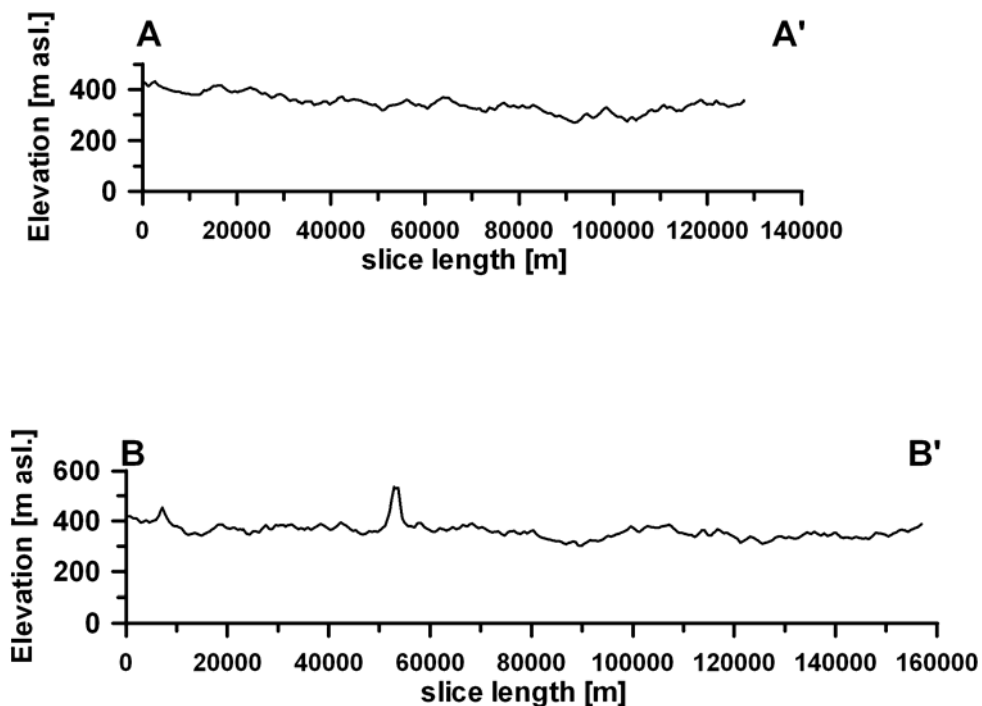


Fig. 3.7: Cross sections A-A' and B-B,' as shown in Fig. 3.6. The z-level is 50 times exaggerated.

Along the trace of the Kandi fault quartzitic crests (Qz) occur. Especially in the northern half of the study area they form a characteristic N-S striking elevation of 30-50 m above surface level. The Kandi fault is as shear fault accompanied at both sides by zones of increased stress due to shear movements. This zone of weakness has promoted erosion

3 Case study: The Upper Ouémé river catchment

but also intrusions of plutonic rock bodies (Wari-Maró massive). Originally of granite or monzodiorite origin, these plutonites were strongly metamorphosed and show gneissic and migmatitic structures. In the southern half of the HVO the trace of the Kandi fault is accompanied by a number of inselbergs.



Fig. 3.8: Inselberg of Wari-Maró (620 m asl) at UTM 407864/1013209.

Characteristic morphological elements of the Upper Ouémé catchment are inland-valleys, also known as *bas-fonds* in Francophone countries or *dambos* in English respectively (FASS 2004). In this text the term *bas-fond* is preferred, as it is commonly used in Benin. *Bas-fonds* constitute the main drainage system in the African surfaces (WRIGHT 1992).

Bas-fonds are seasonally waterlogged bottomlands (MCFARLANE 1987a). They appear in the study area as seasonally swampy, mainly grass-covered depressions of either linear or circular shape. *Bas-fonds* accumulate thick clay deposits in their centre. These deposits are mainly made up by smectite, which indicates stagnant high water levels (Fig. 3.9, MCFARLANE 1992a). Most of the runoff water accumulated in the *bas-fonds* is evapotranspired while a minor part may run off downstream. The evapotranspiration of already concentrated solutions favours the precipitation of smectite which is enriched in *bas-fonds* clays (MCFARLANE 1987a).

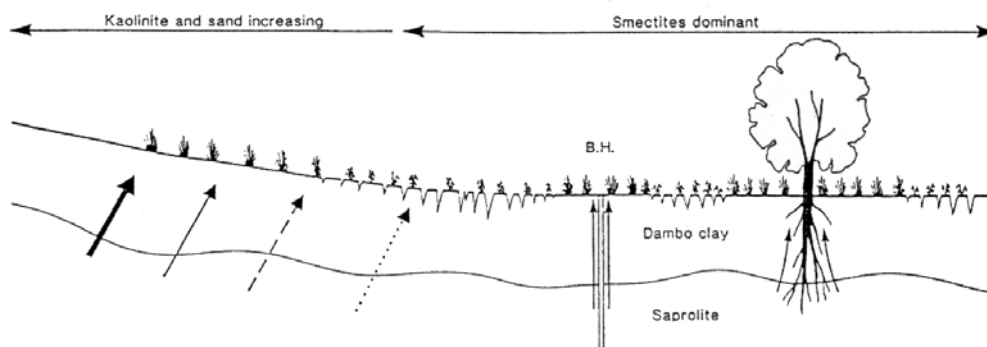


Fig. 3.9: Schematic transect of a *bas-fond* to show the distribution of dominant clay minerals. B.H. = Borehole (taken from MCFARLANE 1987a).

Bas-fonds in the HVO are of varying size but often less than 100 m in diameter. More than 700 *bas-fonds*, or similar structures, were counted in the HVO (oral comm. S. GIERTZ, IMPETUS 2006). Many different models for the evolution of *bas-fonds* are discussed (VON DER HEYDEN 2003; MCFARLANE 1987a and 1992a). However, it seems

3 Case study: The Upper Ouémé river catchment

that the occurrence of bas-fonds is often connected to river systems above densely fractured systems (MCFARLANE 1987a). The groundwater in the bas-fonds clays is connected to the regolith aquifer.

Due to the strong precipitation and the inundation of the bas-fonds during the rainy season most of the settlements are grounded on crests and hilltops. Perennial surface water and groundwater resources are predominantly found downhill.

The biggest rivers in Benin are the Ouémé, the Pendjari, the Niger and the Mono whereby the Ouémé is the most important river. Its complete catchment covers almost half of the countries area.

The source of the Ouémé is within the Monts Taneka in the Northwest of the study area at an altitude of 550 m above sea level. The river's total course is 415 km when it enters the Lake Nokoué close to Cotonou. The slope of its thalweg on the first 12 km is 12.5 m/km. Then the slope progressively declines to attain in average 1.5 to 0.38 m/km (LE BARBÉ et al. 1993). The mean annual discharge of the Ouémé for the period 1951-1995 (SOGREAH and SCET 1997) at Bétérou was 51.14 m³/s, 100 m³/s at Savé and 200 m³/s at Bonou station.

The basin has a total surface of approximately 49,540 km² until it joins the river Zou. In the South of this joining point the limits of the catchment are less easy detectable due to a flat surface (slope = 0.13 m/km) and regular inundations during the rainy season. The Ouémé river bed is in the HVO rocky and shows no terraces or alluvium. Larger tributaries have sandy beds and are accompanied by riverine forests. Smaller tributaries show hydromorphic clay deposits with herbal plant cover and can be associated with bas-fonds (ZOUMARO 1998). The water divide between the Niger and the Ouémé basin roughly follows the 10th parallel, north of the Nikki-Djougou dorsal line (FAURE and VOLKOFF 1997). The northern part of the Ouémé catchment is known as the Upper Ouémé catchment (Fig. 3.1). The main tributaries of the Upper Ouémé are the Téro in the Southwest and the Donga in the Northwest. In the northern part of the HVO people often refer to the Ouémé as the Affon. In this text the term Ouémé is exclusively used.



Fig. 3.10: Riverbed of the Ouémé in the northern half of the HVO during the dry season (UTM 407864/1013209).

3 Case study: The Upper Ouémé river catchment

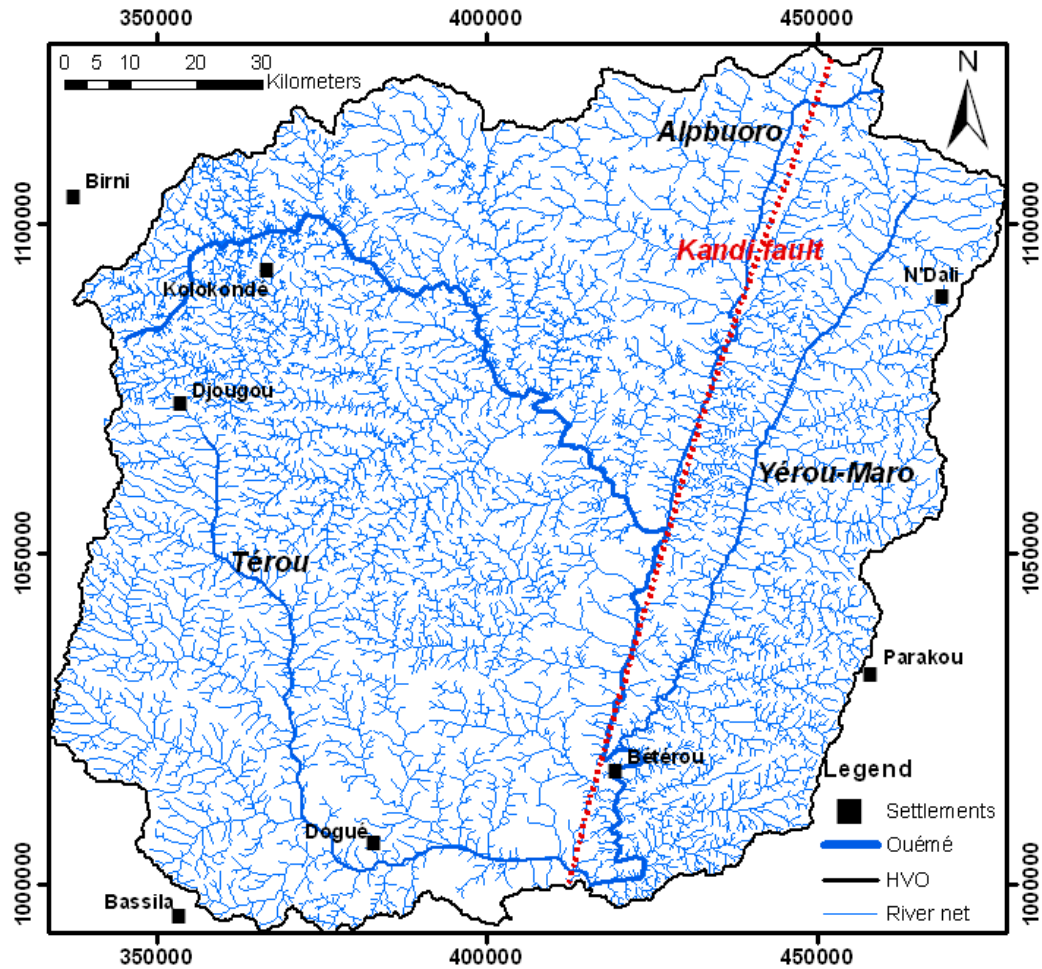


Fig. 3.11: Hydrographic net of the rivers in the HVO catchment. The striking of the Kandi fault has a strong impact on the course of rivers in the East of the HVO. (Projection: UTM, Zone 31P, WGS 84).

Within the catchment the hydrographical net (Fig. 3.11) is quite dense, but during the dry season almost all rivers dry up leaving stagnant puddles and swampy area in the riverbed (Fig. 3.10). Remaining water holes are called “marigot” in Francophone West Africa. For local people without access to wells or other water points the marigots are the only water source during the dry season.

The course of rivers is in general alleged by the direction of fractures and fault zones. The flow net of the Upper Ouémé catchment has been derived from the DEM. The results were compared to general flow patterns on crystalline basement in West Africa given by CEFIGRE (1990).

Most of the rivers show the change between angular and sinuous flow patterns. However, it seems that on this rather rough scale of investigation the angular type prevails.

The angular thalweg generally appears where the riverbed follows fractures or fault zones whose course abruptly changes in sharp angles (see Fig. 3.12). The sinuous river courses are controlled by the topography and the weathering surface. Hills with duricrust cover and inselbergs force the river to turn around them (CEFIGRE 1990). This could be helpful for local analysis of subcatchment characteristics.


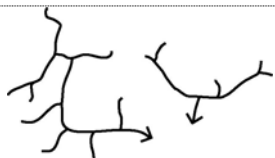
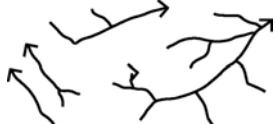
3 Case study: The Upper Ouémé river catchment



Fig. 3.12: a) The water course is controlled by fractures (“en baionette”). b) Sinuosity depends on morphological features and not on fractures (from CEFIGRE 1990).

It is clearly visible that the Kandi fault has a major impact on the river net. The outcrop of the dense and impermeable Kandi quartzite is accompanied to the west and to the east by the almost parallel flowing Alpburo River and Yérou-Marou River. Both rivers join the Ouémé in an area where the Ouémé starts to make sharp angular turns until the Téro River from the West joins it. The course of the river is clearly controlled by the trace of major fractures.

Tab. 3.1: Typical flow net pattern in West Africa taken from CEFIGRE (1990).

Type	Flow net	Observations	Regolith thickness [m]
1		rectangular or askew net with eroded interfluvial; temporary, straight marigots; riverine forests; inselbergs	15-20
2		Gneiss terrain; weak slopes; duricrusts; riverine forests	15-25
3		Schist and granite terrain; all indicators as above may occur to different degree	variable

Tab. 3.1 shows three types of morphological observations which fit to the general flow net and can be identified from satellite images as seen in Fig. 3.13. The descriptions given by CEFIGRE (1990) are in accordance with field observations in the HVO. Type 1 is typically seen along the major rivers in the central part of the study area. Type 2 and 3 share in changing portions the rest of the area in dependence to the geology.

3.5 Vegetation

The HVO is covered mostly by Savannah type vegetation. The Dahomey gap (see Chapter 1.1) is the reason for drier conditions in Benin, and thus, the lack of dense forests. Burning by local people has caused a patchwork of denser and lighter vegetation cover. A bush and grass Savannah is frequent in the northern part of the HVO. Tree Savannah occurs, but with little coverage (20 to 50%). It can be found where duricrusts were eroded and deep soils with much clay remained.

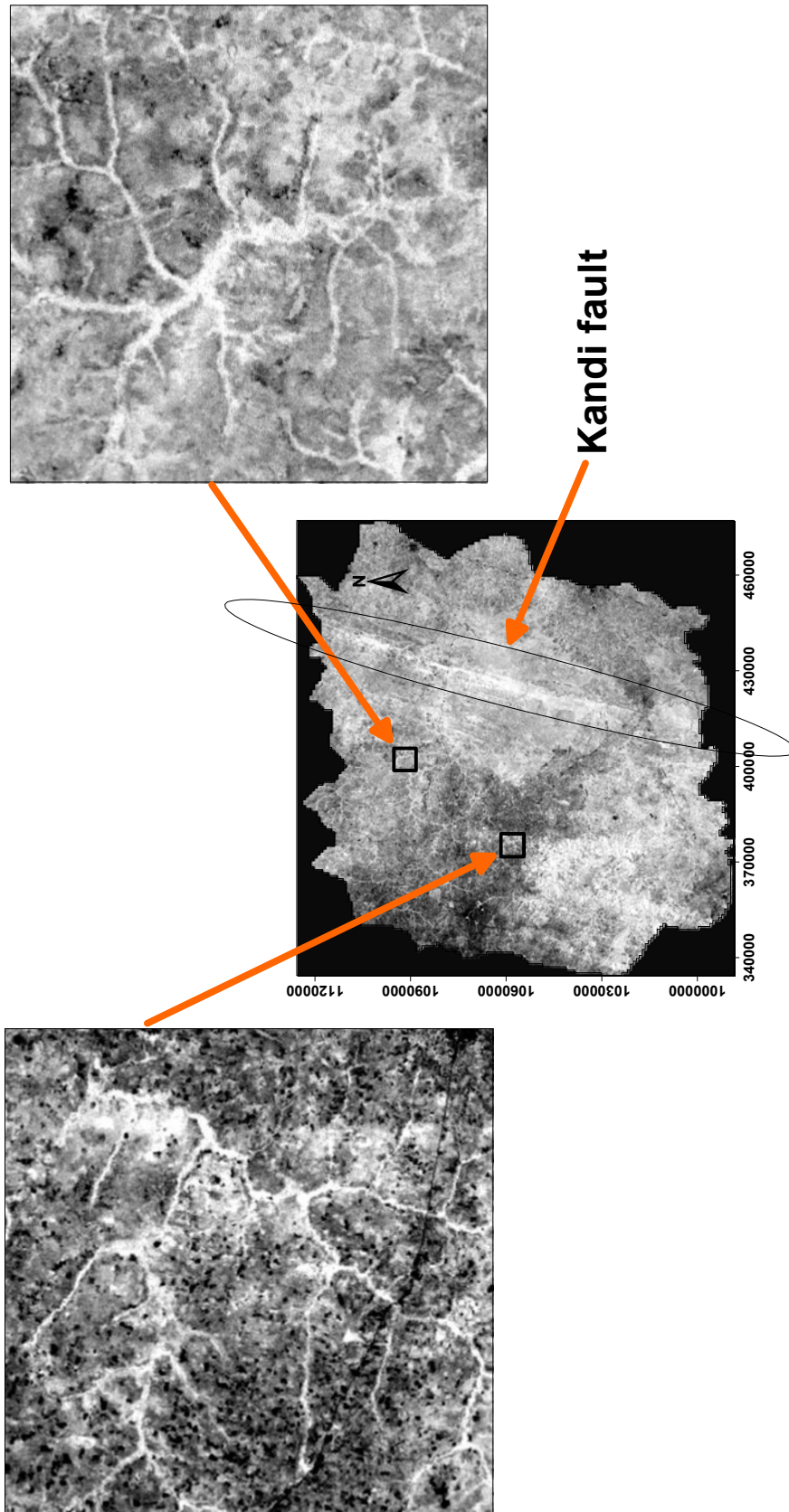


Fig. 3.13: NDVI of Landsat images for the HVO area (period: October 2000). White reflection signifies dense vegetation.

3 Case study: The Upper Ouémé river catchment

Dense woods in the HVO are quite seldom. Only straight along the riverbeds a quite dense forest (tree cover > 80%) may develop (SOGREAH and SCET 1997). In this text it will be referred to them as riverine forests. These riverine forests can easily be identified with a NDVI calculation (Fig. 3.13). A dense stripe of vegetation follows the outcrops of rocks along the Kandi fault from NE to SW. The fault zone is a morphological ridge without settlements and mostly situated in a forest reservation area.

In bas-fonds with strongly changing water tables a purely grass Savannah persists. Dense woods of greater extent occur in the southern half of Benin. The other areas are predominantly covered by bush or grass Savannah with alone standing trees. Deforestation and intense land use have an immediate impact on the persistence of the vegetation cover. Where there is no dense vegetation soils are easily eroded. Duricrusts are formed rather fast on such exposed surfaces (ENGALENC 1978). Accelerated runoff leads to less recharge of the aquifer in the regolith (OMORINBOLA 1982).

Generally, plants are an important guide to groundwater. Certain tree types in the area, e.g. *Tamarindus indica* (Fig. 3.14), are often found in linear constellation and indicate thus the direction of fractures. Water bearing fractures may sustain the vegetation even in dry and drought periods.



Fig. 3.14: A tamarinde tree in the Atacora mountain area. If a second tree is found, there might be high probability to track a fracture along the connecting between the two trees.

3.6 Geology

3.6.1 Regional Geology

The geology of Benin is dominated by the crystalline basement complex of Precambrian age that underlies over 80% of the country. It is a part of the Benino-Nigerian shield and is also called the Dahomeyides. It predominantly consists of granites, granitoid gneisses and gneisses, which are sometimes migmatized. The remaining 20% of Benin are occupied by 4 sediment basins, namely a small part of the Volta basin in the Northwest, the Niger basin in the Northeast, the Kandi basin in the East and the Western Coastal basin (see Fig. 3.15).

Benin is situated at the eastern edge of the West African craton (see Fig. 3.15). In this area some supracrustal belts occur which strike in general NNE-SSW (WRIGHT et al. 1985). The regionally most important is the Togo belt which comprises parts of Ghana, Togo and the Northwest of Benin.

3 Case study: The Upper Ouémé river catchment

These belts are in general dominated by clastic metasediments and plutonic rocks with a high metamorphic grade. Most of the belts are of late Precambrian in age, deformed and metamorphosed during the Pan-African event (500-670 Ma).

In the Nigerian basement area the most common metamorphic grade is the amphibolite facies. To the West granulite facies occurs in Ghana, Togo and in Northwest Benin as well. The supracrustal layers may also show the greenschist facies. Often there are steep metamorphic gradients between basement gneisses and migmatites and supracrustal belts of schist and phyllites (WRIGHT et al. 1985).

The Precambrian Volta Basin which is situated mostly in Ghana and Burkina Faso shares also some area with the Northwest of Benin. The monoclinical flat-lying sedimentary sequences within the Volta Basin are progressively folded and metamorphosed from West to East (AFFATON et al. 1991). The Kandi basin was formed during the Cambro-Silurian. It accumulated Cambrian base conglomerates, Paleozoic sandstones and clays. After reactivation in the Cretaceous sandstones and Post-Eocene and Pre-Quaternary deposits with ferruginous sandstones were concordantly sedimented (ALIDOU et al. 1991). The basin is bounded in the West by a trough induced by the Kandi fault. Several phases of reactivation of the Kandi fault affected the entire basin. The Kandi basin is continued to the Northeast in the Niger basin and leads to the great basin of Iullemeden (BELLION 1987).

The main part of the West African geological formations were affected by multiple orogenic phases which are generally structured in the main directions N-S to NE-SW. These are the main directions of schistosity planes and foliations and sometimes folding axis and faults (WRIGHT et al. 1985, CEFIGRE 1990).

Major fracture and shear zones (NNE-SSW trend) appear to be a feature of the whole region and may be deep-seated lines of structural weakness, repeatedly rejuvenated (WRIGHT et al. 1985).

The superposition of different tectonic phases is shown by the existence of intense fracturing and major faults like the Kandi fault of many kilometres length. In total, the faults are linear and subvertical. The thickness of the fracture zone is variable. Ultramylonite bands may occur which accompany the trace of the faults (CEFIGRE 1990).

Precambrian formations are intensively folded. In the northern central part of Benin the strike of the fold axis is typically NE-SW (SOGREAH and SCET 1999).

In Northwest Benin the external units of the Dahomeyide orogen are represented by the Buem and Atacora structural units. They consist of metasedimentary rocks which are tectonised and metamorphosed equivalents of series from the adjacent Volta Basin (AFFATON et al. 1991).

Folding of the Precambrian formations is strong. Folds appear as long ridges of constant direction and a sometimes strong dip to the East. The striking of fold axis is N-S in the southern areas and NNE-SSW in the North of Benin.

3 Case study: The Upper Ouémé river catchment

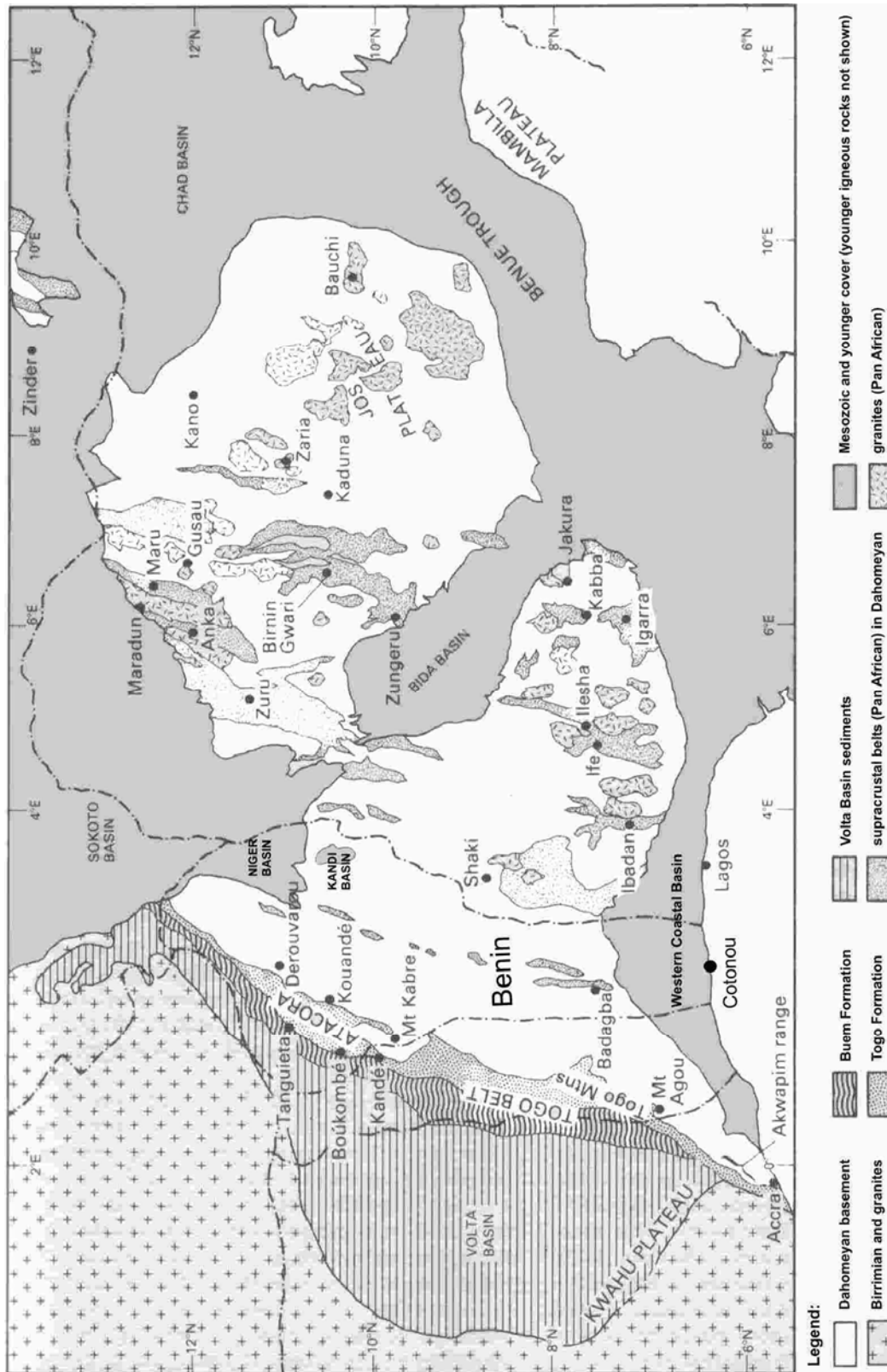


Fig. 3.15: Generalised and simplified map of the main part of the eastern domain of the Pan African of West Africa. Younger igneous rocks are not shown (Geographic projection, WGS 1984; modified from WRIGHT et al. 1985).

Three mayor events of tectonic stress characterize the area of the Dahomeyides and partly all of the West African craton. First of all there is the Pan African orogenesis (500-670 Ma). During the Pan-African orogenesis the West African craton collided with East

3 Case study: The Upper Ouémé river catchment

Saharan cratons and several micro-continental aggregates (TIDJANI et al. 1997). Likewise, the Togo-Benin-Nigeria collided with the eastern borders of the West African craton. Basin sediments of late Proterozoic age in between were thrust towards the West (Fig. 3.16). The so-called Togo belt, of which the Atacora chain is a part of, might be connected to the Pharusian belt of Central Sahara (Fig. 3.17; WRIGHT et al. 1985, TIDJANI et al. 1997).

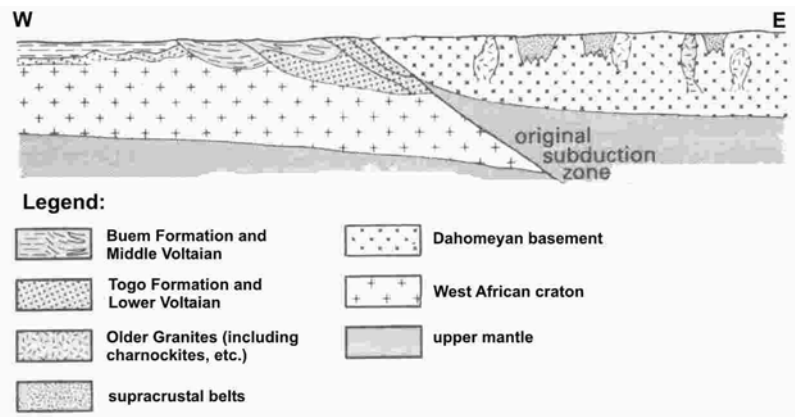


Fig. 3.16: Schematic cross section (not to scale) to illustrate a possible plate tectonic interpretation for the southern part of the eastern Pan African domain in West Africa (from WRIGHT et al. 1985).

During the Triassic and Liassic West Africa experienced a generalised tensional regime accompanied by magmatic events in relation with the opening of the Central Atlantic. Sedimentation was detrital then evaporitic in the rift basins. In the Lower Cretaceous the Western Coastal basin opened. Cretaceous-Tertiary series made up of clays, sands, gravel, ferruginous sandstone overlaid by clayey sands and fluvial deposits makes up most of the basin's sediments (SLANSKY 1962, HOUËSSOU and LANG 1978). Due to rifting the basin is still in subsidence. This subsidence basin strikes from West to East. It is called the Lama depression. It is filled with black clay and covered by marshy vegetation. It extends from Togo to Nigeria (UNITED NATIONS 1988).

At the beginning of the Cenozoic West Africa experienced a warm and humid climate and intense alteration processes. The middle Eocene collision phase between Africa and Europe resulted in slight rework of structures in all basins and surrounding areas and the reactivation of the Kandi fault. The resulting deformation can locally be intense (BELLION 1987).

Many geological features of the pre-rifting phase can be found as well in Brazil (South America), e.g. the Kandi fault. The Kandi fault is a major dislocation and shear zone in Benin. The Kandi fault is a strike-slip-fault whose major axis is marked by ultramylonites which can be traced by satellite images. It strikes NNE-SSW and crosses almost whole Benin. It is the prolongation of a prominent structure which starts at the Algerian Hoggar and reaches into the South of Benin with a general striking of $4^{\circ}50'$. The continuation of the Kandi fault can be found in the Sobral fault of the northeast Brazilian Borborema Complex (see Fig. 3.18, CABY et al. 1981; BRITO NEVES et al. 2001). The sinistral shear movements along the Kandi fault lead to the subsidence of the Kandi basin (ALIDOU 1987). The Kandi fault might be even older than the Pan-African orogenesis and became only reactivated (OBEMINES 1984).

3 Case study: The Upper Ouémé river catchment

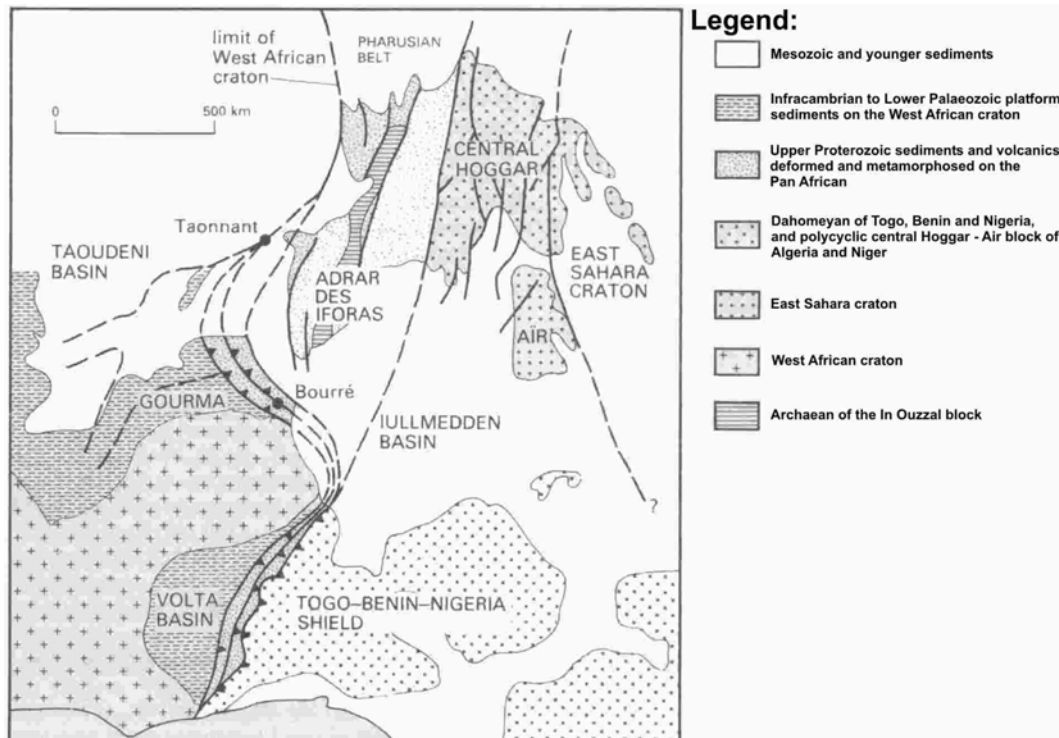


Fig. 3.17: Generalised map to show the extent of correlation between the Precambrian Tuareg shield of the Hoggar and the eastern Pan African domain in the southern part of West Africa (not to scale, from WRIGHT et al. 1985).

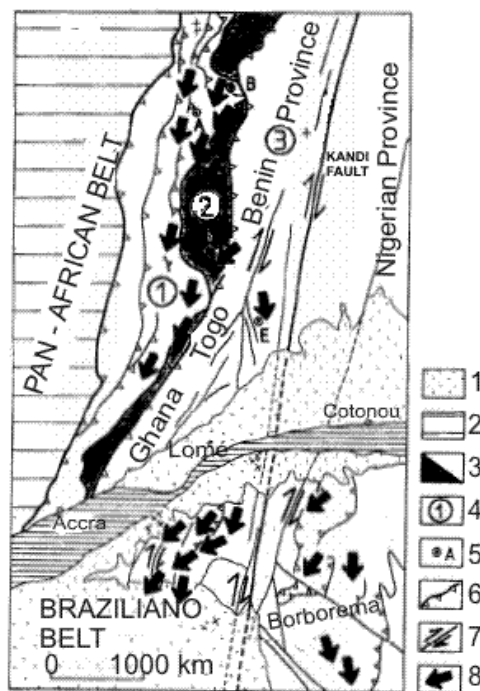


Fig. 3.18: Kinematics of thrusting and wrench faulting in the Pan-African and Brazilian belts of Ghana, Togo and Benin and North eastern Brazil. Legend: 1 = Mesozoic-Cenozoic; 2 = West African craton covered by the Volta Basin; 3 = Pan-African and Brasiliano belts, 4 = external nappes (1), intermediate nappes (2), internal nappes (3); 5 = thermobarometric studies: sampling location in the external nappes (A, B), in the intermediate nappes (C, D) and in the internal nappes (E); 6 = thrust; 7 = dextral transcurrent shear zone; 8 = direction of nappe transport (modified from BRITO NEVES et al. 2001).

3.6.2 Geology of the study area

The Upper Ouémé catchment is situated in central Benin. This area lies completely in the internal parts of the Dahomeyides (Benino-Nigerian shield). The study area is covered by geological maps in a scale of 1:200,000 (Fig. 2.1). The three different legends from these map sheets are homogenised for the HVO in Fig. 3.19. The description of the geological units in the map legends is often imprecise as they include in various cases different metamorphic grades between migmatites and gneisses (e.g. Wé-Wé facies).

It can be seen that in general the geological units strike more or less NE-SW. Eye-catching is the central part of the Upper Ouémé catchment which is marked by an approximately 2-5 km broad band of ultramylonites (Fig. 3.19: umy) along the Kandi fault. The Kandi fault divides the HVO into a western and an eastern part. This central part of the HVO is also called the axis zone (OBEMINES 1984).

In the very East of the HVO lies the migmatite complex of Nikki-Péréré (Fig. 3.19: Mn). The dominating facies is a migmatite with biotite and amphibolite. To the South migmatization is less intense. Thick concordant pegmatites are quite frequent. The major direction of the foliation is N20°-30°E. Between this migmatite complex and the Kandi fault the eastern part gneissic migmatites (Fig. 3.19: Ma) crop out. They belong to the Agramarou group. The orientation of the foliation is mainly N15-20° E, which is the same for the rest of the Ma and for the Mw (Fig. 3.19) facies in the axis zone. The Ma group to the West of the Kandi fault is generally classified as the Sonoumoun-Bariénou facies. Especially this part of Ma is very diverse. Although the metamorphism was quite strong (mesozonal - granulitic) it occurs that in some areas the origin of the gneiss can be identified as greywacke. Higher calcite contents can be distinguished in these rocks (OBEMINES 1984).

The Wé-Wé facies (Fig. 3.19: Mw) appears to be a higher-grade metamorphic part of the Sonoumoun-Bariénou formation and is composed of migmatites and migmatitic granitoids. The quartzites (Fig. 3.19: Qz) which strike along the Kandi fault belong to the Ouémé valley formation. It comprises quartzite, micaschist and gneiss. To the North of Bétérou, the quartzites are folded into a great synclinal structure whose relief is quite pronounced.

In the central North of the HVO the Donga formation (Fig. 3.19: Gdo) appears. This group consists of fine gneiss and biotite-muscovite schist in thin (cm to dm) regularly changing layers. This group has undergone a parametamorphism and is structurally lying on the migmatites of the axis zone. To the western border of the HVO several units appear which represent a series of gneiss of different metamorphic grade. They have in common to be fine grained and thin layered (cm - dm). Leucocratic muscovite rich gneiss (Fig. 3.19: Gd) changes with biotite gneiss (Fig. 3.19: Gy). In some areas appear fine layered quartzites (Fig. 3.19: Qz) sometimes rich in muscovite (Fig. 3.19: Qms).

Intrusive rocks in the HVO are of Pan-African age. Among the intrusions which occur towards the end of the Pan-African orogenesis two types can be distinguished: granites and gabbros (Fig. 3.19: Gb). The granites can be divided into two types of facies:

- porphyric facies (Fig. 3.19: pY)
- fine-grained facies (Fig. 3.19: Y)

3 Case study: The Upper Ouémé river catchment

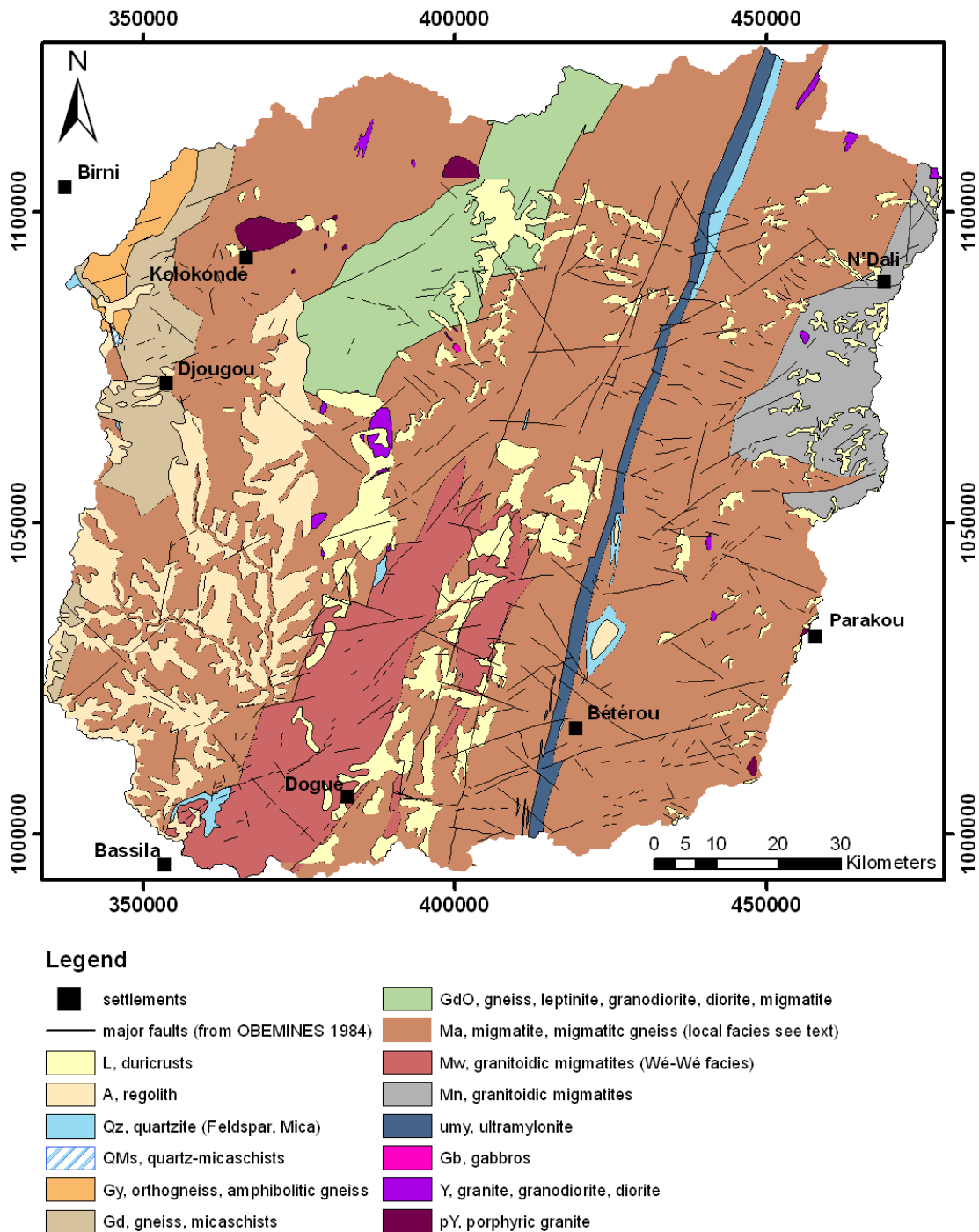


Fig. 3.19: Geological map of the Upper Ouémé catchment. Modified after OBEMINES 1984, 1990 and 1990a (Projection: UTM, Zone 31P, WGS 84). Settlements were chosen for reference.

All granites are in general massive, homogeneous and sometimes planar. The porphyric granites are the most frequent. The granite has medium sized grains and is very heterogeneous with biotite, muscovite and K-feldspar.

The mineralogy of the fine-grained granites is quite the same. All these granites are calcalkaline and leucocrate. Basic intrusions occur only along the Ouémé valley next to the village Affon. These intrusions consist of massive and homogeneous gabbros of green colour.

Pegmatites occur mostly in the axis zone. The migmatites in this area contain numerous dykes. Those are mostly concordant to the foliation of the surrounding rocks. Sometimes they are discordant. Besides quartz and anorthite the pegmatites contain biotite, muscovite sometimes garnet. Additionally tourmaline, apatite and beryllium may occur.

The general orientation of faults in the crystalline basement area of Benin is NNE – SSW (BOUKARI 1985, SOGREA and SCET 1997). The major directions of fracture in the study area are NW – SE and NNW – SSE (FASS 2004).

The occurrences of regolith (A) and duricrusts (L) shown in Fig. 3.19 are taken from the geological map sheet Djougou-Parakou-Nikki from OBEMINES (1984). It is cited that they were originally based on the soil map sheets Djougou (FAURE 1976) and Parakou (DUBROEUCQ 1976).

3.6.3 Regolith formation

The crystalline bedrock is covered by its weathering product – the regolith. TAYLOR and EGGLETON (2001) define regolith as follows: *Regolith is all the continental lithospheric materials above fresh bedrock and including fresh rocks where these are interbedded with or enclosed by unconsolidated or weathered rock materials. Regolith materials can be of an age* (in TAYLOR and EGGLETON 2001).

This definition includes the whole of weathering products lying on the fresh bedrock. The regolith as a whole includes from its top to its bottom the soil zone (often with red soils and ferruginous horizons), the saprolite and the saprock (see Fig. 3.20). The saprock represents the transition zone between bedrock and regolith with a thickness of several meters. This description fits the findings in Benin and is the reason for the complex hydraulic conditions encountered there.

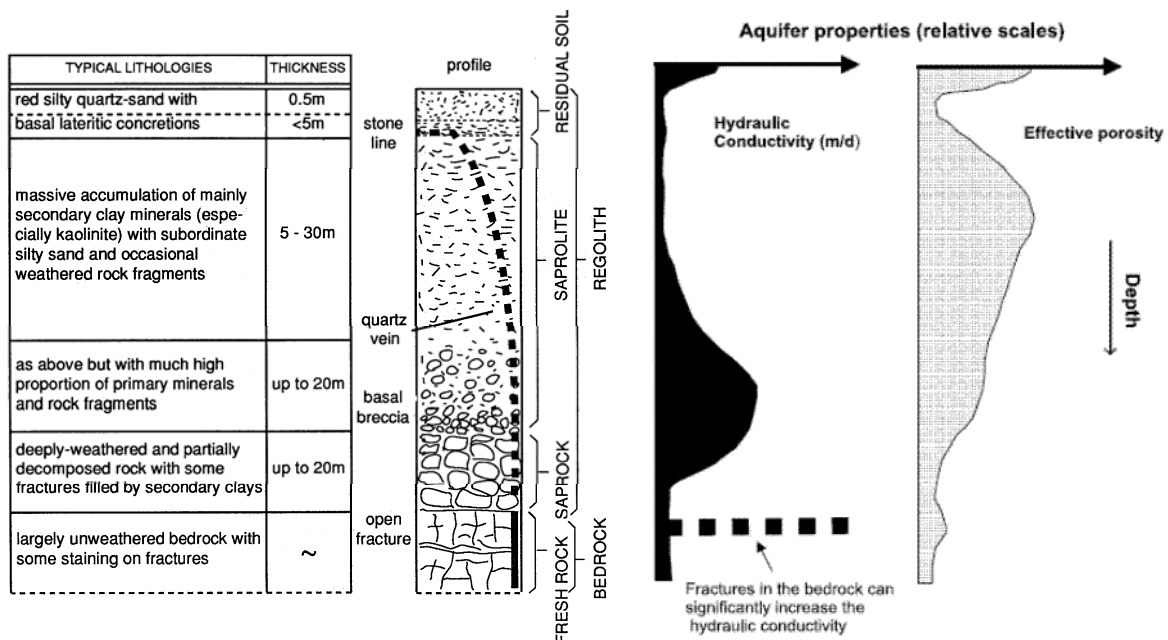


Fig. 3.20: Conceptual hydrogeological model of the crystalline basement aquifers in Africa (modified from CHILTON and FOSTER 1993).

The weathering of the crystalline formations in West Africa is the result of a physico-chemical disaggregation of the magmatic and metamorphic rocks due to 2 climatic factors: water and temperature. The ferralitic weathering of the bedrock occurs in several

3 Case study: The Upper Ouémé river catchment

steps. First the outcropping surface of the original bedrock is transformed. New minerals like sericite, chlorite and serpentine form preferably at the exposed rock surface, e.g. at fissures and fractures (ENGALENC 1978).

While the fresh bedrock is fractured the saprock is additionally strongly fissured. It is a zone of more or less disconnected boulders with a diffuse net of water ways. The texture is lost but still the general structure of the rock is preserved. Weathering is the strongest where fissures intersect. Propagation of weathering along the fissures leads to isolated boulders and rocks in a matrix of regolith. The weathering along fractures in the bedrock proceeds similarly. ENGALENC (1978) showed some typical constellations of the propagation of weathering at fractures (see Fig. 3.21).

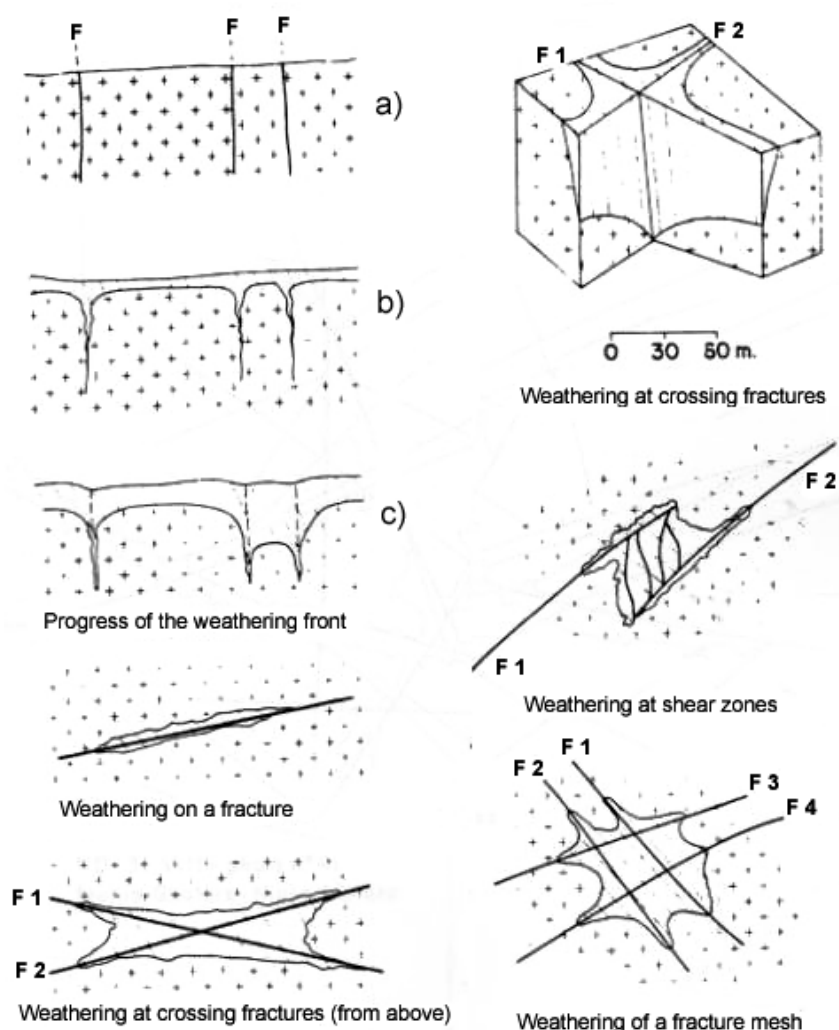


Fig. 3.21: Weathering under different constellations of fractures (from ENGALENC 1978).

The lower parts of the saprolite are usually formed by in-situ weathering; towards the top lateral material transport might be possible (TAYLOR and EGGLETON 2001). The saprolite is coarse grained at the bottom of the mobile layers. It is referred to the upper part of the saprolite as the collapse zone. Boulders and rocks are horizontally deposited in this area. Either transported over short distances (the rocks are well rounded) or deposited in place by collapsing quartz bands or layers (see Fig. 3.22). The original rock structure is mostly conserved but it is completely decomposed. The granulometry is heterogeneous and depends on the bedrock type.

3 Case study: The Upper Ouémé river catchment

The usually encountered red colour is caused by ferric impregnations on the surface of fissures and grains. The weathering of feldspar in the bedrock to kaolinite may cause chalk-white colours.

Greater blocks and boulders are separated. Their core is often harder than the surrounding material. These boulders typically form the smooth hills and domes found in the landscape.

The grade of fissuring depends on the rock type and the intensity of the regional fracturing. The intensity of weathering is as well determined by the morphological position. Below flat plains groundwater is stagnant and badly drained what slows down the weathering. At slopes water circulates better and accelerates weathering. The occurrence of rock anomalies like dykes or mineral laminations will cause variations in the thickness of the regolith.

Associated to the regolith ferruginous incrustations occur (called *duricrusts*). Indurated regolith material may occur near to the surface as a layer of limited extension (see Fig. 3.23). A common form in tropical zones is the ferricrete where the dominant cementing cation is Fe^{3+} (as goethite or haematite). Its appearance in the study area is often pisolitic. Grains of different origin are surrounded by sheets of iron oxides and hydroxides. When this ensemble gets cemented it is called pisolith (TAYLOR and EGGLETON 2001). In literature the term "*laterite*" is synonymously used. There is much discussion about this diffusively used term and therefore it should not be used anymore (TAYLOR and EGGLETON 2001).

Duricrusts are formed by leaching processes of the soils during the rainy seasons. Iron oxides and aluminium oxides get enriched in the soils. If erosion reveals these enriched horizons they dehydrate and incrust. These duricrusts are fine-grained close to clay at the bottom and much coarser to the top ($\emptyset = \text{mm-cm}$). Duricrusts may achieve a thickness of more than 1 m.

Erosion of surface runoff is very much controlled by the existence of duricrusts. The uneven and cavernous surface of the crusts slows down the runoff and protects the layers below. When crusts are absent the strong erosion occurs and carves out large cavities and indentions into the regolith (JACQUIN and SEYGONA 2004). Interfluves in tropical areas are often covered by ferricretes. Due to their hardness they resisted erosion since their formation in the Tertiary. In case of relief inversion they turn from a bottom position into a relatively higher position.

Ferricretes in the HVO cover smaller areas on crests. Evidence is the formation of stepped landmarks and the distributed debris of crusts on the pediments (JUNGE 2004).

Incongruent dissolution of primary silicate minerals, combined with continuous wash-out leads to a strong depletion of sodium, potassium and especially magnesium, calcium and silicon. The most important weathering product within the saprolite aquifer, which is rich in secondary clay minerals, is kaolinite.

3 Case study: The Upper Ouémé river catchment

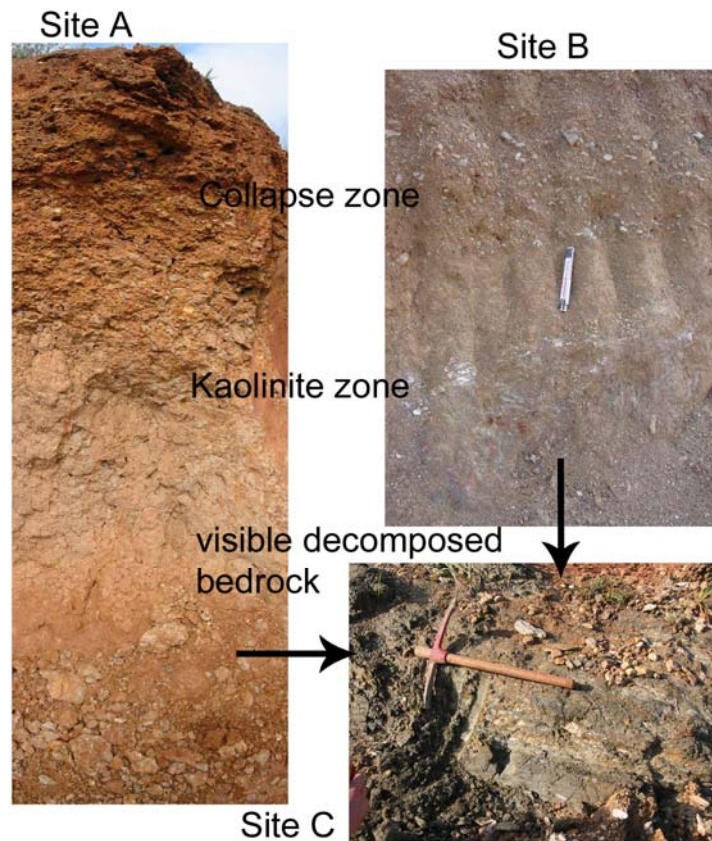


Fig. 3.22: A saprolite profile outcropping at an eroded river valley next to the Okpara barrage. Sites A, B and C are less than 10 m distant from each other (East of Parakou; UTM 470614/1026203).

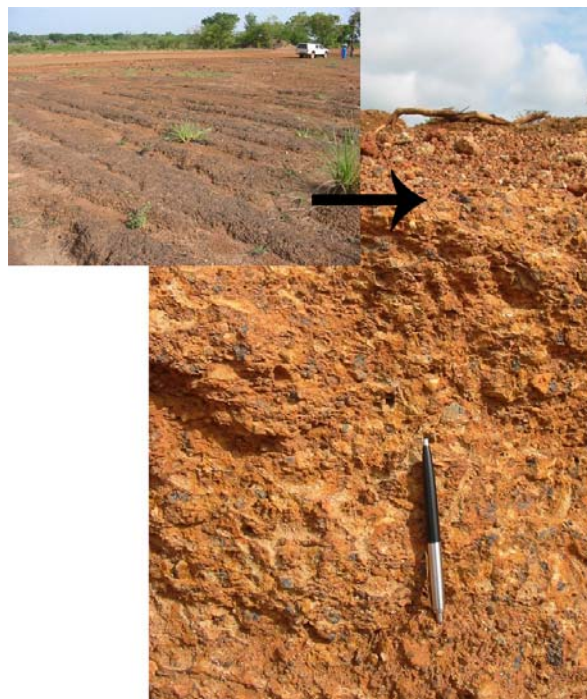


Fig. 3.23: Pisolith at the Okpara dam. Pisolitic iron grains can be identified on the close-up on the right (East of Parakou; UTM 470614/1026203).

3.7 Hydrogeology

3.7.1 Bedrock aquifer

The occurrence of groundwater in Benin is related to the aquifers of the regolith and of the fractured bedrock. Both have very different geological and hydraulic characteristics (Fig. 3.20). The bedrock is a discontinuous aquifer and therefore it is very delicate to handle its exploitation.

However, the most productive regional aquifer is the regolith (SOGREAH and SCET 1999; ENGALENC 1978). Regolith is overlying the bedrock and is found in faults and fractures in the basement. The highest yielding wells and boreholes are found in fairly well fractured and weathered bedrock with a thick regolith cover. The exploitation profits from the rather high permeability of the fractures and from drainable storage of the regolith. The grade and distribution of fractures as well as the effective porosity depends on the bedrock type and the intensity of weathering.

Aquifers in crystalline rocks develop in close relationship to climate, topography and the structural features present in the rocks. While the climate continues to influence the rocks, the impact of tectonic stresses is indirect, having created the structures which facilitate chemical weathering.

Rocks of the basement complex, when not weathered, are impermeable and have no storage capacity. The permeability and the storability of these rocks are solely dependant on secondary structural features like fissures and fractures.

In general fractures close when the lithostatic pressure increases with rising depth. The maximum depth of the exploitable fractured aquifer is around 70 to 80 m (see Tab. 3.2). In major fault zones groundwater may be found occasionally in depths to 120 m (CEFIGRE 1990).

Tab. 3.2: Frequency of final borehole depths for different rock types in the Upper Ouémé catchment [%]. Values of maximum percentage are drawn on grey background (Data source: BDI).

Rock	No. of points	Min. depth [m]	Max. depth [m]	Mean depth [m]	Median depth [m]	Frequency of boreholes for different ranges of depths [%]						
						10 - 20 m	20 - 30 m	30 - 40 m	40 - 50 m	50 - 60 m	60 - 70 m	70 - 80 m
Quartzites	39	16	75	52.2	53	2.56	5.13	10.26	25.64	25.64	28.20	2.56
Migmatites	29	30	69	48.5	49	0.00	3.45	20.69	41.38	20.69	13.79	0.00
Micaschists	8	45	69	60.9	64	0.00	0.00	0.00	25.00	12.50	62.50	0.00
Gneiss	177	32	74	52.5	55	0.00	0.00	15.25	26.55	31.07	26.55	0.56
Orthogneiss	23	23	63	48.5	51	0.00	4.35	17.39	39.13	30.43	8.70	0.00
Granites	76	21	75	51.3	49	0.00	2.63	14.47	28.95	25.00	23.68	5.26

When the groundwater table moves within the regolith aquifer then the fractured aquifer is saturated and is semi-confined or confined. If the regolith does not contain any water

3 Case study: The Upper Ouémé river catchment

then the water table may move free in the fractures. If the water table is still lower than 30 m then the available water resource has to be considered as very low. But this is not the case in the HVO with the exceptions of local anomalies.

Major fault zones like the Kandi fault can be sited in different rock types. They may reach widths of 10 m to more than 100 m. The shear zone is typically filled with mylonite. Being rather impermeable it does not conduct groundwater. But in the fractures accompanying the fault zone important groundwater flow may occur (STOBER 1995).

In the study area longitudinal fractures are the most common structures. Polygonal meshes of fractures needs are homogeneous environment and are not identified. Fracturing induced by regional tectonics is predominant. The occurrence of fractures with lengths of 15 to 25 km is rated to be <10% of all fractures in the study area (ENGALENC 1985 a). Many background information about the formation of fractures in crystalline rocks are given in ENGALENC (1978), SINGHAL and GUPTA (1999) and LLOYD and JACKS (1999).

Groundwater may enter the borewell in different depths. Fig. 3.24 shows that the main influx from water into borewells origins from rather shallow water levels. This water may be conducted through permeable layers within the saprolite or via fracures in the saprock and the crystalline bedrock. Influx is getting rare with rising depth where fractures alone could provide water in important quantities. There is only a slight rise of influx in a depth of around 15 to 25 m. This is the depth where saprock occurs (refer to Fig. 3.20).

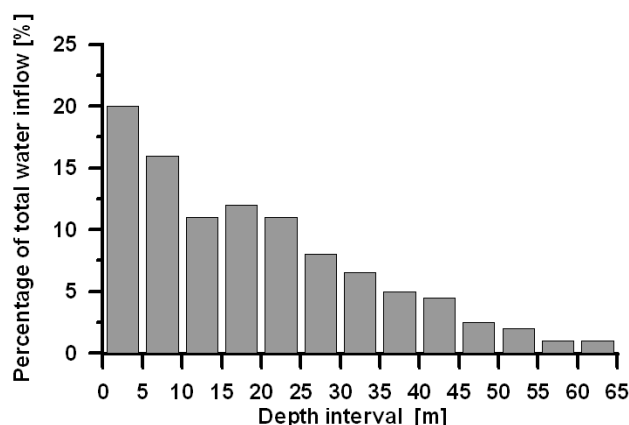


Fig. 3.24: Percentual distribution of the depth (in a 5 m interval) of encountered water inflow into borewells in the crystalline area of Benin (Data from SOGREAH and SCET 1999).

It is important to note that all percolating water must pass through the weathered mantle before the deeper fractured system is reached. The regional groundwater table of the HVO is usually found in the regolith. The fractured bedrock is generally saturated.

The transmissivity of the fractured bedrock is less influenced by the rock type than by the frequency, depth and aperture of fractures. The BDI boreholes were drilled to obtain the maximum productivity. However, the transmissivity data from 358 BDI boreholes was converted into k_f -values by division with the drilled thickness of the bedrock. The k_f -values were lognormalised and interpolated by kriging (linear variogram model). The resulting map (Fig. 3.25) reveals a k_f pattern which is reflecting the major geological structure units in the HVO. The central axis zone shows a relatively higher hydraulic conductivity than the granitic Nikki-Péréré complex in the East and the Atacora foreland in the West (compressive tectonics). The central axis zone was most affected by stress

3 Case study: The Upper Ouémé river catchment

and strain due to lateral movements along the Kandi fault and thus shows a stronger and deeper fracturing. The pumping test data is interpreted by the BURGEAP-method (1988) and serves only for relative considerations between different boreholes. These pumping tests were applied on the fractured aquifer only.

The hydrogeological pumping tests realised by BOUKARI et al. (1985) are more reliable (see Tab. 3.3). The pumping tests were done at the end of the wet season and have to be considered as relatively high.

Tab. 3.3: Mean values for transmissivity and storativity in the Collines. Average calculated from 5 pumping test interpretations (taken from BOUKARI et al. 1985).

Aquifer	Transmissivity [m ² /s]	Storativity [-]
Regolith	7E-04	0.01
Bedrock	1E-03	0.00001

ENGALENC (1978) classifies rocks with a transmissivity (T) between 1E-06 m²/s and 1E-05 m²/s as well fractured and rocks with a transmissivity higher than 1E-04 m²/s are either fissured or faulted.

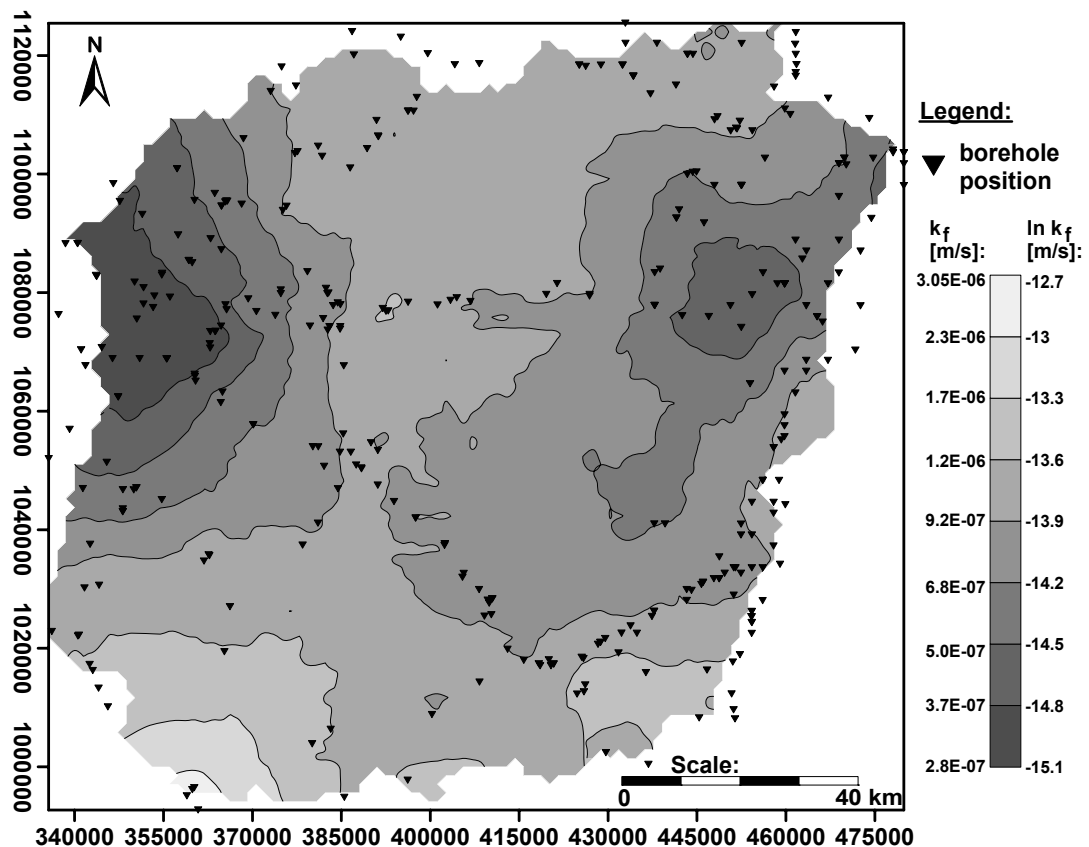


Fig. 3.25: Distribution of lognormal k_f values in the bedrock aquifer and the limits of the k_f zones achieved from the BDI data (Projection: UTM, Zone 31P, WGS 84).

The recharge of the bedrock is indirect by vertical drainage and downward percolation from the regolith aquifer at the top. Outcrops of the bedrock aquifer are generally limited to local occurrences and therefore are negligible for regional recharge.

3 Case study: The Upper Ouémé river catchment

After LELONG (1966) more than 1300 mm of rainfall are needed in tropical Africa to recharge the groundwater table in around 20 m depth. ENGALENC (1985a) estimates that in case of outcropping bedrock a small fraction of around 40 to 80 mm of the total precipitation would be sufficient to renew the usable content of a fractured reservoir.

SOGREAH (1997) calculates a potential recharge of around 20% from precipitations of around 1000 to 1200 mm/a. Like ENGALENC (1985a) they based their calculation on a water balance taking only evaporation into account. Transpiration and interflow were not included. SINGHAL and GUPTA (1999) refer to a lesser recharge of 5 to 15% of the precipitation. In accordance to field observations in Benin the real recharge in the crystalline area is assumed to be very low with around 5% of the precipitation (oral comm. C. ZUNINO, DANIDA, and J.-L. LAVALADE, ANTEA). However, recharge depends on the saturation of the shallow regolith aquifer. The groundwater level raises fast during the first rainfall events of the rainy season. Once the regolith is saturated, abundant rain water will rather flow away as interflow or surface runoff than producing recharge. This means that possibly more water could infiltrate if the regolith aquifer is unsaturated. Afterwards the groundwater storage depletes and returns towards a general base level (Fig. 4.1 and Fig. 4.2). This rather constant base level observed for the period from 2004 to 2006 still remains although a visible decline of the piezometric heads during the rainy season occurs.

The first infiltrated water is used to balance the humidity deficit in the unsaturated zone. Only then the groundwater table can rise. The rise is very strong because of the low effective porosity (ENGALENC 1978). Recharge of the fractured aquifer is higher when the regolith zone is thinner. Even in times of droughts there would be enough water available to refill the fractures of the bedrock.

Most of the groundwater in the HVO is found in the regolith. The quantity stored in the bedrock is small by comparison. Tab. 3.4 gives a generalised overview on the relationship between bedrock and regolith aquifer.

Tab. 3.4: General hydrogeologic characteristics of the geological units of the Upper Ouémé catchment area (modified, from DANIEL et al. 1997).

Hydrogeologic characteristics	Hydrogeologic terrains	
	Massive or foliated bedrocks, thick regolith	Massive or foliated bedrocks, thin regolith
Topographic Relief	low to average	see left column
Recharge	precipitation on topographic highs	see left column
Discharge	to streams	see left column
Type of porosity or permeability	intergranular in regolith, fracture	fracture
Type of flow	diffuse, fracture	fracture
Depth of flow [m]	5-15	5-20
Confined or unconfined	mostly unconfined	mostly unconfined
Regolith storage	large	small
Well yield	proportional to regolith thickness	low

3.7.2 Regolith aquifer

The regolith contains important water resources suitable for rural water supply in Benin (SOGREAH and SCET 1999; ENGALENC 1978). The yield of regolith aquifers in crystalline basement areas is generally very low. The regolith is not a compact homogenous porous milieu. A fine net of fissures can be observed in great diameter wells. This net is a heritage of the original mother rock. The original texture prevails while the structure is decomposed to clay. Thus the flow is faster within the fissures than in the clay matrix.

Despite the undulating landform the regolith forms and continuous aquifer together with the fractured bedrock. Its pressure heads equilibrate over all the area and a common table can be drawn (ENGALENC 1978). The piezometric surface is almost parallel to the topography. However, the highest levels are found at the interfluves the lowest levels are found below river valleys. In case of regressive erosion of the slopes towards the river valley may disrupt the groundwater table. The adaptation of the table may result in general water levels below the riverbed (10 to 30 m; ENGALENC 1978).

Especially in plain areas, the groundwater table is horizontally extended and rather shallow. Wherever the groundwater table is relatively deep, at slopes, interfluves and in areas of weak precipitation, the aquifer is scattered to water bearing pockets in the regolith. The appearance of these pockets is of strong local nature. In areas with high piezometric amplitude the water volume trapped in the pockets can decrease rapidly during the dry season (ENGALENC 1978). Perched aquifers may exist permanently in hardened (e.g. duricrusts) or impermeable clay layers. Wells placed in these perched aquifers may dry out rather fast when the overall water level sinks.

The low yield of the regolith is explained by its low permeability due to its high share of clay minerals. For exploitation the low yield has to be compensated by a higher thickness. In general the water level is around 5 to 10 m below ground. In zones where schist and clay weathering is dominant the water level depth is even shallower than 10 m (SOGREAH and SCET 1999).

For a withdrawal of 1 m³/h following requirements for the planning of a borewell are expected (BURGEAP 1976):

- a depth of 5 to 10 m to the groundwater table below ground but with a minimum water column in the borehole of 12 m,
- 1m of security distance from the groundwater table to the pump
- 1 m from the borehole bottom for the sedimentation fosse.

As consequencel a minimum borewell depth of around 24 m is mandatory. All borewells in the HVO do respect this criterion and are generally deeper.

Comparison of geological log-data from 75 wells in the Donga catchment in the northwestern part of the HVO showed an average thickness of the regolith from 16.2 m with a maximum of 30 m and a minimum of 3 m (JACQUIN and SEYGONA 2004). The BDI data shows differing results for the whole HVO area (see Tab. 3.5). The mean value of the average regolith thickness for the different rock types is around 20 m and only around 16 m for gneissic rocks. Quartzite forms denser and harder rocks and it is therefore astonishing that its mean weathering thickness is as intense as the one of the micaschists. However, the minimum thickness of regolith above the quartzite is the

3 Case study: The Upper Ouémé river catchment

lowest for all the HVO. It is nevertheless advisable not to be too confident with the data quality of the BDI.

Tab. 3.5: Thickness of the regolith in relation to the mother rock. Data is taken from the BDI.

Rock	Number of points	Mean thickness [m]	Median thickness [m]	Minimum thickness [m]	Maximum thickness [m]
Quartzites	39	20.62	22	3	42
Migmatites	29	20.17	19	5	38
Micaschists	8	20	21.5	7	30
Gneiss	177	17.65	10.5	5	20
Orthogneiss	23	15.83	11	5	31
Granites	76	20	21	7	47

FASS (2004) realised pumping tests for the regolith aquifer in the HVO next to the village of Dogué (see Tab. 3.6). The range of hydraulic conductivities is comparable to published values for regolith aquifers found under similar conditions in other African countries. The values are situated at the lower limit of the data range. The average storage coefficient for the regolith is around 0.03 (SOGREAH and SCET 1997). The value 0.01 proposed by BOUKARI et al. (1985) in Tab. 3.3 is still somewhat lower. In regard to the greater data base used by the first authors it seems that 0.03 is likely to describe the general storage coefficient for larger areas in Benin.

Tab. 3.6: Hydraulic conductivities of regolith aquifers.

Country	Conductivity		Reference
	[m/d]	[m/s]	
Malawi / Zimbabwe	0.08 – 0.7	9.3E-07 – 8.1E-06	CHILTON and FOSTER (1993)
Zimbabwe	0.02 – 4.9	2.4E-07 – 5.7E-05	WRIGHT (1992)
Burkina-Faso	0.26 – 1.12	3E-06 - 1.3 E-05	ENGALENC (1978)
Uganda	0.04 – 0.7	4.6 E-07 – 8E-06	TAYLOR and HOWARD (2000)
Ghana	0.22 – 2.2	2.5E-06 – 2.5E-05	MARTIN (2006)
Benin	0.009 – 0.09	1E-07 – 1E-06	SOGREAH (1997)
Benin (Dogué)	0.005 – 0.02	6E-08 – 1.7E-07	FASS (2004)

An overall value of 2.5E-03 m²/s for the diffusivity (quotient of T/S) is calculated on the data set from ENGALENC (1978) and indicates slow transmittance of changes of the groundwater table in the regolith. This is demonstrated by the observation of groundwater drawdown during pumping.

A 24-hour pumping test does not affect more than a radius of 12 m around the borewell. The routine duration of exploitation per day is around 10 hours. This produces an area of influence of 9 m² (see Tab. 3.7).

A supposed period of pumping for one year would produce an area of drawdown of around 260 m². However, pumping tests are expensive. To prevent boreholes or wells having impact on another a minimum distance of 200 to 250 m should be respected.

It is encouraged that a pumping test should last longer than 10 days to make Jacob's equation applicable and the result effectively defines the aquifer system of concern.

3 Case study: The Upper Ouémé river catchment

Tab. 3.7: Area of influence for pumping tests in the regolith zone (ENGALENC 1978).

Pumping period [h]	Area [m ²]
10	9
24	12
120 (5 days)	34

The regolith aquifer obtains direct recharge due to the infiltration of parts of the precipitated water. Infiltrated water will relatively fast discharge to lower areas as interflow in shallow depths (0 to 3 m bgl). The interflow can be classified as a floating (perched) aquifer which is existent during the rainy season. The low electric conductivity measured in this depth (20 to 50 $\mu\text{S}/\text{cm}^2$) is caused by the relatively fast transit of water in an already eluted zone. The water which is not lost by interflow, evapotranspiration or human consumption is stored in the regolith aquifer.

The surface runoff, interflow and probably some groundwater base flow end up in the bas-fonds respectively in the river valleys. Recharge occurs mainly at the exposed interfluves (see Fig. 3.26). The bas-fonds (dambos) show important clay layers. A higher proportion of runoff would be expected as soon as the smectites have expanded to fill its cracks and tighten the clay surface (McFarlane 1987a). Lateral flow is possible either above the clay layer at the surface or else below the clay in the contact zone with the saprolite.

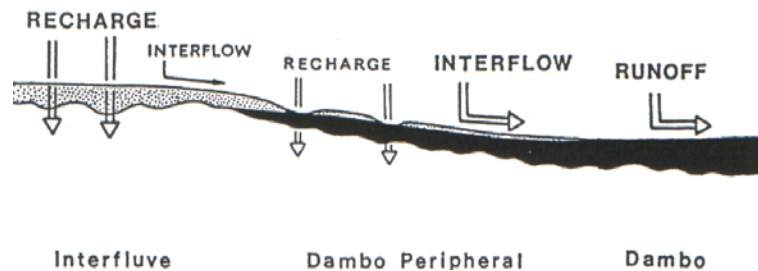


Fig. 3.26: The theoretical relative distribution of recharge, interflow and runoff in the centre and the periphery of bas-fonds (dambos) and at the interfluves (from McFarlane 1987a). The occurrence of smectitic deposits is marked by the black layer.

4. Piezometry

4.1 Data logger time series

The piezometric data shows different levels of periodical fluctuation. The measured amplitude between the lowest measurements of the groundwater table during the end of the dry season and the highest groundwater table at the end of the rainy season varies from 4 to 6 m.

The lowest groundwater tables are observed with 8 to 10 m below ground. The piezometer HVO-1 shows the deepest groundwater level with around 14 m (Fig. 4.1 and Fig. 4.2). HVO-9 at Bétérou shows the shallowest water level with around 6 m. Recharge in the rainy season lifts the groundwater table to a depth of 4 to 6 m. This means a general rise of 4 to 6 m for each observation well. The only exception is HVO-9 with a rise of only 2 m. This limited recovery at HVO-9 may indicate the fact that water in shallower depths is controlled by the surface morphology and flows horizontally away to any effluent, for example as interflow.

The rise of the groundwater table in 2005 due to the rainfalls is for some loggers less accentuated as for others. The groundwater level at HVO-1, HVO-3 and HVO-11 recovers less than for the other piezometers. The piezometers of concern are situated in the North and the Northwest of the study area. The difference is caused by the retarded and lower precipitation in the year 2005. This is already an indication for a regionally different recharge pattern and is underlined by the trend analyses made later in this chapter.

Theoretically the morphological position of the observation borehole should have a certain influence on the groundwater level and its reaction towards recharge. Most of the observation boreholes are situated at crest positions or in the upper slope.

HVO-9, instead, is placed on the foothills of a slope. HVO-9 is the only borehole with a relatively high groundwater table during the whole year. Water flows from the crests towards its position and thus the groundwater table stays generally higher. HVO-8 and HVO-10 are situated on top of crests. The two hydrographs are quite equilibrated and do not show sharp rise or fall. Recharge at crests would rather runoff towards the slopes than to prevail at the crests. At slopes the recharge of the groundwater table would fast accumulate the water coming from the crests and let it run through towards the lower valleys.

The longer time series (HVO-1, HVO-3, HVO-6, HVO-9 and HVO-11) show very well a decrease in the annual recharge for the years 2005 and 2006 due to reduced rainfalls. For the same period the base groundwater level instead is not decreasing. This means that a certain part of the aquifer stays saturated all the year long and is only slightly affected by dynamic changes of the water level.

Furthermore there is a daily fluctuation of the groundwater table in the observation wells which is thus not caused by pumping or other human intervention. Its amplitude ranges from 8 to 10 cm (see Fig. 4.3). This fluctuation is not only caused by evapotranspiration as it can be seen that the groundwater table descends as well in the night with almost the same amplitude. The observed fluctuations are supposed to be caused by diurnal tidal movements. This effect was also seen by A. Kolodziej (GeoConsult) during

geophysical field experiments in the Collines department in 2004 and 2005. During the rainy season these signals are less clear because of strong recharge.

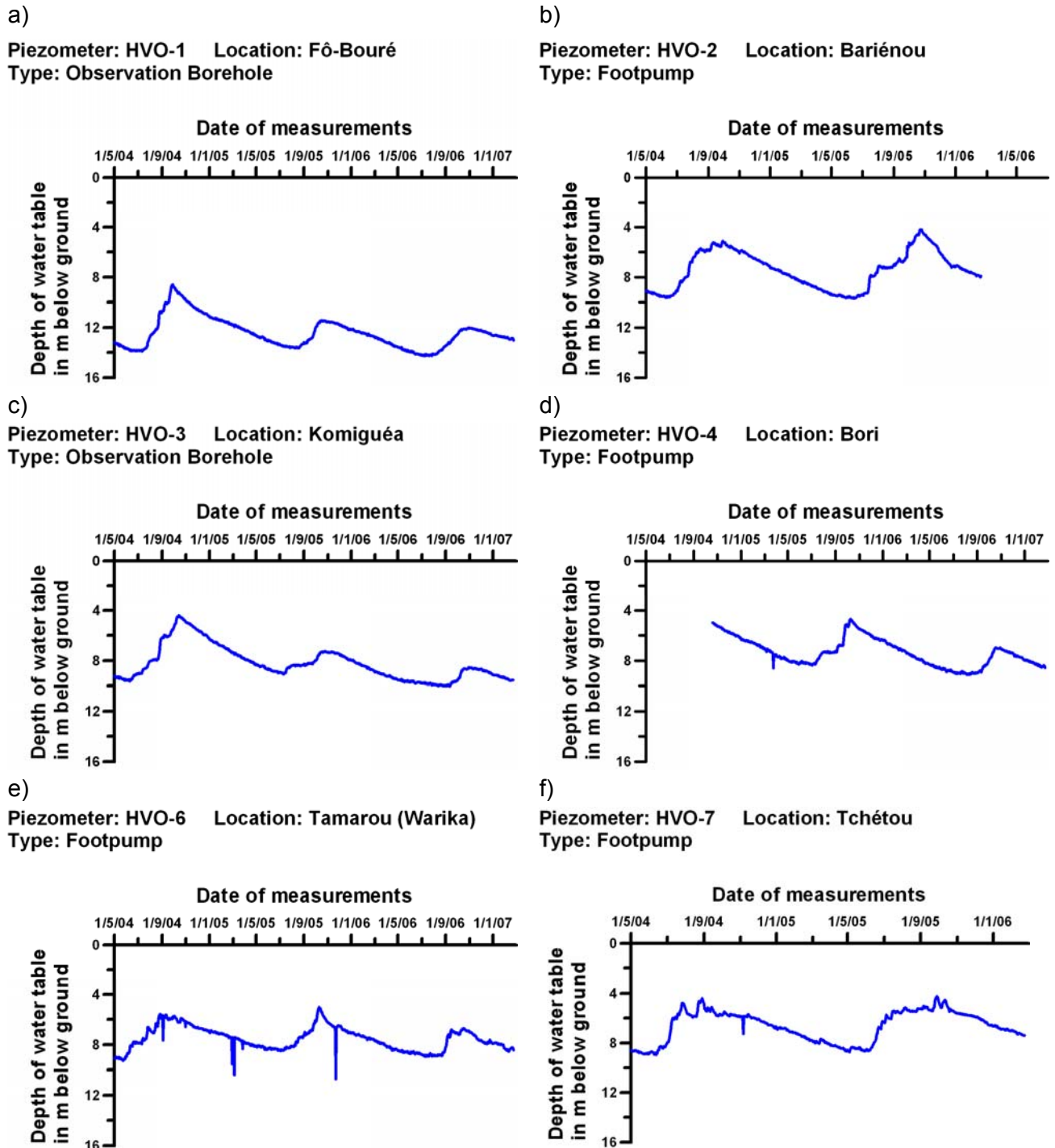
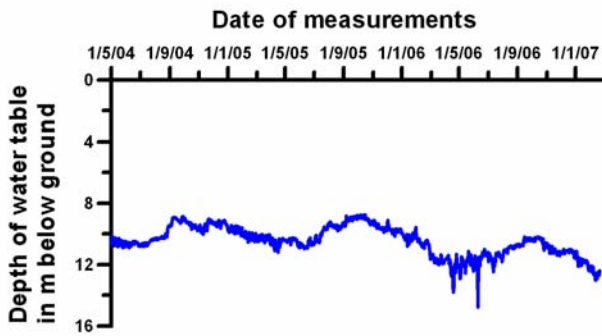


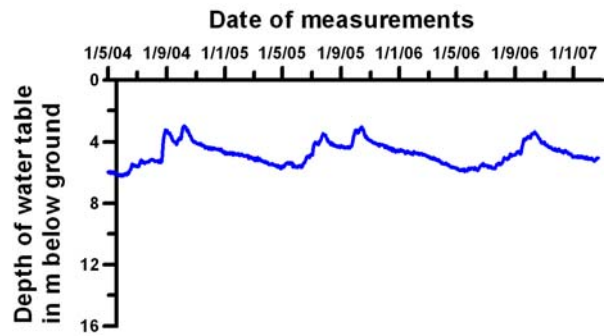
Fig. 4.1: Groundwater head time series of the HVO data loggers. The data sets are filtered. Only the measurements at 5 am are shown.

4 Piezometry

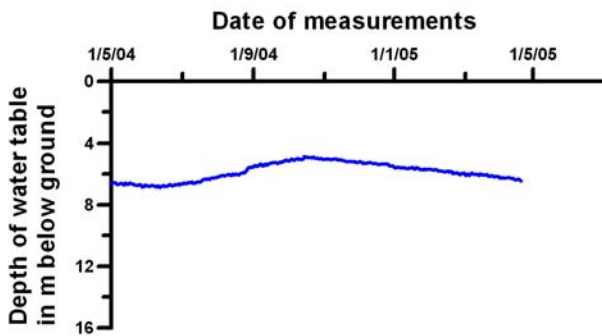
g)
Piezometer: HVO-8 Location: CEG Djougou
Type: Footpump



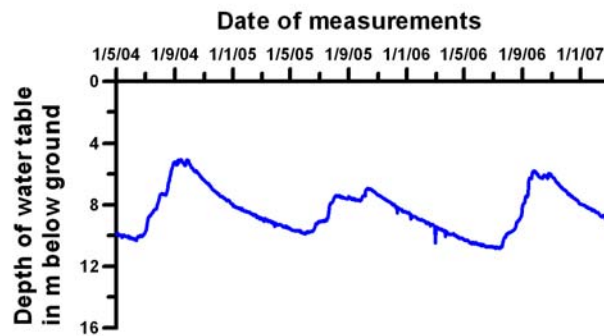
h)
Piezometer: HVO-9 Location: Bétérou
Type: Observation Borehole



i)
Piezometer: HVO-10 Location: Tchatchou
Type: Observation Borehole



j)
Piezometer: HVO-11 Location: Kolokondé
Type: Footpump



k)
Piezometer: HVO-12 Location: Dogué
Type: Observation Borehole

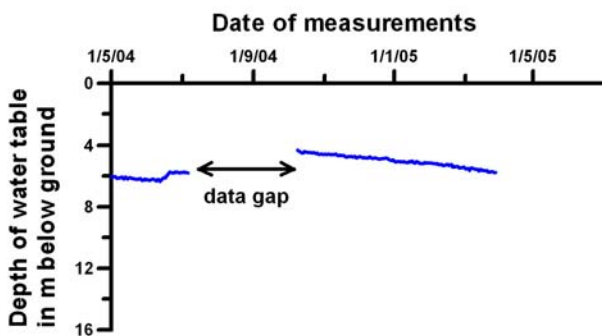


Fig. 4.2: Groundwater head time series of the HVO data loggers (continued). The data sets are filtered. Only the measurements at 5 am are shown.

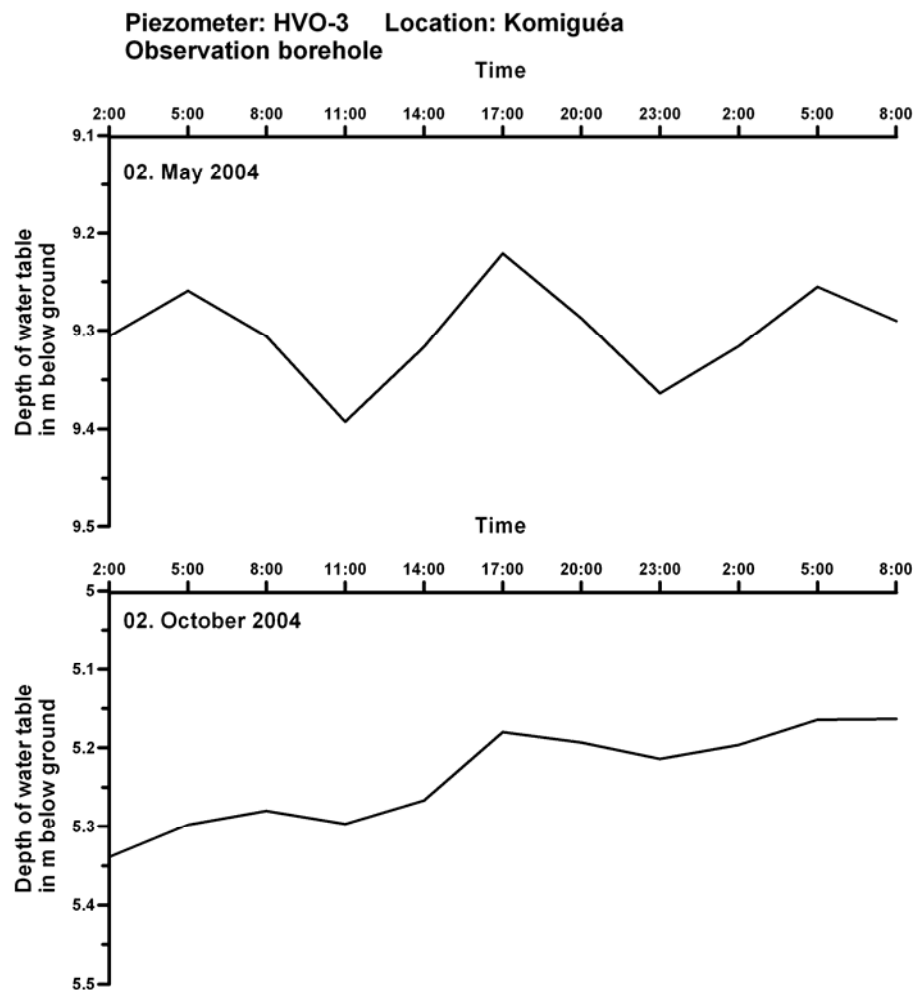


Fig. 4.3: The enlarged view on the groundwater hydrograph of HVO-3 (unfiltered) for two different dates in 2004. The view at the top shows the daily fluctuations of the groundwater table in the dry season, the screenshot at the bottom respectively the rainy season.

The installation of the data loggers depended on already existing boreholes. The financial means for drilling new observation boreholes close to existing installations like river gaugers and pluviometers were not disposed. However, some divers are next to these stations and their data series (as far as available) can be used for comparison.

The groundwater hydrograph of HVO-9 reacts to rainfalls with fast and sharp rises of the water level (Fig. 4.4). As the observation wells are drilled into the bedrock this reaction cannot be caused by real recharge towards the aquifer. It is rather the hydrostatic equilibrium which transfers the increasing pressure on the diver's transducers. This fast exchange needs preferential pathways. Those can be fracture structures running out close to the surface. Therefore this location was chosen for an investigation with geoelectric profiling. BOHNENKÄMPER (2006) measured thus two structures which can be interpreted as coarse grained clastic materials like quartz bands. Such bands might be remnants from fracture fillings (CHILTON and FOSTER 1993).

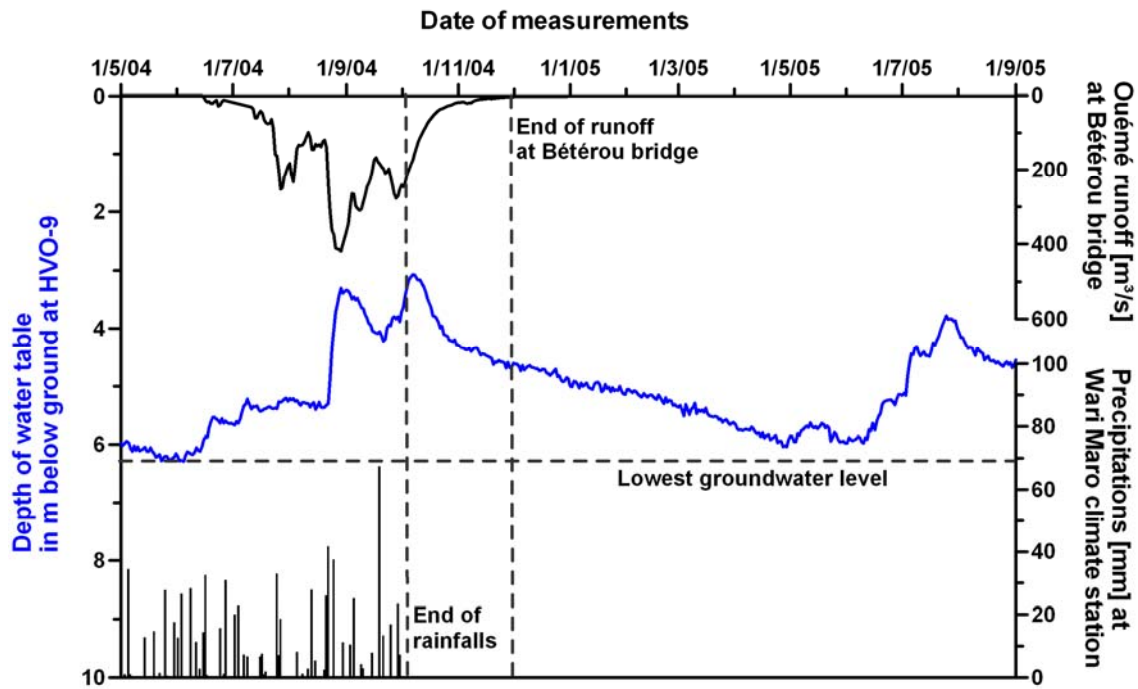


Fig. 4.4: Comparison of rainfall, runoff and groundwater levels at Bétérou (HVO-9) for the year 2004. The data set is filtered for 5:00 am measurements only.

The river runoff reacts almost simultaneously with the groundwater levels. This means that the retention through the aquifer is of less importance. Most of the precipitation runs off at the surface or by interflow towards the river. Only when the rainfalls stop it can be seen that there is still base flow from the aquifer towards the Ouémé. But it is as well seen that the groundwater level still falls after the river already ran dry (Fig. 4.5). It is assumed that the withdrawal of the groundwater table during the dry season is due to deep rooting plants. Similar behaviour of an aquifer had been watched for example in studies in Botswana (BAUER et al. 2003).

The data series in Fig. 4.6 shows a gap during the important rainy season. Nevertheless, the groundwater table depletes even after the end of the river runoff. It would be interesting to compare the losses from the groundwater table with a regional estimation of plant's water consumption.

In all cases the water table drops after the end of the river runoff still for 1.50 to 2 m. Any long range transport in riverbed sediments is not probable as for example the riverbeds of the Ouémé and the Téro River consist of bedrock only along long distances. Flow in fractures depends on their connectivity.

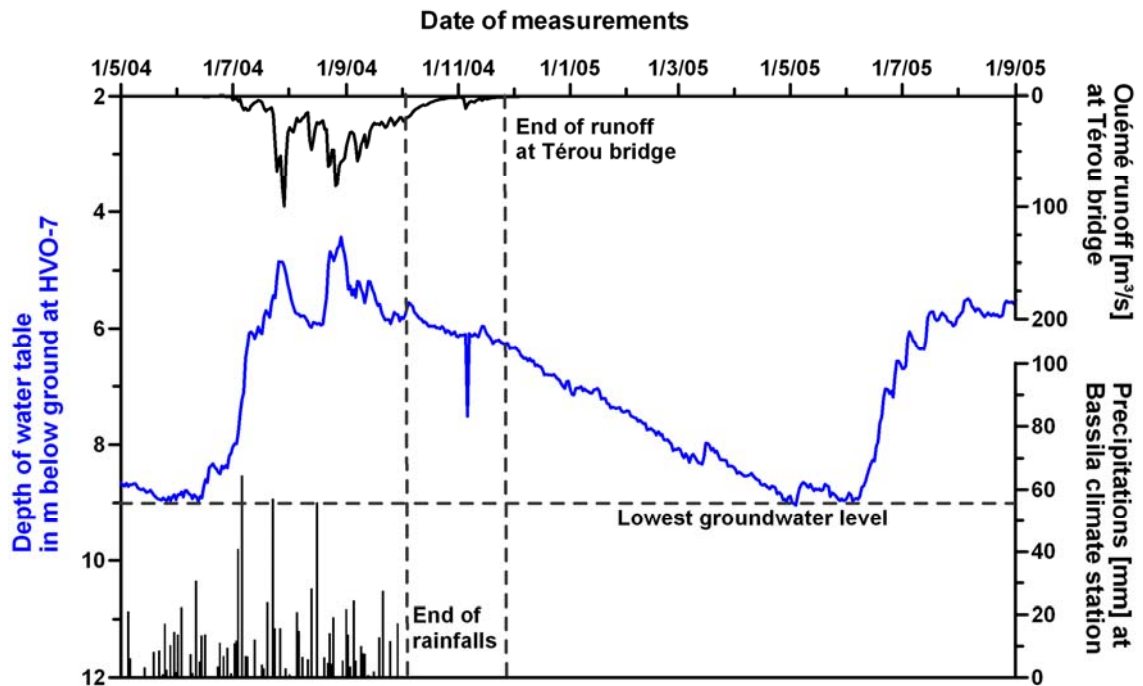


Fig. 4.5: Comparison of rainfall, runoff and groundwater levels at Tchétou (HVO-9 for the year 2004). The data set is filtered for 5:00 am measurements only.

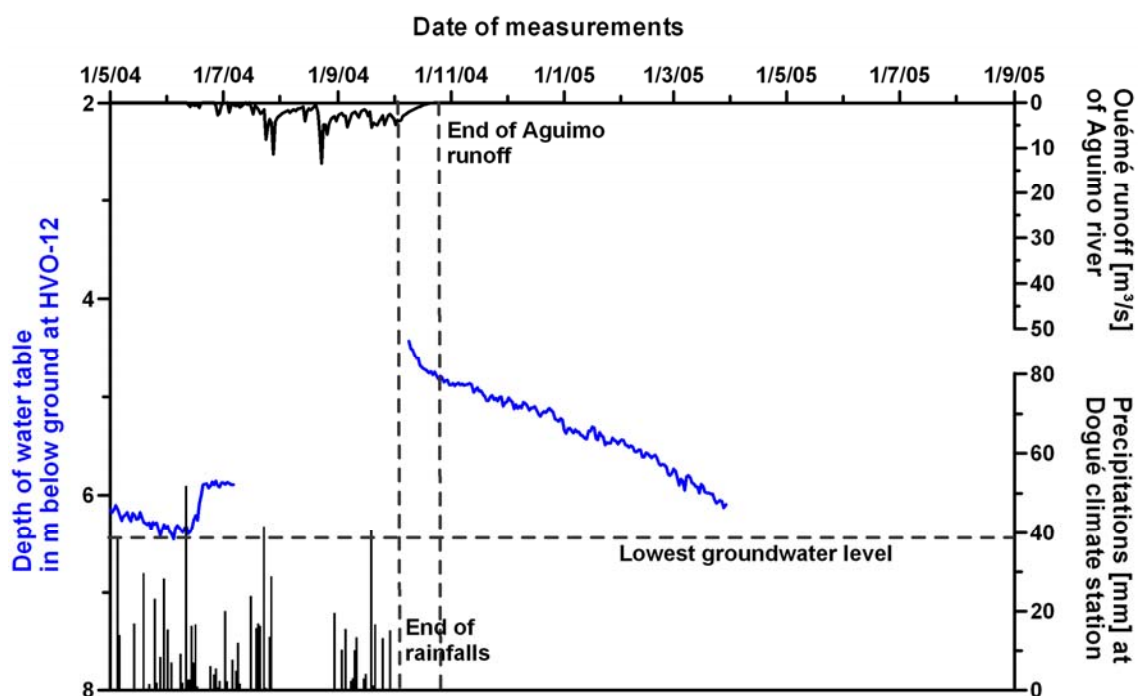


Fig. 4.6: Comparison of rainfall, runoff and groundwater levels at Dogué (HVO-12) for the year 2004. The data set is filtered for 5:00 am measurements only.

The distance groundwater may cover in the bedrock depends on the fracture connectivity. The degree of connectivity within the HVO remains unknown, but is estimated to a maximum of some hundred meters only. The most probable reason for the groundwater depletion during the rest of the year is as said above outtake by plants and evaporation.

4 Piezometry

For long term interpretation of the time series a trend analysis was done. For each fully available data time series (daily 5:00 am measurements only) the recorded number of days and the measurements are summed up and multiplied.

These values are used to calculate the sums of the squared deviation (Q) of the groundwater level below ground (x). For each time series the individual number of time steps (n) is used. The results are found in Tab. 4.1.

$$Q_x = \sum x^2 - \frac{(\sum x)^2}{n} \quad (\text{Eq. 4.1})$$

$$Q_t = \sum t^2 - \frac{(\sum t)^2}{n} \quad (\text{Eq. 4.2})$$

$$Q_{xt} = \sum xt - \frac{\sum x \cdot \sum t}{n} \quad (\text{Eq. 4.3})$$

with

xt = share of the trend

t = time step of the measurement

The squared sums of deviation are used to compute the coefficients b_0 and b_1 of the trend equation.

$$b_0 = \frac{Q_{xt}}{Q_t} \quad (\text{Eq. 4.4})$$

$$b_1 = \frac{\sum x}{n} \quad (\text{Eq. 4.5})$$

The quality of the trend can be evaluated by the linear correlation coefficient r (Eq. 4.6) (see LANGGUTH 1980):

$$r = \frac{Q_{xt}}{\sqrt{Q_x \cdot Q_t}} \quad (\text{Eq. 4.6})$$

The trend equation is formulated as follows:

$$xt = (b_0 \cdot t) + b_1 \quad (\text{Eq. 4.7})$$

Tab. 4.1: Trend analyses of piezometric time series data.

Diver	Sum (x ^a)	Sum (t ^b)	Sum (xt)	Sum (x ²)	Sum (t ²)	Q _x ^c	Q _t ^c	Q _{xt} ^c	b ₀ ^d	b ₁ ^d	r ^e
HVO-1	1.3E+04	5.3E+05	6.7E+06	1.6E+05	3.6E+08	1.5E+03	3.6E+08	1.3E+05	3.6E-04	12.64	0.17772
HVO-2	4.9E+03	2.2E+05	1.6E+06	3.8E+04	9.6E+07	1.5E+03	9.6E+07	-3.2E+04	-3.4E-04	7.30	-0.085
HVO-3	8.5E+03	5.3E+05	4.6E+06	7.2E+04	3.6E+08	1.9E+03	3.6E+08	2.3E+05	6.3E-04	8.56	0.27834
HVO-4	6.3E+03	3.7E+05	2.8E+06	4.7E+04	2.1E+08	1.0E+03	2.1E+08	1.3E+05	6.1E-04	7.60	0.27102
HVO-6	7.7E+03	5.3E+05	4.1E+06	5.9E+04	3.6E+08	8.8E+02	3.6E+08	7.5E+04	2.1E-04	7.64	0.13276
HVO-7	4.4E+03	2.2E+05	1.4E+06	3.0E+04	9.7E+07	1.0E+03	9.7E+07	-3.5E+04	-3.6E-04	6.52	-0.111
HVO-8	1.1E+04	5.6E+05	6.0E+06	1.2E+05	3.9E+08	9.3E+02	3.9E+08	1.7E+05	4.4E-04	10.69	0.28274
HVO-9	4.9E+03	5.3E+05	2.5E+06	2.4E+04	3.6E+08	5.6E+02	3.6E+08	-1.1E+04	-3.0E-05	4.77	-0.02435
HVO-10	2.1E+03	6.3E+04	3.6E+05	1.2E+04	1.5E+07	1.2E+02	1.5E+07	-8.6E+03	-5.8E-04	5.75	-0.199
HVO-11	8.6E+03	5.3E+05	4.5E+06	7.4E+04	3.6E+08	2.2E+03	3.6E+08	4.0E+04	1.1E-04	8.43	0.04457
Average:									1.05E-04	7.99	

^a x = groundwater level below ground [m].

^b t = day of the measurement x; starting with the first measurement on day zero (0).

^c Q = squared deviation.

^d b = regression coefficients of the trend equation.

^e r = correlation coefficient.

4 Piezometry

SACHS (1997) presents a way how to prove the correlation coefficient directly. He proposed critical values for comparison with the values of r in order to identify any statistical significance. The critical values are related to the number of measurements and their grade of freedom respectively and can be read from tables presented in SACHS (1997).

$$GF = n - 2 \quad (\text{Eq. 4.8})$$

with

$GF = \text{degree of freedom}$

$n = \text{number of measurements}$

If the amount of r is bigger as the critical values than the 5% significance is statistically assured. The comparison is given in Tab. 4.2.

Tab. 4.2: Critical values of r for the HVO divers.

Diver	n	GF	r	critical value 5% significance ¹
HVO-1	1028	1026	0.17772	0.0505
HVO-2	661	659	-0.08500	0.0740
HVO-3	1029	1027	0.27834	0.0505
HVO-4	856	854	0.27102	0.0619
HVO-6	1028	1026	0.13276	0.0505
HVO-7	663	661	-0.11100	0.0740
HVO-8	1057	1055	0.28274	0.0505
HVO-9	1030	1028	-0.02435	0.0505
HVO-10	355	353	-0.19900	0.105
HVO-11	1028	1026	0.04457	0.0505

¹ from SACHS (1997).

Out from 10 data series 5 seem to have a significant statistic time-measurement-relationship (HVO-1, HVO-3, HVO-4, HVO-6 and HVO-8). HVO-11 fails this test only close but is included into the above group. All approved series show a positive trend.

At the actual state of observation the properties of the time series are changing too strong that neither stationary nor non-stationary behaviour in time could be determined (MIDDLETON 2000).

The regarded data represents groundwater level below the ground surface. A sufficiently high value of r assures the trend equation. A positive trend would mean a further depletion of the groundwater table while a negative trend represents the opposite. Thus the 6 diver data series with the assured trend would rather represent a general trend to a depletion of the groundwater table (see average trend curve in Fig. 4.7). The remaining 4 series who failed the significance test show all a negative trend. It should be mentioned that their data series are much shorter (with the exception of HVO-9). Thus any trend calculation is much more uncertain.

However, r is only a statistical value. A close view to the data of the 6 approved data series reveals that the measurements started in the end of the dry season at a very low level and ended in most of the series at relatively higher levels. As the available time

series is still very short the influence of the last measured season on the overall series is considerably strong.

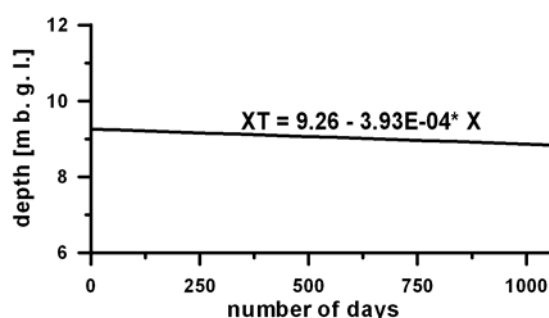


Fig. 4.7: Average trend equation XT for the 6 data logger time series with an approved statistical relevance.

The comparison of 5:00 am measurements at observation wells and at pumped boreholes showed no relevant difference in the depth of the groundwater table. It seems that the groundwater recovers almost fully during the night after being pumped at daytime. In rural areas with low water extraction rates the approach to install data loggers even under non-stationary conditions is reasonable when measurements are taken after sufficient recovery time. More frequently used pumps, e.g. in urban areas, might very well not recover at all.

Tab. 4.3: Coordinates of the IRD piezometers in the Donga catchment.

ID	Locality	Type	X (UTM)	Y (UTM)
ANANPZ	Ananinga	dug well	380252	1074308
BABAPZ	Babayaka	dug well	342425	1077927
BELEPZ	Belefoungou	dug well	359868	1085200
BORTOKOPZ	Bortoko	dug well	379276	1083944
CPR-SOSSOPZ	CPR-SOSSO	piezometer	362792	1087601
DEND1PZ	Dendougou	dug well	360612	1076431
DJAKPINGPZ	Djakpingou	dug well	354966	1082777
DJOUGOUPZ	Djoungou	piezometer	353994	1073376
FOUNGAPZ	Founga	dug well	345498	1071177
FOYOPZ	Foyo	dug well	383357	1073726
GANGPZ	Gangamou	dug well	374354	1088880
GAOUNGAPZ	Gaounga	piezometer	384600	1076758
KOKOPZ	Koko Sika	dug well	383108	1079976
KOLOPZ	Kolokonde	dug well	366117	1093400
KOUAPZ	Koua	dug well	367437	1079381
MONEMOSPZ	Mone mosquée	dug well	373542	1075300
PAMIPZ	Pamido	dug well	350265	1074369
SANKPZ	Sankoro	dug well	369989	1091610
SERIVERIPZ	Sérivéri	dug well	361901	1074174
TCHAPZ	Tchakpaissa	dug well	359596	1073986
TEWAMOUPZ	Téwamou	dug well	377571	1085723

The same ambivalent information is given by trend analyses from different piezometers in the Donga catchment⁸. Since the beginning of the year 2000 the IRD measures the groundwater table with 21 data loggers installed in open dug wells and observation wells distributed in this catchment (see Tab. 4.3). The data was available for analysis by the kind permission of Luc Séguis (IRD Cotonou). The time series were controlled through and equally analysed for trends and periodicity. The very same phenomena are seen in this data set. The correlation coefficient r is sometimes fitting well sometimes not. Trends are in some cases slightly positive in others slightly negative. However, these data series comprises only the years 2000 to 2003. This is hardly more than the time series from the IMPETUS divers and thus is still not sufficient for a clear interpretation.

It was shown in this chapter that the available time rows of piezometric data are still not sufficient to determine any trend of the groundwater table development. Actually the impact of increasing groundwater consumption by the people or of the declining precipitation in 2005 and 2006 on the general groundwater table cannot be determined. Longer time series would give the opportunity to investigate in detail the periodicity and autocorrelation of the data.

4.2 Regionalisation of piezometric data

It is a common procedure to generate contour lines of the groundwater table for regional research. Groundwater contours allow the determination of the groundwater flow direction. The regional distribution of local groundwater levels is hereby achieved by kriging.

These measurements are interpolated applying the kriging algorithm on the depth of the groundwater table below the ground. The depth of the groundwater level is equal to the thickness of the unsaturated zone. The thickness of the unsaturated zone can be subtracted from the DEM (see Fig. 4.11).

Many parts of the HVO are not accessible or do not show any settlements with wells or other groundwater points. Furthermore the DEM showed that the surface of the Area is slightly undulated and shows a number of smaller subcatchments. Each subcatchment has an individual distribution of crests, slopes and valleys. And at each of these positions the groundwater level would differ. No representative data for groundwater levels for all these subcatchments and their morphological characteristics is available. Only a general picture of the major groundwater flow direction in the HVO can be given. Groundwater flow would be on a local scale directed towards the locally draining river. On the regional scale flow is roughly directed towards the Ouémé valley and from there towards the South. But it has to be understood that the groundwater contours generally follows just the morphological features as the water table is quite close to the surface.

The distance between the data logger positions makes it impossible to integrate the actual morphology in interpolation algorithms unless an extremely simplified terrain model is used. However, during the field campaigns the depth of the groundwater table was regularly measured at numerous open dug wells (Fig. 4.8 and Tab. 4.4, for details see Annex 3). In respect to the size of the HVO, the completion of each measurement campaign required several weeks. The open dug wells are always in use by the villagers.

⁸ A subcatchment in the Northwest of the HVO. The Donga catchment is object of intensive research of the CATCH project of the IRD.

Thus, the water table is not stationary, except for measurements in the early morning hours.

Tab. 4.4: Number of manual piezometric measurements on wells realised in and around the study area during different seasons from 2004 to 2006.

Season	N° of measurements
Dry season 2004	113
Rainy season 2004	110
Dry season 2005	187
Rainy season 2005	83

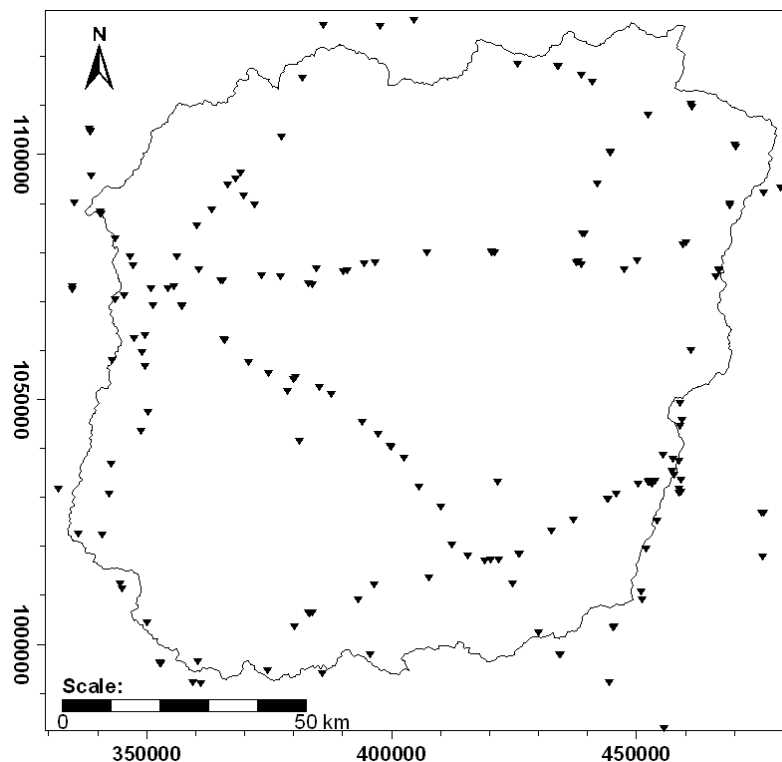


Fig. 4.8: Regional distribution of all manual and automatic piezometric measurements realised in the vicinity of the study area (Projection: UTM, Zone 31P, WGS 84).

The software package SURFER[®] has been used to produce contour maps for the dry seasons 2004/2005 and for the rainy seasons 2004/2005. Each data set was kriged. The resulting grid data was arranged in the same dimensions as the DEM. The same grid size facilitates mathematical grid operations.

The difference between the groundwater surfaces of the dry season 2004 and the rainy season 2004 (Fig. 4.9) and respectively the same for the year 2005 (Fig. 4.10) was calculated. The remaining volume was then multiplied with the storage coefficient for the regolith aquifer (4% as proposed by ENGALENC 1978) in order to obtain the volume of effectively gained groundwater at the end of the rainy season considered as recharge towards the aquifers. The effective recharge between the dry season 2004 and the dry season 2005 was then calculated by the same procedure (Fig. 4.12).

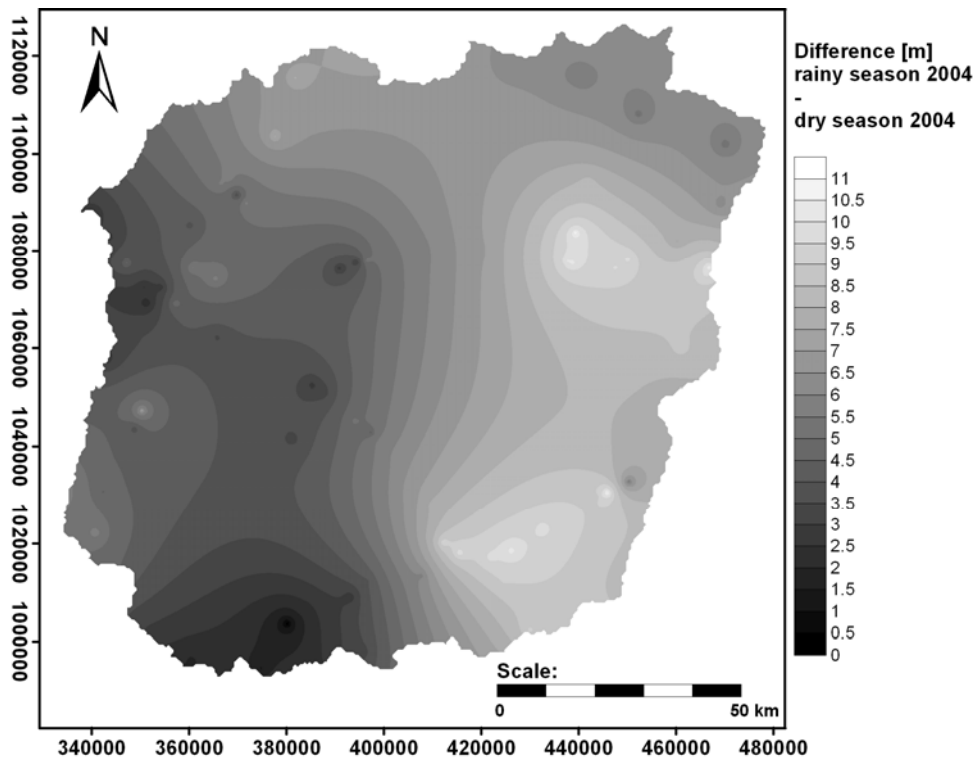


Fig. 4.9: The groundwater levels during the rainy season are generally higher as in the dry season 2004 (Projection: UTM, Zone 31P, WGS 84).

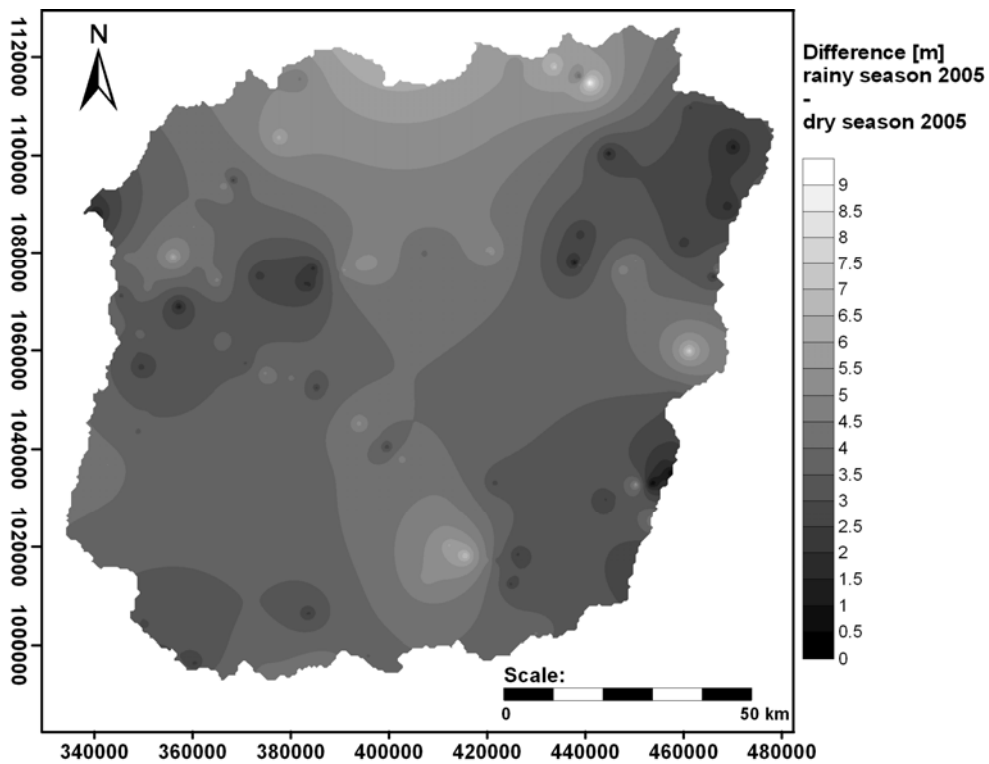


Fig. 4.10: Distribution of the groundwater differences in 2005 (Projection: UTM, Zone 31P, WGS 84).

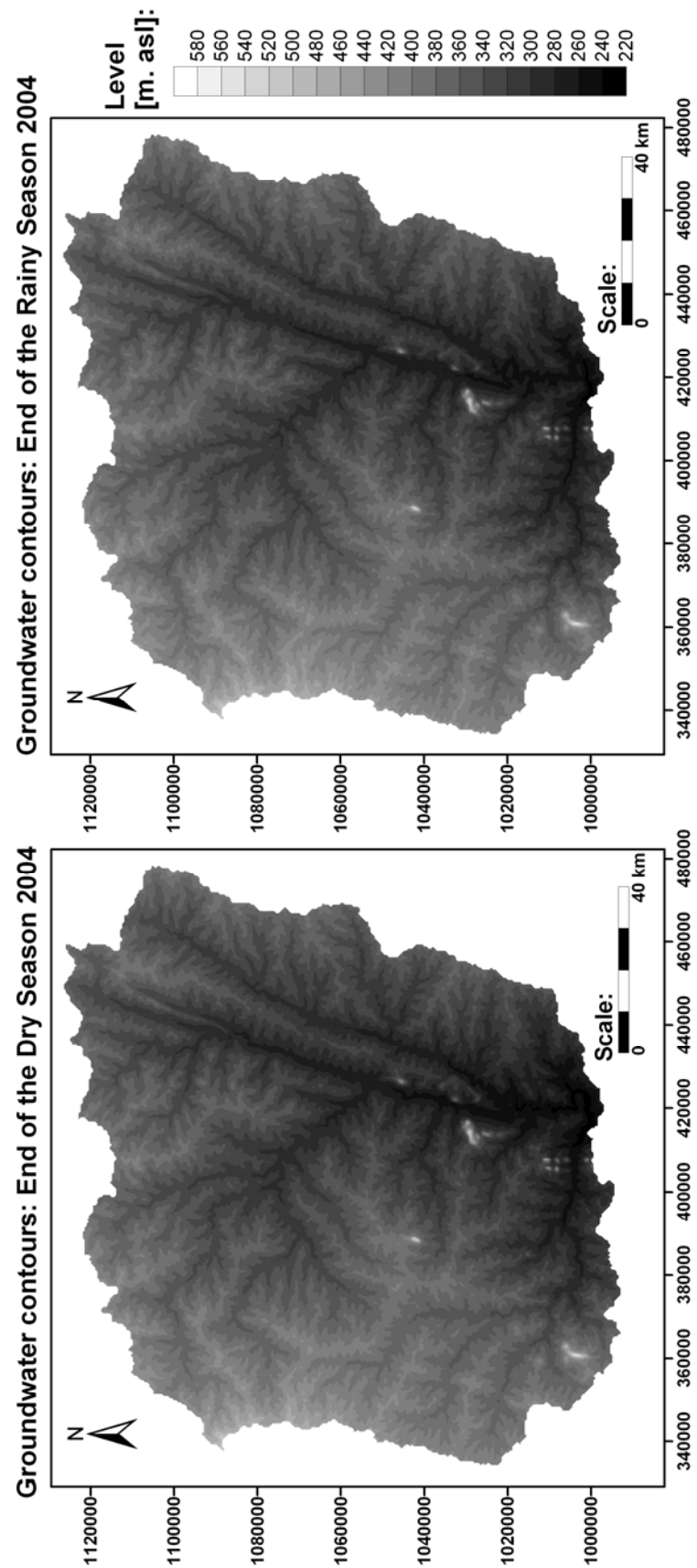


Fig. 4.11: Exemplary interpolation of manually made groundwater measurements. The data was interpolated and then subtracted from the DEM.

5 Hydrochemistry

By this procedure a recharge of 240 mm in the year 2004 and 158 mm for the year 2005 was calculated for the HVO area. Both values are too high in comparison to values of 30 to 100 mm/a proposed by GIERTZ (2005), ENGALENC (1978), ENGALENC (1985), SANDWIDI et al. (2006) and SOGREAH and SCET (1997).

Tab. 4.5: Results from the grid based recharge calculation. The volume is calculated by subtracting the grids of the interpolated manual field measurements.

Grid	Storage Volume [m ³]	Recharge [mm]
Rainy – Dry 2004	3408108893.79	240
Rainy – Dry 2005	2243401570.47	158
Dry 2005 – Dry2004	455483045.27	32

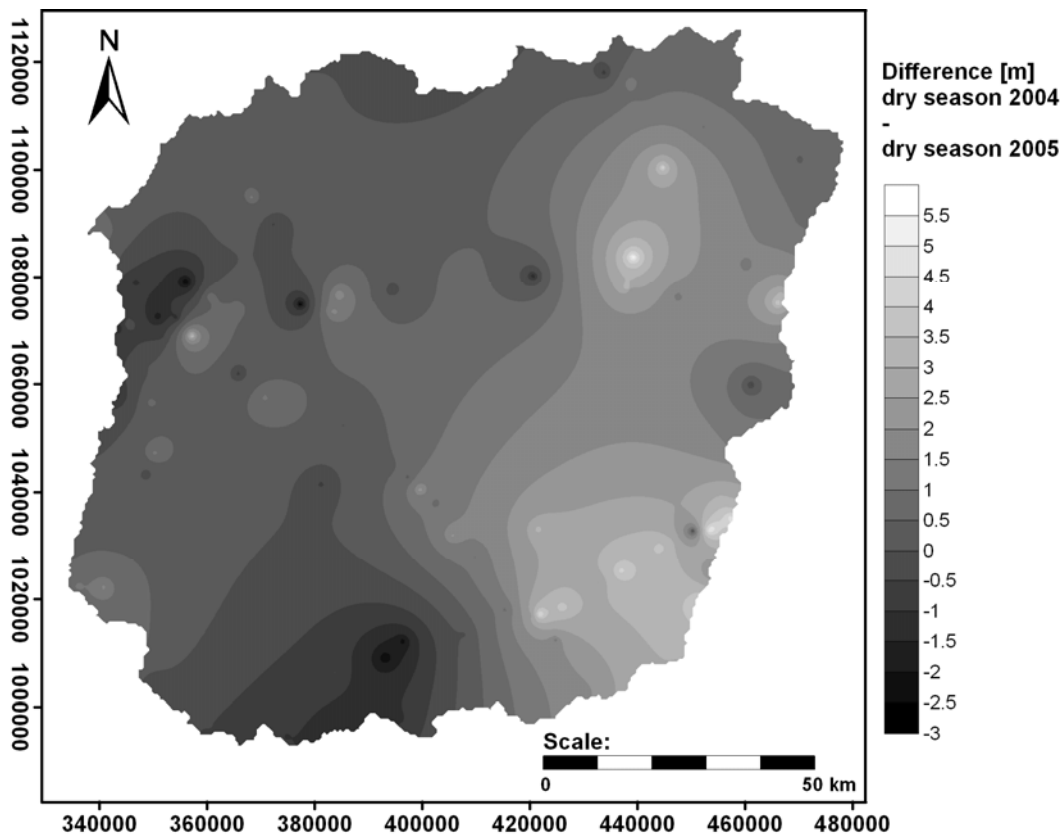


Fig. 4.12: Difference between the two dry seasons of the years 2004 and 2005 (Projection: UTM, Zone 31P, WGS 84).

The recharged water between the end of the dry season 2004 and the end of the dry season 2005 was calculated as 32 mm. This means that the groundwater table rose in total from one year to the other. The amount of 32 mm fits very well with the general assumptions for recharge made by the above citations.

The elevated groundwater table differences in the figures above are due to the regional distribution of precipitation but as well by the great time intervals between the measurements. The groundwater contours of the dry season 2004 are used as initial head conditions of the numerical model (Chapter 8).

5. Hydrochemistry

5.1 Physico-chemical characteristics

5.1.1 Temperature

Air and water temperature (in °C) have been measured on-site for each sample. In general, water from the regolith aquifer was sampled from open dug wells where it is in direct contact with the atmosphere. The borewells instead are fully cased. The temperature in borewells is slightly elevated (~1-2°C) compared to the dug wells. The solarised metallic casings (in general Ø=8") conduct the heat from the surface towards the relatively small water volume stocked inside.

Tab. 5.1 gives an overview about the population statistics of measured water temperatures for all sampling campaigns. Correlation of water against air temperature (Fig. 5.1) showed only a small but positive correspondence ($r^2=0.3$). The water temperature principally depends on the general climatic conditions during the sampling period and not from any inflow from another hydrogeological background as it might be suspected in a fractured environment.

Tab. 5.1: Population statistics of temperature measurements.

	water temperature (°C)
Number	246
Mean	29.49
Median	29.5
St. dev.	1.48
Minimum	25
Maximum	35.7

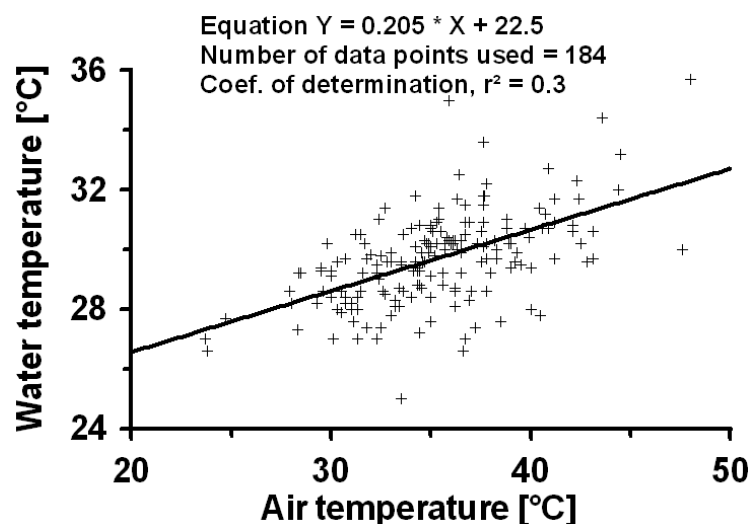


Fig. 5.1: Determination of correlation between air and water temperature.

5.1.2 pH

The pH besides redox potential and water temperature controls the solubility of many agents in groundwater. It further influences the ion exchange and the sorption capacity of

the surrounding rock. The value of pH ranges for the borewells from 5.7 to 7.47 and for the dug wells from 5.43 to 8.03 (see Fig. 5.2).

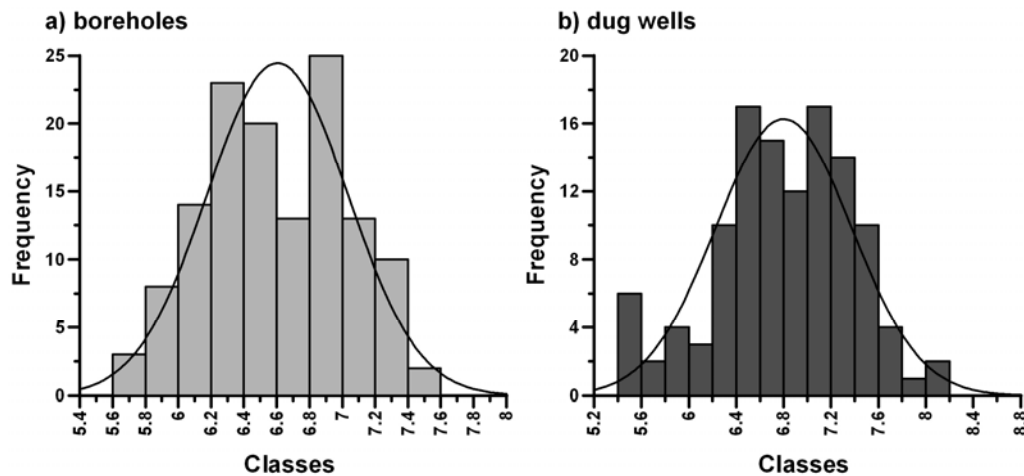
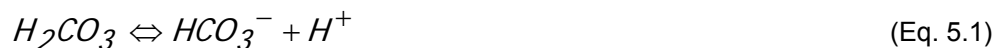


Fig. 5.2: pH data of boreholes (a) and dug wells (b) presented respectively in histograms.

A pH around 7 is generally typical for rainwater, and may indicate recently infiltrated recharge or just perched shallow aquifers. Changes of pH values in natural waters are often caused by different contents of carbonic acid. Bicarbonate in water buffers the acid and equilibrates the pH within the range of 5.5 to 8.0 (HÖLTING 1996). When $\text{pH} < 5.5$ silicates, like feldspar and clay minerals, may work as buffers. The buffering consumes H^+ . The content of H_2CO_3 declines and HCO_3^- increases. The reaction follows the simplified equilibrium reaction:



Precipitation is in equilibrium with atmospheric CO_2 which has a partial pressure of $10^{-3.5}$ atm. Due to microbial reactions the soil zone holds more CO_2 . Typical partial pressures of CO_2 achieved in the soil zone are $10^{-2.0}$ to $10^{-1.5}$ atm (DREVER 1997).

A higher content of CO_2 in the groundwater increases the solubility of CaCO_3 . Thus more HCO_3^- dissolves. For each partial pressure pCO_2 a certain relationship of pH/HCO_3^- is achieved. Fig. 5.3 demonstrates the relationships for 3 different pCO_2 . The curve for atmospheric pCO_2 shows a gradual increase of bicarbonate only for higher pH values. This scatter plot gives a general footprint for recharge mechanisms in the study area. Most of the samples are from different sources and taken during different seasons and plot around the curves of the typical pCO_2 in soil zones. This means that all sampled water passed through the soil zone.

If groundwater is directly recharged from the surface, for example by open fractures, the samples would plot closer to the curve for $\text{pCO}_2 = 10^{-3.5}$ atm. If groundwater travelled a rather long passage under higher pCO_2 conditions the scatter of points would be below the soil zone pCO_2 relationships.

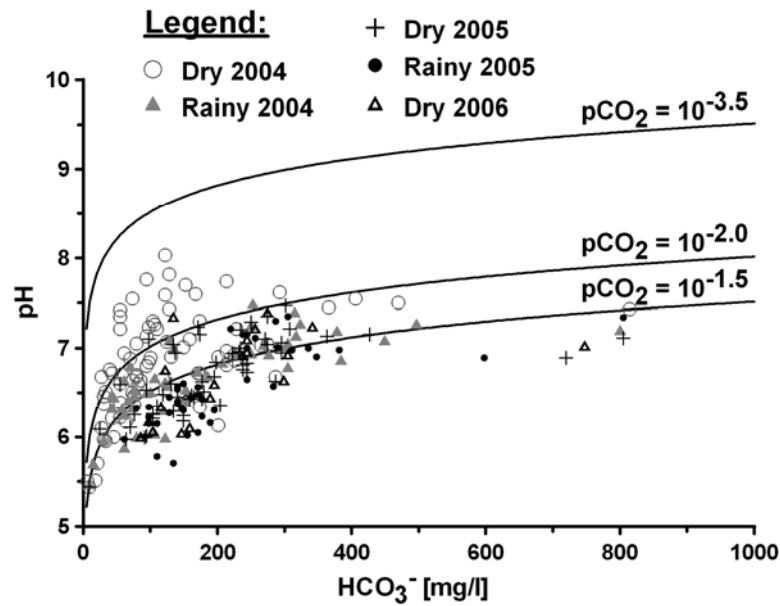


Fig. 5.3: Plot of pH and bicarbonate from all sample campaigns. Curves show the pH-bicarbonate relationship for partial pressures of CO_2 in the atmosphere ($10^{-3.5}$) and for the soil zone (2 examples: $10^{-1.5}$ and $10^{-2.0}$).

5.1.3 Electrical conductivity

During sampling it was recognised that the electric conductivity (EC) at most locations did not change during the seasons (see Chapter 5.3). At some dug wells relatively high values are measured (800 to >1500 $\mu\text{S}/\text{cm}$). This behaviour is observed at these points for all seasons. The same is seen for nearby borewells. EC ranges for borewells from 92 to 1780 $\mu\text{S}/\text{cm}$ and for dug wells from 10 to 1725 $\mu\text{S}/\text{cm}$. The histograms a) and b) in Fig. 5.4 do not show a clear Gaussian normal distribution for all samples. In each of the histograms a second population appears with typically higher charges. The possible extend of the two additional population is marked by circles.

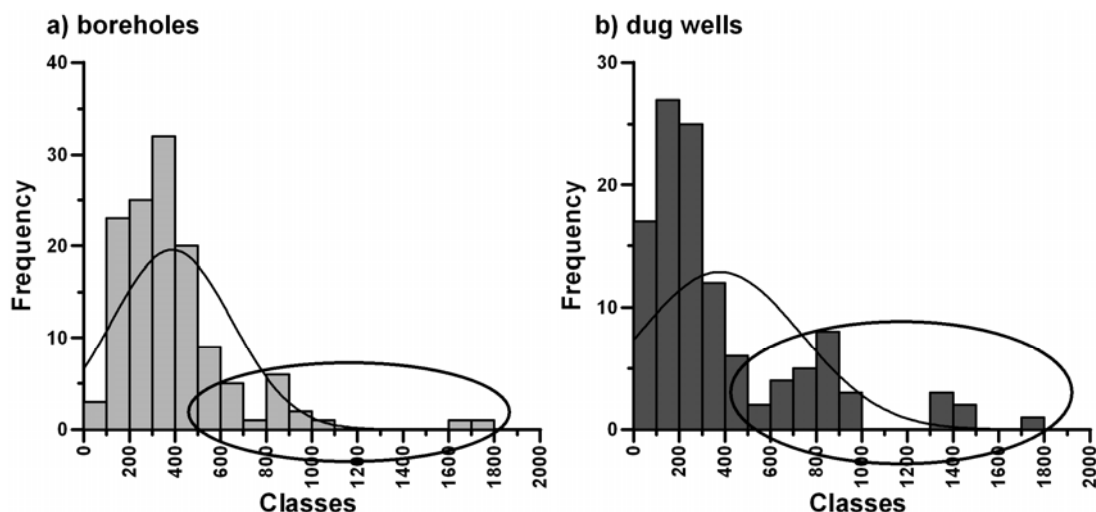


Fig. 5.4: EC data of boreholes (a) and dug wells (b) presented respectively in histograms.

This picture demonstrates that the source for the higher charge must be in the regolith aquifer wherefrom groundwater infiltrates the bedrock.

5 Hydrochemistry

The data sets for the dug wells and the boreholes were regionalised by kriging (Fig. 5.5a and Fig. 5.5b). From multiple measurements at the same point only the median EC value was included. The variogram includes a nugget effect of 10 and an exponential model. The comparison of the data shows that elevated EC appears more often in wells. But it is seen as well that the higher charged boreholes are situated where already higher electric conductivities in wells were measured.

Higher EC values appear especially in the South of the study area. This area includes the villages of Dogué, Wari-Maró, Ouannou and Kikélé. While in Dogué, Wari-Maró and Ouannou the high conductivity is observed in borewells too, in Kikélé and Igbomakoro (a village next to Dogué with a handpump) instead no increase of EC in the pumps is observed. It seems that not in all villages higher charged groundwater from the regolith aquifer infiltrated towards the bedrock. These findings will be discussed in Chapter 5.2.

The case of Sonoumoun is discussed in Chapter 5.4.3. At Kori the regolith layer is very thin (<5 m). Contamination from the surface might pass to the bedrock rather fast. Increased concentration at the pump of Séróu might have geogenic origins in regard to its hydrochemical composition (see Annex 1 and Fig. 5.24).

A map generated by kriging of EC measurements taken from the BDI shows that southward of the HVO the EC is generally elevated (see Fig. 5.6). Especially around Dassa and in its South the EC values are higher. The reason for it is a thinner regolith and thus a direct contamination of groundwater due to human activities. The South of the HVO instead is characterised by very thick regolith. At Dogué the regolith is thicker than 20 m. The elevated EC might be caused by a special hydrochemical environment (Chapter 5.2.3).

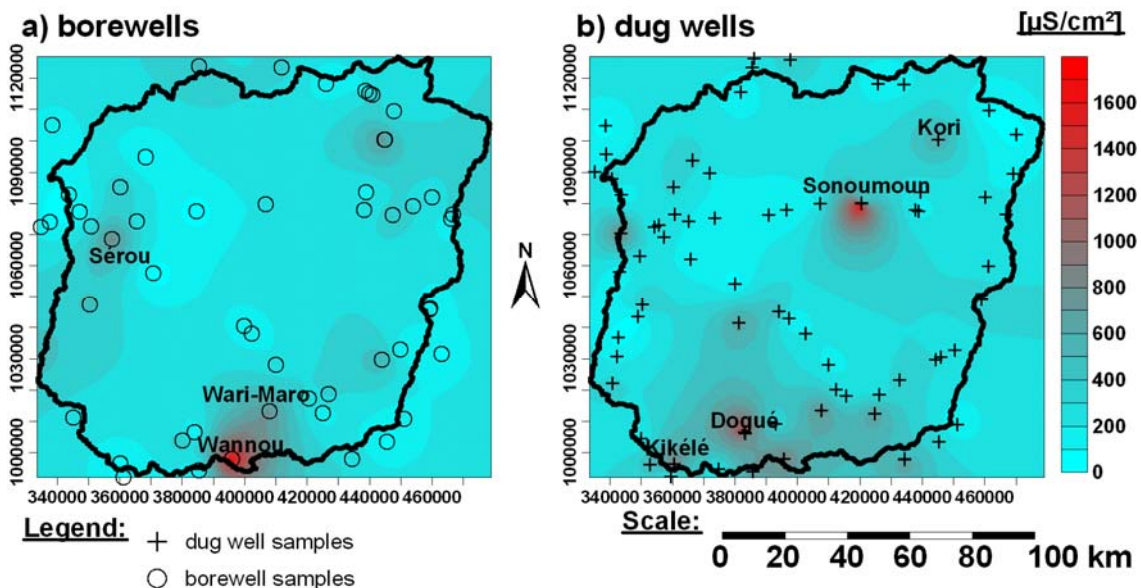


Fig. 5.5: Regionalised EC data for the (a) bedrock aquifer and for the (b) regolith aquifer (Projection: UTM, Zone 31P, WGS 84).

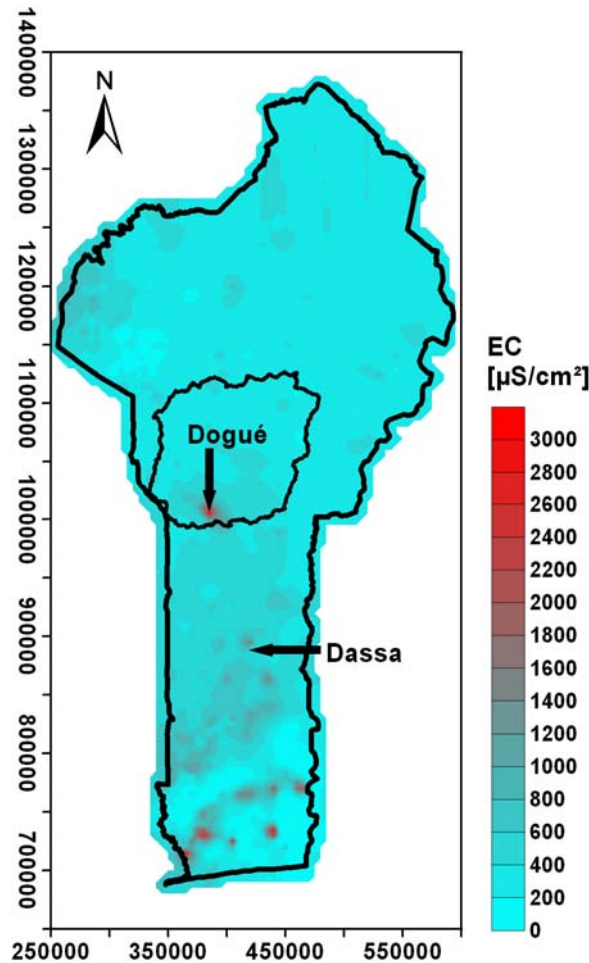


Fig. 5.6: Kriging of EC measurements made on borewells after completion of the drilling phase (Source: BDI) (Projection: UTM, Zone 31P, WGS 84).

5.1.4 Redox potential

Redox levels in groundwater are mostly determined by the quantity of oxygen and nitrate, by pH and by the relation of the redox couples ($\text{Fe}^{2+}/\text{Fe}^{3+}$, $\text{Mn}^{2+}/\text{Mn}^{3+}$, $\text{S}^{2-}/\text{SO}_4^{2-}$). The most important variables (after DREVER 1997) in natural systems are therefore:

- Oxygen content of recharge water.
- Distribution of potential redox buffers in the aquifer. The redox levels in groundwater often corresponds to buffering by the redox pairs $\text{Mn}^{2+}/\text{MnO}_2$, $\text{Fe}^{3+}/\text{FeOH}_3$, or $\text{Fe}^{2+}/\text{Fe}_2\text{O}_3$.
- Circulation rate of the groundwater. The pe of groundwater depends very much on its residence time in the aquifer. Longer residence time causes a lower pe.

The electron activity can be expressed in units of volts (Eh) or in units of electron activity (pe). Eh [V] and pe [-] are related by the equation:

$$pe = \frac{F}{2.303 \cdot R \cdot T} \cdot Eh \quad (\text{Eq. 5.2})$$

F = Faraday's constant (96.484 KJ)

T = Temperature [K]

R = gas constant [8.314E-03 kJ/K*mol]

At 25°C pe can be approximated by:

$$pe = 16.9 \cdot Eh \tag{Eq. 5.3}$$

The scatter (Fig. 5.7) of oxygen measurements against the redox potential as electron activity (pe) reveals a rather good correlation ($r^2 = 0.84$).

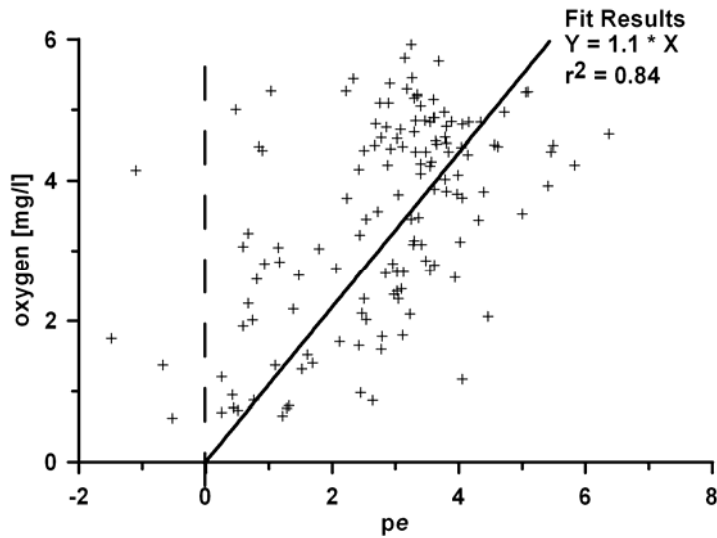


Fig. 5.7: The oxygen content plotted against the redox potential.

Almost all samples from ground and surface water show Eh values of generally oxidising conditions (compare with Fig. 5.8). 4 samples showed negative values. All of them are borewells (D04-H-ANM-1, R05-H-OUB-P, D06-H- WEWE -P, D06-H-BET-P). The borehole at Ouberou (OUB-P) is defect since a long time. The water is already ochre because of corrosion. Its water must be stagnant and not very well aerated. This sample is excluded from further interpretation.

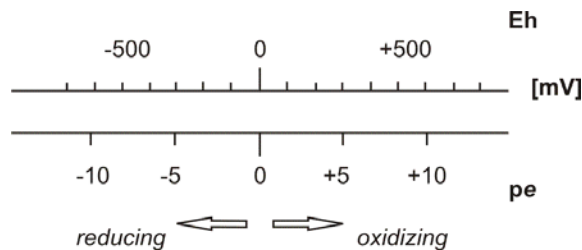


Fig. 5.8: Redox potential and pe range encountered in natural systems at near-neutral pH (modified from SIGG 1999).

The other three borewells are regularly used. They show negative values only during the dry season. But Tab. 5.2 a) - d) demonstrates that there is no typical trend towards low redox potentials during the dry seasons. Borewells and dug wells may even show the opposite behaviour. Possibly the three borewells were still fed by water stored in extended fractures with less oxygen contents before being recharged by fresher water from the regolith aquifer.

The redox electrode needs a long time to stabilise during the measurement. SIGG (2000) showed that only the use of a comparing electrode, e.g. hydrogen, in the laboratory deliver reasonable redox values. The influence of atmospheric oxygen, which can modify

the redox potential, cannot be excluded during field measurements (KÄSS and SEEBURGER 1989).

Tab. 5.2: Population statistics of redox measurements in the study area for boreholes (a+c) and wells (b+d) for the dry seasons and for the rainy seasons.

a) Dry season		b) Dry season	
<i>boreholes</i>		<i>wells</i>	
Number	66	Number	85
Mean	140.8	Mean	197.6
Median	139	Median	201
Modus	224	Modus	225
st. Dev.	92.8	st. Dev.	73.6
Minimum	-65	Minimum	28
Maximum	320	Maximum	377
c) Rainy season		d) Rainy season	
<i>boreholes</i>		<i>wells</i>	
Number	63	Number	30
Mean	138.1	Mean	154.2
Median	148	Median	155
Modus	180	Modus	182
st. Dev.	66.9	st. Dev.	53.7
Minimum	15	Minimum	51
Maximum	264	Maximum	255

5.1.5 Oxygen

The mean and the median values of oxygen of well samples for all sampling campaigns are higher than those for the borehole samples (see Tab. 5.3). In wells and boreholes groundwater remains rather stagnant under constant exchange with the atmosphere. Thus oxygen contents at these places are barely representing conditions in the aquifer. Whirling and ventilation occur during pumping and drawing of the water by the villagers. This might be the reason why no further correlations between oxygen and other measurements or chemical constituents were found. Oxygen was not regarded for further investigations.

Tab. 5.3: Population statistics of oxygen measurements of boreholes (left) and wells (right).

boreholes	content	saturation	wells	content	saturation
	[mg/l]	[%]		[mg/l]	[%]
Number	67	67	Number	73	73
Mean	2.33	31.39	Mean	4.58	63.89
Median	2.43	33	Median	4.61	66
St. dev.	1.05	14.34	St. dev.	0.69	10.64
Minimum	0.62	8.4	Minimum	2.01	26.4
Maximum	4.62	65.7	Maximum	5.93	82.3

5.2 Hydrochemical parameters

5.2.1 Distinction of hydrochemical groups

Due to the field conditions and the lack of technical data it was concluded that dug wells penetrate only the regolith aquifer while the borewells tap water from fractures in the bedrock. The measurements of the electrical conductivity (Chapter 5.1.3) revealed that the groundwater from each aquifer is not normal distributed. A number of samples from both aquifers showed a relatively high conductivity which might be caused by a different hydrochemical environment. In order to describe the different chemical characteristics from each aquifer it was necessary to distinguish between samples with a common lower EC and those with elevated EC.

The results of rang analysis (Fig. 5.9) for dug well samples and for borewell samples plot in the beginning as smooth curves. Both curves have a steep slope after the turning point at 450 $\mu\text{S}/\text{cm}$.

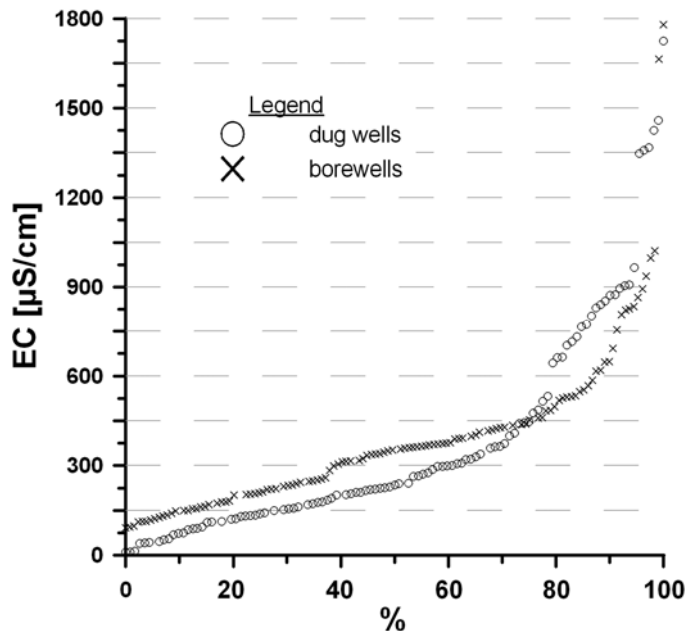


Fig. 5.9: Rang distribution in percent of all electric conductivity measurements for dug wells and borewells made in the field during the period of 2004 to 2006.

The dug well samples plot generally lower than the bedrock samples. But above the inflexion point at $\sim 75\%$ (dug wells) and at $\sim 80\%$ (borewells) respectively, it is seen that the higher charge is principally found in the regolith aquifer. However the maximum EC values are for both groups similar.

The samples above the inflexion points are assigned to a so-called group 3. Comparatively, the revised samples from dug wells are called group 1 and the revised borewell samples are called group 2 (see Tab. 5.4). In Chapter 5.3 it is explained that some samples from the regolith aquifer (Group 1) show a strong precipitation signature. They are discarded from the group 1 samples.

As described in Chapter 5.1.3, anthropogenic contamination is the reason for high charges at some locations (Kori, Sonoumoun). Typically, human influence on

groundwater quality is marked by elevated nitrate and chloride values. Samples with excessive nitrate ($\text{NO}_3^{2-} > 100 \text{ mg/l}$) are excluded from group 3 (see Tab. 5.5).

Additionally it was necessary to exclude 5 samples (Tab. 5.6) from group 2. They are borewells which were already suspicious during sampling because of either low redox values or very high iron and manganese concentrations. All of these borewells were visibly old and people complained about its smell and taste. It appears that corroding casings or clogged filters have changed sufficiently the quality of the water tapped in these boreholes.

Tab. 5.4: Assignment of aquifers to sample groups.

Group	Groundwater	Source	Seasons
1	regolith*	dug wells	all
2	bedrock	borewells	all
3	regolith + bedrock	dug wells + borewells	all

*Samples with strong precipitation signature were discarded.

The map in Fig. 5.10 shows the distribution of the group samples. Most samples from group 3 are taken in the southern part of the HVO. In group 3 dug wells plot generally higher than the borewells (Fig. 5.9). This may indicate that the origin for this higher charge is to be found in the regolith itself, either by contamination from the surface or by special hydrogeochemical conditions.

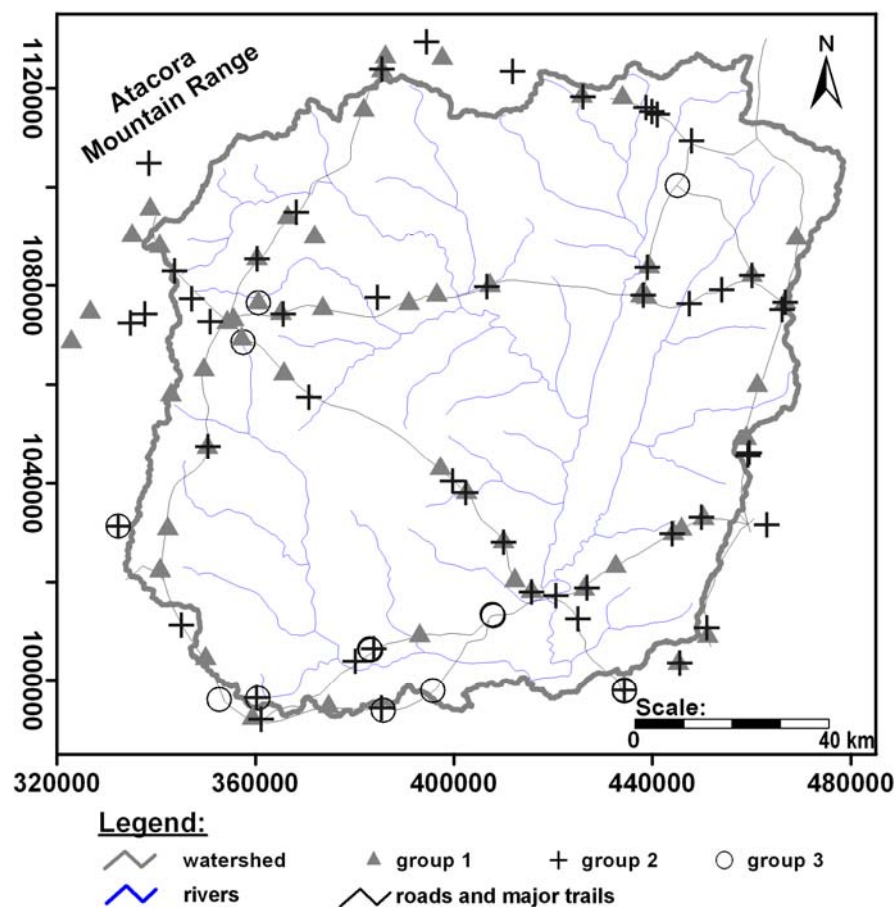


Fig. 5.10: The distribution of all hydrochemical groups in the study area (Projection: UTM, Zone 31P, WGS 84).

5 Hydrochemistry

Tab. 5.5: Samples excluded from group 3 because of too high grades of contamination.

Sample*	Location	X UTM	Y UTM
D04-W-BANI-1	Banigri	424768	1012407
R04-W-BANI-1	Banigri	424768	1012407
D06-W-BDOG-1	Dogué	383221	1006210
D04-W-DAR-1	Daringa	393970	1045257
D04-H-KAR-1	Kari	444818	1100288
D05-W-KAR-2	Kari	445010	1100335
D05-H-OUN-P	Ouannou	395894	997902
R05-H-OUN-P	Ouannou	395894	997902
D05-F-PRE-1	Pérére	499279	1083351
D04-W-PELE-1	Pélébina	350353	1047339
D05-W-PELE-1	Pélébina	350353	1047339
R05-H-SEB-P	Sébou	443940	1029716
D06-H-SEB-P	Sébou	443940	1029716
D04-W-SON-1	Sonoumoun	420434	1079934
D05-W-SON-3	Sonoumoun	420535	1080105
R04-W-TAR-2	Tamarou	466791	1076529

Tab. 5.6: Samples excluded from group 2.

Sample*	Location	X UTM	Y UTM
D04-H-ANM-1	Anoum	334784	1072403
D05-F-GNG-1	Guingamou	494107	1057124
R05-H-IGER-P	Igbéré	385405	994399
R05-H-KPS-P	Kpéssou	409973	1028012
R05-H-OUB-P	Ouberou	415657	1018023

5.2.2 Hydrochemical characteristics of the groundwater in the HVO

Recharge for all hydrochemical groups in the HVO area originates in precipitation (see also Chapter 6). Percolating downward towards the bedrock, the recharged water alternates progressively with increasing depth. The change is generally so smooth that clear hydrochemical boundaries cannot be drawn. In order to describe the general composition of each hydrochemical group population statistics were taken (Tab. 5.7).

Tab. 5.7: Population statistics of the hydrochemical parameters for each group (see Annex 1).

Group 1	pH	EC [µS/cm]	HCO ₃ ⁻ [mg/l]	Cl ⁻ [mg/l]	SO ₄ ²⁻ [mg/l]	NO ₃ ²⁻ [mg/l]	PO ₄ ³⁻ [mg/l]	SiO ₂ [mg/l]	Na ⁺ [mg/l]	K ⁺ [mg/l]	Ca ²⁺ [mg/l]	Mg ²⁺ [mg/l]	Fe _{total} [mg/l]	Mn ²⁺ [mg/l]
Min	5.43	85	9.15	0.38	0	0	0.074	4.79	3.08	1.19	6.6	0.55	0	0.006
Max	7.76	409	244	56.45	30.71	105.47	2.175	54.44	50.5	39.14	50.96	21.06	0.745	1.75
Mean	6.76	206	94.55	5.43	2.3	6.66	0.715	30.3	14.71	4.12	22	4.98	0.06	0.034
Median	6.8	215.71	97.25	10.08	3.48	18.39	0.94	29.93	14.84	5.46	21.49	6.05	0.093	0.081

Group 2	pH	EC [µS/cm]	HCO ₃ ⁻ [mg/l]	Cl ⁻ [mg/l]	SO ₄ ²⁻ [mg/l]	NO ₃ ²⁻ [mg/l]	PO ₄ ³⁻ [mg/l]	SiO ₂ [mg/l]	Na ⁺ [mg/l]	K ⁺ [mg/l]	Ca ²⁺ [mg/l]	Mg ²⁺ [mg/l]	Fe _{total} [mg/l]	Mn ²⁺ [mg/l]
Min	5.7	92	61	0.4	0.275	0.275	0.015	7.83	9.9	2.4	6.1	1.12	0	0.0025
Max	7.47	567	335.5	49.7	22.69	108.3	5.2	49.13	31	18	71	36	3.3	0.882
Mean	6.48	324	161.65	3.3	1.7	0.39	0.67	32.77	16.3	5.6	30	10	0.55	0.033
Median	6.56	306	174.35	8.2	2.94	12.5	0.77	32.55	17.3	5.7	31.57	11.95	0.6	0.085

Group 3	pH	EC [µS/cm]	HCO ₃ ⁻ [mg/l]	Cl ⁻ [mg/l]	SO ₄ ²⁻ [mg/l]	NO ₃ ²⁻ [mg/l]	PO ₄ ³⁻ [mg/l]	SiO ₂ [mg/l]	Na ⁺ [mg/l]	K ⁺ [mg/l]	Ca ²⁺ [mg/l]	Mg ²⁺ [mg/l]	Fe _{total} [mg/l]	Mn ²⁺ [mg/l]
Min	6.68	446	228.75	9.11	3.87	3.7	0.043	9.88	20.48	3.19	35	18.9	0	0.01
Max	7.62	1458	814.35	110.2	160.4	95	2.11	38.5	149.9	96	125.7	81	0.47	0.57
Mean	7.13	835	347.7	43.66	34.5	35.86	0.57	27.57	41.1	12	71	31.83	0.03	0.046
Median	7.13	883.74	409.3	55.65	43.64	46.53	0.69	26.23	61.33	20.06	74.97	38.8	0.07	0.13

In Fig. 5.11 the box plots for EC measurements from group 1 (dug wells in the regolith) and group 2 (borewells in the bedrock) are compared. The 25- and the 75-percentile of each plot cover mostly the same range of EC. This picture is conclusive as the groundwater of both aquifers has the same source. The median of group 1 is lower than for the group 2. This is explained by the dilution of regolith groundwater by fresh rainwater, while Bedrock groundwater prevails in the fractures and gets more concentrated.

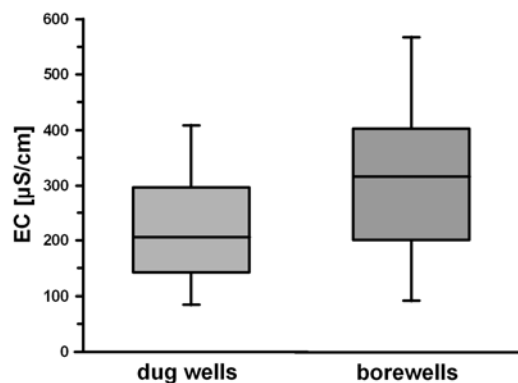


Fig. 5.11: Whisker-Box-Plot for the electric conductivity measured from dug wells and borewells.

The plot of all three groups into a Piper diagram shows very well their overlapping hydrochemical characteristics (Fig. 5.12). Groundwater in the HVO is generally of a Na-Ca-(Mg)-HCO₃ type and is rich in silicon. This type of water is typical for shallow groundwater systems in crystalline areas (SINGHAL and GUPTA 1999). With increasing depth an increase of magnesium is observed. Any other differentiation is at least hidden.

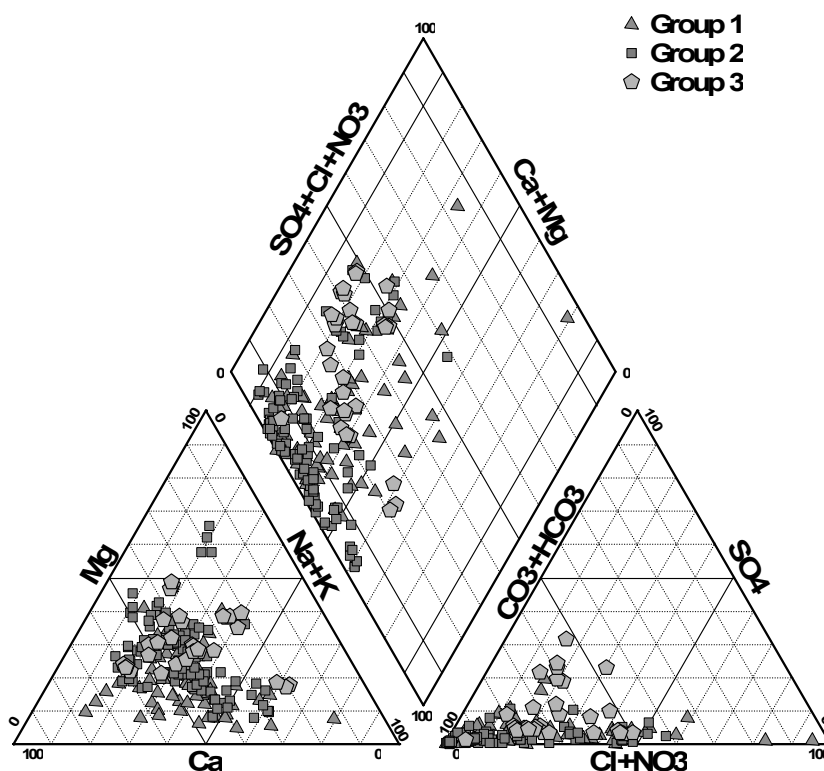


Fig. 5.12: Piper plot of all three hydrochemical groups in the HVO.

The Schoeller diagram (Fig. 5.13) shows the original rainfall composition in relation to the designed hydrochemical groups. It is striking that the sulphate concentration for group 1 and group 2 equals that of the precipitation. The general hydrochemical facies of precipitation, group 1 and group 2 are comparable and represent the dissolution of mineral phases during the downward percolation of groundwater.

The ionic make-up of groundwater is driven by weathering reactions and is controlled by the pCO₂ of the recharge water (HUTCHINGS and PETRICH 2002). Plagioclase feldspars, biotite, and other dark minerals weather more rapidly than K-feldspars or quartz (APPELO and POSTMA 1999; HUTCHINGS and PETRICH 2002).

Potassium and magnesium are derived primarily from biotite (HUTCHINGS and PETRICH 2002). Chloride and sulphate are not dissolved by silicate weathering but generally indicate mixing of water from other sources (see Chapter 5.2.3). The concentration of dissolved silicon depends almost entirely on the weathering of plagioclase and related minerals. Kaolinite is the first alteration product formed by silicate weathering.

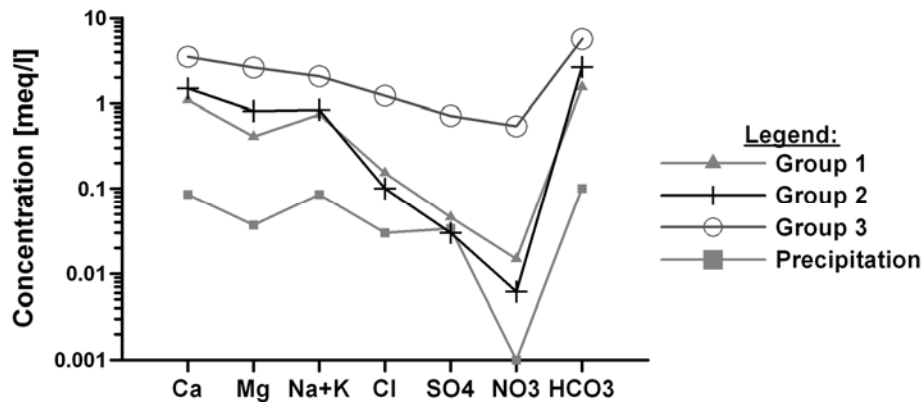


Fig. 5.13: Schoeller diagram of the median group composition.

Analysis results show that the dominating anion is bicarbonate whose amount is directly dependant from the availability of organic substances and the pH of the precipitation water.

Fresh precipitations are generally slightly acidic. A decrease in pH will weather albite to gibbsite and then to kaolinite. When the water remains stagnant then Na-montmorillonite is formed. The leaching effect depends on the intensity of the rainfalls. Stronger leaching links to kaolinite while less rainfall plots towards the montmorillonite zone (APPELO and POSTMA 1999). Leaching forms kaolinite in the surface layers. This is well demonstrated by the milky coloured water of surface runoff, rivers and shallow dug wells.

Hydrochemical analyses made at the Nalohou test site (UTM 347124/1077311) shows that under a slightly acid pH more Al^{3+} is dissolved (Fig. 5.14). Under neutral pH conditions in the deeper regolith Al^{3+} gets less soluble. It is assumed that the remaining aluminium remains in the weathering product. The charge of the dissolved cations must be balanced with H^+ .

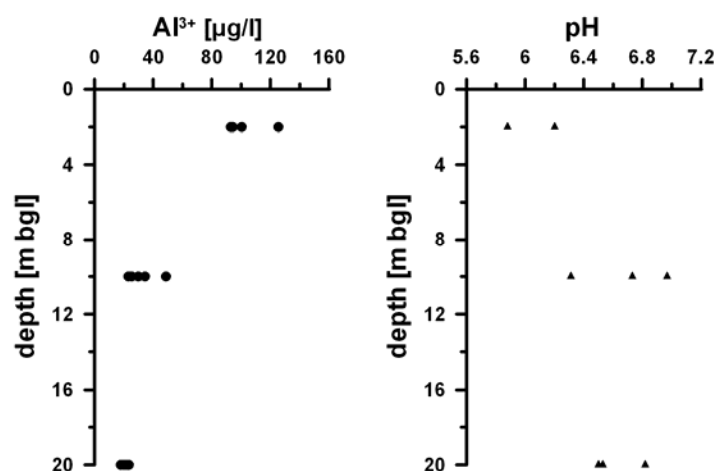


Fig. 5.14: Change of the aluminium concentration in relation to pH with increasing depth (with the kind permission of Luc Séguis, IRD 2007) at Nalohou test site (UTM 347124/1077311). Site description: 3 boreholes with different filter depths at 2 m, 10 m and 20 m.

Influences of rock and soil types are hardly to be found in seepage water and phreatic groundwater regardless of the differences in climate or vegetation (LOEHNERT 1988). Maturation occurs within the saturated zone in which groundwater composition might be affected by the rock nature.

5 Hydrochemistry

A high CO₂ content related to a decrease of pH causes an accelerated silicate weathering with an increasing HCO₃⁻-value. The hydrolysis of silicates liberates the cations Na⁺, K⁺, Ca²⁺, Mg²⁺ and Fe^{2+/3+}. Additionally, a higher partial pressure of CO₂ increases the solution of Ca- and Mg-carbonates (STOBER 1995). Sodium and silicate dioxide are less absorbed by plant roots and are hence relatively enriched in groundwater against other cations. The modification of the Ca²⁺/Mg²⁺-ratio at the expense of the latter is not observed in the unsaturated zone and is definitely established in the saturated zone (ROOSE and LELONG 1981).

The deeper the fractures the deeper groundwater can enter the massif. Groundwater flow in hydrogeological massifs is exclusively connected to fractures and faults. Especially the silicate dioxide content can be used to describe the deep circulation of waters. The plots of Fig. 5.15a) and b) show the relatively similar silicon concentration in all three groups. Group 1 shows the widest range of scatter which is caused by dilution in shallower zones and as well by the very heterogeneous build up of the dug wells. Fig. 5.15a) and b) shows that group 3 has the highest chloride and calcium concentration but does not differ in its silicon concentration.

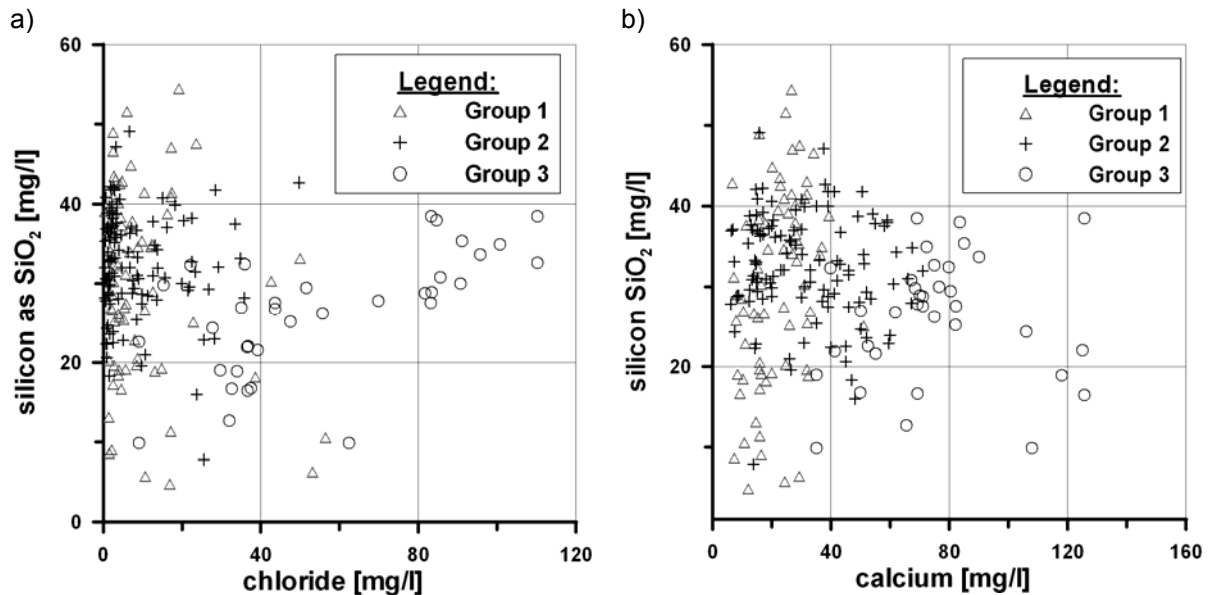
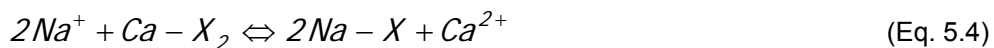


Fig. 5.15: a) Plot of silicon against chloride and b) plot of silicon against calcium.

Group 2 is the most homogeneous. Its samples scatter mostly in a well limited area for most of the presented diagrams. Fig. 5.16a) shows that the concentration of sodium in group 2 is rather constant, while chloride gets relatively concentrated. Both groups 1 and 3, instead, show a relative increase of the two parameters. On the other hand it is seen as well in Fig. 5.16b) that sodium stays in constant concentration against calcium. The relationship Na/Ca is roughly interpreted as 1:2 and can be explained by ion exchange on clay minerals as represented by Eq. 5.4:



Montmorillonite is a typical agent for ion exchange. The observed changes of the concentration of calcium and sodium are probably caused by the following ion exchange reaction (Eq. 5.5) from Ca-montmorillonite to Na-montmorillonite.

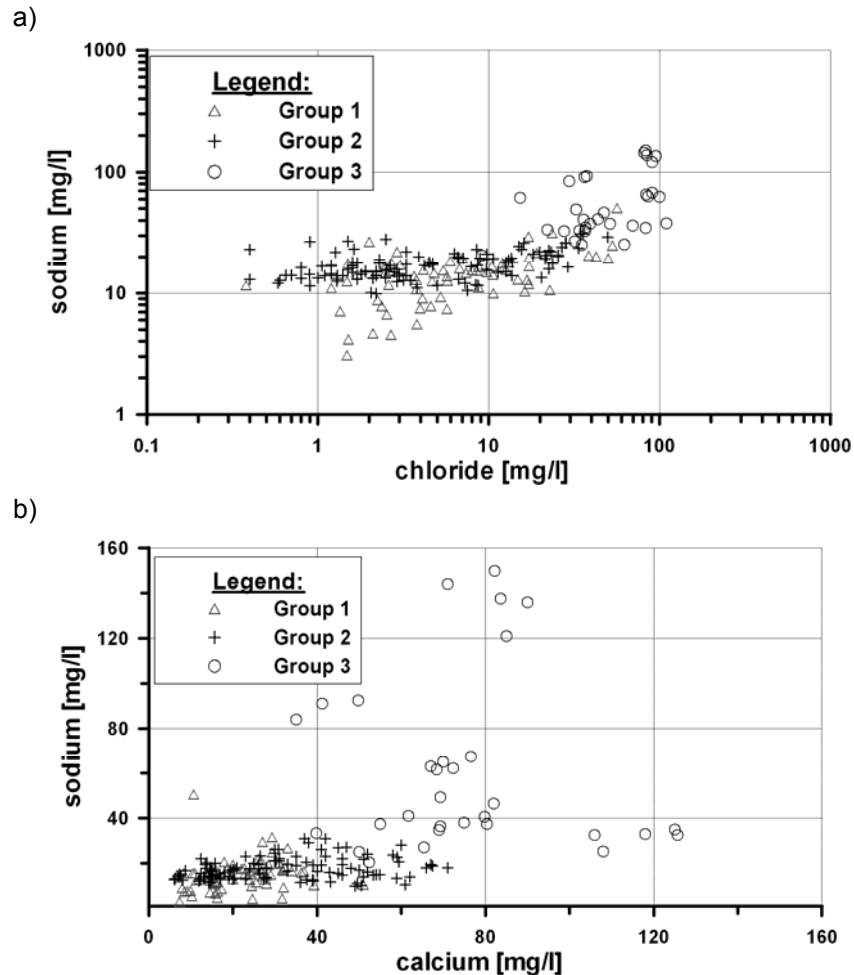
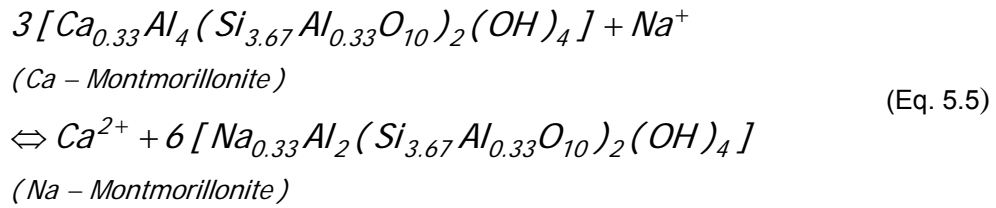


Fig. 5.16: Scatter diagrams of sodium against chloride (a) and against calcium (b).

5.2.3 Discussion of group 3 – the southern province

As the median concentration for all major ions of group 3 is elevated (Fig. 5.13), it is suggested that besides anthropogenic contamination (high concentrations of anions) a special hydrochemical environment exist. The increase of magnesium and calcium is considerable and suggests long residence times of the groundwater. The highest concentrations were found in dug wells, while borewells close to the same were either not affected or mostly to a lesser degree. It is therefore concluded that the hydrochemistry of group 3 is originally under influence from the regolith aquifer.

Most of the samples from group 3 belong to the southern part of the HVO (Fig. 5.10). This regional concentration and the often observed thick regolith layer (>20 m thickness) point at geogenic origins for the elevated EC.

The general thickness of the regolith was interpolated from BDI borehole logs all over the HVO. The resulting map in Fig. 5.17 demonstrates roughly the increased thickness of the

regolith in the southwestern part of the HVO. The map indicates as well thicker regolith layer to the East of the HVO. The groundwater samples from the townships of Nikki and Péréré in the East and outside of the HVO are part of group 3. The direct correlation between regolith thickness and ionic charge, however, is not conclusive as the sampled dug wells of group 3 have different depths and do not always penetrate the whole of the regolith. The eventual siting of boreholes in fracture fillings cannot be determined from the available data.

Group 3 is observed on different rock types and geological series (Fig. 3.19) and though any geogenic influence of bedrock geochemistry is for a start widely excluded.

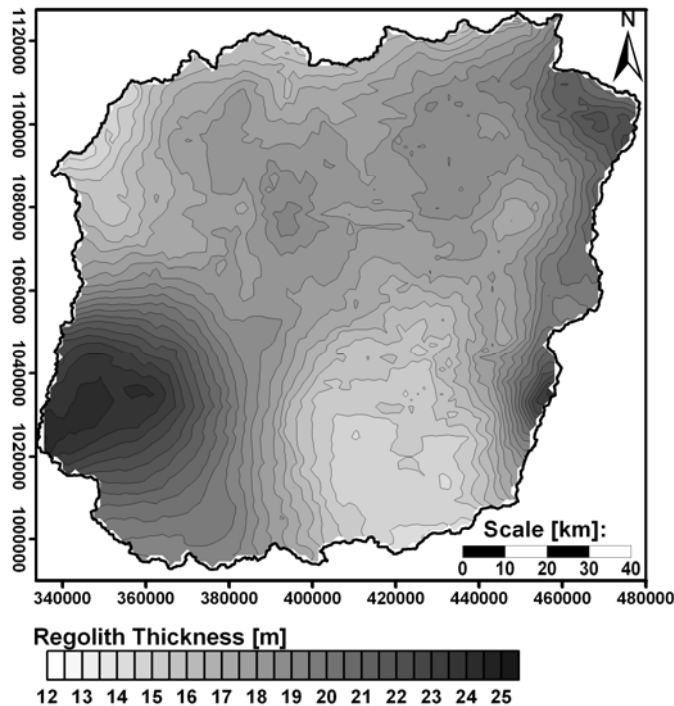


Fig. 5.17: Interpolation of regolith thickness from BDI data (Projection: UTM, Zone 31P, WGS 84). Kriging was done with an exponential variogram.

Stability diagrams computed from ion activities with the software PhreeqC (PARKHURST and APPELO 1999) showed that group 3 plots mostly in the field for Na-montmorillonite. But once more the strong overlapping between all groups is seen (Fig. 5.18) and, partly, samples from the other groups are placed in the same field too. The Na-montmorillonite stability field is an indicator for stagnant or slowly moving water. The kaolinite field is typical for fast flow and groundwater table variations causing a rather fast weathering and transport of dissolved components (APPELO and POSTMA 1999).

TAYLOR and EGGLETON (2001) subdivide the saprolite zone into a succession of layers of different weathering characteristics. At the top, the zone of groundwater table fluctuations is described as kaolinitic. Below this kaolinite zone the saprolite remains saturated without any change. Weathering is slower but very intense and forms as dominant clay mineral montmorillonite.

Some of the group 3 samples belong to dug wells whose depth is definitely below the range of groundwater fluctuations (depth >15 m) they belong certainly to the Na-montmorillonite zone.

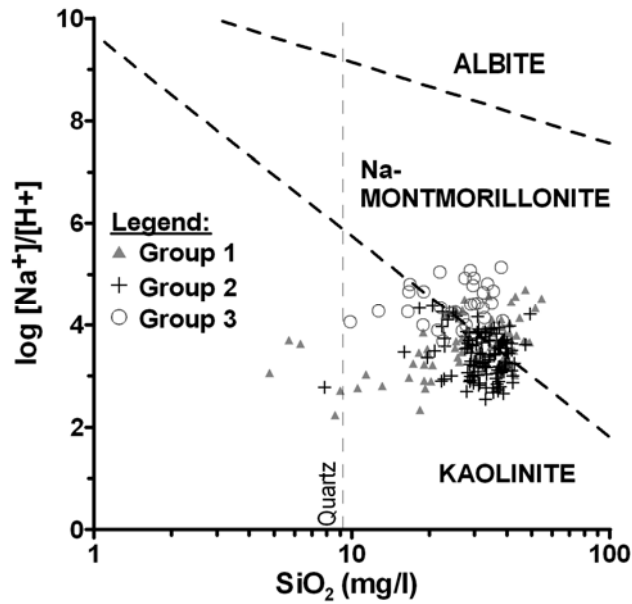


Fig. 5.18: The stability diagram for albite and its weathering products kaolinite and Na-Montmorillonite.

The kaolinite-montmorillonite reaction quotient for the hydrochemical data exhibit a sharp increase from about -10 (precipitation) to more than $+12$ (dug wells) (Fig. 5.19). This means that most of the dug well samples achieved an equilibrium with a single weathering product (kaolinite) but tend already to a horizontal asymptote where an equilibrium exists between kaolinite and montmorillonite (GARRELS 1967). The picture is the same for Ca- and Na-montmorillonite. The first conclusion drawn is that recharge only contributes to a lesser extent to the regolith hydrochemistry. Most of the infiltrating precipitation does, finally, not meet the groundwater body. A second conclusion is that group 3 is not influenced by ion exchange as mentioned for group 2.

If we take it as a typical pattern that the majority of group 3 is placed in the Na-montmorillonite field still some questions remain open. Stagnant water should be relatively older. Tritium analysis (Chapter 6.3) has not shown an important increase in water age with rising depth within the regolith. Therefore it is difficult to say that groundwater of group 3 would be older than those of the other groups. The high share of nitrate and chloride due to contamination demands supply of contaminated water in order to maintain the nitrate input. Nitrate is not stable under the current groundwater conditions (see Chapter 5.4.3).

The high contents of sulphate in group 3 derive either from human input or by the pyrite oxidation. Pyrite (FeS_2) is found in traces in many types of crystalline bedrock facies and dykes and is possibly oxidised to sulphate. Sulphate concentrations vary widely in group 3. Only 2 (H-PTA-1 and H-SER-P) wells show constantly elevated concentrations twice as high as for the rest of this group. The correlation between chloride and sulphate in Fig. 5.20 shows a clear linear trend for all groups. Thus, the sulphate concentration may have been caused by contamination.

On the other hand it is principally among the samples from group 3 that elevated fluoride occurs (see Chapter 5.4.2). Weathering of basement rocks under stagnant groundwater conditions and ion exchange releases fluoride what is affirmed by the explicative approach made in this chapter.

5 Hydrochemistry

Further considerations about the hydrochemistry of group 3 will rest assumptive as the level of contamination obscures the natural signals.

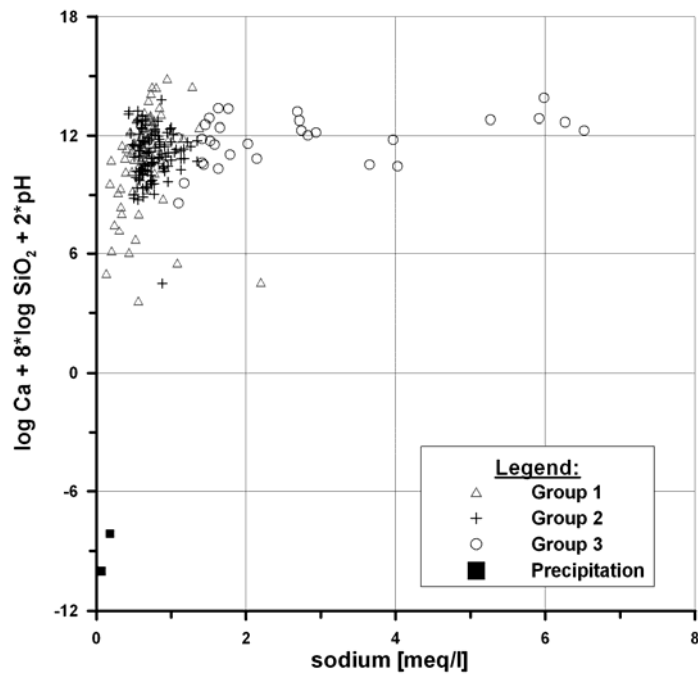


Fig. 5.19: Changes in the kaolinite-montmorillonite reaction quotient for the hydrochemical groundwater groups in the HVO (modified after GARRELS 1967).

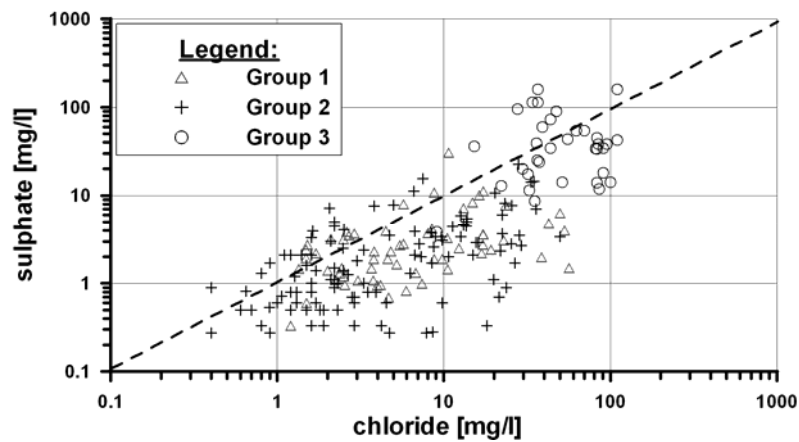


Fig. 5.20: Correlation diagram of sulphate against chloride. The dashed line represents a 1:1 relationship for both constituents.

5.3 Seasonal variations

The hydrochemical analyses from all campaigns and independent from any group affiliation were screened for seasonal changes caused by precipitation and/or evaporation. The plot of all seasonal data in Gibb's diagrams (see Fig. 5.21) revealed that the influence of precipitation and evaporation on groundwater chemistry is generally low for most of the samples.

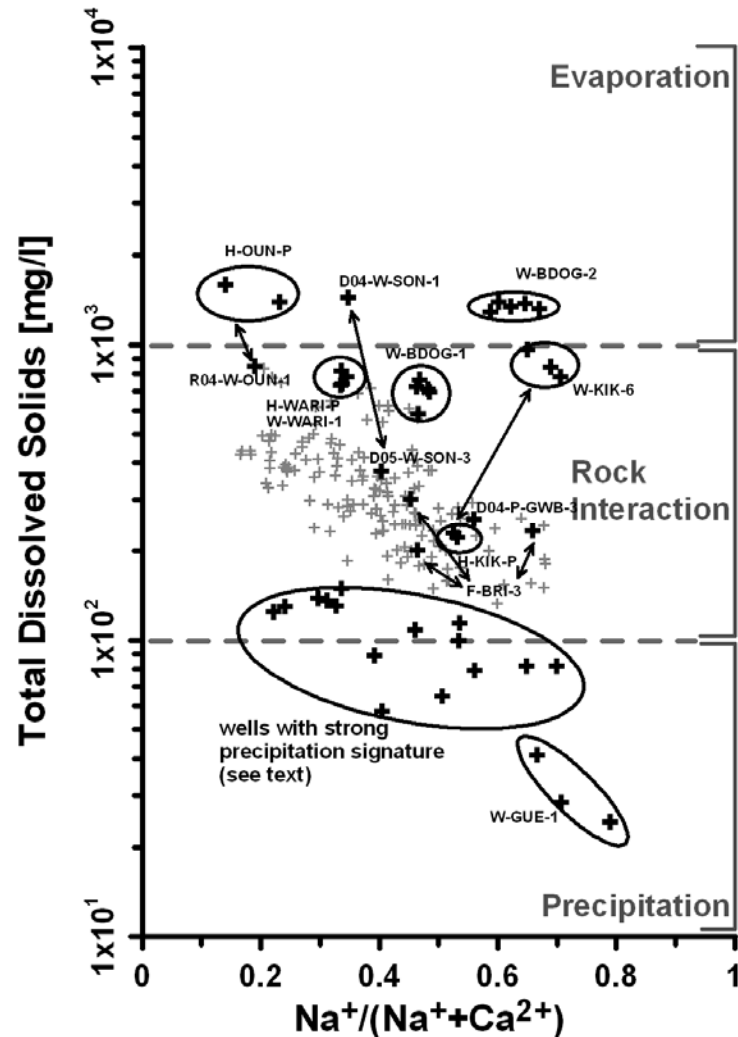


Fig. 5.21: Plot of all groundwater samples (grey and black crosses) in Gibb's diagram. Samples discussed in the text are marked with black crosses. Arrows show the relative position of different samples from the same location. Circles embrace samples of the same sampling point or equal habits. The wells with strong precipitation signature are found in Tab. 5.8.

In general it is seen that those samples taken from the same location plot as well in the vicinity of one to another. This means that most of the wells are not affected by surface processes, although the open dug wells are directly exposed to the atmosphere.

On the other side it is shown that wells from the same village or region do not plot necessarily nearby in the diagram. Note for example that the samples from W-BDOG-1 and W-BDOG-2 for all seasons form separated clusters although the wells are only a few hundred meter distant from each other. Furthermore, the sample from D04-P-GWB-3, which lies in the vicinity of Dugué, plots even more distant from the others. This borehole

is only half as deep as the dug wells in Dogué and outside of the village. Dilution or contamination may play a more important role in these shallow depths. In the village of Sonoumoun different characteristics for closely situated wells are observed too. D04-W-SON-1 is a well with high mineral charge in the centre of the village; D05-W-SON-3 is a well at the village periphery, which is only moderately charged.

Samples from borewells (fractured aquifer) and from dug wells (regolith aquifer) differ in different ways. In the village of Kikélé the well KIK-6 plots closer to the field of evaporation than the handpump KIK-P. In Ouannou it is the handpump (H-OUN-P) sample which plots in the evaporation field while the dug well W-OUN-1 plots below. In contrast to these examples the village of Wari-Maró shows that the sampled well and the handpump plot equally in the very same cluster (W-WARI-1 and H-WARI-P). The 3 samples from the footpump in Birni (F-BRI-3) instead plot in every season differently.

These observations show that even in a comparatively small area like a village (generally a few km² only) the hydrogeological and hydrochemical conditions may change profoundly horizontally from one well to another and vertically from wells in the regolith aquifer towards pumps in the bedrock aquifer. Therefore local particularities cannot be explained by a generalised regional sampling. The detection of local contamination sources demands intensified local research (see Chapter 5.4).

The local existence of perched aquifers in the weathered crystalline basement areas has been described in literature before (WRIGHT 1992 and ENGALENC 1978) and was proven for the HVO by FASS (2004) and BOHNENKÄMPER (2006). The hydrochemistry of wells which exploits this aquifer is mainly influenced by precipitation. The well of Guéssou (D04/R04/D05-W-GUE-1) is situated in a perched aquifer (BOHNENKÄMPER 2006). Eventually, other wells are situated in perched aquifers too. The wells with an assumed strong precipitation signature are represented in Tab. 5.8.

Tab. 5.8: Names of samples under strong precipitation influence.

Sample*	Location	X UTM	Y UTM
D04/R04/D05-W-BODI	Bodi	342672	1036773
D04/D05-W-TCH-1	Tchatchou	451119	1009028
D04-W-PAP-2	Partago	379998	1054149
D04-W-BRI-1	Birni	338520	1104741
D04/R04/D05-W-GUE-1	Guéssou	461405	1109699
R04-W-WEWE-2	Wé-Wé	402344	1038032
R04-W-KBG-1	Kpabégou	343561	1082842
D04-W-BAK-1	Bakou	397280	1042949
D04-W-BUV-1	Djougou	354286	1072507
D04/R04-W-GOS-1	Gosso	396533	1077975
R04-W-KAKI-S	Kakikoka	426212	1018523
R04-W-OSA-1	Wassa	349599	1063068

* Samples from the same location but from different seasons are put together by just repeating the season's code.

Two wells and a handpump (W-BDOG-2, W-SON-1 and H-OUN-P) show an influence of evaporation. But under close regard it is not very reasonable to take just evaporation as the reason for the higher charge of these water points. OUN-P is a closed handpump, SON-1 is a well which is clearly contaminated by human residues and W-BDOG-2 shows

such a general increase in mineralisation that any increase of chloride cannot be clearly caused by evapotranspiration.

Spots of evaporation would be depressions with ponds of water, principally during the dry season. In these locations generally no wells or borewells are found. However, the observations made by isotope analysis (Chapter 6) reveal no evaporation signature on groundwater.

In order to observe the seasonal variation in each village Schoeller diagrams were made to visualise differences between each sampling campaign (see Fig. 5.22 to Fig. 5.25).

In general it can be said that the hydrochemical facies for each site (wells and boreholes) does not change much during the year. Especially the wells of Dogué show that fluctuations due to dilution or concentration by evaporation are very low. The same is seen for a couple of other wells (Kikélé, Pénéssoulou and Kakikoka). At some places it is observed that the well water gets diluted during the rainy season (e. g. R04-W-WEWE-2 in the village of Wé-Wé; R04-W-PEB-1 in Pélébina; R04-W-OSA-1 in Wassa). The opposite behaviour may occur as well (e. g. D05-W-DDU-1 in Dendougou, R04-W-OUB-1 in Oubérou).

A reason for this may be the extraction of water by the local people. Already during the early morning hours (around 6 am) people starts looking for water. At Dogué and at Dendougou it was observed that the women are able to extract enough water to lower the groundwater table for a couple of meters in a few hours only. Therefore the sampling for this thesis is regularly done on groundwater freshly seeped in from the aquifer.

It is a common habit in Benin to disinfect their wells regularly with concentrated disinfectants or chlorine. Other contamination sources are possible as well, e.g. dead animals fallen into the wells or the simple water clogging devices used by the women which often stored on the ground without cleaning before the next use.

For many pumps no change in hydrochemistry is observed during the year (e. g. Bétérou, Bio-Sikka, Kikélé, Parakou, Sérou in Fig. 5.22 to Fig. 5.25). Water in fractures is not directly recharged from the surface but by a passage via the regolith first.

During the cooperation with other IMPETUS Workgroups possible pathways for bacteria and virus contaminations of well water were discussed. This here presented study concentrates on a regional scale. Answers to the posed questions demand more detailed local observations. From the hydrochemical observation no typical hint can be deduced to say whether or not rainfall may flush surface deposits and faeces directly into a well or into a badly cased borehole. One point of interest was the pump of Vanhoui. The analyses showed that sample R04-H-VAN-1 has a higher anion charge, principally in chloride but nitrate as indicator for faecal contamination was not detected. The bacteriologically critical wells of Kakikoka show no seasonal fluctuations.

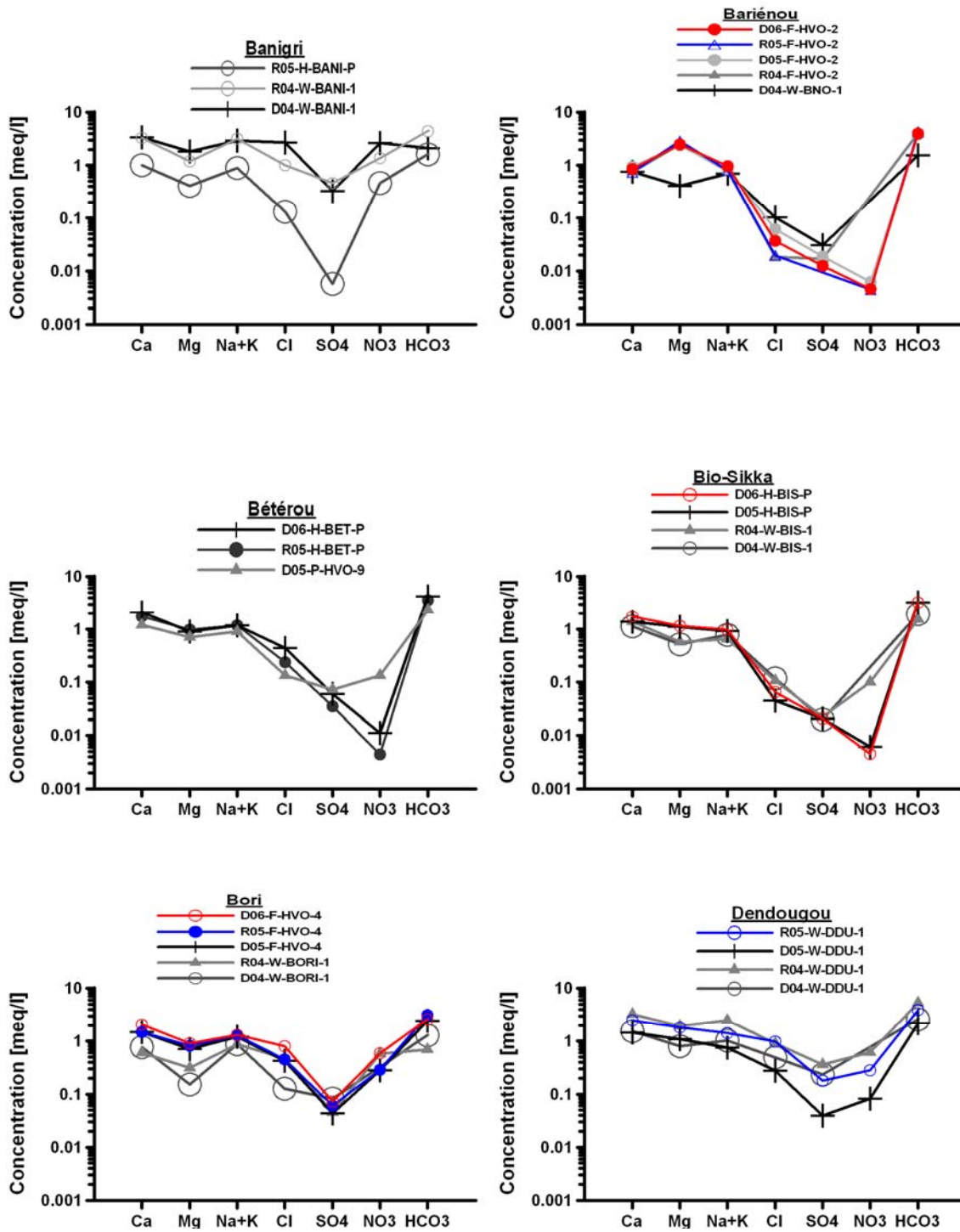


Fig. 5.22: Hydrochemical facies of different points in the HVO represented in Schoeller diagrams. The diagrams combine the seasonal samples from all points within the vicinity of a village (with exception of the village of Dogué, because of visibility). The villages are in alphabetical order.

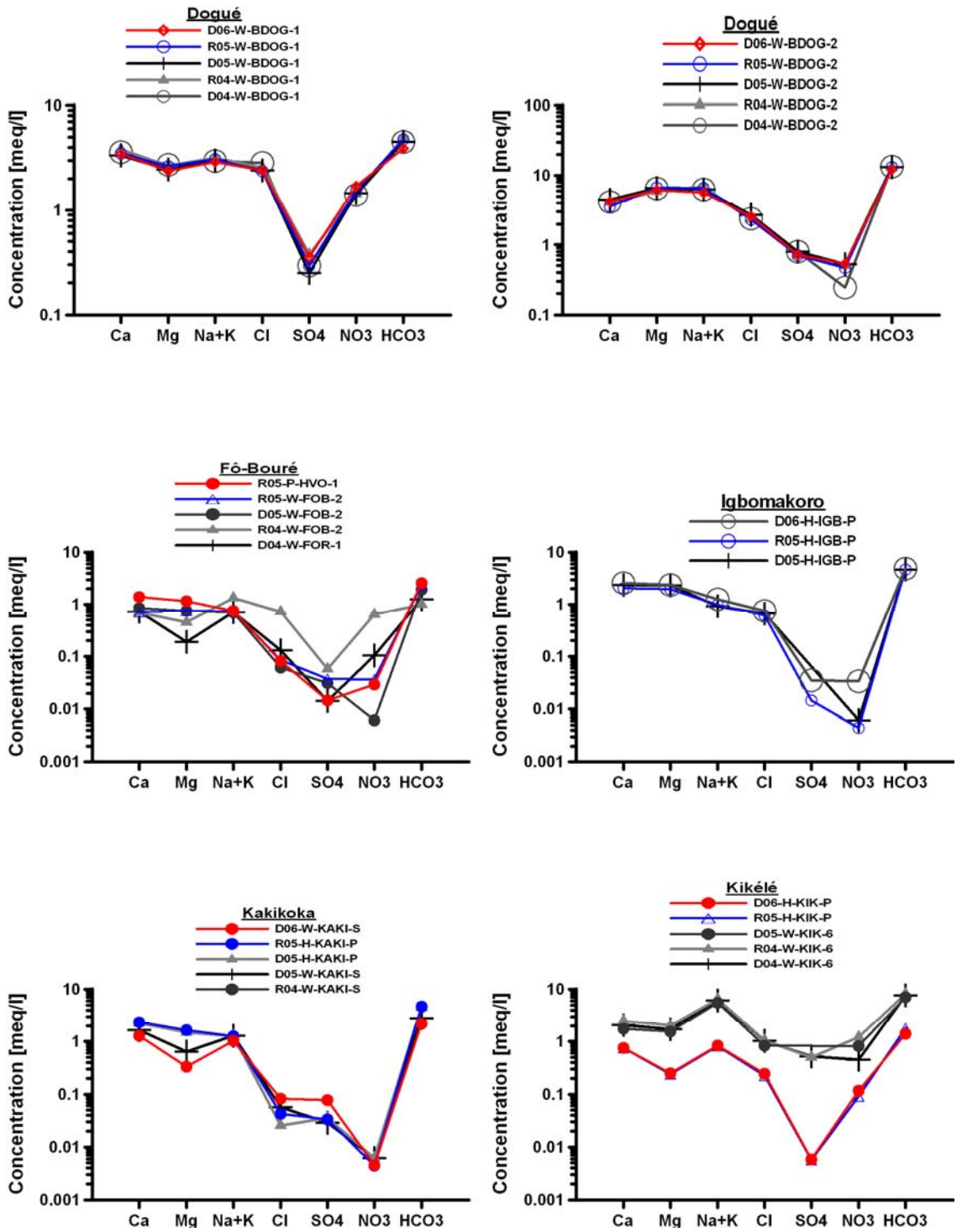


Fig. 5.23: (continued) Hydrochemical facies of different points in the HVO represented in Schoeller diagrams. The diagrams combine the seasonal samples from all points within the vicinity of a village (with exception of the village of Dogué, because of visibility). The villages are in alphabetical order.

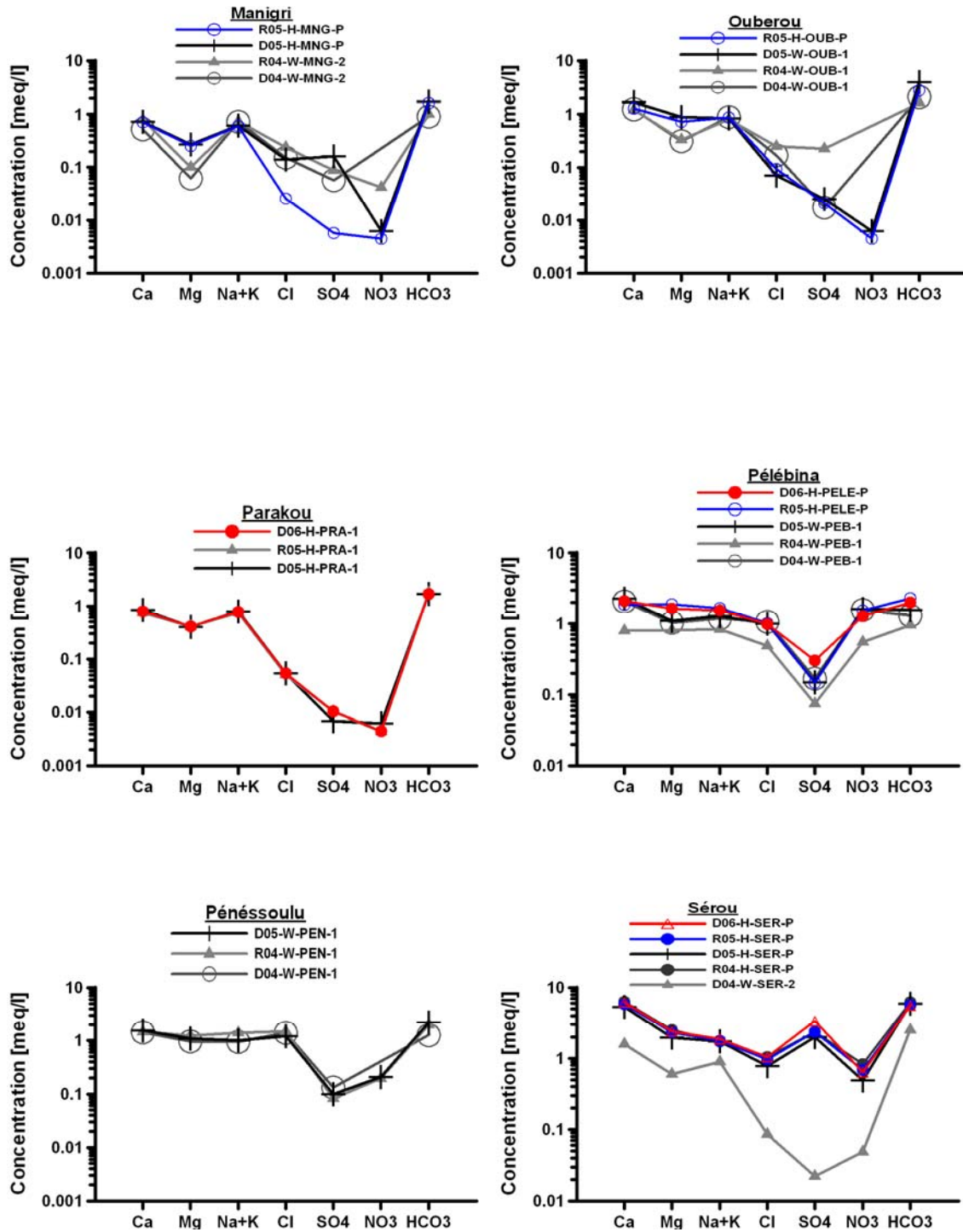


Fig. 5.24: (continued) Hydrochemical facies of different points in the HVO represented in Schoeller diagrams. The diagrams combine the seasonal samples from all points within the vicinity of a village (with exception of the village of Dogué, because of visibility). The villages are in alphabetical order.

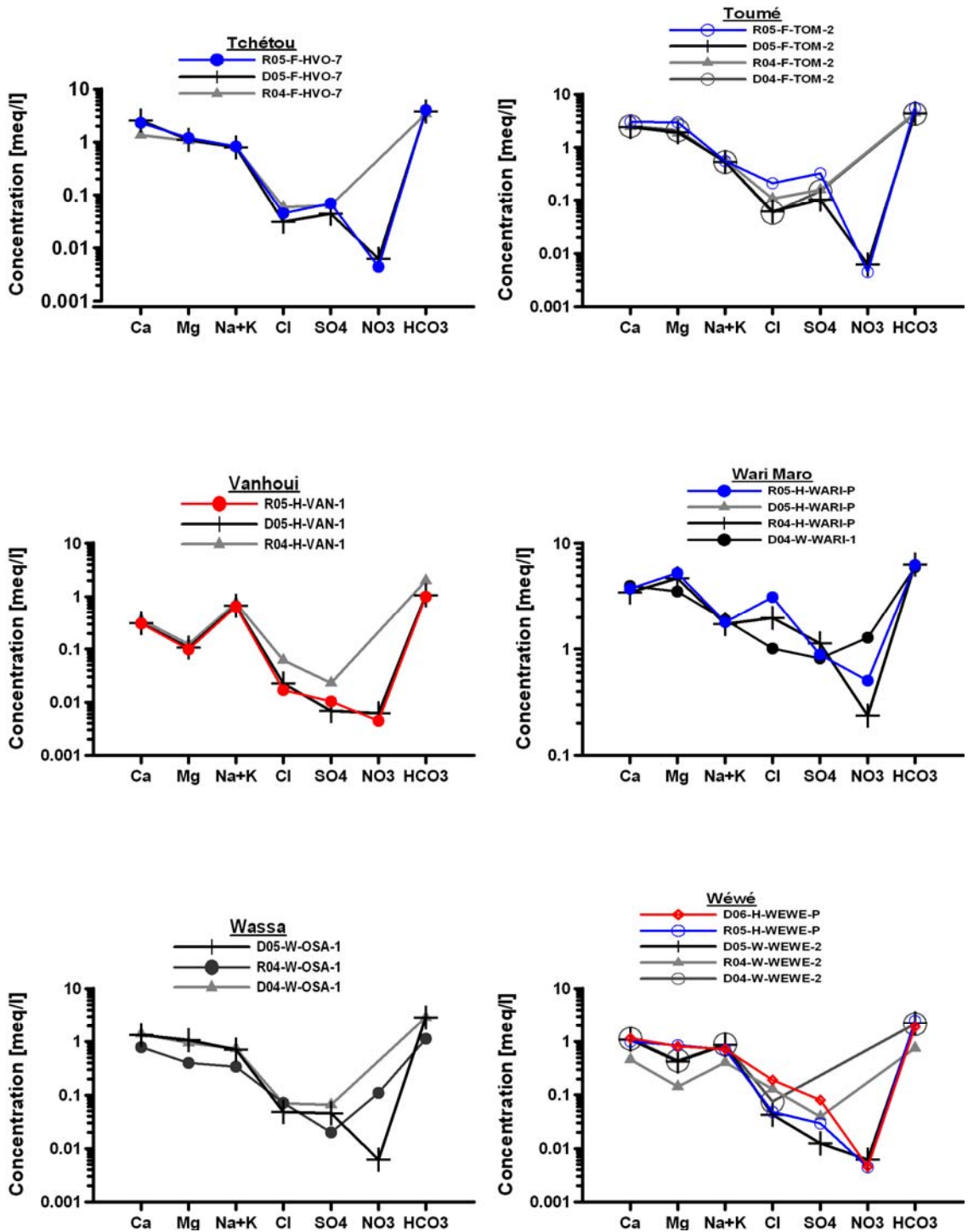


Fig. 5.25: (continued) Hydrochemical facies of different points in the HVO represented in Schoeller diagrams. The diagrams combine the seasonal samples from all points within the vicinity of a village (with exception of the village of Dogué, because of visibility). The villages are in alphabetical order.

5.4 Groundwater quality

5.4.1 Physico-chemical quality

The general physico-chemical quality of groundwater in the HVO is good, with the exception of elevated nitrate concentrations (see Chapter 5.4.3) in water points close to settlements.

Contents of major ions are all in acceptable limits (WHO 2004). Elevated values for potassium, magnesium, iron and manganese are not rigorously limited but can be objected by consumers because of aesthetic or physiological considerations. Water temperature is often elevated but generally water is stored in cooler places before consumption. In total 94% of the samples in the HVO satisfied the WHO drinking water guideline values.

When asked, the rural people underline that they rather prefer water from the regolith wells than from the borewells because of its taste. It was observed that most of the people do not like to drink the water with too high charge, e.g. the well B-DOG-2 in Dogué. In some cases elevated fluoride values are related to samples with a higher electric conductivity. Its appearance is discussed in Chapter 5.4.2 Fluoride.

The disposal of water points to contamination due to their proximity to locations of diverse daily use, e.g. market places, latrines, showers, in combination to a shallow water table is of major concern for groundwater quality. Nitrate as a good indicator for this source of contamination. The results from the analyses are explained in Chapter 5.4.3.

A greater thickness of the unsaturated zone provides more time for the downward percolation of contaminated water and, consequently, enhanced protection of groundwater (HOWARD et al. 2005). But during the rainy season, the water table rises often to very small distance towards the surface (3-5 m). The groundwater table is thus on the same level as the latrine holes and their deposits.

5.4.2 Fluoride

5.4.2.1 Geological sources

In crystalline areas groundwater is mostly sensitive to high fluoride concentrations where granites and alkaline rocks occur (TRAVI 1993, FLEISCHER and ROBINSON 1963). It is present in primary minerals (fluorite, biotite, hornblende and apatite). Fluoride can be leached out during weathering and circulation of water in rocks and soils.

Metamorphic rocks have a fluoride concentration from 100 ppm (regional metamorphism) up to > 5000 ppm (contact metamorphism). In these rocks the original minerals are enriched with fluoride by metasomatic processes (FRENCKEN 1992).

Fluoride contents in most freshwaters are low (< 1 mg/l). Fluoride can replace hydroxide ions on mineral surfaces under low and neutral pH. In presence of Ca^{2+} the fluoride content is controlled by the solubility product of fluorite (CaF_2).

High fluoride concentrations can be built up in groundwater which has a long residence time (FRENCKEN 1992). Increased fluoride concentrations are possible when the Ca^{2+} -

activity decreases, for example due to ion exchange in Na-SO₄-HCO₃-water (MATTHESS 1990).

Dykes and pegmatites bear high concentrations of fluoride. It is likely that these rocks could be providing higher fluoride to groundwater during weathering (SINGHAL and GUPTA 2005).

The WHO (2004) determined the upper limit of Fluoride in drinking-water as 1.5 mg/l for daily consumption. Repeated ingestion of high fluoride concentrations over a long period may cause fluorosis of bones and teeth. A minimum dose of fluoride is essential for dental health (Tab. 5.9).

Tab. 5.9: Impact of fluoride in drinking water on health (DISSANAYAKE 1991).

Concentration of fluoride [mg/l]	Impact on health
0	limited growth and fertility
0.0 - 0.5	dental caries
0.5 - 1.5	promotes dental health
1.5 - 4.0	dental fluorosis (mottling of teeth)
4.0 - 10.0	dental and skeletal fluorosis (pain in back and neck bones)
> 10.0	crippling fluorosis

For livestock breeding fluorosis symptoms must be compared to the economical usefulness of an animal. The acceptable level of fluoride in the feedstuff without economic loss of the animal is around 30-40 ppm (LEEMANN 1970).

5.4.2.2 Fluoride in the study area

Around Benin fluorosis cases are reported from Niger (TRAVI 1993) and Ghana (BGS 2006). The DGEau is therefore worried about its occurrence in Benin. Until 2005 fluoride values from 5 to 80 mg/l were measured in 56 boreholes in Benin (Tab. 5.10, oral comm. L. DOVONAN, DGEAU 2005). Until recently, none of these boreholes is restricted to public use. Information about their exact position and geological environment was not available at time. The highest values had been observed in the village of Bouloum next to Sérou in the Department Donga.

Tab. 5.10: Borewells contaminated by fluoride in Benin (oral comm. L. DOVONAN, DGEAU, March 2005).

Department	contaminated pumps
Collines	42
Borgou	13
Donga	1

The groundwater samples in the study area show only low or not detectable values in most cases. Tab. 5.11 shows the most affected wells (all are open dug wells).

The results of the two field campaigns in 2004 showed constant increased values for the well W-BDOG-2 in Dogué. For all later field campaigns no fluoride content above the detection limits was measured. This effect might be caused by a changed sensitivity of IC analysis in the laboratory or as well by dilution, but rainfall occurred as well during the

5 Hydrochemistry

early field campaigns. The general level of fluoride in the sampled wells is low and there is no object for concern despite the well W-BDOG-2 in Dogué who shows a generally high mineralization.

The markedly local occurrence of high fluoride values is due to the eventual appearance of fluoride bearing rocks such as pegmatite or crystallised drop outs in fractures.

Because of the spatially distribution of such rocks and fracture fillings it is not to be excluded that unsampled wells and pumps in the study area show higher fluoride values.

Tab. 5.11: Fluoride concentrations observed at three well during the seasons from 2004 to 2006.

Sample location	dry season 2004	wet season 2004	dry season 2005	wet season 2005	dry season 2006
W-BDOG-2	1.26	1.8	< 1	< 1	< 1
W-KAKI	1.2	< 1	< 1	< 1	< 1
W-KIK-6	0.83	1.3	< 1	< 1	< 1

5.4.3 Nitrate and Nitrite

5.4.3.1 Nitrogen compounds in the environment

Almost all nitrogen (N) found in the soil and subsoil originates from the atmosphere which is made of 78.1% nitrogen. In water nitrogen may oxidise and occur as nitrate (NO_3^-) or nitrite (NO_2^-), in reduced form nitrogen may appear as ammonium (NH_4^+). They circulate in the natural environment in the so-called nitrogen cycle (MATTHESS 1994). Natural background nitrate concentrations are evaluated in the report of ECETOC (1988) to be 0 to 10 mg/l in groundwater and up to 5 mg/l in surface water. Excessive concentrations of nitrate in drinking water may cause methamoglobinemia to small children (blue-baby syndrome). It hinders the oxygen transport in the blood and leads to suffocation (HEM 1985). The internationally mostly respected limits for nitrate in potable water are given in Tab. 5.12.

Tab. 5.12: Limits for nitrate in drinking water in international use. It should be noted that some countries may chose other limits following their own policies.

Limit [mg/l]	Reference
50	WHO (2004)
44.3	US EPA (2002)

In this thesis nitrate analyses are reported as mg/l NO_3^- . Some laboratories may refer to the nitrogen content of the analysed nitrate ($\text{NO}_3\text{-N}$). 1 mg/l of $\text{NO}_3\text{-N}$ equals 4.43 mg/l of NO_3^- .

APPELO and POSTMA (1999) consider the extensive application of fertilizers and manure in agriculture as the main cause of high nitrate concentrations in shallow groundwater. Artificial fertilisers are generally used on cotton fields which are generally distant from villages. Cotton planters use around 200 kg/ha of nitrogen bearing fertilisers (oral comm. T. MARTIN, IRD Cotonou 2007).

The study area is mainly of rural character. Industrial influx of nitrate can therefore be excluded. Besides agricultural and industrial nitrate sources it is human excreta which contains considerable amounts of nitrate and N-compounds.

Within the study area, the population either uses simple pit latrines or has no form of sanitation at all. Nitrate contaminations under equal conditions are found all over in Africa, as in Botswana (JACKS et al. 1999), Tanzania (NKOTAGU 1996) and The Republic of Guinea (GÉLINAS et al. 1996). Up to 95% of the nitrate derived from the human excreta originally belongs to urine (JACKS et al. 1999).

Nitrate is fast transported in flowing groundwater. Disposal of human excreta for example in latrines are therefore commonly known as origin of nitrate contamination of the groundwater. Further on the traditional village wells are often in a poor condition. Cracks and lack of sealing may cause the infiltration of contaminated water.

5.4.3.2 Nitrate in the study area

Analysis of groundwater samples from all field campaigns revealed high amounts of nitrates. The highest nitrate content, found in the study area, is 648.77 mg/l at a well in the village Sonoumoun (D04-W-SON-1) during the dry season 2004. All analysis results are represented in the Annex 1.

Of the 164 groundwater samples taken within the study area, 93 samples (56.7%) were found to have nitrate concentrations above 10 mg/l, which indicates anthropogenic influence (ECETOC 1988). 42 among these samples have nitrate concentrations exceeding 50 mg/l (45.2% of the 93 samples and 25.6% of the total population).

The plot of all samples in a pe-pH diagram (see Fig. 5.26) reveals that the ruling conditions favour a complete decay of all nitrogen compounds to nitrogen. Therefore the encountered nitrate concentrations are either conserved in some part of the aquifer with other redox conditions or there is a continuous enrichment.

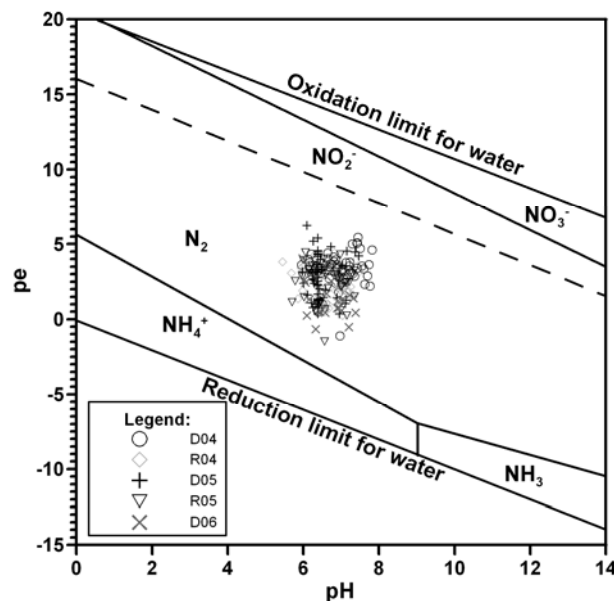


Fig. 5.26: Stability phases of nitrogen compounds in a pe/pH diagram (N-O-H system). The samples are plotted for each season respectively.

BARRETT et al. (2000) suggest that a good correlation between NO_3^- and Cl^- is given when they are of the same source. Furthermore, a low $\text{Cl}^-/\text{NO}_3^-$ -ratio is indicative of a

faecal origin when $\text{NO}_3^- > 10 \text{ mg/l}$ (MORRIS et al. 1994). This is shown for the study area in Fig. 5.27. Human activity can therefore be interpreted as origin of contamination. Isotope investigations in the groundwater of the Collines department by CRANE (2006) proofed the very same. Human waste and manure are the principal origin of nitrate (Fig. 5.28).

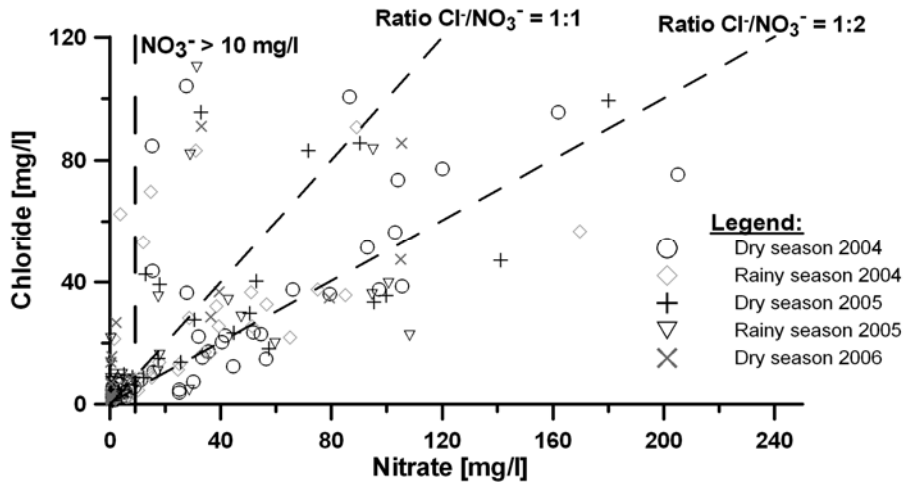


Fig. 5.27: Correlation of chloride against nitrate (after BARRETT et al. 2000).

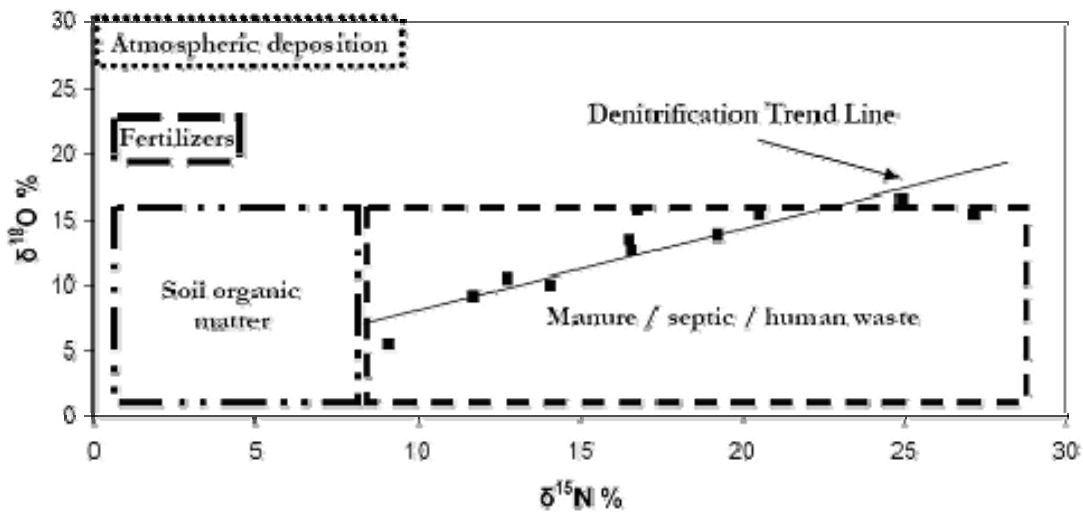


Fig. 5.28: Nitrogen and oxygen isotopes of nitrate in groundwater samples from the Collines department in Benin, rainy season 2003 (taken from CRANE 2006). The source composition is from ROCK and MAYER (2002). The trend line has a slope of ~ 0.5 , indicative of behaviour consistent with denitrification. All 11 samples were taken from open dug wells.

A borehole drilled in 2002 in the village of Dogué (UTM 383200/1006349) was abandoned because of bad water quality ($\text{EC} > 4000 \mu\text{S/cm}^2$). In 2002 nitrate concentration was determined as 16.83 mg/l (Source: BDI). In 2007 at the same location a much higher nitrate concentration was found ($>400 \text{ mg/l}$). This value was proven by the hydrochemical laboratory of the DGEau at Cotonou as well as by the IMPETUS laboratory at Parakou. The occurrence of exposed excrements at the surface around the borewell was reported by A. UESBECK (IMPETUS subproject A5). The high nitrate concentration in this borehole is therefore caused anthropogenic contamination.

Such a high nitrate value is only reported from the open dug well in the centre of the village Sonoumoun (D04-W-SON-1, UTM 420434/1079934) with a nitrate concentration of 648.77 mg/l. The origin of this very high value is clear. The regolith layer in Sonoumoun is very thin (< 1 m). Mica schist is outcropping directly in the dug well which is almost enclosed by near standing houses and latrines. This well has only a depth of around 14 m. Contaminated water may infiltrate almost directly from latrine pits into the well. The borewell at Dogué, instead, is deeper than 40 m and is installed in a regolith with a thickness of around 25 m. Preferential flow paths (macropores, fissures) or a bad boreholes casing would be the cause of the observed contamination

Alternatively, other possible sources of high nitrate levels in groundwater exist. SCHWIEDE et al. (2005) describe high nitrate contents in soils and sandstone aquifers in Botswana due to cattle rising (up to 600 mg/l). Cattle breeders are the half nomadic Fulbe people who come by casually and cannot be seen as relevant source for nitrate contamination. BOLGER et al. (1999) found in arid Australia soil nitrate concentrations around termite mounds of up to 2,000 mg/l. In Benin termite mounds can be found all over the country therefore it is not convincing that only the village of Dogué would be affected by a termite induced nitrate contamination. Elevated nitrate contents occur as well in spinifex and other grasses, leaf litter in mulga, in surface crusts and in bare sandy soil covered with bushfire ash. When rain falls, this nitrate is leached from the ash and percolates toward the groundwater table. In Benin it is a common practice to burn wild grasses to clear area and fertilise agricultural soils.

In Dogué two dug wells (W-BDOG-1 at the central market place and W-BDOG-2 at the village edge) were investigated from 2001 until 2006. Both show elevated nitrate values but a different behaviour during the last years (see Fig. 5.29).

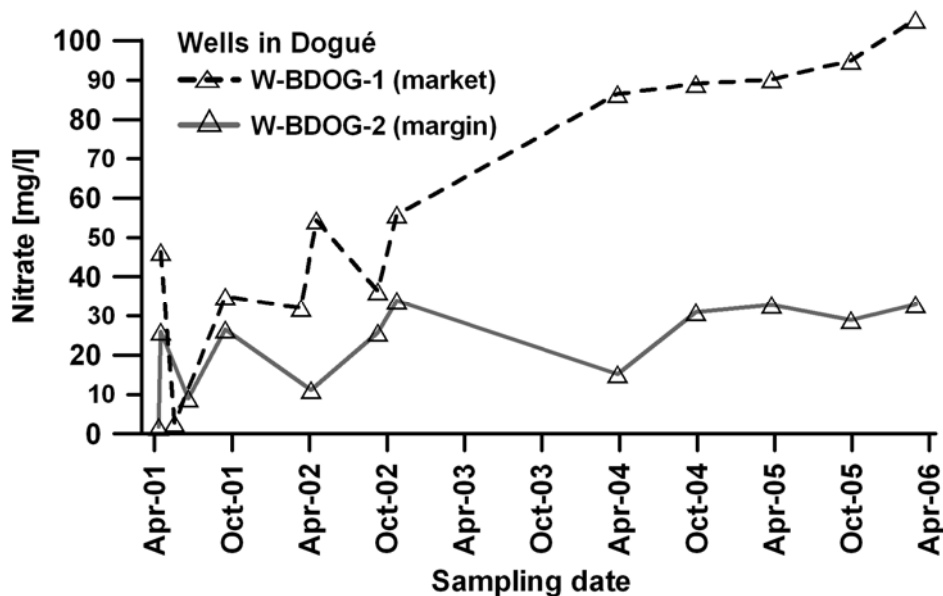


Fig. 5.29: Evolution of nitrate concentrations in groundwater from W-BDOG-1 and W-BDOG-2 in Dogué from 2001 – 2006. Data from 2001 to 2002 was collected by FASS (2004). No field campaign in 2003.

The well at the village edge is around 500 m distant from the market place. Its nitrate level is rather constant during the time with a level of around 20 to 30 mg/l. The other

well instead shows an increasing level of nitrate with already 90.2 mg/l in the dry season 2006.

The differing nitrate levels of both wells can be clearly explained by the difference in use and location. The market place is regularly frequented by many people and shows many buildings while the other well is only achievable by a small tray and is encircled by some trees. Nevertheless both wells are regularly frequented but the well W-BDOG-2 is not used for drinking water. This seems paradox as it shows at least less nitrate. The villagers refer to it as having a bad taste which they refuse. The reason might be the generally higher level of solved minerals in this well (see Tab. 5.13).

Tab. 5.13: Average mineralisation of the two regularly sampled dug wells in Dogué.

Location	Depth [m]	Average mineralisation [mg/l]
W-BDOG-1	22	694.8
W-BDOG-2	24	1343.9

The distribution of nitrate within the regolith might be either advantaged by microfissures in the saprolite clay or by lateral flow in the interface zone between sandy soils and argillaceous saprolite.

5.4.4 Heavy metals

The elements with a density $>4.5 \text{ g/cm}^3$ are called heavy metals. Although groundwater contamination of heavy metals is often related to the infiltration of industrial water and slugs. A geologic origin is as well possible. Crystalline rocks contain heavy metals in variable concentrations. Mn^{2+} and Fe^{2+} are separately described together with the major cations.

The HVO is a rural area without any industries except at Parakou. But all over the area especially in the vicinity of settlements disposals like car batteries, energy cells and many others are found. Sometimes the disposals can even be found in wells. It is as well often seen that people wash their cars, trucks and motorcycles directly next to water points or even parking inside lakes, rivers or bas-fonds. In order to determine any impact of these disposals on the shallow groundwater in the HVO, samples from the rainy season 2004 and from the dry season 2005 were additionally analysed for a limited variety of heavy metals, among them arsenic (As), cadmium (Cd), copper (Cu), lead (Pb) and nickel (Ni), was analysed. For the results and the drinking water limits (WHO 2004) refer to Annex 1.

All of them are very poisonous (APPELO and POSTMA 1999). Cu is less toxic but it is good indicator for contamination by simple industrial forms as steel and metal work. Cd and Pb are typically found in energy cells and are therefore investigated (WHO 2004). Contamination by geogenic arsenic is reported from many places in the world, for example in Bangladesh, India or Mexico (AGGARWAL et al. 2000). Arsenic can be released from the rock matrix to groundwater under anaerobic conditions but also in acidic groundwater under oxidising conditions. The later case tends to occur in arid and semiarid settings resulting from extensive mineral reaction and evaporation (WSP 2005). Cases of arsenic in rural groundwater are reported from Ghana by SMEDLEY et al. (1996). In the rainy season 2004 53 samples were analysed, in the dry season 2005 66

samples. The samples include groundwater from the regolith and from the bedrock aquifer. Surface water from lakes and rivers were tested as well. The reservoirs of Djougou (DJO-BR) and Parakou (OKP-1) are almost exclusively in use for the public water supply of these cities. No traces of any contamination by the here presented heavy metals were found (see Annex 1).

5.4.5 Sodium adsorption ratio (SAR)

Artificial irrigation is not popular in Benin. Longer drought periods and new agricultural policies may change this in future. In the HVO groundwater is available throughout the whole year and may serve as an important source for decentralised irrigation.

In order to prove the suitability of groundwater for this purpose the sodium adsorption ratio (SAR) was calculated. The SAR (Eq. 5.6) was proposed by the US DEPARTMENT OF AGRICULTURE (USDA 1954) as classification scheme for groundwater.

$$SAR = \frac{Na^+}{\sqrt{\frac{1}{2}(Ca^{2+} + Mg^{2+})}} \quad (\text{Eq. 5.6})$$

with

SAR = Sodium adsorption ratio

Na^+ , Ca^{2+} , Mg^{2+} in meq/l

The SAR of the groundwater samples is plotted against their electric conductivity [$\mu\text{S}/\text{cm}$] respectively into a classification diagram (Fig. 5.30). The salinity hazard is described by 3 intervals of electrical conductivity (C1, C2 and C3). The higher the grade the more likely it is that the irrigated soil gets saline. The sodium hazard (S1, S2 and S3) indicates how far harmful levels of exchangeable Na^+ are produced in the soil water. The majority of the samples represent a low ($EC < 250 \mu\text{S}/\text{cm}$) or medium salinity hazard ($250 - 750 \mu\text{S}/\text{cm}$) when used for irrigation. There is couple of samples with a relatively high salinity hazard ($EC > 750 \mu\text{S}/\text{cm}$). In general those are always the same samples for each season. They belong mainly to group 3.

High salinity water cannot be used on soils with restricted drainage (USDA 1954). The locations of concern (Tab. 5.14) are mostly situated in the southern part of the HVO. But other areas as well outside the HVO are indicated (for example F-NIK-2 and F-PRE-1). The SAR is an appropriate method to check long term influence of groundwater hydrochemistry on the soil properties. Groundwater within the study area can generally be used for irrigation with a low risk of sodium hazard.

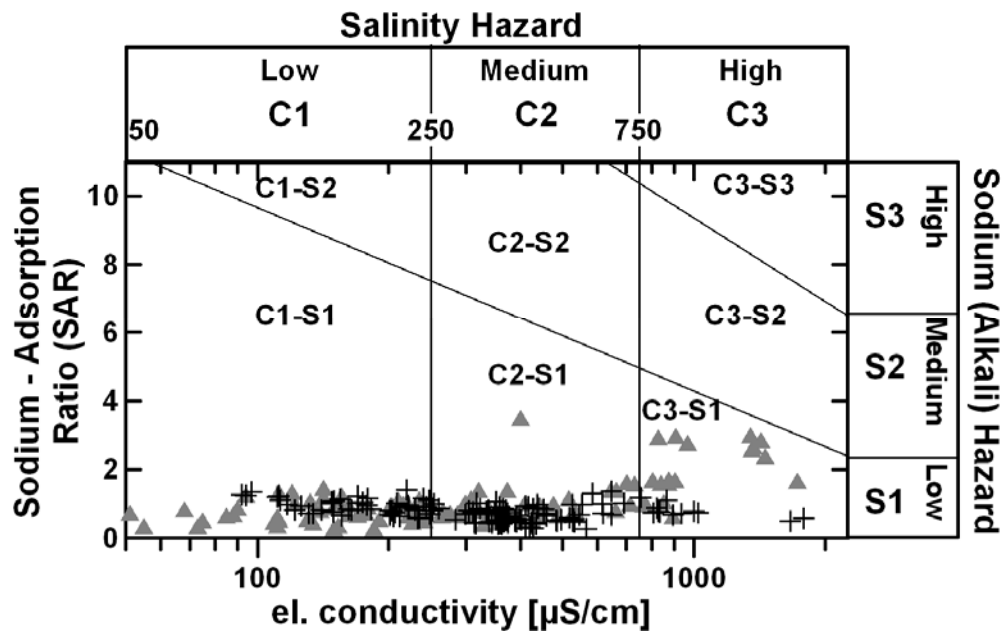


Fig. 5.30: Groundwater classification for the HVO for all sampled seasons. Grey triangles = dug wells; black crosses = borewells.

Tab. 5.14: Sample locations with high salinity hazard.

Village	Sample	N° of samples from March 2004 to March 2006
Alfakpara	W-ALF-1	1
Dogué	W-BDOG-1	5
	W-BDOG-2	5
Kari	H-KAR-1	1
Kikélé	W-KIK-6	3
Nikki	F-NIK-2	1
Ouannou	H-OUN-P	2
	W-OUN-1	1
Péréré	F-PRE-1	1
Sérou	H-SER-P	4
Sonoumoun	W-SON-1	1
Tamarou	W-TAR-2	1
Wari-Maró	W-WARI-1	1
	H-WARI-P	3

6. Environmental isotopes

6.1 Stable isotopes in precipitation and surface water

Since the rainy season 2004 precipitation was regularly sampled at three sites in the HVO. They are at Sérrou (UTM 357472/1068612), Dogué (UTM 383034/1006505) and Parakou (UTM 459862.5/1035435.8). More than 210 precipitation samples were taken for analysis until the dry season 2006. By the time of writing this thesis the results of these samples were still not available. Thus, only 8 rainfall samples taken during the field campaigns 2004 were used (see Annex 2). 13 samples from earlier campaigns (FASS 2004) were added.

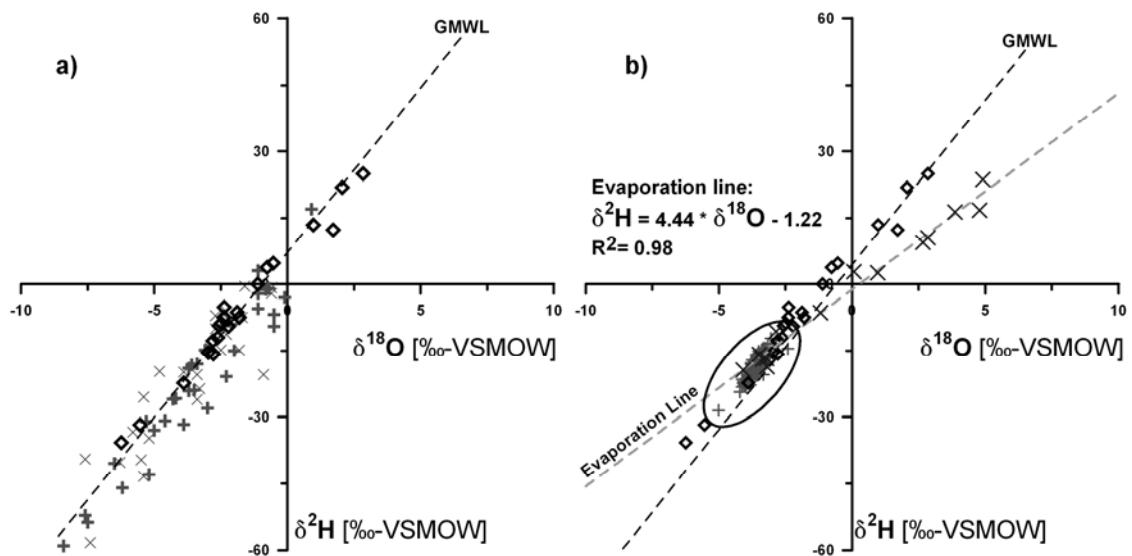


Fig. 6.1: a) Comparison of GNIP data (Kano-Nigeria = light grey x / Niamey-Niger = grey +) with the HVO rainfall data (black rhombus). The global meteoric water line (GMWL as gray dashed line) is calculated by Craig's notation (Eq. 6.1). b) Groundwater analyses (grey +) are shown in relation to the GMWL. Analyses from surface waters (grey x) are grouped around an evaporation line (light gray dashed line).

From the GNIP database (IAEA/WMO 2004) the measurements from Niamey and Kano were additionally chosen. All data sets were compared with the GMWL (Fig. 6.1 a). The isotopic range of HVO precipitation in 2002 to 2004 lies between -6.24‰ and 2.845‰ for $\delta^{18}\text{O}$, and between -35.75‰ and -24.95‰ for $\delta^2\text{H}$. The stable isotope composition of the HVO samples plots around the GMWL with a median d-excess of approximately 9. The relative plot of the groundwater samples shows that they are much less scattered as the precipitation samples (see Fig. 6.1 b).

The surface water samples are plotted into the same diagram. They are influenced by evaporation and plot around an evaporation line with the equation:

$$\delta^2\text{H} = 4.44 \cdot \delta^{18}\text{O} - 1.22 \quad (\text{Eq. 6.1})$$

The evaporation line crosses the GMWL in the scatter of the groundwater samples in the encircled area. This means that surface water and groundwater types have the same

6 Environmental isotopes

origin. The groundwater reservoir is a mainly semi-confined aquifer. It is the mixing pot for all isotopic rainwater signatures. Another origin of groundwater in the HVO is not distinguished. Groundwater samples are not affected by evaporation in contrast to the sampled surface waters. This implies that the principal source of groundwater recharge in the HVO is the direct infiltration of rainfall. The remaining surface water runs off via rivers or gets evaporated in residual lakes or bas-fonds.

6.2 Stable isotopes in Groundwater

Stable isotopes were regionally sampled from wells and pumps (see Annex 2). It was observed that no clear distinction can be made between the regolith and the bedrock samples (Fig. 6.2). The relative position of the samples marked by letters (a to h) shows that the isotope composition even in the deeper bedrock aquifer is not stable. As shown in Fig. 6.2 groundwater plots around the GMWL. Bedrock and regolith groundwater has infiltration of rain water as common source. The isotope composition may change during the time as a result of mixing either with fresh water or with downward percolating water due to extraction.

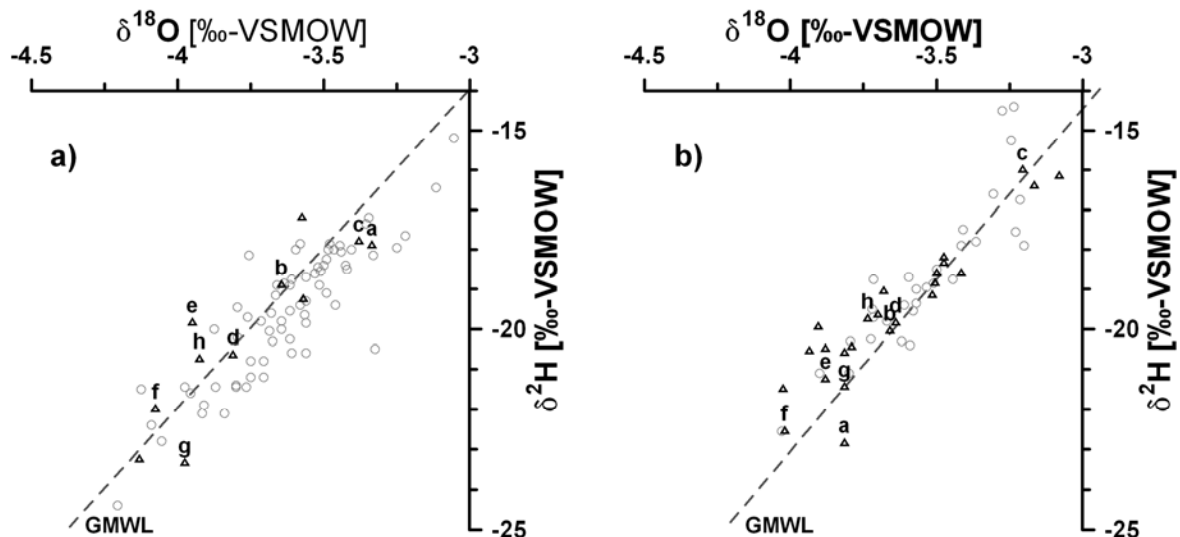


Fig. 6.2: left) Dry season 2004: Isotope relationships for groundwater samples from wells (circles=regolith) and pumps (triangles=bedrock). right) Rainy season 2004: Isotope relationships for groundwater samples from wells (circles=regolith) and pumps (triangles=bedrock). The letters (a) to (h) signify a choice of samples from the same locations.

While all samples plot during the dry seasons around the GMWL (Fig. 6.3 left) they show a different behaviour in the rainy seasons (Fig. 6.3 right). Mainly the samples from the rainy season 2002 (from FASS 2004) show a higher D-Excess. The D-Excess for these samples has been re-calculated by a strict linear fitting to be rather +12 (the value of +12.5 was originally determined by FASS 2004).

At the village of Dogué water from precipitation was regularly sampled and analysed for its stable isotope content (samples for the period 2001 – 2002 from FASS 2004). The time row from 2001 to 2004 shows a rise in D-excess in when the rainy season in 2002, and respectively in 2004, starts (Fig. 6.4).

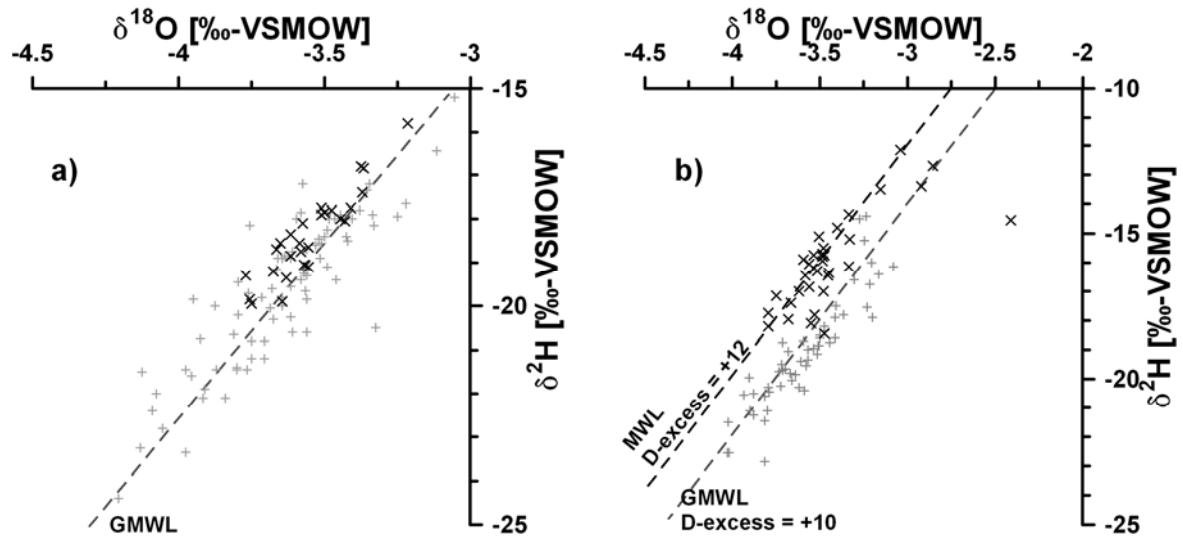


Fig. 6.3: left) Comparison of groundwater samples from the dry season 2002 (black x, FASS 2004) and from the dry season 2004 (grey +). right) Comparison of groundwater samples from the rainy season 2002 (black x, FASS 2004) and from the rainy season 2004 (grey +).

A D-excess $> +10$ can be explained when air masses are enriched by condensed water which rises up from evapotranspiration surfaces. These may occur when the air passes areas of lakes or dense forests (among others: oral comm. by Y. TRAVI in 2005, KENDALL and McDONNELL 1998, CLARK and FRITZ 1997).

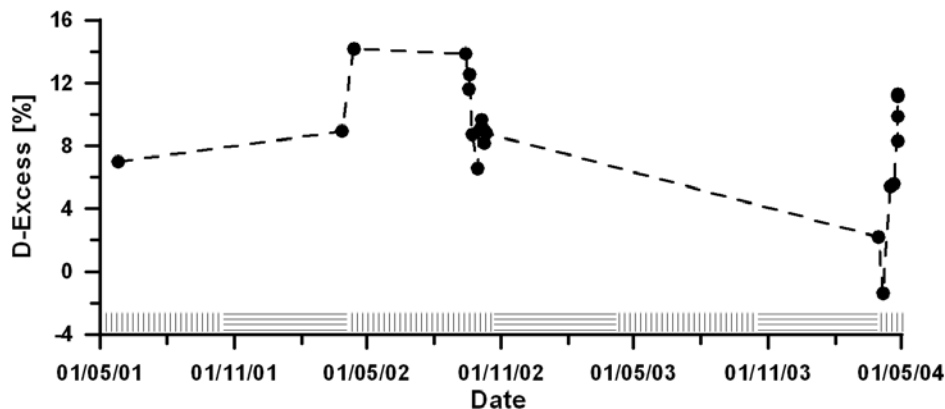


Fig. 6.4: D-excess measured from precipitation samples at the village of Dogué in the years 2002 and 2004. In 2003 no sampling took place. Horizontal lines = dry season; vertical lines = rainy season.

The continuation of stable isotope sampling from groundwater and precipitation helped to prove that the observed difference in the D-Excess is not a result of differing origins of the groundwater but rather of the different isotope composition of the precipitation during the year as shown by Fig. 6.4. In correspondence to the pH observations (Fig. 5.3) and the interpretation of the seasonally sampled hydrochemical analyses (in Chapter 5.2 and 5.3) the local character of recharge by precipitation can be assumed.

Groundwater flow over distances of several kilometres from distant areas, e.g. outside the HVO, through a rather thin regolith aquifer (average thickness = 5-15 m) remains unimaginable. Chapter 4 showed that subsurface flow in the regolith of the slightly

6 Environmental isotopes

undulated HVO area heads towards the local depressions. The conclusion can only be that the groundwater available in local subcatchments is first of all a product of local recharge.

No clear end members can be defined in this hydraulic system. As consequence stable isotopes serve not to determine mixing ratios in order to separate groundwater base flow to rivers from surface runoff. Other tracers might be more promising for this task.

6.3 Tritium data from the HVO

In total 34 samples for tritium analyses were chosen on hydrogeological base and in order to receive a regional distribution across the whole HVO (see Annex 2). The samples were taken from groundwater in different depths. Samples from open dug wells normally shall describe the TU contents of groundwater in the regolith while samples from pumps reflect conditions in the fractured bedrock.

Additionally 33 results from tritium sampling during the rainy season 2002 from FASS (2004) are available (including samples from 2 rainfalls, 5 surface water sources and 26 shallow groundwater sources).

Tritium concentrations in precipitation and surface waters in the study area have been compared to measurements from the GNIP stations at Bamako (Mali), Kano (Nigeria) and N'Djamena (Chad) and for reference at São Tomé as published by the IAEA/WMO (2004). The first three stations are more or less all at the same latitudes. Kano is the closest station to the HVO in Benin. São Tomé has been chosen to show the increase of tritium concentrations moving from the seaside to the inner continent (see Fig. 6.5). The Fig. 6.7 shows that the course of the curves is quite similar for Kano, Bamako and N'Djamena and tritium units fluctuate around the same amounts.

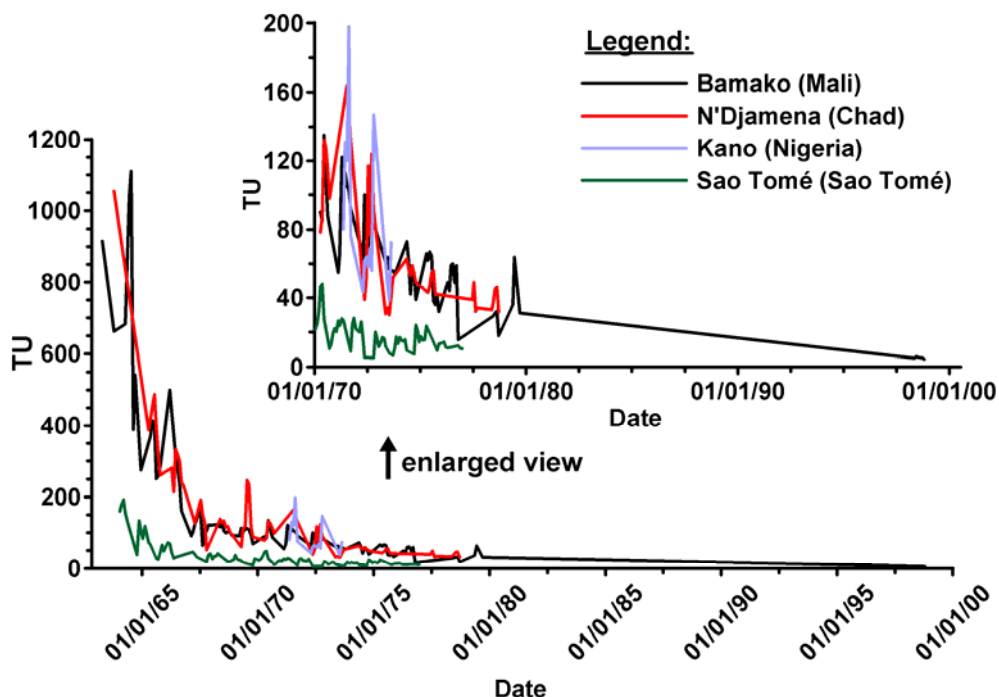


Fig. 6.5: Seasonal fluctuations of TU in precipitation measured at different stations of the GNIP database (IAEA/WMO 2001) with an enlarged view for the years 1970 to 2000.

It is seen that for N'Djamena and Bamako the development of the curves is quite comparable. Both start in the early 60ies with values exceeding 1000 TU when monthly variations are still the strongest. In the midst of the 1970s values decreased to around 50 TU. Bamako shows consequently in 1998 as last and lowest measurement 4.7 TU. Analyses of precipitation and surface waters in the HVO show a range of 2.8 to 3.8 ± 0.7 TU. This is slightly less than at Bamako but reasonable as the whole study area is situated more meridional. The decrease of tritium towards the South can be seen as well by the course of the curve for São Tomé which shows the same trend but lower values.

Tritium analyses for precipitation and surface water from the rainy season 2002 (FASS 2004) show an equal range of 2.7 to 3.9 ± 0.7 TU. By comparison of these few samples from the dry and the rainy season no seasonal variations in tritium contents are obvious. For further considerations the median of the available results 3.5 ± 0.7 TU is assumed as the average content of fresh recharge water. It cannot be excluded that precipitation with > 4 TU might occur as for example the oral communication with TRAVI (2005) revealed an actually expected tritium concentrations in precipitations in the Sahel (including the North of Benin) vary between 6 – 10 TU.

6.4 Tritium age determination of groundwater in the HVO

Most of the samples were taken from dug wells and boreholes. As dug wells normally penetrate the regolith zone in depths from 5 to 20 m, boreholes catch water most of times in the fractured bedrock in depths > 30 m. Fig. 6.6a) show that tritium contents of the samples vary with the depth. Most of the analyses of the samples from shallow groundwater tables show TU in the range of the precipitation reported above. Most of the samples from groundwater belonging to the bedrock aquifer show tritium concentrations < 2 TU instead. Still a couple of samples from dug wells as from boreholes show concentrations of > 5 TU although actual rainwater has only 2.2 – 4.6 TU. Rainwater with originally higher tritium contents is still stored in some layers. These layers are most probable within the montmorillonitic weathering zone where less water is exchanged or in the bedrock where water from above infiltrates. Pumping lowers the water level within the fractures quite fast as they have usually only a small storage capacity (see Fig. 6.6). The older pre-bomb test water (age > 50 years) is then mixed with younger water producing elevated values of TU.

Tab. 6.1: Comparison of the seasonal differences of TU-contents of groundwater samples from different sites and depths in the HVO-area.

Sample*	Wet season TU	Dry season TU	st. Dev. $\pm 2\sigma$	Depth [m]
PELE - 1	3.8	7.3	0.7	12.68
WEW - 2	3.0	4.3	0.7	11.28
OUB - 1	3.1	3.7	0.7	20.2
GWB-3	3.0 (GWB-1)	2.1	0.7	11.60
SER - 2	3.0	2.7	0.7	12.56
DRG	3.0	2.9	0.7	12.62

* All locations are open dug wells with the exception of GWB 1 and 3. These are observation wells within the regolith which were installed by FASS (2004).

6 Environmental isotopes

When the TU exceeds the value of the precipitation samples it can clearly be said that recharge belongs to the bomb-linked water. The question remains how water from that period still prevails in open dug wells when fresh water regularly infiltrates. As said in Chapter 4 most of the dug wells do not dry up completely during the dry season. They are still connected to a water table within the regolith aquifer. It might be possible that layers or lenses, e.g. perched aquifers, of older bomb-water prevail and are still infiltrating into these wells too. A higher amount of TU can be admixing this older groundwater.

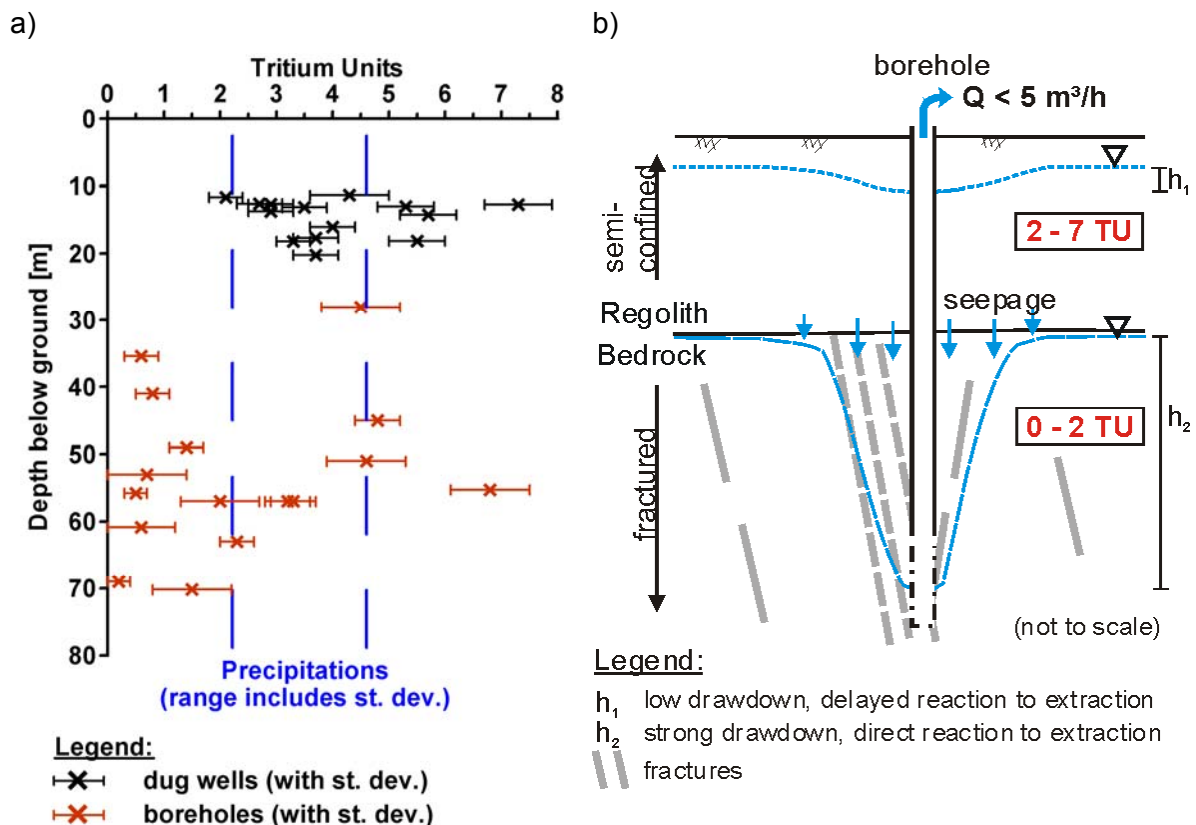


Fig. 6.6: a) Distribution of tritium in relation to the sample depth. b) Drawdown of the groundwater level in fractures causes seepage from the regolith aquifer above and thus mixture of younger with older water.

Comparison of samples from the dry seasons 2004 and 2005 with data from the rainy season 2002 shows a sharp increase of the tritium amount at PELE-1, WEW-2 and OUB-1. In the case of SER-2 the value for TU stays the same or is even decreasing but keeps including the standard deviation still in the range of the precipitation tritium (see Tab. 6.1).

Age signals of tritium may be hidden in mixed water. The age of recent water correlates positively with tritium concentrations in precipitation. Sampling of fracture water is only possible at pumped boreholes where it gets mixed (see above). Some samples from the bedrock aquifer show $TU < 0.5$. This water must have been recharged before 1952 (MAZOR 1997). Groundwater recharged since that time got mixed already during infiltration into the aquifer and continued percolating downward. Therefore it could still exist a layering of different water ages in the aquifer. The highest observed value for TU is 7.3.

Some assumptions were made for calculating mixing ratios and determine the percentage of actual precipitation in groundwater (Eq. 6.2). For the precipitation the mean value of 3.5 TU is just considered as non-changing and as well the mean value of 0.7 for bedrock samples is not modified as well. A further assumption is that there is no decay of tritium during precipitation and infiltration to the groundwater.

$$X = \frac{T_P - T_F}{T_R - T_F} \cdot 100 \quad (\text{Eq. 6.2})$$

x = share of recharge in the mixing water in %

T_R = TU of the regolith mixing water (from 4.0 to supposed 10 TU)

T_F = TU of the fracture water (mean: 0.7 TU)

T_P = TU of the precipitation (mean: 3.5 TU)

Under these assumptions the maximum mixing ratio between recent recharged water to sampled older water can be calculated to be somewhere between 30.1 to 85.0% (Tab. 6.2). This shows that recharge water delivers for samples with > 6 TU only around 50% of the mixing water. This value emphasises the presence of “older” water. The calculation above is only a first approach. It must be kept in mind that the sampled groundwater from fractures could as well be mixed. More data is needed to base conclusions on these findings.

Tab. 6.2: Mixing ratio of recently recharged water to groundwater from the regolith and the bedrock aquifer. Results from Eq. 6.2.

Regolith water [TU]	Fracture water [TU]	Precipitation [TU]	Mixing ratio [%]
4	0.7	3.5	85
5	0.7	3.5	65.1
6	0.7	3.5	52.8
7	0.7	3.5	44.4
8	0.7	3.5	38.4
9	0.7	3.5	33.7
10	0.7	3.5	30.1

Nevertheless, attempts were made to calculate some eventual water ages by black-box-models using the Boxmodel V2-3 sheets of ZOELLMANN and AESCHBACH-HERTIG (2001). As reference tritium measurements of the GNIP database at Bamako, Mali, were used. Restriction is given by the lack of yearly data. Mean values were calculated for each year and the interpolated linearly over the years without measurements. The program calculates reasonable water ages only until the year 2000 but this is sufficient taking in account that values in the rainy season 2002 are not that different from values measured in the following years. It has to be kept in mind that regional recharge is only around 10 to 15% from the total amount of precipitation. The dispersion model (DM) was chosen as it serves well to simulate partly covered aquifers with samples from different depth levels (DVWK 1995).

The choice of input parameters is presented in Tab. 6.3. The year of observation is technically limited to the year 2000. In order to obtain a possible age for the groundwater

6 Environmental isotopes

with > 6 TU a value of 10 TU is entered. Residence times between 30 to 50 years are assumed. BAUER (2004) determined dispersion parameters by forced gradient tracer tests in the Aguima catchment. Values for P_D range from 0.003 to 0.11 with an average of 0.05 which is used in the DM. During modelling values had been adjusted and changed several times. As a result the DM results show that older groundwater should be recharged in the 70ies (1968 – 1980).

The mean atmospheric concentration of tritium measured at Kano from 1971 to 1973 was calculated as 69 TU. All mixing processes excluded, radioactive decay in groundwater would lead to 12.25 TU in the year 2000. The more southwards situated HVO should show lesser concentrations in the precipitation in 2000 (longitudinal effect).

Considering the above outlined processes it seems possible that originally recharged groundwater in deep or bad connected fractures could be very well much older than 50 a.

Tab. 6.3: Entry parameters into the user interface of the Boxmodel V2-3[®] (by IHW, ETH-Zurich, ZOELLMANN et al. 2001).

USER INTERFACE	
Model Code (pm,em,dm)	dm
Tau [a] (for transfer and output graphs)	30
Tau Step [a] (for tau graph)	1
Delta (dispersion parameter, P_D)	0.5
Tritium Factor (tritium input scaling)	1
Tracer Code (tr, cfc, kr, he)	tr
Year of Observation	2000
C_obs (observed concentration)	
tr (TU)	10

The study of CEFIGRE (1990) presented results from a tritium research (BRGM-AQUATER 1986) on borehole groundwater in the Leo-Ranch area in Burkina Faso during 1984 to 1985. It showed that in the crystalline massif of Burkina Faso water ages ranges around 30 years – younger towards the North and older towards the South. DRAY et al. (1988) used isotopes (^3H and ^{14}C) to determine groundwater age in the coastal basin of Benin. They showed that groundwater in the Mesozoic aquifers has an age of around 2000 a in the North and is getting older towards the South (>6000 a). The coastal basin aquifers are recharged by mainly by surface waters in the northern unconfined areas while the South of the basin is mainly confined. In relation to the crystalline basement it can be stated that there is a certain amount of water which is transferred from the basement towards the coastal basin too.

Age determination by the ^{14}C -method is reasonable when the minimum age of the sample is >1000 a (oral communication by W. STICHLER, GSF 2005). Although a high percentage of bedrock water should be much higher age than 50 a, mixture occurs especially around places with pumping where samples can be taken. Therefore it is not reasonable to take such water to ^{14}C analysis. Within the scope of this study it was not priority to know the exact groundwater age. But the tritium analysis revealed the relatively slow regional vertical exchange of groundwater and a very homogeneous horizontal distribution with the exception of locally pumped areas.

7. Conceptual hydrogeological model

The observations described in the foregoing chapters are fitting to the regional model for regolith areas (Fig. 7.1) as proposed by DANIEL et al. (1997). Recharge occurs areally at the ground's surface but principally at the crests (Chapter 3.7.2). The valleys are preferential for groundwater discharge, either by transpiration or by fracture flow. Groundwater flow heads towards local depressions. The groundwater table moves mostly within the regolith and is the lowest at valleys.

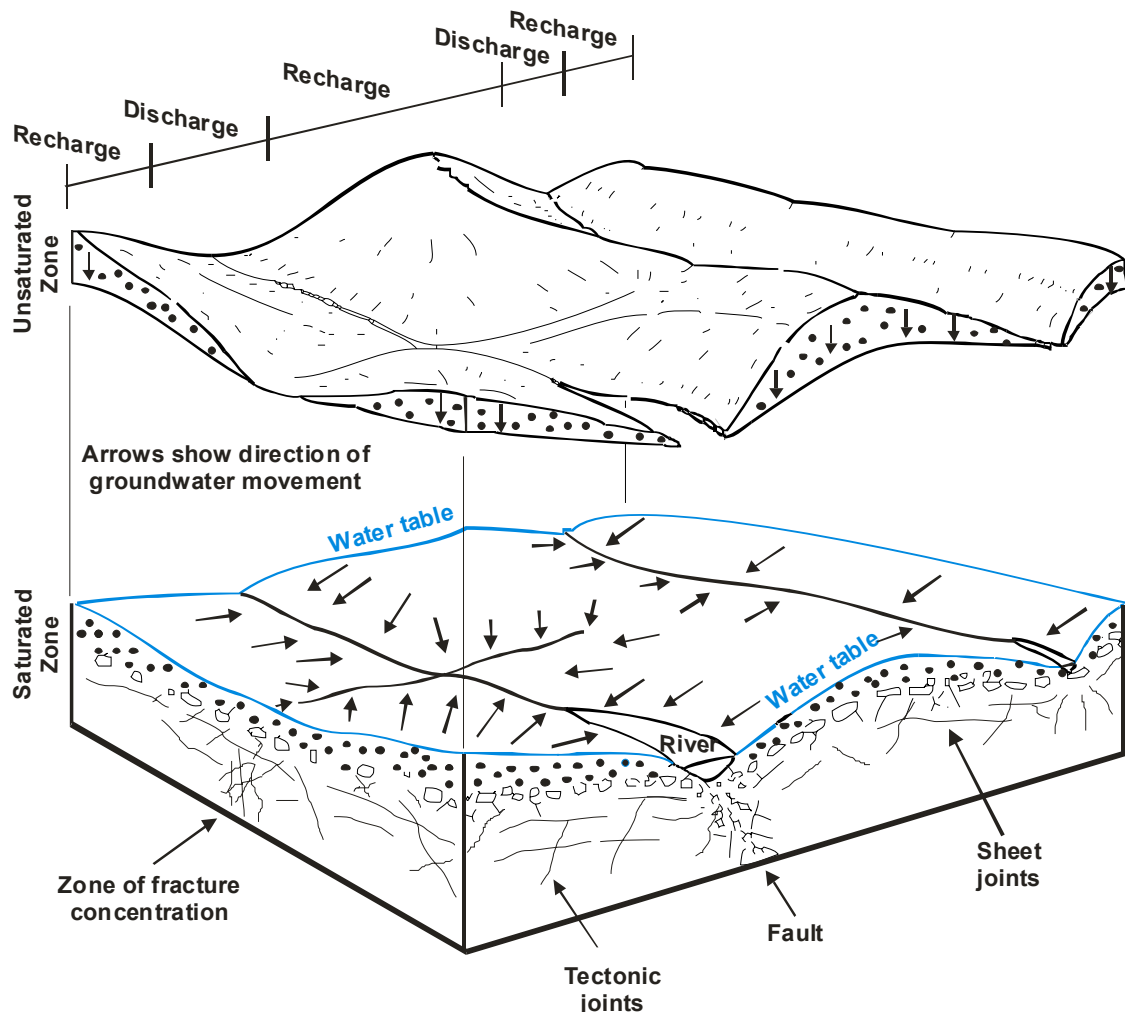


Fig. 7.1: Conceptual model of the regional hydrogeology (modified from DANIEL et al. 1997; not scaled; vertically exaggerated). Effective recharge takes place at tophill – discharge downhill. The groundwater table (blue) is set in the regolith. Groundwater in the saturated zone flows towards local morphological depressions. Flow in the bedrock is limited to the fracture zones.

The results from the piezometric observations (Chapter 4) and the investigation in hydrochemistry (Chapter 5) and environmental isotopes (Chapter 6) revealed that groundwater recharge and flow highly depend on local fractures systems.

Regional flow in the bedrock can be excluded due to its lacking fracture connectivity. A regional flow pattern in the regolith is unlikely too, due to the low overall gradient of the terrain (from Northwest to Southeast around 1.5 m/km). Additionally the terrain is undulated and the average median regolith thickness only around 20 m. Groundwater flow would therefore head towards the drains of the local subbasins.

7 Conceptual hydrogeological model

As consequence the groundwater table reflects the surface elevation (Fig. 4.11). Groundwater flow is therefore limited to the local subcatchments. Local conceptual models from the literature represent mostly x-sections of these subcatchments (e.g. MARTIN 2006, FASS 2004, CEFIGRE 1990 and ENGALENC 1978).

The case example from a subcatchment of the Ara River in the North of Djougou shows that groundwater levels in valleys are very diverging (Fig. 7.2). In the boreholes with 2 m depths at all three positions the water table is generally shallow, but in the valley it is the shallowest. The deeper boreholes (10 m and 20 m) show instead that the water levels measured in the valleys are the deepest. Those measured at the crest are still deeper than along the slope. This means for the valleys that perched aquifers on top of clayish valley fillings exist. Below these fillings the groundwater table is lowered either by the extraction from deep rooting plants in the riverine forests (compare with Chapter 3.5) or either by a system of well connected fractures draining off the water towards any distant feature of discharge.

The groundwater table at the crest is relatively lower than at the slope. This behaviour is caused by the equilibration of the piezometric surface in relation to the morphologically higher situated borehole position at the crest.

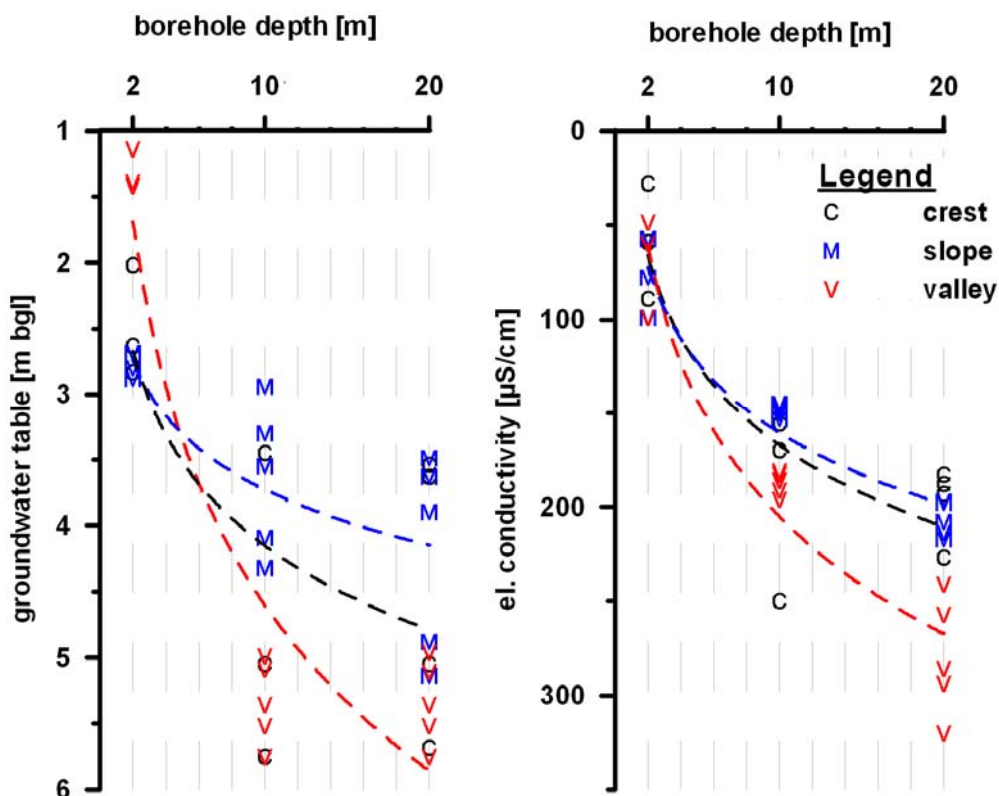


Fig. 7.2: Nalohou test site, Ara catchment (UTM 347124/1077311): Measurements from three boreholes of different filter depths (upper screen depth: 2 m, 10 m and 20 m; screen length: 1 m respectively). Boreholes positioned on the crest, the slope and the valley. Left – Observation of the groundwater table. Right – Measurements of the electric conductivity. Raw data received with the kind permission of L. Séguis, IRD (2007).

The comparison of EC measurements at Nalohou revealed an increase of concentration downhill. The highest values were observed in the deeper groundwater levels of the valleys. It is supposed that outwash and dissolved content from the crest and the slope is

accumulated within the valley filling. Assuming that the valley is formed on a well drained fracture zone, groundwater should experience a relatively rapid exchange and thus a decrease in EC. This is not the case; instead it has to be assumed from the observation described for Fig. 7.2 that the lower groundwater level in the river valleys is caused by transpiration through the riverine forests. The roots of trees in these forests but as well of the alone standing trees and in the tree Savannah can easily achieve depths from 10 to 20 m (L. SEGUI, IRD, oral comm. 2007; C. ZUNINO, oral comm. 2006; Y. TRAVIS, LHA, oral comm. 2005). Thus, they are able to extract groundwater throughout the whole year. This assumption was also made before by L. SÉGUI (IRD, oral communication 2007) and by ENGALENC (1978) for comparable sites in Benin and in West Africa.

As said before in Chapter 1.3 only a few regional groundwater models in a sub-Saharan setting are described in literature. In two case studies from southern Africa groundwater models were developed including discharge of groundwater by trees. KLOCK et al. (2001) assumed a discharge of 20-30 mm/a from Kalahari aquifers by Acacia trees.

BAUER (2004) determined the groundwater discharge by riverine forests in the Okavango delta as varying between 21.9 and 1569.5 mm/a. He also observed that the downstream groundwater velocity is very low compared to the lateral flow velocities feeding the water demand by the riverine forests.

The interaction of groundwater with surface water is discussed in Chapter 4. The probably very small contribution of groundwater from deeper aquifer levels in the regolith and the bedrock is additionally demonstrated by the electric conductivity. The general electric conductivity of running river water is $< 100 \mu\text{S}/\text{cm}$. Groundwater is progressively higher charged with increasing depth. Thus any infiltration would only be caused by the shallowest groundwater levels and interflow. FASS (2004) calculated the possible share of bedrock groundwater on rivers as 2%. But his references for bedrock water were the wells and observation boreholes of Dogué which, although relatively deep, are not dug in the basement.

It is concluded that bedrock groundwater has generally no influence on surface water. Wherever surface water bodies (lakes and rivers, bas-fonds) are connected to the fractured aquifer below it would certainly influence its hydrochemistry. This area of influence is controlled by the fracture connectivity. Elsewhere the influence of surface water on groundwater chemistry was excluded by isotopic evidence (Chapter 6).

8. Groundwater flow model

8.1 Objectives of the model

In the previous chapters it was already described that the hydrogeological conditions of the crystalline basement aquifers in Central Benin as well as the available data base limit the application of a regional groundwater modelling approach. The encountered groundwater hydraulics does not fit the conditions found in other catchment areas of comparable size with thick sedimentary aquifers and a considerable groundwater flow velocity. Instead, the HVO catchment consists of many subcatchments that are not necessarily well connected among another. Regional flow is limited through the fracture connectivity and the very low general permeability of the regolith. The total aquifer thickness (regolith + bedrock) achieves a maximum of 80 m. The relationship between this value and the horizontal extension HVO area is roughly equal to 1:100.000. This means the aquifer only represents a very thin layer parallel to the surface. Under such measures described before it seems not reasonable to build a detailed regional numerical model. Further on there exist not enough piezometric time rows at sufficient observation points in the HVO. The uncertainty of model results could not be controlled by any other means than by the comparison with the generally observed position of the groundwater level at different seasons. Accepting that the lack of input would cause uncertainties within a several meters range they would almost always fit the originally observed groundwater levels.

As consequence only a general approach was applied for simulating groundwater flow in the HVO area as described by the conceptual model in Chapter 7. The resulting model simplifies the HVO area to a great measure by its geometric dimensions and by the distribution of its hydraulic parameters. It was tried to use parameter values within the order of observed field data, values from literature and from other models.

The purpose of the model is to prove the assumption made for the conceptual model that the average groundwater level observed in the field can be maintained by recharge/discharge within the model area.

The constraints given to this modelling approach are discussed in the following chapters respectively. The impact of groundwater exploitation on the groundwater resources was considered under regard of the IMPETUS-scenario information.

8.2 Model geometry

The numerical groundwater flow model is a three-dimensional finite element model with triangular elements of different size. The model area covers almost the whole HVO (Fig. 8.2). The natural boundary of the catchment is the hydrological watershed. The course of the natural watershed is very complex and shows many turns and edges. Discretisation close to the course of this boundary demands an increased number of mesh nodes on the boundary itself. Thus the numerical weight of the boundary elements would greatly influence the inner model solution. To avoid this problem the outline of the model area is chosen within the HVO area and is straighter than the watershed's course. The model area is about 13,985 km² and thus 3.5% smaller than the total HVO area. The average element size is, under regard of their number per layer, approximately 1 km² (Tab. 8.1).

Local features like inselbergs, duricrusts and bas-fonds were not modelled. The regolith aquifer is generally unconfined.

Horizontally the finite element mesh was automatically distributed by the T-mesh Delaunay procedure (DIERSCH 2005). The refinement along the rivers was done manually. Initial model tests showed that a refinement around the villages was not necessary. Only in the case of Djougou the model mesh around the village's coordinates was refined to reduce the sphere of influence of drawdown caused by groundwater exploitation in this area.

Tab. 8.1: Number of nodes and elements in the model after the final refinement.

Layers	N° Elements	N° Nodes
single layer	13,635	9,284
all layers	40,905	27,852

Vertically the model is structured in three layers. The bottom layer represents the fractured bedrock aquifer while the two top layers simulate the regolith layer. The total thickness of the regolith aquifer was assumed to be 20 m (see Fig. 8.1). The regolith aquifer was then divided by equal parts into an upper and a lower layer for numerical reasons given by DIERSCH (2005). DIERSCH (2005) advises to divide thin layers in two or more layers to produce more elements for water exchange. The bottom depth of the bedrock aquifer was determined as 80 m below ground. This is the maximum depth where groundwater can be exploited from boreholes in Benin under economical conditions (SOGREAH and SCET 1997).

The model slices are determined as plane (Fig. 8.1). Note that the top elevation of the first slice is zero. Groundwater heads are measured as meters below ground level.

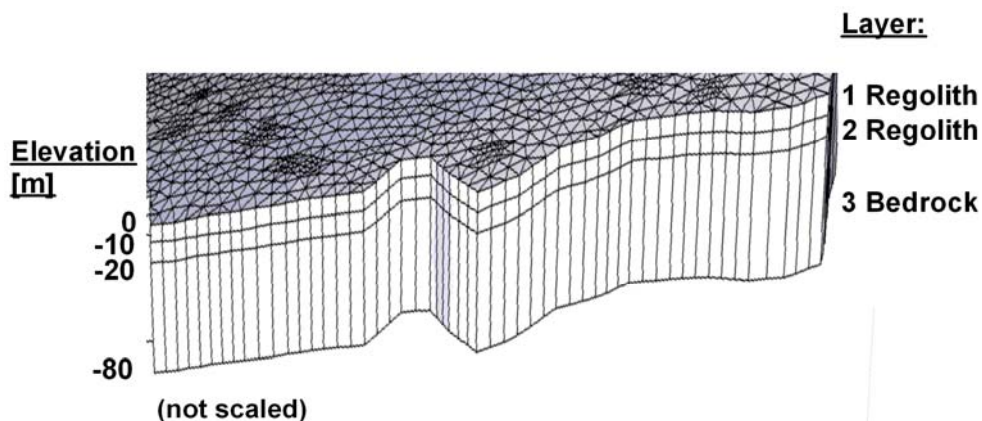


Fig. 8.1: Presentation of the model area in a 3D sketch. Three layers, with a plane surface but a dip from the North to the South, represent the regional geology.

8.3 Boundary Conditions

The schematic Fig. 8.2 shows the distribution of the boundary conditions (BC) of the model area.

It is assumed that the hydrogeological watershed of the HVO is at the same position as the hydrological. This is likely because of the shallow water table and the observation of a generally morphology driven groundwater flow (Fig. 8.3 a). The connectivity of

8 Groundwater flow model

fractures especially in the bedrock aquifer may result in different flow ways (see Fig. 8.3 b). In regard to the size of the HVO it is assumed that inflow and outflow of groundwater beyond the model boundary are in general equal.

The whole HVO groundwater divide is considered as a BC of the 2nd type – constant flow (also known as Neumann condition). In this special case it is a no-flow boundary (flow = 0). Flux in and out along the HVO groundwater divide may occur but is because of the slow groundwater movement which is based on local subbasins only of importance for the subbasins very close to this divide (refer to Chapters 7 and 8.1).

In FEFLOW[®] special constraints can be given to each boundary condition. It was chosen to supply the Neumann condition with a head constraint of minimum 8 m bgl to a maximum of 5 m bgl. This procedure was chosen to assure that boundary nodes would not fall dry and is in accordance to the head observations made in the HVO area as described in Chapter 4.

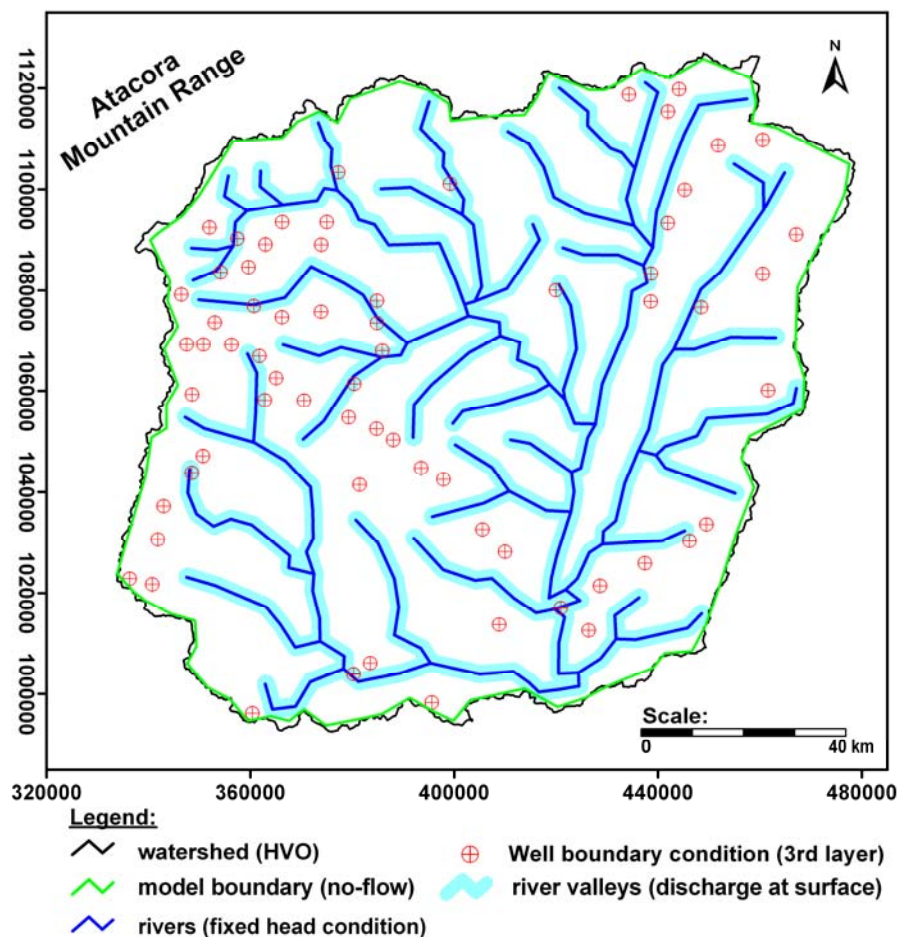


Fig. 8.2: Distribution of the boundary conditions in the model area for the 3rd layer (bedrock). For the regolith layer the distribution is the same, but without the well boundaries (Projection: UTM, Zone 31P, WGS 84).

The model needs water discharge in its internal area otherwise it would stockpile without limit. As stated before regional groundwater flow is excluded. Downstream flow appears under these conditions (Chapter 4 and 7) not effective enough to deliver an important discharge function. In regard to the assumptions made in Chapter 7 discharge through vegetation was included into the model. Based on the conceptual model a buffer area around the rivers was created to represent the riverine forests (see Chapter 8.4).

These buffers areas had to be secured from running dry as water transfer due to the relatively low overall aquifer permeability (Chapter 8.4) would be too slow for a refilling in time. Therefore the rivers were configured as fixed head conditions of the 1st type (Dirichlet condition) with a general value of 10 m bgl. This is a couple of meters deeper than where the groundwater table's position is found according to the observation in Fig. 7.2. The reason was to provide generally more space for groundwater fluctuations below the top layer of the model.

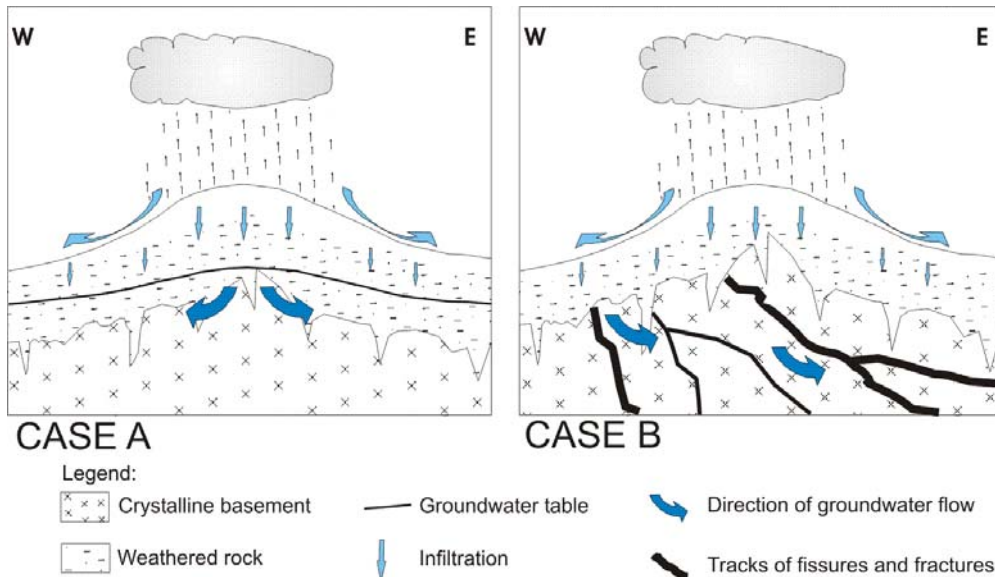


Fig. 8.3: Case A - Accordance of the hydrological and hydrogeological watershed. Case B – Shift of the hydrogeological watershed due to fracture connectivity.

FEFLOW[®] defines wells and pumps as 4th kind BCs. The position of the well conditions is copied to every model layer but the extraction is assigned to the bottom nodes only (Fig. 8.4). Ideally the extracted water at the bottom layer should be equilibrated by water from the 2nd layer. Exploitation rates for domestic use are rather small and generally negligible for regional models.

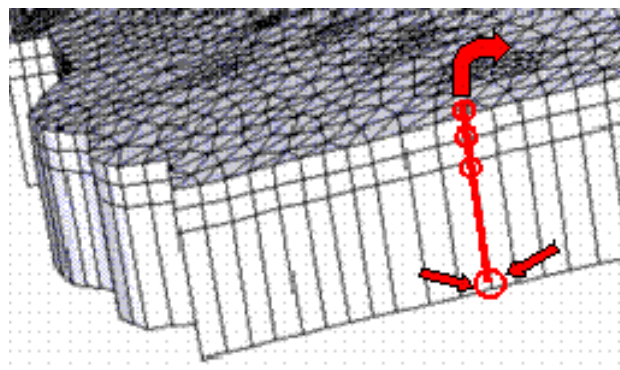


Fig. 8.4: The placement of the well conditions at the bottom of the third model layer is based on the assumed filter position in drill holes. Extracted water leaves the model without any redistribution. Therefore the mesh nodes of concern in the 1st and 2nd layer are described as well conditions with 0 m³/d extraction. The nodes set vertically above one to another will act numerically as a connected tube. Extracted water will be equilibrated by inflow from the other layers.

8.4 Hydraulic parameters

The characterisation of the hydraulic properties of the HVO aquifers demanded a high grade of generalisation of the most important parameters for saturated flow: the hydraulic conductivity and the storage coefficient.

It is quite difficult to generalise k_f -values in the regolith aquifer due to local differences like macropores, roots, duricrusts or different weathering intensity as presented by FASS (2004) and BAUER (2004). However, most of the k_f values found in the Beninese regolith vary from 1E-04 m/s to 1E-08 m/s. In respect to the regional scale, the fractured bedrock was considered as a porous medium with a lower permeability. The values applied in Tab. 8.2 are found during the process of model calibration. A lower permeability would hinder the exchange of groundwater in this model and it would start to pile up. Higher permeabilities caused the regional equilibration of the groundwater table and the discharge areas became disguised.

The storage coefficients presented in Tab. 8.2 were taken from literature (SOGREAH and SCET 1997; BOUKARI et al. 1985). FEFLOW[®] requests vertical hydraulic conductivities which were assumed as 1E-01 less than those of the horizontal hydraulic conductivity (LANGGUTH 2004).

Tab. 8.2: Hydraulic parameters as applied to the model layers.

Layer	Type	Horizontal k_f [m/s]	Vertical k_f [m/s]	Storage coefficient S [-]
1	Regolith	5E-06	5E-07	0.03
2	Regolith	5E-06	5E-07	0.03
3	Bedrock	1E-08	1E-09	0.00001

Recharge was applied on the top layer. Details about the recharge distribution are given in Chapter 8.5.3. In accordance with the conceptual model (Chapter 7) it was necessary to establish discharge areas close to the river net. A buffer area with its limit in 1 km distance from the river to each direction was created (Fig. 8.2). By this way an area of 2,291 km² got covered (16.4% of the total model area).

It is likely that discharge through transpiration by plants is an important factor in the water budget. Most of the trees in the study area have roots reaching deeper than 10 m. Their water consumption might be the reason for the seasonal draining of the groundwater level. The constant base level of the groundwater hydrographs may thus represent a general balance between recharge and evapotranspiration.

Evapotranspiration was already subtracted from the recharge calculation by the UHP model (chapter 8.5.3). But transpiration still is an important process affecting the groundwater table in greater depths.

The extension of the river buffers is greater than the riverine forest cover in reality. But the buffer area shall represent as well all off the assumed area in the HVO covered by trees with root systems feeding from the groundwater table (compare with the dense vegetation pattern in Fig. 3.13). Fig. 3.26 shows that the preferential zones for effective recharge are found uphill in the area of the interfluves. Thus the river buffers are representing the areas without recharge but with discharge instead. Additionally, the creation of the distinct buffers serves the model purpose to create local flow patterns towards the local drains. The manifold branches of the real river system in the HVO are

difficult to identify and cannot be included in such detail into a regional numerical model. Thus only the main rivers were included and the buffers chosen can only be coarse approximation to the real tree cover area with impact on the groundwater table.

A value of 73 mm/a is consigned to the discharge area of the river buffers (Fig. 8.2) on the top layer where it replaces the net recharge. The value mentioned for discharge is a compromise between values from literature (BAUER 2004, KLOCK et al. 2001 and KLINE et al. 1970) and an iterating approach on both the stationary and the transient models (Chapter 8.6). However, the choice of the size of the river buffers is mainly assumptious and serves primarily the intention to create a simplified model for regional flow.

8.5 Integration of scenario information

8.5.1 Climate scenarios

The Intergovernmental Panel on Climate Change (IPCC) described in its Special Report on Emission Scenarios (SRES published as IPCC 2000) different pathways for the world's future development until the year 2001. A set of 4 divergent but still plausible storylines (A1, A2, B1 and B2) was created. The storylines are subdivided by emission schemes or other assumptions. The outcome is a whole family of possible scenario descriptions for every storyline. IMPETUS refers to the scenarios A1B and B1 as input of driving forces to their models (BRÜCHER et al. 2005). A short description of the scenarios is taken from the SRES (IPCC 2000):

- A1** – A future world with rapid economic growth and a global population that peaks in mid-century and declines thereafter and the rapid introduction of new and more efficient technologies. The A1 scenario family develops into three groups that describe alternative directions of technological change in the energy system. The three A1 groups are distinguished by their technological emphasis: fossil intensive (A1FI), non-fossil energy sources (A1T), or a balance across all sources (A1B) (where balanced is defined as not relying too heavily on one particular energy source, on the assumption that similar improvement rates apply to all energy supply and end use technologies).
- B1** - A convergent world with the same global population that peaks in mid-century and declines thereafter, as in the A1 storyline but with rapid change in economic structures toward a service and information economy, with reductions in material intensity and the introduction of clean and resource-efficient technologies. The emphasis is on global solutions to economic, social and environmental sustainability, including improved equity, but without additional climate initiatives.

The results from the global climate model ECHAM 5 (ROECKNER et al. 2003) for each IPCC-scenario was downscaled to a regional climate model REMO (JACOB 2001) applied by H. Paeth (IMPETUS A1, PAETH 2006). The REMO integrates as well the land use scenarios modelled by the IMPETUS subproject A3. REMO delivers the climatic input parameters for the hydrological modelling with the UHP model for the A1B and the B1 scenarios.

8.5.2 Socio-economic scenarios

IMPETUS (2006) worked out different scenarios for the development of Benin embedded in a general global context. These scenarios and their general storyline background are in short abbreviated as follows:

- BI** - Economic growth and stable decentralisation;
- BII** - Economic stagnation and institutional uncertainty;
- BIII** - Business as usual.

The scenarios should cover the eventual socioeconomic changes in the Ouémé catchment for the future. However, it was necessary to make a regional subdivision. The catchment was structured in three parts: the Upper Ouémé, Middle Ouémé and Lower Ouémé. Their limits were chosen based on general environmental features and not on hydrological boundaries. The impact of the socio-economic scenarios in regard to HVO groundwater resources concerns mostly the development of the rural population (see Chapter 8.5.4). The scenario data of the Upper Ouémé scenario subregion was adapted to the smaller HVO area.

8.5.3 Recharge

The value for recharge was derived from data computed by S. Giertz (IMPETUS subproject A2, Workpackage Hydrology) with the conceptual, hydrological model UHP-HRU 1.1 (BORMANN and DIEKKRÜGER 2003, GIERTZ 2004). The UHP model subdivided the HVO area in 525 so-called hydrological response units (HRU) with an average size of 30.5 km². The software automatically determines the coverage of the model area by HRUs as function of the prescribed area and the terrain elevation. Flow to the aquifer storage is described as net recharge. The climate input data for all HRUs is exclusively taken from the Parakou climate station. Precipitation data was obtained from several climate stations installed by the IMPETUS project in the HVO area.

The average trend of recharge in Fig. 8.5 was calculated by the unweighted average of recharge at all HRUs at each time step respectively. The UHP model starts already in the year 1993 (GIERTZ et al. 2006). The groundwater model instead operates with an initial recharge amount calculated from the UHP model results for the year 2001.

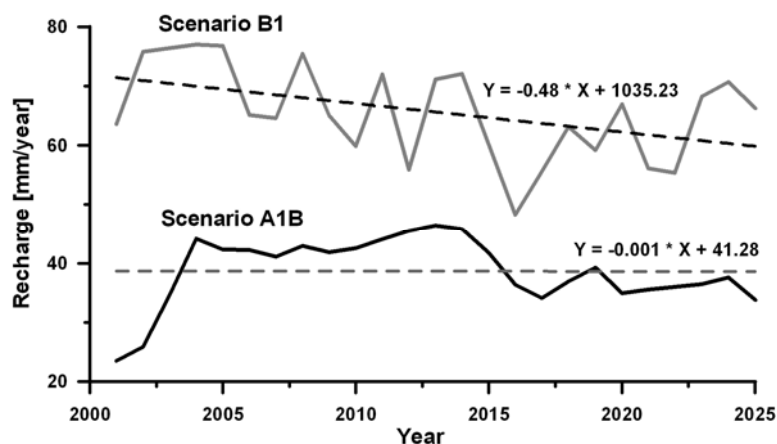


Fig. 8.5: Average yearly recharge (unweighted) from all HRUs for each scenario A1B and B1 with trend (dashed lines) and trend equation (original recharge data from GIERTZ 2004).

The recharge in the B1 scenario is generally higher than for the A1B scenario but is fluctuating stronger during the year. However, the average curve for B1 (Fig. 8.5) shows a clearly decreasing trend, although in the case of some HRUs the recharge in 2025 is still higher than in 2001.

This groundwater model was only produced in the aftermath of the scenario calculations by the UHP model. A coupled approach for both models to compute the net recharge towards the aquifers was not achieved.

The actual simplified groundwater model uses the initial average recharge for both scenarios (44 mm/a) in the year 2001 for the whole HVO area as entry parameter. Scenario A1B shows no change of recharge during the transient model period because of the almost linear recharge trend. For scenario B1 the annual change of recharge in the HVO was calculated by the B1 trend equation (see Fig. 8.5).

In the transient model it was distinguished between dry months and months with recharge notable the dry season and the rainy season (Fig. 8.6). During the dry season (October to April) recharge was set to zero. The total yearly recharge was distributed to the months of the rainy season (May to September).

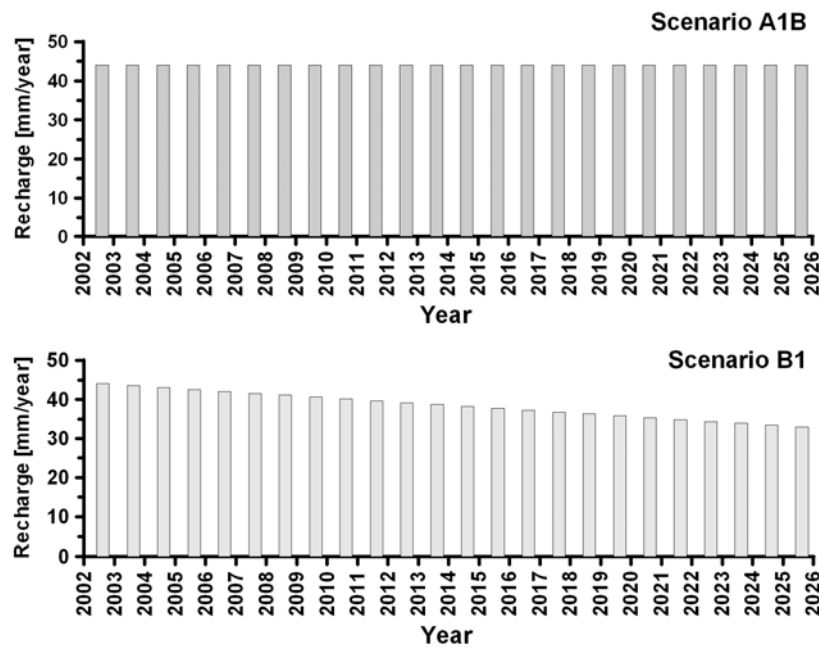


Fig. 8.6: Effective recharge towards the groundwater table; calculated input data for the model scenarios A1B and B1. Recharge is limited to the months of the rainy season. The model starts in the beginning of the year 2002 in the middle of the dry season. Scenario A1B shows constant recharge while B1 is characterised by a decreasing recharge.

8.5.4 Water use

Many hundreds of wells and pumps are found in the HVO area. As mentioned in Chapter 2.2 efforts are made to register the public water points in the BDI. As the BDI remains incomplete in regard to the private dug wells and unofficial water points it was decided to calculate the groundwater extraction from the model area preferentially from the average consumption of the inhabitants. Therefore the numerous water extraction points in a township are combined to a single well condition. The total water consumption by the inhabitants respectively is summed up. The potential demographic development for the scenarios BI, BII and BIII is based on the national census data (INSAE 2003) from 2002 (see Fig. 8.7).

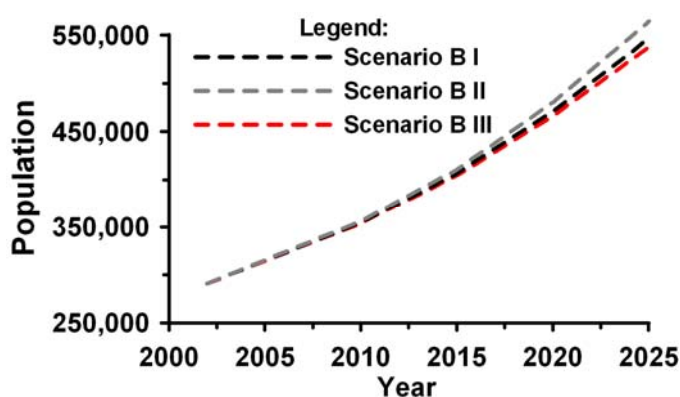


Fig. 8.7: Projection of the demographic development in the HVO until 2025 for the three IMPETUS scenarios (data from U. SINGER, IMPETUS subproject A5).

The census counted 119 townships in the HVO area. They are converted to water extraction points. When close to another, they were unified to simplify the finite element net. In total 66 extraction points remained and were implemented into the model as well conditions (see Fig. 8.8). The townships Djougou and Tourou (in the periphery of Parakou) are considered as towns, all the others are classified as villages.

The water consumption analysis of SCHOPP (2004) proved that the improved water supply in urban and peri-urban areas and water abundance during the rainy season cause higher water consumption (Tab. 8.3).

Tab. 8.3: Mean values of the water consumption in l/d per capita in different types of townships in the HVO as measured from 2002 to 2003 (SCHOPP 2004).

Month	Town	Periphery	Village
Jul	24.9	22.3	22.0
Aug	46.4	22.8	17.9
Sep	39.0	19.6	20.9
Oct	26.1	19.5	18.6
Nov	24.6	20.9	15.1
Dec	10.4	19.9	12.0
Jan	12.0	14.5	14.9
Feb	18.3	13.7	14.2
Mar	31.8	12.8	14.4
Apr	22.8	15.7	13.2
May	12.1	17.7	15.4
Jun	11.8	16.0	15.2
Mean:	22.8	17.9	16.2

Tapped water from the public supply system originates from surface water resources. Based on the water consumption analysis (SCHOPP 2004) it was tried to identify the share of groundwater on public supply (Tab. 8.4). The observed period comprises not a complete hydrological year but only the period from August 2002 to April 2003.

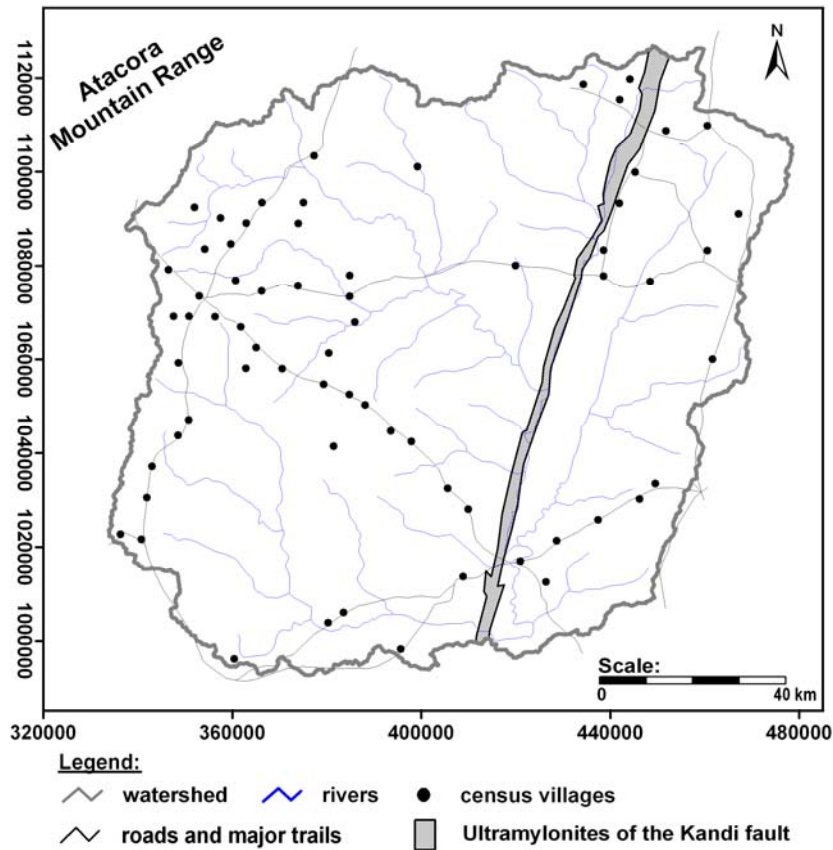


Fig. 8.8: Position of the remaining 66 villages after aggregation of the census data set from INSAE (2003). Each village presents a well condition in the model mesh (Projection: UTM, Zone 31P, WGS 84).

Tab. 8.4: Distributed use of the different water sources used to satisfy the general water demand based on the observations of SCHOPP (2004).

Month	Well	Marigot	Rain	Pump	Groundwater (Well+Pump)
Aug	92.19	7.59	0.22		92.19
Sep	90.48	9.51			90.48
Oct	87.88	12.12			87.88
Nov	89.3	10.69			89.3
Dec	80.82	19.16			80.82
Jan	67.8	16.25		15.94	83.74
Feb	10.17	19.45		70.38	80.55
Mar	17.88	16.17		65.95	83.83
Apr	30.53	9.14		60.35	90.88

During the months of the rainy season water from wells is preferentially used (approx. 90% of the water needs). Water from marigots is used as well although more for cleaning and washing. The village wells are less productive during the dry season. Hence people start to look for water elsewhere, from marigots in the first place. From the middle of the dry season on, pumps become the principal water source. In general it can be said that

8 Groundwater flow model

groundwater abstraction covers around 80% of the total water consumption in the rainy season, and respectively 90% in the dry season. It is assumed that these percentages stay constant during the modelled time period. The water consumption for each of the 66 townships is calculated by multiplying the population respectively with the daily consumption [m³/d] and the seasonal percentage of groundwater extraction. The resulting data is imported into FEFLOW[®] as the 4th boundary condition.

A simplified calculation demonstrates the great potential of groundwater in the HVO to satisfy the public demand (Tab. 8.5). Assuming a worst case scenario the water content for both aquifers is assumed to be very low and recharge is ignored. Maximum water extraction from a population as projected for the year 2025 is added (Scenario B2). Human consumption will thus discharge the total aquifer storage only by 1.4%.

Tab. 8.5: Groundwater volume in the aquifers of the HVO. Minimum water content for both aquifers is assumed (low saturation level for one year). Recharge is ignored. Maximum water extraction from a population as projected for the year 2025 is added (Scenario B2).

Aquifer	Saturated thickness [m] ¹	Storage coefficient ²	Area [km ²]	Water Volume [m ³]
Regolith	5	0.03	14,300	21,450,000,000
Bedrock	20	0.00001	14,300	2,860,000
Total Volume				21,452,860,000
Exploitation (2025)				3,056,950.11
Partition of exploitation on total water volume				0.014 (1.4%)

¹Minimum values for the saturated zone.

²Minimum values from ENGALENC (1978).

The calculation of discharge by pumping for the HVO area (Tab. 8.6) in the years 2002 and 2025 show that the groundwater exploitation by humans is negligible in comparison to the recharge. However, local exhaustion by extensive pumping, eventually in combination with bad hydraulic conditions, cannot be excluded.

Tab. 8.6: Calculation of the discharge (in mm/a) caused by pumping in the HVO area for the comparison with the regional recharge.

	Year 2002	Year 2025
Population (HVO)	291,125	564,125
Consumption [l/d]	20	20
Total consumption [l/a]	2,125,212,500	4,118,112,500
Areal discharge [mm/a]	0.15	0.28

It is seen that the demographic development for all IMPETUS scenarios differs only slightly after the year 2015 (Fig. 8.7). The FEFLOW[®] model is therefore run with the well exploitation data for the scenario BII which shows the strongest increase in population and in water use respectively.

8.6 Stationary model

In regard to the seasonal conditions observed in the HVO it was difficult to decide about the setting of the stationary model. A stationary model for the dry season (no recharge) would produce only the piezometric base line as shown in the Fig. 4.4, Fig. 4.5 and Fig. 4.6. The model would be obsolete. On the other side it is obvious that a model representing recharge conditions will display an overflowing with water which could be managed only by artificial outlets. However, this second option was chosen to quantify the surplus of water and cope with it in the transient models.

The stationary model for the HVO represents an average rainy season. It was run with an initial recharge of 44 mm/a and a discharge of 73 mm/a as discussed above. All hydraulic parameters and geometric proportions remain constant.

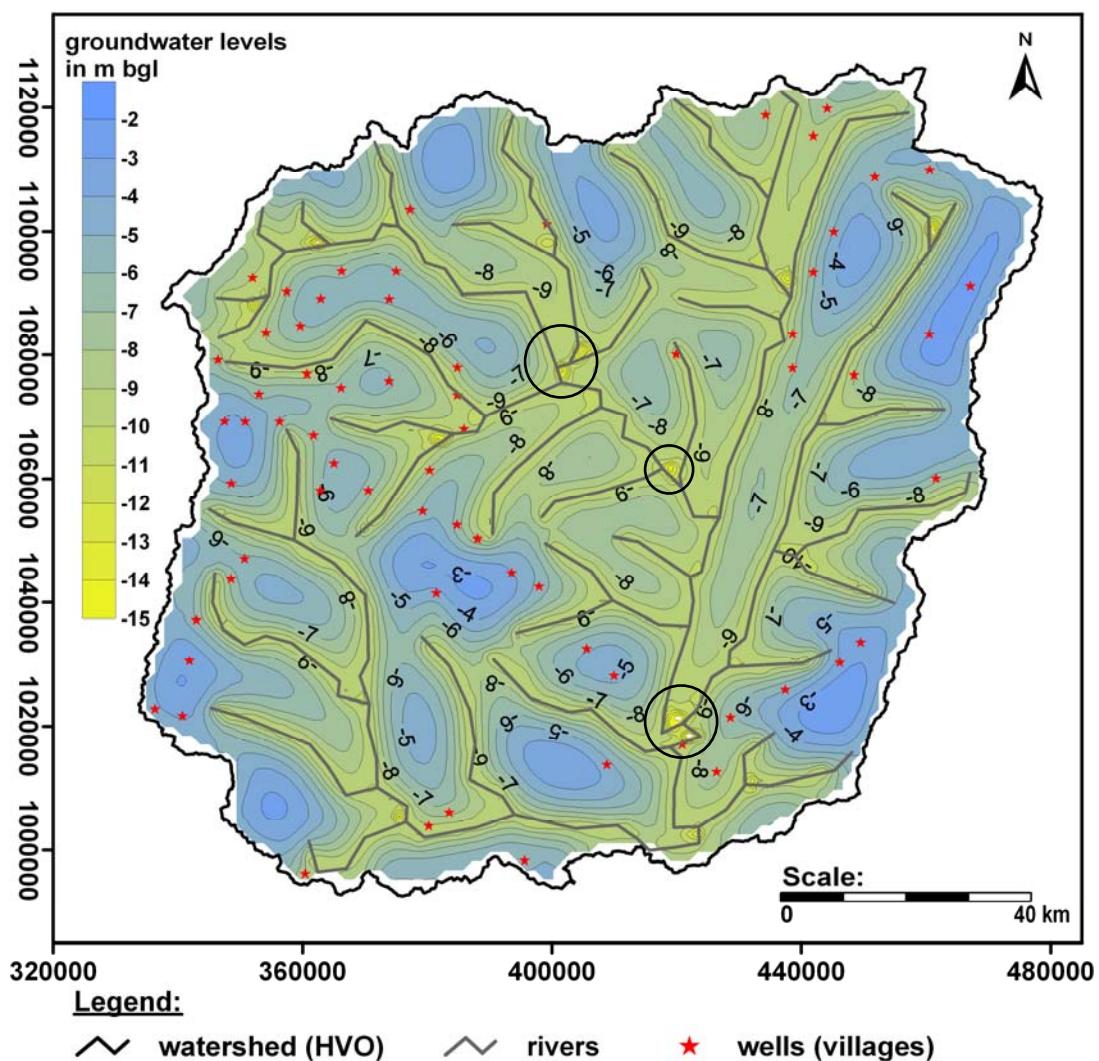


Fig. 8.9: Groundwater contours of the HVO model area from the stationary model with 44 mm/a recharge. Groundwater flow heads generally towards the closely lying river system. Black circles show joints of rivers with a strong drawdown motivated by numerical reasons (see text).

The resulting groundwater heads are in accordance with the conceptual model. The modelled groundwater contours are represented in Fig. 8.9. The groundwater flow regime is under control by the discharge from the areas around the closest river system

8 Groundwater flow model

respectively. Supraregional flow patterns are not observed. Drawdown by pumping does not show impact on the groundwater table under stationary conditions.

In some areas the groundwater table are lower than 10 m bgl. These areas are generally found close to river joints. Some are marked by black circles. The reason for this decrease is simply the areal extent of the discharge zone without a nearby recharge. However, these areas are only a few and were ignored as the aim of this model is showing the regional trends and not the exact analogue to natural conditions.

The total water balance for the stationary model reveals (Tab. 8.7) that the boundary conditions (especially the 1st BC) transfer quite big amounts of water to the outside of the model.

Tab. 8.7: Total water balance of the stationary model. The well flux occurs at the 3rd layer only.

Flux type	Flux in (+) Q [m3/d]	Flux out(-) Q [m3/d]
Dirichlet, 1 st BC	1.55E+04	-9.72E+04
Neumann, 2 nd BC	1.88E+03	-9.33E+03
Well flux	0	-3.16E+03
Aereal flux	1.23E+05	-3.08E+04
Imbalance	0	-5.4

The comparison of discharge and recharge shows that recharge in the stationary model is about three times greater than the discharge (Tab. 8.8). The excess water is removed by the BCs by the order of 28.6 mm/a. The 1st order BC is applied only to the river course itself and not to the total river buffer area. The elements of concern cover an area of around the half of the buffer area. Thus the influence of the 1st BD is objectionable. A more adjusted water balance would be achieved if a lower recharge of 22 to 33 mm/a would be applied. Then the discharge and recharge would compensate related to the area of concern.

Tab. 8.8: Comparison of discharge and recharge in the HVO model related to their share of the HVO surface.

Parameter	Coverage of the total HVO area	Water input/output related to the area of concern [mm/a]
Recharge (5 months per year) ¹	83.62 %	15.3
Discharge (buffer area)	16.38 %	12
Imbalance stationary model		24.8
Imbalance transient model		3.3
1 st BC	50 % (of the total buffer area)	26

¹ Reduction of recharge in scenario B1 leads to 11.5 mm/a in the year 2025 and thus a gradual equilibration of the water balance takes place.

For the transient models instead it has to be kept in mind that the original recharge is only distributed to 5 months of the yearly rainy season. The imbalance of the water

budget is then smaller. A difference of around 3.3 mm/a is computed which is automatically equilibrated by the BCs. In regard to the very simple model conditions this value appears relatively small and adjustable by minor corrections of the chosen parameters. These changes would not essentially change the order of the here chosen values for recharge and discharge. The simplified model approach supports the assumption that a regional groundwater flow is not needed to maintain the hydraulic groundwater conditions as observed in the field but rather a local flow control by drainage due to the riverine vegetations on a subcatchment scale. As consequence of the lack of field data to quantify and finally prove this assumption the model results remain unsatisfying.

The groundwater contours are used as initial head distribution in the transient models afterwards (Chapter 8.7). In FEFLOW® the stationary model has to be run first before the transient model in order to conserve the general flow system.

The stationary model was proved on its sensitivity to recharge. Therefore it was run with values for recharge ranging from zero to 200% changing in 25% steps (Tab. 8.9). The limit for the numerical head error was determined as 1E-03. In most cases the iteration was successful after 4 computing steps.

Tab. 8.9: Stepwise variation of recharge as input for the stationary model. For each case the error on the hydraulic heads was controlled. Minimum limit for successful computing is 1E-03 in less than 12 iteration steps (FEFLOW® default conditions, DIERSCH 2005).

Case	1	2	3	4	5*	6	7	8	9
Recharge [%]	0	25	50	75	100	125	150	175	200
Recharge [mm/a]	0	11	22	33	44	55	66	77	88
Iteration steps	>12	>12	4	4	4	4	4	4	4

**initial case*

For each case the average standard deviation of the areal groundwater head distribution was computed and is shown in Fig. 8.10. The model solutions for cases 1 and 2 are numerical insufficient in computing the residual heads. Adjustment in other parameters is needed, e.g. discharge. The options for modification are manifold and the lack of hard data does not justify any special approach. Case 6 still shows groundwater tables below ground surface. As shown above, this is due to the boundary conditions. All other cases with higher recharge produce tables partly above the surface.

The solutions with decreasing recharge show a lower deviation. However, the cases 3 to 6 produce all groundwater table contours within the range of the observations made in nature (Chapter 4). The recharge applied to these cases fit also to the assumptions made before in Chapter 4.2. Recharge may vary about -50% to +25% and is not very sensitive parameter for model calibration. An areal recharge of 22 mm/a could be outbalanced by the discharge introduced and thus represent a probable better start value. However, it preference was given to a higher value closer to the less assumptive UHP model results.

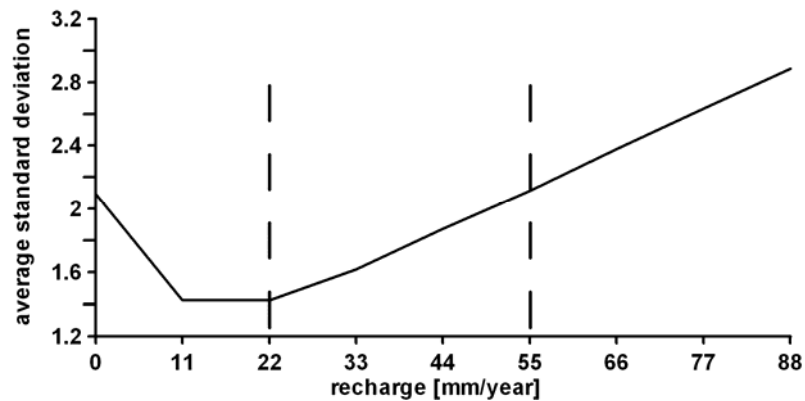


Fig. 8.10: Standard deviation of model solutions for different recharge cases. The area between the 22 and 55 mm/a represents equally reasonable model solutions.

8.7 Transient models

The transient models A1B and B1 use the same input parameters and geometric conditions. The initial conditions of both models are described by the stationary model (see Chapter above). Both models start at the 01.01.2002 and run until the 31.12.2025. The models compute daily time steps. The input data about exploitation from wells varies in monthly time steps (Chapter 8.5.4).

The only difference between both models is the data input of recharge. Recharge changes in seasonal steps (Chapter 8.5.3). While model A1B shows constant recharge (44 mm/a), model B1 shows an annual decrease of around 0.48 mm/a.

The calculation in Tab. 8.5 hints already that changes in recharge will have only a minor influence on the model results. But the models show as well the increasing groundwater exploitation by the population.

8.7.1 Scenario model A1B

The groundwater contours at the final time step of model A1B (Fig. 8.11) is mostly similar to the result of the stationary model (Fig. 8.9). Drawdown around villages is principally seen at Tourou. Tourou belongs already to the outskirts of Parakou and is one of the major settlements in the HVO. It has more than 13,000 habitants in 2002 (> 30,000 in 2025). Although Djougou has a higher population (> 50,000 habitants in 2002) drawdown cones are not observed in the same extent. The reason is the relative position of both locations in relation to the discharge zones. At Djougou water is exploited but in the same time it receives additional water from flow towards the rivers. Tourou instead is located closer to a centre of interfluves. Groundwater flow heads towards the two adjacent rivers additionally.

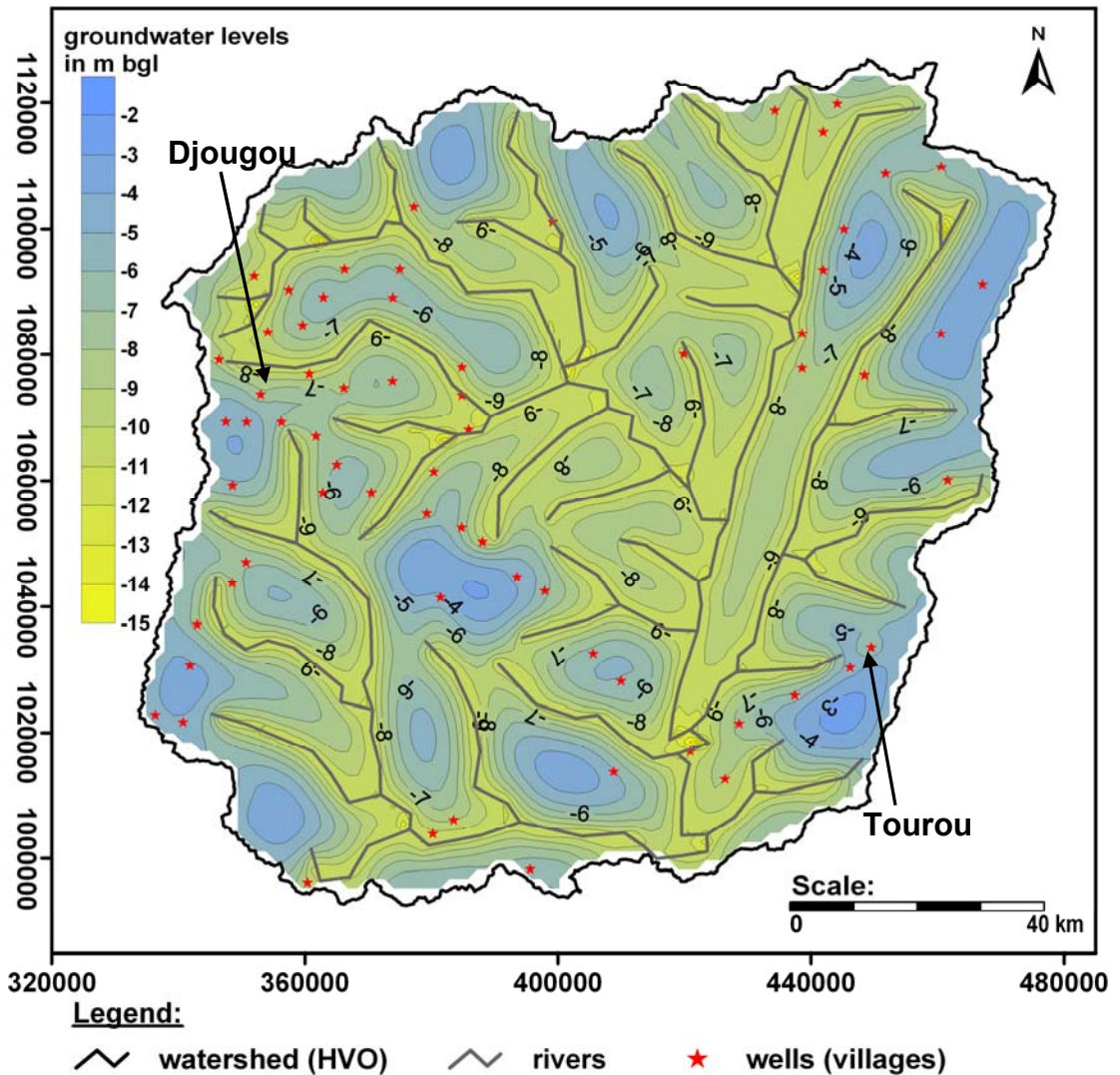


Fig. 8.11: Groundwater contours of the HVO model area from the final time step of the A1B scenario model. Groundwater flow heads generally towards the closely lying river system. Especially around the village of Tourou (see arrow) groundwater drawdown can be observed.

The map of groundwater differences in the HVO shows that the relative drawdown of the groundwater table is only concentrated on areas around wells (Fig. 8.12). Most of the area is only slightly affected by a lowering the groundwater table (< 0.5 m). The relative drawdown around is even more visible by this kind of presentation. In some cases the initial groundwater levels are lower than in the final phase of the scenario model. Those areas are mostly the same which has shown already stronger drawdown (Fig. 8.9). Some areas close to the model boundaries have slightly higher groundwater levels too. This is caused by remaining recharge from the rainy season before and which is still not equilibrated all over the area due to the relatively low hydraulic permeability.

As said before the natural reaction of the aquifers might be very different due to their fractured characteristics.

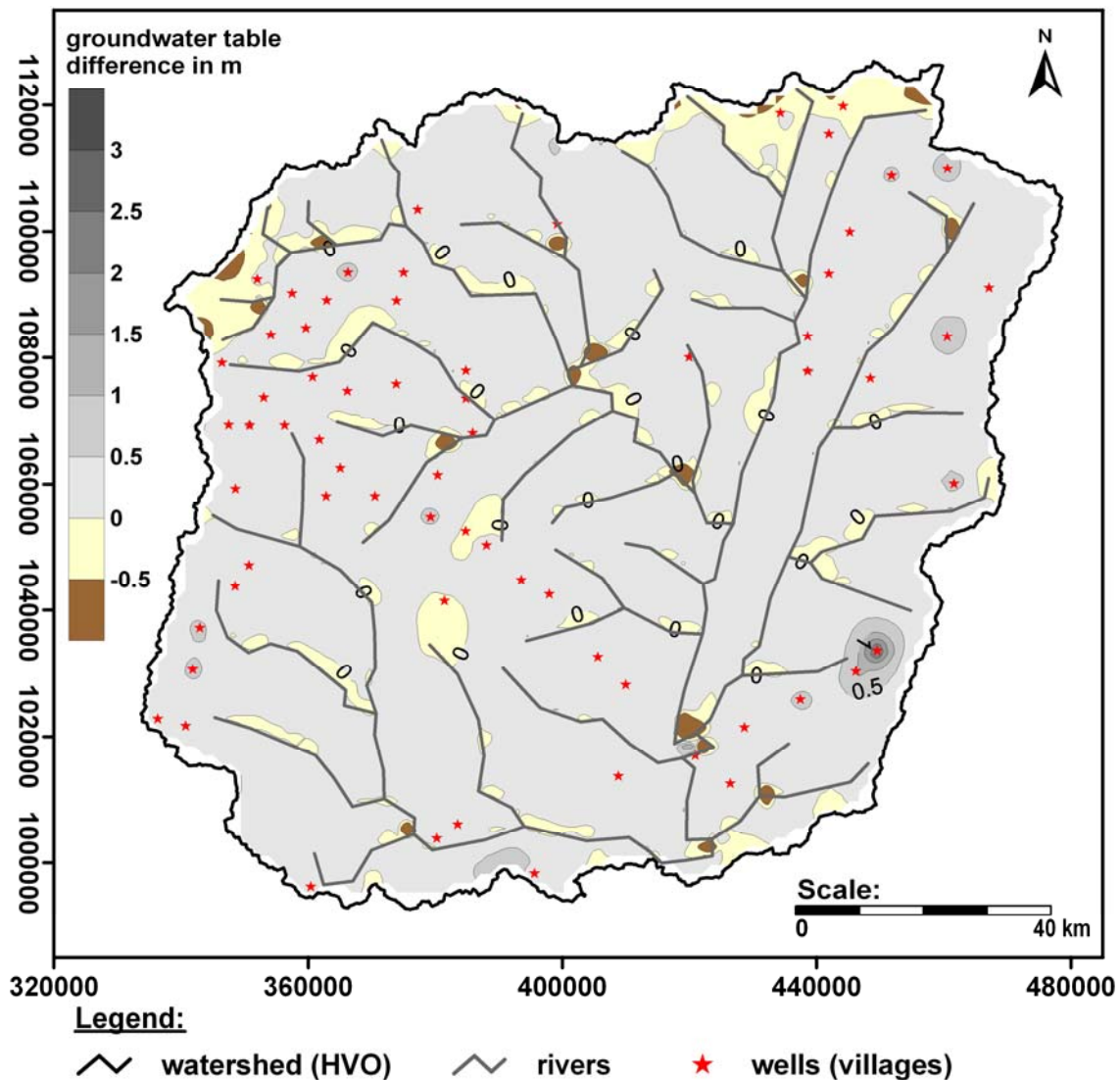


Fig. 8.12: Groundwater table differences between the final time step of model A1B and the initial conditions from the stationary model. Positive values indicate the drawdown of the groundwater table in the A1B model in relation to the initial conditions.

8.7.2 Scenario model B1

The groundwater contours at the final time step of model B1 (Fig. 8.13) show as well no significant changes in the groundwater flow pattern. Drawdown around Tourou is consequently more evident than in the A1B model. Around other villages as well drawdown cones can be recognised.

The contour map of the table differences (Fig. 8.14) between the final time step of model B1 and the initial head distribution shows for this scenario more extended areas of drawdown. At many interfluves the general groundwater level is lowered around 0.5 to 1 m. The total drawdown at Tourou is still the same as in the A1B model. This means that still sufficient horizontal flow may occur to cover the losses by pumping at this location.

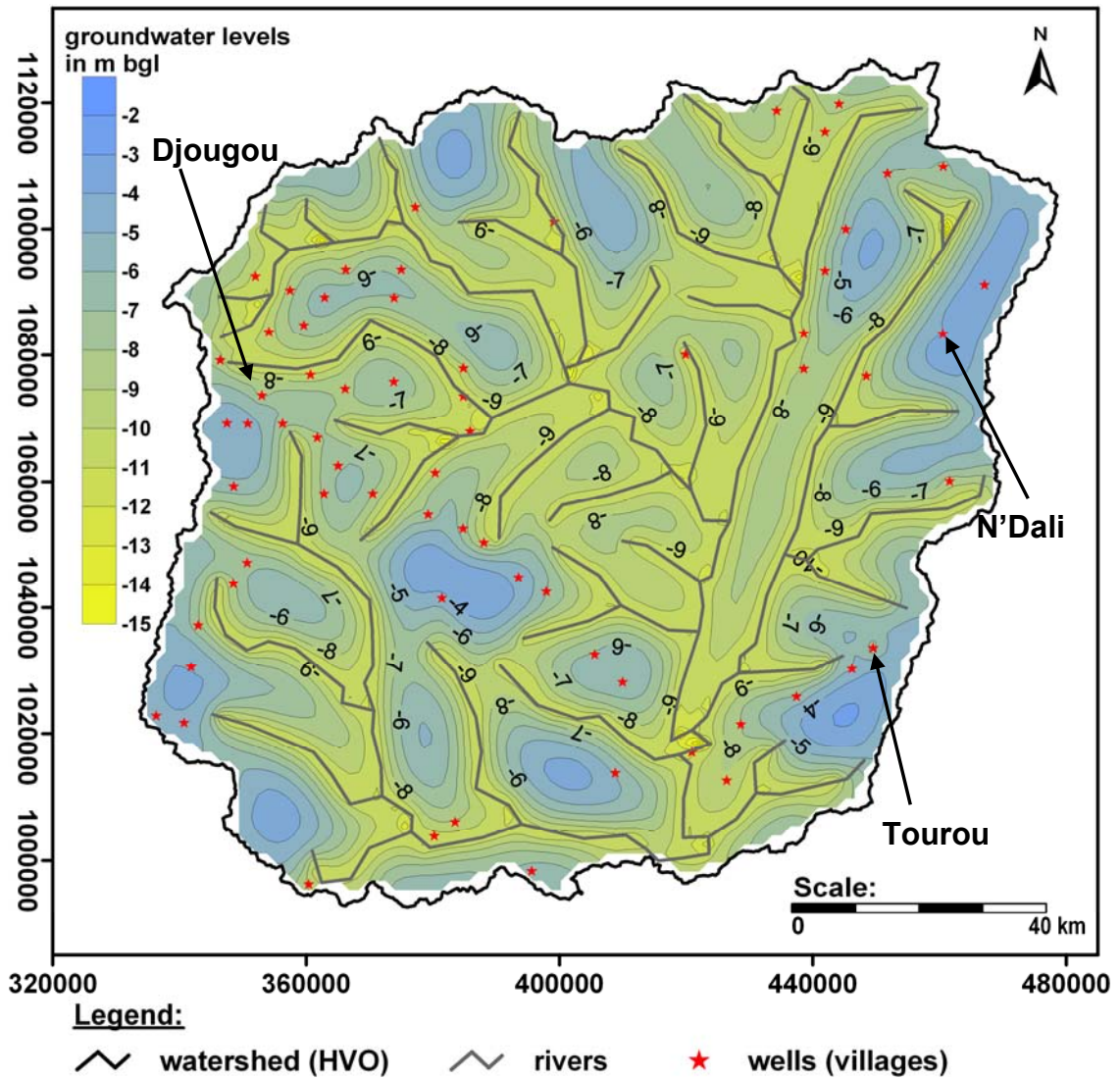


Fig. 8.13: Groundwater contours of the HVO model area from the final time step of the B1 scenario model. Groundwater flow heads generally towards the closely lying river system. Especially around the village of Tourou (see arrow) groundwater drawdown can be observed.

The areas with a higher groundwater table in the final stage of the transient model are decreased. Especially around the rivers they lack but still some are found close to the boundaries. This shows that the lower recharge in the final seasons modelled in the B1 scenario does need less equilibration.

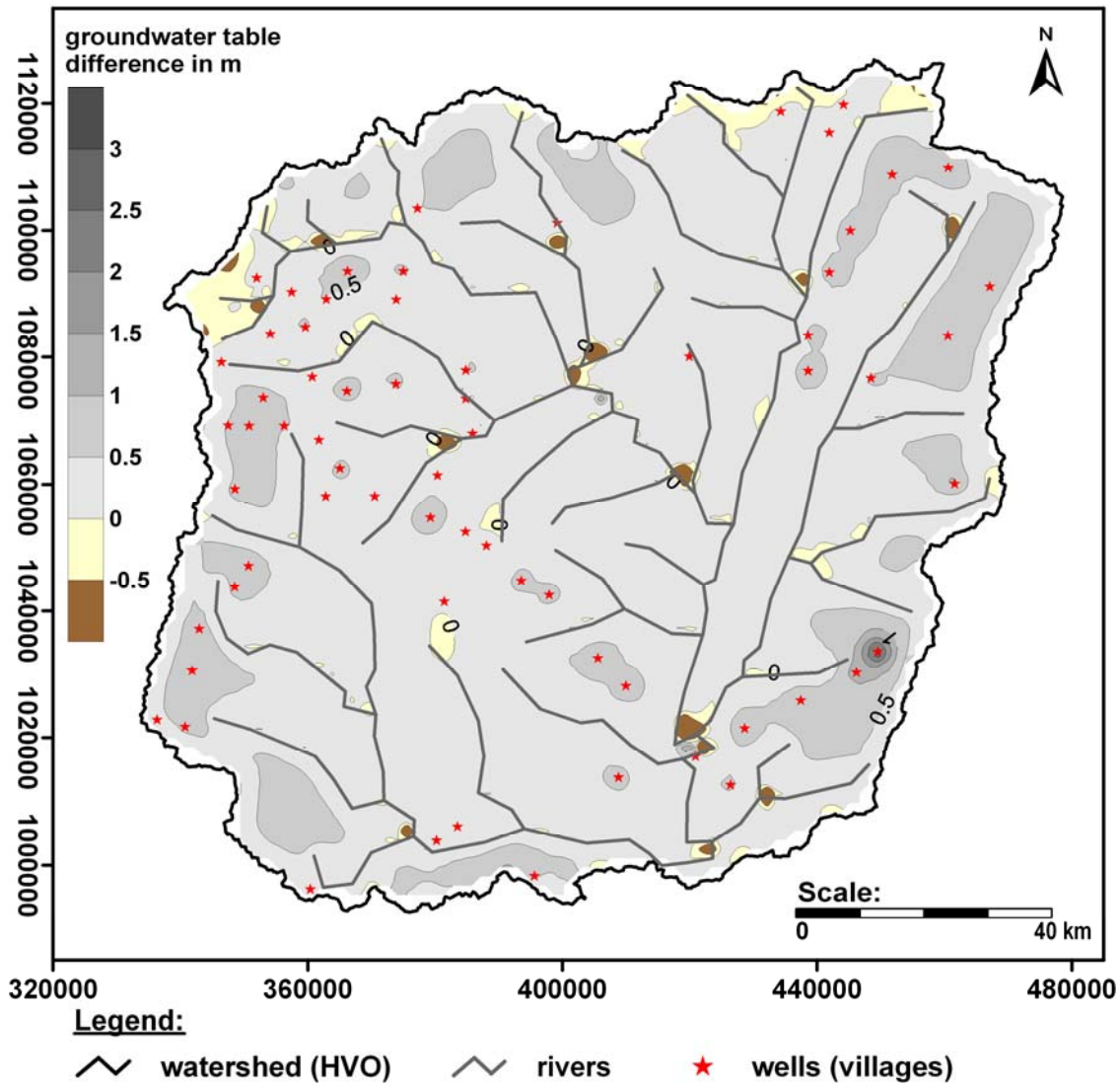


Fig. 8.14: Groundwater table differences between the final time step of model B1 and the initial conditions from the stationary model. Positive values indicate the drawdown of the groundwater table in the B1 model in relation to the initial conditions.

8.7.3 Model comparison

As described above the two scenarios show no important change in regional groundwater flow. It is observed that especially in model B1 local drawdown cones around the villages occur and may locally influence the groundwater direction. The calculation of the difference of the groundwater contours for each scenario is visualised in Fig. 8.15. The general difference between the two contour maps ranges from 0 to 0.35 m. The difference between the transient models is relatively small. The drawdown exemplarily measured at the observation point set into the village of Tourou remains almost the same for both models. The curve observed over the model period of the A1B scenario is only slightly higher (5 to 10 mm) than the one of the B1 scenario. The dynamic is identical. Fig. 8.16 shows the hydrograph of the well at Tourou in the A1B model. The figure shows that the groundwater table is locally mostly under influence of the seasonally adapted water consumption pattern.

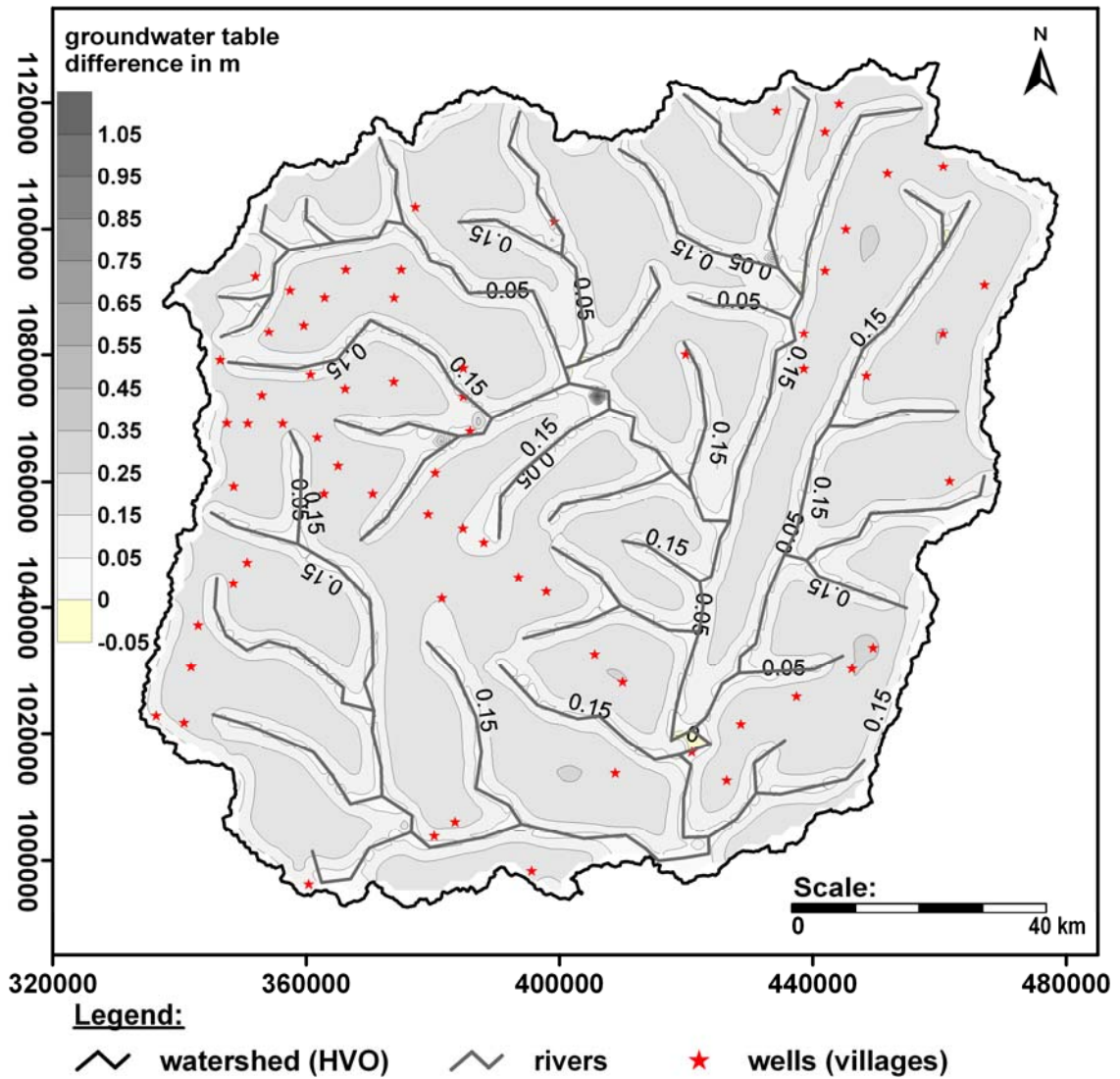


Fig. 8.15: Groundwater level differences between the final time steps of model A1B and model B1. Positive values indicate the drawdown of the groundwater table in the A1B model in relation to the initial conditions.

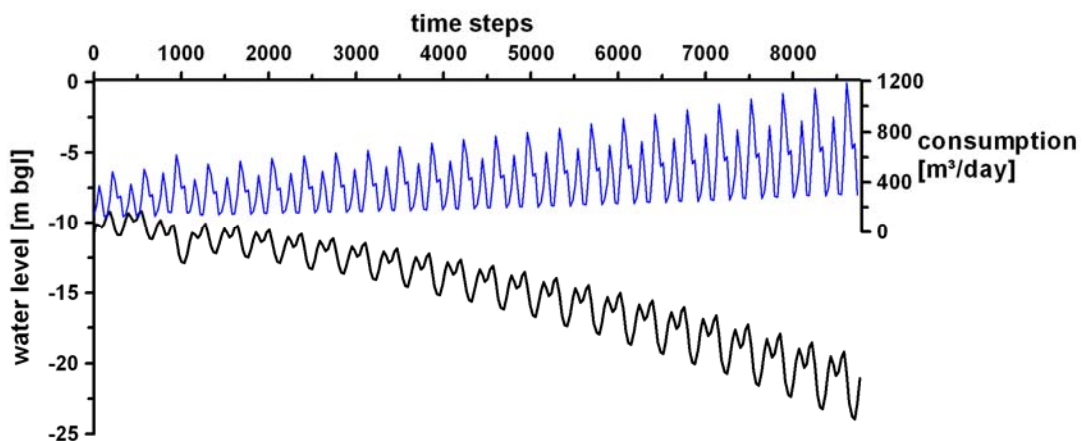


Fig. 8.16: Drawdown at the pumping well of Tourou (black line) and the consumption by its population (blue line). The seasonal fluctuations of water consumption can be traced by the behaviour of the modelled groundwater table.

The groundwater table depletes with the ongoing modelling time and seems to be locally more affected by the increasing local withdrawal from wells and generally less by

8 Groundwater flow model

decreasing recharge. The amplitude of groundwater fluctuations ranges from 1 to 5 m which is in accordance to the observations described in Chapter 4.

The transient model B1 simulates slightly decreasing groundwater tables due to decrease in recharge. The drawdown is relatively small and thus it is assumed that decreasing recharge is actually no threat to the development of groundwater resources in the HVO area. The aquifers of the HVO will not run dry. But it can be predicted, e.g. by the case of Tourou, that it is possible to exhaust the aquifers locally by continuous pumping. This problem was already considered in the planning of water supply for the bigger settlements in the study area, like Djougou, Bassila or especially Parakou and its periphery. For these settlements lake reservoirs were developed to allow public water supply throughout the year. Decentralised water supply by groundwater pumping for customers at the urban periphery and for rural settlements is in general no problem. Exceptions may exist where the local hydrogeology is not in favour for sufficient groundwater storage.

8.8 Uncertainties and constraints

The major constraints to regional modelling in the HVO are explained below. A quantification of the error of the calculation of the piezometric heads in the model is not possible. The reason is that a fractured environment is modelled as a porous milieu (see section e). However, the modelling results represent an average solution. The following points give a general overview about the general problems limiting the application of a regional numerical groundwater flow model for the HVO area:

a) Scaling problem: The model covers an area of around 14,000 km². The smooth changes of the vertical terrain elevation are negligible when compared to the horizontal model extension. An intensive mesh refinement in order to achieve a better representation of the surface demands extensive computational power and a very refined digital elevation model as input source.

b) Piezometric data: Piezometer time series are very important for transient models. The piezometric data obtained from the IMPETUS data loggers covers a period of two hydrological years (May 2004 to February 2006). Model prediction for more than twice the time of the gauged period is not recommended (ESSINK 2000; BEAR 1992). Additionally the piezometer groundwater hydrographs may show very individual reactions of the groundwater caused by local features e.g. fractures as discussed in the case of HVO-9 (Chapter 4.1). The regional model approach is not able to integrate these local features. A direct comparison of model data with observed piezometric data seems therefore unreasonable. However, it was possible to compare the modelled data with the overall level of the groundwater table in the studied area.

c) Conceptual model: The conceptual model makes difference neither for the differing bedrock types nor for the regolith formed through weathering out of the first. A reason is the lack of consistent data about relevant outcrops and boreholes and the unrefined level of the hydrogeological and geological maps available for the study area. The achieved data gave no clue for differing hydraulic characteristics of the bedrock. As consequence

the conceptual model generalises the main flow components for the whole study area. Single terrain features, e.g. the Kandi fault and the Inselbergs, are not integrated because of the reasons given above (lack of data, scale problem).

d) Hydrological data: For the here presented model only average recharge values were applied. The order of magnitude was derived from the regionally differentiated UHP model data (IMPETUS subproject A2, Workpackage Hydrology). As the groundwater model design is simpler as the UHP model an approach to calibrate the net recharge towards the aquifer by coupling the models was not realised.

e) Fractured bedrock aquifer: The bedrock layer is modelled like a porous, homogeneous continuum. Thus, the in nature observed sharp peaks and immediate reaction of the groundwater table to precipitation cannot be reproduced in the model. In a porous aquifer the groundwater table outbalances itself and reacts smoother on external influences.

f) Regolith aquifer: The model demanded a simplification of the regolith structure. The occurrence of thus semi-confined conditions, due to duricrusts and intensely weathered clay layers, is ignored. Additionally, a constant thickness of the regolith is supposed. Field observations revealed the strongly varying regolith thickness and changes in texture and mineral composition over short distances.

g) Model limits: The groundwater divide of the HVO is supposedly equal to the surface water divide. In reality no information about the position and nature of the real groundwater divide is available.

9. Conclusions

In the beginning of this study data about the regional hydrogeological and hydrochemical character of the regolith and the bedrock aquifer was only available through geological and hydrogeological maps. It was therefore necessary to undertake several measurement campaigns in order to get an overview about the regional groundwater resources.

The interpretation of results from analyses of groundwater hydrochemistry, stable isotope composition of water resources, tritium and piezometric measurements produced important information about recharge, water age and the evolution of hydrochemical facies.

Based on these results a conceptual regional model was designed. In regard to this conceptual model and some general assumptions about hydraulic parameters in the study area it was tried to create and perform a numerical model for the Upper Ouémé catchment.

The transfer of the hydrogeological features of the HVO into a regional numerical model demanded for strong simplification because of the great extent of the study area. A regional groundwater flow field is assumed for this measure but in the same time its existence remains disputable. As shown in Chapter 4 groundwater tables in the HVO are a reprint of the general surface morphology. Pumping or other types of groundwater extraction would have only very local impact on the available groundwater resources.

It is obvious that the major objective for the numerical model in this environment is not to predict exact piezometric heads but to prove the general assumptions made about the conceptual model. The discussion about the regional groundwater flow model may serve as reference for the development of other regional groundwater models in such areas of complex hydrogeological conditions like the crystalline bedrock with its regolith cover in Central Benin. However, the actual state of available input data reminds that the here model is only a simplified starting point for further modelling.

In relation to the IMPETUS scenario data the groundwater model was able to show that, despite declining recharge, supply of groundwater for public demand until the year 2025 will be sufficient. The experience from the field shows that still some villages are found sparse of groundwater during the dry season. Those villages are found mostly in areas where the regolith is thin or almost not existent and thus lacks important groundwater storage. Additionally important water bearing fractures in the bedrock may lack or where failed to be localised by groundwater exploring activities. But in such places the provision of water supply is rather more a problem of infrastructure and investment than that of a general water shortage.

Reason for concern is the groundwater quality in the vicinity of settlements. Here contamination by human activities is omnipresent. The nitrate concentration in the groundwater already achieved alerting levels in many places. Health risks from fluoride or heavy metals could be excluded for the HVO area.

In respect to the heterogeneous character of the aquifers in the Upper Ouémé catchment it is necessary to underline that all investigations for this study were realised on a regional scale and thus conclusions drawn on them have to be regarded absolutely under this generalising aspect.

Nevertheless, the here presented regional approach produced a good conceptual idea about hydrogeological conditions and hydrochemical processes in the crystalline basement aquifers of Central Benin. Many findings are made in agreement with those of other researchers at comparable sites. Citations are found in the text above.

The regional field work produced a large database about hydrogeology, piezometric measurements, hydrochemistry and environmental isotope concentrations in the HVO area. It completes the already vast data base collected by the IMPETUS fellow researchers and may thus, hopefully, serve well for future research in the Upper Ouémé catchment and in adjacent areas.

10. Recommendations and outlook

In rural areas of Benin and elsewhere in Africa groundwater is still the best solution for water supply (WURZEL 2001). The relatively small borehole yields are sufficient for rural water needs (ENGALENC 1985). Groundwater is ubiquitous albeit water bearing fractures have first to be localised.

The clue to better implantation strategies are intensive geophysical investigations, the development and exploitation of consistent borehole databases (e.g. BDI), the interpretation of morphological features from a DEM and interpretation of satellite image data. Any improvement in these fields of research is of great concern for the local water supply.

Multi-seasonal observation of the hydrochemical data revealed less importance of seasonal factors for the deeper regolith and the bedrock aquifer. But vertical changes of hydrochemical characteristics especially in the regolith seem to give more information about flow velocity and weathering processes. Detailed hydrochemical research in the regolith in comparison with soil analyses would be of interest. The great number of already available hydrochemical analyses permits as well a profound statistical study and hydrochemical modelling, for example with the PHREEQC modelling software.

Tritium proved the existence of different ages in a vertical sequence in the aquifers. A closer view to the tritium ages in combination with transport models (e.g. with the NETPATH model) could give a better understanding to flow velocities in the regolith (e.g. BORONINA et al. 2005).

Since October 2004 rainwater was collected at three locations in the HVO (Parakou, Dogué and Sérrou). The samples were sent to the GSF research centre in order to measure the content of deuterium and oxygen-18. It might be interesting to include these measurements in meteorological models in order to locate the origin of precipitation causing recharge. These samples may serve as calibration tool in meteorological models. An exemplary application is described in STURM et al. (2005).

The groundwater monitoring via data loggers should be continued in order to obtain substantial time series for conclusive statistical analysis of trend components and periodicity.

The here presented FEFLOW[®] model permits the easy integration of new data. Further refinement can be done in areas of interest and closer investigation. FEFLOW[®] provides a free programmable interface. This interface can be used for coupling with procedures from other models, e.g. the hydrological UHP model, in order to obtain a conclusive modelling environment. Model coupling was not part of this thesis but would be a great task for further model work in Benin.

References

- ADEPELUMI, A., AKO, B. and AJAYI, T. (2001): "*Groundwater contamination in the basement-complex area of Ile-Ife, southwestern Nigeria: A case study using the electrical-resistivity geophysical method.*" *Hydrogeology Journal* 9(6), pp. 611-622.
- AFFATON, P., RAHAMAN, M. A., TROMPETTE, R. and SOUGY, J. (1991): "*The Dahomeyide Orogen: Tectonothermal evolution and relationships with the Volta basin.*" in: *The West African orogens and circum-Atlantic correlatives.* Editors: D. DALLMEYER and J. P. LÉCORCHÉ. Springer Verlag, pp. 107-122., Berlin, Heidelberg, New York.
- AGGARWAL, P. K., BASU, A. R., POREDA, R. J., KULKARNI, K. M., FROEHLICH, K., TARAFDAR, S. A., ALI, M., HUSSAIN, N. A. A., RAHMAN, M. and AHMED, S. R. (2000): "*Isotope Hydrology of Groundwater in Bangladesh: Implications for Characterization and Mitigation of Arsenic in Groundwater.*" IAEA – TC Project (BGD/8/016). Vienna, Austria.
- AKIN, H. and SIEMES, H. (1988): "*Praktische Geostatistik.*" 1st edition, 315 p., Springer Verlag, Berlin, Heidelberg, Germany.
- ALIDOU, S. (1987): "*Etude géologique du bassin paleo-mesozoïque de Kandi. Nord-Est du Bénin (Afrique de l'Ouest).*" Occasional Publication No. 13, Université Nationale du Bénin, Université de Dijon, CIFEG, Paris, France.
- ALIDOU, S., LANG, J., BONVALOT, J., ROMAN, E. and SEILACHER, A. (1991): "*Marine influences in the so-called continental sediments of the Palaeozoic-Mesozoic Kandi Basin (Northern Benin – West Africa).*" *Journal of African Earth Science* Vol. 12(1-2), pp. 55-65.
- APPELO, C. A. J. and POSTMA, D. (2005): "*Geochemistry, groundwater and pollution.*" A.A. Balkema Publishers, Rotterdam, The Netherlands.
- ANDERSON, M.P. and WOESSNER, W.W. (1994): "*Applied Groundwater Modeling – Simulation of Flow and Advective Transport.*" 381 p., Academic Press, San Diego, USA.
- BARKER, J. A. and HERBERT, R. (1992): "*Hydraulic Tests on Well Screens.*" *Applied Hydrogeology* 0/92, pp. 7-19.
- BARRETT, M., HOWARD, G., PEDLEY, S., TAYLOR, R. and NALUBEGA, M. (2000): "*A comparison of the extent and impacts of sewage contamination on urban groundwater in developed and developing countries.*" in: *Water, Sanitation & Health.* Editors: L. CHORUS, U. RINGELBAND, G. SCHLAG and O. SCHMOLL, Schriftenreihe des Vereins für Wasser-, Boden- und Lufthygiene, No. 105.
- BAUER, F. (2004): "*Transportvorgänge in der ungesättigten Bodenzone (IMPETUS-Testfeld Aquima, Benin, Westafrika).*" Geological Institute. Rheinischen Friedrich-Wilhelms-Universität, unpublished Diploma Thesis, Bonn, Germany.
- BAUER, P., THABENG, G., STAUFFER, F. and KINZELBACH, W. (2003): "*Estimation of the evapotranspiration rate from diurnal groundwater level fluctuations in the Okavango Delta, Botswana.*" *Journal of Hydrology* 288, pp. 344-355.

References

- BAUER, P. (2004): "*Flooding and Salt Transport in the Okavango Delta, Botswana: Key issues for a sustainable wetland management.*" Swiss Federal Institute of Technology Zurich, Dissertation ETH N° 15436, 177 p., Zurich, Switzerland.
- BEAR, J., BELJIN, M. S. and ROSS, R. R. (1992): "*Fundamentals of Ground-Water Modeling.*" Ground Water Issue, United States Environmental Protection Agency, 11 p., Ada, USA.
- BELLION, Y. J.-C. (1987): "*Histoire géodynamique post-paléozoïque de l'Afrique de l'ouest d'après l'étude de quelques bassins sédimentaires (Sénégal, Taoudeni, Iullemeden, Tchad).*" Université d'Avignon et des Pays de Vaucluse, CIFEG, Paris, France.
- BESTO, T. T. (1987): "*The extent, characteristics and recharge conditions of groundwater in crystalline basement rocks in Australia.*" Proceedings: Groundwater exploration and development in crystalline basement aquifers, Zimbabwe, Commonwealth science council.
- BGR (2000): "*Erfassung und Bewertung ausgewählter Vorkommen von Ornamentsteinen in der Republik Benin.*" Bundesanstalt für Geowissenschaften und Rohstoffe, Technical Cooperation, Project-No. 1998.2166.1, 201 p., Hannover, Germany.
- BGS (2006): "*Water quality fact sheet: Fluoride.*" British Geological Survey.
- BISCALDI, R. (1967): "*Etude statistique des forages et carte hydrogéologique des régions à substratum éruptif et métamorphique en Afrique Occidentale.*" BRGM-CIEH, Ouagadougou, Burkina-Faso.
- BOHNENKÄMPER, L. (2006): "*Regionale Charakterisierung des Saprolith im oberen Ouémé-Einzugsgebiet / Benin durch geoelektrische Sondierungen und Bohrlochansprachen.*" Institut für Geologie und Mineralogie. University of Cologne, unpublished Diploma Thesis, 136 p., Cologne, Germany.
- BOLGER, P., STEVENS, M., DILLON, P., WILLIAMS, M. and OTTO, C. (1999): "*Contamination of Australian Groundwater Systems with Nitrate.*" Land and Water Resources Research and Development Corporation, Canberra, Australia.
- BORMANN, H. (2005): "*Evaluation of hydrological models for scenario analyses: signal-to-noise-ratio between scenario effects and model uncertainty.*" Advances in Geosciences 5, pp. 43-48.
- BORMANN, H. and DIEKKRÜGER, B. (2003): "*Analyse der Unsicherheiten bei der hydrologischen Modellierung im Benin (West Afrika) im Rahmen des IMPETUS-Projektes.*" Kassel University Press, Kassel, Germany.
- BORONINA, A., FAVREAU, G., ZAÏRI, R., DIEULIN, C. and COUDRAIN, A. (2005): "*Data scarcity in the large semiarid Lake Chad basin: incorporating environmental tracers as a priori information for groundwater modeling.*" Proceedings: 5th International Conference on Calibration and Reliability in Groundwater Modelling. From Uncertainty to Decision Making, ModelCARE 2005, IAHS, The Hague, The Netherlands.
- BOUKARI, M. and GUIRAUD, R. (1985): "*L'hydrogéologie des régions de socle de l'Afrique intertropicale: l'exemple de Dassa-Zoumè (Bénin méridional).*" Journal of African Earth Sciences 3(4), pp. 491-503.

- BOUKARI, M., GAYE, C. B., FAYE, A. and FAYE, S. (1996): "*The impact of urban development on coastal aquifers near Cotonou, Benin.*" *Journal of African Earth Sciences* 22(4), pp. 403-408.
- BRGM-AQUATER (1986): "*La recharge naturelle des aquifères de socle sous climats Sahélien et Soudanien - Étude expérimentale au Burkina-Faso.*" BRGM.
- BRGM (1978): "*Carte géologique à 1/200.000 de la République du Togo et de la R.P. du Bénin entre les 9e et 10e de lat. N. Feuilles de BASSARI-DJOUYOU et PARAKOU-NIKKI.*" Office Béninois des Mines, Cotonou, Benin.
- BRITO NEVES, B. B., VAN SCHMUS, W. R. and FETTER, A. H. (2001): "*Noroeste da África – Nordeste do Brasil (Província Borborema) - Ensaio comparativo e problemas de correlação.*" *Revista do Instituto de Geociências - USP* 1, pp. 51-78.
- BROOKS, N. (2004): "*Drought in the African Sahel: Long term perspectives and future prospects.*" Working Paper 61, Tyndall Centre for Climate Change Research, 37 p., Norwich, UK.
- BRÜCHER, T., FINK, A. H. and SPETH, P. (2006): "*Klimasimulationen im Rahmen des interdisziplinären Forschungsprojektes IMPETUS.*" Annual Report, IMPETUS West Africa 7 p., Cologne, Bonn, Germany.
- BURGEAP (1976): "*Evaluation du débit d'exploitation des puits dans les régions à substratum cristallin d'Afrique tropicale.*" CIEH, 39 p., Ouagadougou, Burkina-Faso.
- BURGEAP (1988): "*Essais de débit simplifiés sur forages d'hydraulique villageoise - Normalisation des modalités d'exécution et des méthodes d'interpolation.*" CIEH, Ouagadougou, Burkina-Faso.
- BURGEAP (2004): "*Notice d'utilisation de la BDI Bénin (Manuel de référence).*" Cotonou, Benin.
- BUTT, C. R. M. and ZEEGERS, H., Eds. (1992): "*Regolith Exploration Geochemistry in Tropical and Subtropical Terrains.*" Handbook of Exploration Geochemistry. Elsevier, Amsterdam, The Netherlands.
- CABY, R., BERTRAND, J. M. and BLACK, R. (1981): "*Pan-African ocean closure and continental collision in the Hoggar-Iforas Segment, Central Sahara.*" Precambrian plate tectonics. A. KRÖNER. Elsevier, pp. 407-431., Amsterdam, The Netherlands
- CARUTHERS, R. M. and SMITH, I. F. (1992): "*The use of ground electrical survey methods for siting water-supply boreholes in shallow crystalline basement terrains.*" in: Hydrogeology of Crystalline Basement Aquifers in Africa. Editors: E. P. WRIGHT and W. G. BURGESS, British Geological Society. 66, pp. 203-220.
- CEFIGRE (1990): "*Synthese des connaissances sur l'hydrogéologie de l'Afrique de l'Ouest – Socle cristallin et cristallophyllien Sédimentaire ancien.*" Université d'Avignon, Ministère de la Coopération et du Développement, France.
- CHIANG, W.-H. and KINZELBACH, W. (2000): "*3D-Groundwater Modeling with PMWIN – A Simulation System for Modeling Groundwater Flow and Pollution.*" Springer-Verlag, Berlin-Heidelberg-New York.
- CHILTON, J. P. and FOSTER, S. S. D. (1993): "*Hydrogeological Characterisation and Water-Supply Potential of Basement Aquifers in Tropical Africa.*" *Hydrogeology Journal* 3(1), pp. 36-49.

References

- CIA (2007): "*Benin*." The World Factbook of the Central Intelligence Agency, from <https://www.cia.gov/library/publications/the-world-factbook/>.
- CIEH (1990): "*Hydrogéologie de l'Afrique de l'Ouest*." Ministère de la Coopération et du Développement, Ouagadougou, Burkina-Faso.
- CLARK, I. D. and FRITZ, P. (1997): "*Environmental Isotopes in Hydrogeology*." CRC.
- DIWI CONSULT and BIDR (1994): "*Etudes d' Réhabilitation des Points d' Eau Existants*." Bureau d'Ingénierie pour le Développement Rural.
- COOK, P. G. and HERCZEG, A. L., Eds. (2000): "*Environmental Tracers in subsurface hydrology*." Water Resources Research, 529 p., Kluwer Academic Publishers, Boston, USA.
- COOK, P. G., SOLOMON, D. K., SANFORD, W. E., BUSENBERG, E., PLUMMER, J. N. and POREDA, R. J. (1996): "*Inferring shallow groundwater flow in saprolite and fractured rock using environmental tracers*." Water Resources Research 32(6), pp. 1501-1509.
- CRAIG, H. (1961): "*Isotopic variations in natural waters*." Science (133), pp. 1702-1703.
- CRANE, P. E. (2006): "*Implementation of a sustainable groundwater quality monitoring program in rural Benin, West Africa*." Master Thesis in Civil Engineering and Geological Sciences, University of Notre Dame, 165 p., Notre Dame, Indiana, USA.
- CZEGKA, W., BEHREND, K. and BRAUNE, S. (2004): "*Die Qualität der SRTM-90m Höhendaten und ihre Verwendbarkeit in GIS*." 24. Wissenschaftlich-Technische Tagung der DGPF, Halle, Germany.
- DAHI, E., MTALO, F., NJAU, B. and BREGNHJI, H. (1996): "*Defluoridation using the Nalgonda Technique in Tanzania*." New Delhi, India.
- DANIEL, C. C., SMITH, D. G. and EIMERS, J. L. (1997): "*Hydrogeology and simulation of ground-water flow in the thick regolith-fractured crystalline rock aquifer system of Indian Creek Basin, North Carolina*." USGS, USA.
- DANSGAARD, W. (1964): "*Stable isotopes in precipitation*." Tellus (16), pp. 436-468.
- DEUTSCH, W. J. (1997): "*Groundwater geochemistry: Fundamentals and applications to contamination*." Lewis, New York, USA.
- DFID (2001): "*Addressing the Water Crisis: Healthier and more productive lives for poor people. Strategies for achieving the international development targets*." Department for international Development, UK.
- DGH (2005): "*Strategie nationale del'approvisionnement en eau potable en milieu rural du Benin 2005 – 2015*." Ministère des Mines, de l'Energie et de l'Hydraulique, Cotonou, Benin.
- DIEKAU, R., BRABB, E. E. and MARK, R. M. (1991): "*Landform Classification of New Mexico by Computer*." USGS, USA.
- DIERSCH, H.-J. G. (2005): "*FEFLOW - Finite Element Subsurface Flow & Transport Simulation System*." WASY GmbH Institute for Water Resources Planning and System Research, Berlin, Germany.
- DISSANAYAKE, C. B. (1991): "*The fluoride problem in the groundwater of Sri Lanka – environmental management and health*." International Journal of Environmental Studies 38, pp. 137-156.

- DRAY, M., GIACHELLO, L., LAZZAROTTO, V., MANCINI, M., ROMAN, E. and ZUPPI, G. M. (1988): "*Etudes isotopique de l'aquifère Crétace du bassin côtier béninois.*" « Développement des techniques isotopiques et nucléaires en hydrologie et hydrogéologie dans les pays du Sahel ». IAEA, Niamey, Niger.
- DREVER, J. J. (1997): "*The geochemistry of natural waters – surface and groundwater environments.*" Prentice Hall, New York, USA.
- DUBROEUCQ, D. (1977): "*Carte Pédologique de Reconnaissance de la République Populaire du Bénin à 1: 200,000. Feuille Parakou.*" 1 map and report, 37 p., ORSTOM.
- DVWK (1995): "*Speicher-Durchfluss-Modelle zur Bewertung des Stoffein- und Stoffaustrags in unterschiedlichen Grundwasserzirkulationssystemen.*" Wirtschafts- und Verlags-gesellschaft Gas und Wasser mbH, Bonn, Germany,
- ECETOC (1988): "*Nitrate and drinking water.*" European Chemical Industry Ecology and Toxicology Centre, Brussels, Belgium.
- EDET, A. and OKEREKE, C. (2005): "*Hydrogeological and hydrochemical character of the regolith aquifer, northern Obudu Plateau, southern Nigeria.*" Hydrogeology Journal 13(2), pp. 391-415.
- EDMUNDS, W., FELLMAN, E., GONI, I. and PRUDHOMME, C. (2002): "*Spatial and temporal distribution of groundwater recharge in northern Nigeria.*" Hydrogeology Journal 10(1), pp. 205-215.
- EHINOLA, O. A., OPOOLA, A. O. and ADESOKAN, H. A. (2006): "*Empirical analysis of electromagnetic profiles for groundwater prospecting in rural areas of Ibadan, southwestern Nigeria.*" Hydrogeology Journal 14(4), pp. 613-624.
- ENGALENC, M. (1978): "*Methode d'étude et de recherche de l'eau souterraine des roches cristallines de l'Afrique de l'Ouest.*" CIEH, Ouagadougou, Burkina-Faso.
- ENGALENC, M. (1985a): "*Notice explicative de la carte hydrogéologique à 1/500.000 du Bénin.*" Géohydraulique, 21 p., Maisons Alfort, France.
- ENGALENC, M. (1985b): "*Notice explicative de la carte hydrogéologique à 1/200.000 du bassin sédimentaire du cotier du Bénin.*" Géohydraulique, 21 p., Maisons Alfort, France.
- ESSINK, O. (2000): "*Groundwater Modelling.*" Interfaculty Centre of Hydrology, 201 p., Utrecht, The Netherlands.
- FARNHAM, I. M., STETZENBACH, K. J., SINGH, A. S. and JOHANNESSEN, K. H. (2002): "*Treatment of nondetects in multivariate analysis of groundwater geochemistry data.*" Chemometrics Intelligent Lab. Sys. 60, pp. 265-281.
- FASS, T. (2004): "*Hydrogeologie im Aquima Einzugsgebiet in Benin/Westafrika.*" Mathematisch–Naturwissenschaftliche Fakultät. Rheinische Friedrich-Wilhelms-Universität. Dissertation, 161 p., Bonn, Germany.
- FAURE, P. (1976): "*Carte Pédologique de Reconnaissance à 1: 200,000. Feuille Parakou.*" ORSTOM.
- FAURE, P. and VOLKOFF, B. (1998): "*Some factors affecting regional differentiation of the soils in the Republic of Benin (West Africa).*" Catena 32.
- FAYE, S., NIANG DIOP, I., FAYE, C., EVANS, D. G., PFISTER, M., MALOSZEWSKI, P. and SEILER, K. P. (2001): "*Seawater intrusion in the Dakar (Senegal) confined aquifer:*

References

- calibration and testing of a 3D finite element model.*" In Proceedings: New Approaches Characterizing Groundwater Flow. Proceedings of the XXXI IAH Congress, Munich, 10-14 Sept. 2001. Editors: K. P. SEILER and S. WOHNLICH, A.A.Balkema, Lisse/Abingdon. 2, pp. 1183-1186.
- FILLIPI, C., MILVILLE, F. and THIERY, D. (1990): "*Evaluation de la recharge naturelle des aquifères en climat Soudano-Sahélien par modélisation hydrologique globale: Application a dix sites au Burkina Faso.*" Hydrological Sciences 35(1), 20 p.
- FLEISCHER, M. and ROBINSON, W. O. (1963): "*Some problems of the geochemistry of fluorine.*" in: Studies in analytical geochemistry. Editor: D. M. SHAW, R. Soc. Can. 6, pp.58-75.
- FONTES, J. C., GASSE, F. and ANDREWS, J. N. (1993): "*Climatic conditions of holocene groundwater recharge in the Sahel Zone of Africa.*" in: Isotope techniques in the study of past and current environmental changes in the hydrosphere and the atmosphere, IAEA, pp. 231–248, STI/PUB/908, Vienna, Austria.
- FRENCKEN, J. E., Ed. (1992): "*Endemic Fluorosis in developing countries, causes, effects and possible solutions.*" NIPG-TNO, Leiden, The Netherlands.
- GARRELS, R. M., Ed. (1967): "*Genesis of some ground waters from igneous rocks.*" Researches in Geochemistry, John Wiley, New York, USA.
- GAT, J. R. (1996): "*Oxygen and hydrogen isotopes in the hydrologic cycle.*" Annu. Rev. Earth Planet Sci.(24), pp. 225-262.
- GAT, J. R., BROWSER, C. and KENDALL, C. (1994): "*The contribution of evaporation from the Great Lakes to the continental atmosphere: estimate based on stable isotope data.*" Geophys. Res. Lett. (21), pp. 557-560.
- GÉLINAS, Y., RANDALL, H., ROBIDOUX, L. and SCHMIT, J. (1996): "*Well water survey in two districts of Conakry (Republic of Guinea), and comparison with the piped city water.*" Water Research 30(9), pp. 2017-2026.
- GIERTZ, S. (2004): "*Analyse der hydrologischen Prozesse in den sub-humiden Tropen Westafrikas unter besonderer Berücksichtigung der Landnutzung am Beispiel des Aguima-Einzugsgebietes in Benin.*" Mathematisch–Naturwissenschaftliche Fakultät. Rheinische Friedrich-Wilhelms-Universität. Dissertation, 267 p., Bonn, Germany.
- GIERTZ, S., DIEKKRÜGER, B., JAEGER, A. and SCHOPP, M. (2006): "*An interdisciplinary scenario analysis to assess the water availability and water consumption in the Upper Ouémé catchment in Benin.*" Advances in Geosciences 9, pp. 3-13.
- GONI, I. B. (2006): "*Tracing stable isotope values from meteoric water to groundwater in the southwestern part of the Chad basin.*" Hydrogeology Journal 14(5), pp. 742-752.
- GOSWAMI, P. and HIMESH, S. (2002): "*Coupled atmospheric-hydrologic models to forecast spatio-temporal variability of water resources.*" CSIR, 27 p., Bangalore, India.
- HARBAUGH, A. W., BANTA, E. B., HILL, M. C. and McDONALD, M. G. (2000): "*MODFLOW 2000, the U.S. Geological Survey Modular Groundwater Model - User Guide to Modularization concepts and the Groundwater Flow Process.*" Open File Report 00-92, USGS, 130 p., Reston, USA.

- HEIDWEILLER, V. M. L. (1990): "*Fluoride removal methods. In: Proc. Symposium on Endemic Fluorosis in Developing Countries: Causes, Effects and Possible Solutions.*" J. E. FRENCKEN. NIPG-TNO, pp. 51-85., Leiden, The Netherlands.
- HEM, J. D. (1985): "*Study and interpretation of the chemical characteristics of natural water.*" USGS, USA.
- HERRMANN, L. and VENNEMANN, K., Eds. (2000): "*Atlas of natural and agronomic resources of Niger and Benin.*" Institute of Soil Science and Land Evaluation, University of Hohenheim, Stuttgart, Germany.
- HOEFS, J. (2004): "*Stable Isotope Geochemistry.*" 340 p., Springer, Berlin, Germany.
- HÖLTING, B. (1996): "*Hydrogeologie.*" 326 p., Ferdinand Enke-Verlag, Stuttgart, Germany.
- HOUSSOU, A. and LANG, J. (1978): "*Contribution à l'étude du "continental terminal" dans le Bénin méridional.*" Sciences Géologique Bulletin Vol. 31(4), pp 137-149.
- HOWARD, G., JAHNEL, J., FRIMMEL, F. H., MCCHESENEY, D., REED, B. and SCHIJVEN, J. (2005): "*Human excreta and sanitation: Information needs.*" Protecting groundwater for health: managing the quality of drinking-water sources, from www.who.int/water-sanitation-health/resourcequality/groundwater2004/en.
- HOWARD, K. W. F., HUGHES, M., CHARLESWORTH, D. L. and NGOBI, G. (1992): "*Hydrogeologic Evaluation of Fracture Permeability in Crystalline Basement Aquifers of Uganda.*" Applied Hydrogeology 1(1), pp. 55-65.
- HUTCHINGS, J. and PETRICH, C. R. (2002): "*Groundwater recharge and flow in the regional Treasure Valley aquifer system - Geochemistry and Isotope study.*" Idaho Water Resources Research Institute Research Report. Idaho Water Resources Research Institute, 91 p., Boise, USA.
- IAEA/WMO. (2004): "*Global Network of Isotopes in Precipitation.*" The GNIP Database, from <http://isohis.iaea.org>.
- IMPETUS (2003): "*Final Report 2000 - 2003.*" IMPETUS West Africa Project, 156 p., Cologne, Bonn, Germany.
- IMPETUS (2006): "*Final Report 2003 - 2006.*" IMPETUS West Africa Project, 286 p., Cologne, Bonn, Germany.
- INSAE (2003): "*Third General Population and Housing Census of February 2002 in Benin.*" Cotonou, Benin.
- IPCC (2000): "*Special Report Emissions Scenarios.*" Summary for policymakers, WMO, UNEP, p. 27.
- ISTOK, J. (1989): "*Groundwater modeling by the finite element method.*" Washington, USA, American Geophysical Union.
- JACKS, G., SEFE, F., CARLING, M., MAMMAR, M. and LETSAMAQ, P. (1999): "*Tentative nitrogen budget for pit latrines – eastern Botswana.*" Environmental Geology 38(3), pp. 199 – 203.
- JACQUIN, F. and SEYGONA, Z. Y. (2004): "*Contribution à l'étude du fonctionnement hydrodynamique des aquifères du bassin versant de la Donga.*" ORE AMMA/CATCH, IRD, Cotonou, Benin.

References

- JØRGENSEN, N. O. and BANOENG-YAKUBO, B. K. (2001): "*Environmental isotopes (18O, 2H, and 87Sr/86Sr) as a tool in groundwater investigations in the Keta Basin, Ghana.*" Hydrogeology Journal 9, pp. 190-201.
- JUBELIN, F. (2006): "*A la poursuite de la mousson africaine.*" Sciences et Avenir, No. 9, pp. 62-67.
- JUDEX, M. (2003): "*Analyse und Erklärung der Landbedeckungs- und Landnutzungsänderungen im Upper Oueme Catchment (Benin, Westafrika) durch die Verknüpfung von LANDSAT-Daten mit sozioökonomischen Daten.*" Geographical Institute. Rheinischen Friedrich-Wilhelms-Universität. Diploma thesis, Bonn, Germany.
- JUNGE, B. (2004): "*Die Böden des oberen Ouémé-Einzugsgebietes in Benin/Westafrika - Pedologie, Klassifizierung, Nutzung und Degradierung.*" Landwirtschaftlichen Fakultät. Rheinischen Friedrich-Wilhelms-Universität. Dissertation, 307 p., Bonn, Germany.
- KAMAGATE, B. (2006): "*Fonctionnement hydrologique et origine des écoulements sur un bassin versant de milieu tropical de socle au Bénin: bassin versant de la Donga (haute vallée de l'Ouémé).*" Université Montpellier II Sciences et Techniques du Languedoc. phd, 320 p., Montpellier, France.
- KÄSS, W. and SEEBURGER, I. (1989): "*Grundwasser-Redoxpotentialmessungen und Probenahmegeräte.*" Parey, Hamburg-Berlin, Germany.
- KENDALL, C. and MCDONELL, J. J., Eds. (1998): "*Isotope Tracers in Catchment Hydrology.*" Elsevier Science B.V., Amsterdam, The Netherlands.
- KITANIDIS, P. K. (1997): "*Introduction to Geostatistics: Application to Hydrogeology.*" Cambridge University Press, New York, USA.
- KLINE, J. R., MARTIN, J. R., JORDAN, C. F. and KORANDA, J. J. (1970): "*Measurement of Transpiration in Tropical Trees with Tritiated Water.*" Ecology, Vol. 51, No. 6, pp. 1068-1073.
- KLOCK, H., KÜLLS, C. and UDLUFT, P. (2001): "*Estimating recharge values using hydrochemical and geological data: a case study from the semiarid Kalahari catchment of northern Namibia.*" in *Impact of Human Activity on Groundwater Dynamics*. Editors. H. Gehrels, N.E. Peters, E. Hoehn, K. Jensen, C. Leibundgut, J. Griffioen, B. Webb, and W.J. Zaadnoordijk. IAHS Publication No. 269.
- LAMB, P. J. and PEPPLER, R. A. (1991): "*West Africa.*" in: *Teleconnections linking worldwide climate anomalies*. Editors: M. GLANTZ, R. W. KATZ and N. NICHOLLS, pp. 121-188.
- LANGGUTH, H.-R. and VOIGT, R. (2004): "*Hydrogeologische Methoden.*" Springer Verlag, Berlin, Heidelberg, Germany.
- LARES (1999): "*Atlas de sécurité alimentaire du Bénin.*" Laboratoire d'Analyse régionale et d'expertise sociale, Ministère du Développement Rural, Cotonou, Benin.
- LE BARBE, L., ALE, G., MILLET, B., TEXIER, H., BOREL, Y. and GUALDE, R. (1993): "*Les ressource en eaux superficielles de la République du Bénin.*" ORSTOM (IRD), Paris, France.
- LEEMANN, W. (1970): "*Fluorosis in cattle.*" in: *Fluoride in Medicine*. Editor: T. L. VISCHER, Hans Huber Publishers, Bern, Switzerland.

- LELONG, F. (1966): "*Régime des nappes phréatiques contenues dans les formations d'alteration tropicale.*" Science de la Terre Vol. 12(2), pp. 201-204.
- LLOYD, J. W. and JACKS, G. (1999): "*Groundwater chemistry.*" Water resources in hard rock aquifers. J. W. LLOYD. Paris, France, UN.
- LOEHNERT, E. P. (1988): "*Major chemical and isotopes variations in surfaces and subsurface waters of West Africa.*" Journal of African Earth Science 7(3), pp. 579-588.
- LOEWE, M. (2005): "*Die Millennium Development Goals: Hintergrund, Bedeutung und Bewertung aus Sicht der deutschen Entwicklungszusammenarbeit.*" DIE, 39 p., Bonn, Germany.
- MACDONALD, A. M. and DAVIES, J. (2002): "*A brief review of groundwater for rural water supply in Sub-Saharan Africa.*" British Geological Society (BGS), Nottingham, UK.
- MACDONALD, A. M., DAVIES, J. and DOCHARTAIGH, B. (2002): "*Simple Methods for Assessing Groundwater Resources in Low Permeability Areas of Africa.*" British Geological Society, Nottingham, UK.
- MAIGNIEN, R. (1966): "*Compte-rendu de recherches sur les latérites.*" Paris, France, UNESCO.
- MAILU, G. M. (1994): "*The influence of Precambrian metamorphic rocks on groundwater in the Chyulu Area, Kenya.*" Applied Hydrogeology, Vol. 2(2), 26 p.
- MALOMO, S., OKUFARASIN, V. A., OLORUNNINO, M. A. and OMODE, A. A. (1990): "*Groundwater chemistry of weathered zone aquifers of an area underlain by basement complex rocks.*" Journal of African Earth Science 11(3/4), pp. 357-371.
- MARSAL, D. (1989): "*Finite Differenzen und Elemente.*" Springer Verlag, Berlin, Heidelberg, Germany.
- MARTIN, N. (2006): "*Development of a water balance for the Atankwidi catchment, West Africa – A case study of groundwater recharge in a semi-arid climate.*" Cuvillier Verlag, Göttingen, Germany.
- MATTHESS, G. (1994): "*Die Beschaffenheit des Grundwassers.*" Gebrüder Borntraeger, Berlin, Stuttgart, Germany.
- MAZOR, E. (1997): "*Chemical and isotopic groundwater hydrology: The applied approach.*" M.Dekker, New York, USA.
- MCFARLANE, M. J. (1987a): "*Dambos - Their characteristics and geomorphological evolution in parts of Malawi and Zimbabwe, with particular reference to their role in the hydrogeological regime of surviving areas of African surface.*" Proceedings: Groundwater exploration and development in crystalline basement aquifers, Zimbabwe, in: Water & Mineral resources Technical Paper, Vol. 237, Commonwealth science council, pp. 254-302.
- MCFARLANE, M. J. (1992a): "*Groundwater movement and water chemistry associated with weathering profiles of the African surface in parts of Malawi.*" in: Hydrogeology of Crystalline Basement Aquifers in Africa. Editors: E. P. WRIGHT and W. G. BURGESS, Geological Society Special Publication. 66, pp. 101-130.
- MCFARLANE, M. J., CHILTON, P. J. and LEWIS, M. A. (1992b): "*Geomorphological controls on borehole yields; a statistical study in an area of basement rocks in central Malawi.*" in: Hydrogeology of Crystalline Basement Aquifers in Africa. Editors: E. P.

References

- WRIGHT and W. G. BURGESS, Geological Society Special Publication. 66, pp. 131-154.
- MERKEL, B. J. and PLANER-FRIEDRICH, B. (2003): "*Integrierte Datenauswertung Hydrogeologie.*" TU Bergakademie Freiberg, Germany.
- MIDDLETON, G. V. (2000): "*Data analysis in the Earth Sciences using Matlab.*" Prentice Hall, New Jersey, USA.
- MORRIS, B. L., LAWRENCE, A. R. and STUART, M. E. (1994): "*The impact of urbanization on groundwater quality (Project summary report).*" Technical Report BGS.
- NATIONS, U. (1988): "*Groundwater in North and West Africa.*" Natural Resources/Water Series. New York, Department of Technical Co-operation for Development and Economic Commission for Africa, pp. 37-50.
- NKOTAGU, H. (1996): "*Origins of high nitrate in groundwater in Tanzania.*" Journal of African Earth Sciences 21(4), pp. 471 – 478.
- OBEMINES (1984): "*Notice explicative de la carte géologique à 1/200.000 - Feuilles DJOUGOU – PARAKOU – NIKKI.*" Office Béninois des Mines, Cotonou, Benin.
- OBEMINES (1989): "*Notice explicative de la carte géologique à 1/200.000 – Feuille KARIMAMA.*" Office Béninois des Mines, Cotonou, Benin.
- OKEREKE, C. S., ESU, E. O. and EDET, A. E. (1998): "*Determination of potential groundwater sites using geological and geophysical techniques in the Cross River State, southeastern Nigeria.*" Journal of African Earth Science 27(1), pp. 149-163.
- OMORINBOLA, E. O. (1982): "*Systematic decline of groundwater level in the regoliths of the Nigerian basement complex due to human activities.*" in: Improvement of methods of long term prediction of variations in groundwater resources and regimes due to human activity. IAHS.
- OWEN, R. J., GWAVAVA, O. and GWAZE, P. (2005): "*Multi-electrode resistivity survey for groundwater exploration in the Harare greenstone belt, Zimbabwe.*" Hydrogeology Journal 14(1-2), pp. 244-252.
- PAETH, H. (2006): "*The climate of tropical and northern Africa – a statistical-dynamical analysis of the key factors in climate variability and the role of human activity in future climate change.*" Bonner Meteorologische Abhandlungen, Vol. 61, 340 p., Bonn, Germany.
- PAN-INTERNATIONAL (2000): "*Endosulfan deaths in Benin.*" Pesticide News 48, pp. 17.
- PARKHURST, D. L. and APPELO, C. A. J. (1999): "*User'S guide to PHREEQC (Version 2) - A computer program for speciation, batch-reaction, one-dimensional transport, and inverse geochemical calculations.*" Water-Resources Investigations Report, U.S. Geological Survey, 326 p., Denver, USA.
- PEIFFER, S. (2000): "*Characterisation of the redox state of aqueous systems - towards a problem-oriented approach.*" in: Redox - Fundamentals, Processes and Measuring Techniques. Editors: J. SCHÜRING, H. D. SCHULZ, W. R. FISCHER, J. BÖTTCHER and W. H. M. DUIJNESVELD. Springer Verlag, Berlin, Germany.
- RAJMOHAN, N. and ELANGO, L. (2004): "*Identification and evolution of hydrogeochemical processes in the groundwater environment in an area of the Palar and Cheyyar River Basins, Southern India.*" Environmental Geology 46, pp. 47-61.

- RIVERTWIN (2007): "*A Regional Model for Integrated Water Management in Twinned River Basins.*" from <http://www.rivertwin.de/Publications&Reports.htm>.
- ROBAIN, H. and WUBDA, M. (2004): "*Rapport de mission au Bénin du 12 octobre au 22 novembre 2004.*" IRD.
- ROBINS, N., DAVIES, J., HANKIN, P. and SAUER, D. (2002): "*Groundwater and data – an African experience.*" *Waterlines* 21(4), pp. 19-21.
- ROECKNER, E., BÄUML, G., BONAVENTURA, L., BROKOPF, R., ESCH, M., GIORGETTA, M., HAGEMANN, S., KIRCHNER, I., KORNBLUEH, L., MANZINI, E., RHODIN, A., SCHLESE, U., SCHULTZWEIDA, U. and TOMPKINS, A. (2003): "*The atmospheric general circulation model ECHAM5. Part I: Model description.*" Hamburg, Germany.
- ROOPE, B. P. (2003): "*Analysis of elevated Uranium and Impact of the Cotton Industry on Groundwater in Benin, Africa.*" Civil Engineering and Geological Sciences Institute, University of Notre Dame, Master of Science, Notre Dame, Indiana, USA.
- ROOSE, E. J. and LELONG, F. (1981): "*Factors of the chemical composition of seepage and groundwaters in the Intertropical Zone (West Africa).*" *Journal of Hydrology*, pp. 1-22.
- SACHS, L. (1997): "*Angewandte Statistik.*" Springer Verlag, Berlin, Heidelberg, Germany.
- SALATI, E., DALL'OLLIO, A., MATSUI, E. and GAT, J. R. (1979): "*Recycling of water in the Amazon basin, an isotopic study.*" *Water Resources* (15), pp. 1250-1258.
- SANDER, P. (1999): "*Mapping methods.*" in: *Water resources in hard rock aquifers.* Editor: J. W. LLOYD. United Nations, Paris, France.
- SANDWIDI, J.-P., VAN DE GIESEN, N. C., RODGERS, C., BOGARDI, J. J. and VLEK, P. L. G. (2006): "*Groundwater potential assessment in Kompienga dam basin using multiple methods.*" Zentrum für Entwicklungsforschung (ZEF), 6 p., Bonn, Germany.
- SARVAN, M. (2005): "*Characterisation of the groundwater in the Upper Ouémé catchment (Benin, West Africa) employing hydrochemical and isotope data.*" Geological Institute. Rheinischen Friedrich-Wilhelms-Universität, unpublished Diploma Thesis, 93 p., Bonn, Germany.
- SAVADOGO, N. A., NAKOLENDOUSSE, S. and DIALLO, S. (1997): "*Étude comparée de l'apport des méthodes électromagnétique MaxMin et électriques dans l'implantation des foragès à gros débits dans les régions de socle cristallin du Burkina Faso.*" *Journal of African Earth Science* 24(1-2), pp. 169-181.
- SBEE (2003): "*Rapport d'activités EAU – Exercice 2003.*" Ministère des Mines, de l'Energie et de l'Hydraulique, Cotonou, Benin.
- SCHAFMEISTER, M.-T. (1999): "*Geostatistik für die hydrogeologische Praxis.*" Springer Verlag, Berlin, Heidelberg, Germany.
- SCHOPP, M. (2004): "*Wasserversorgung in Benin unter Berücksichtigung sozioökonomischer und soziodemographischer Strukturen - Analyse der Wassernachfrage an ausgewählten Standorten des Haute Ouémé.*" Landwirtschaftliche Fakultät, Rheinischen Friedrich-Wilhelms-Universität. Dissertation, 318 p., Bonn, Germany.
- SCHWIEDE, M., DUIJNISVELD, W. H. M. and BÖTTCHER, J. (2005): "*Investigation of processes leading to nitrate enrichment in soils in the Kalahari Region, Botswana.*" *Physics and Chemistry of the Earth*, Vol. 30, 712-716 pp.

References

- SHEKWOLO, P. D. and BRISBE (1999): "*Bacteriological properties of groundwater in parts of Niger state, Nigeria.*" Journal of Environmental Hydrology 7(12), pp. 1-9.
- SIGG, L. (2000): "*Redox Potential Measurements in Natural Waters: Significance: Concepts and Problems.*" Redox - Fundamentals, Processes and Measuring Techniques. J. SCHÜRING, H. D. SCHULZ, W. R. FISCHER, J. BÖTTCHER and W. H. M. DUIJNESVELD. Springer Verlag, Berlin, Germany.
- SINGHAL, B. B. S. and GUPTA, R. P. (1999): "*Applied hydrogeology of fractured rocks.*" Kluwer Academic Publishers, Dordrecht, The Netherlands.
- SITRA.HM (2003): "*Etude d'implantation et controle des travaux de 11 piezomètres dans les départements du Borgou et de l'Alibori. Final Report.*" Ministère des Mines de l'Energie et de l'Hydraulique (MMEH), Direction de l'Hydraulique, Cotonou, Benin.
- SLANSKY, M. (1962): "*Contribution à l'étude géologique du bassin sédimentaire côtier du Dahomey et du Togo.*" BRGM, 11, 270 p., Ed. Technip.
- SMEDLEY, P. L., EDMUNDS, W. M., WEST, J. M., GARDNER, S. J. and PELIG-BA, K. B. (1995): "*Health problems related to groundwaters in the Obuasi and Bolgatanga areas, Ghana.*" Technical Report, British Geological Survey (BGS), 122 p.
- SOGREAH and SCET (1997): "*Potentialités des aquifères discontinus des formations du socle.*" MMEH and MPREPES, Cotonou, Benin.
- SOLSONA, F. (1985): "*Water defluoridation in the Rift Valley, Ethiopia.*" UNICEF Technical Report, 27 p., Addis Abbeba, Ethiopia.
- STOBER, I. (1995): "*Die Wasserführung des kristallinen Grundgebirges.*" Enke, Stuttgart, Germany.
- STRAHLENSCHUTZ, F. F. (1995): "*Empfehlungen zur Überwachung der Umweltradioaktivität.*" Loseblattsammlung des Arbeitskreises Umweltüberwachung, Fachverband für Strahlenschutz.
- STURM, K., HOFFMANN, G., LANGMANN, B. and STICHLER, W. (2005): "*Simulation of $\delta^{18}O$ in precipitation by the regional circulation model REMOiso.*" Hydrological Processes 19, pp. 3425-3444.
- SUBHA RAO, N. (2002): "*Geochemistry of groundwater in parts of Guntur district, Andhra Pradesh, India.*" Environmental Geology Vol. 41, pp. 552-562.
- SUKHIJA, B. S., REDDY, D. V., NAGABHUSHANAM, P., BHATTACHARYA, S. K., JANI, R. A. and KUMAR, D. (2006): "*Characterisation of recharge processes and groundwater flow mechanisms in weathered-fractured granites of Hyderabad (India) using isotopes.*" Hydrogeology Journal 14(5), pp. 663-674.
- TAYLOR, G. and EGGLETON, R. A. (2001): "*Regolith Geology and Geomorphology.*" John Wiley & Sons, Chichester, UK.
- TAYLOR, R. G. and HOWARD, K. W. F. (1996): "*Groundwater recharge in the Victoria Nile basin of east Africa: support for the soil moisture balance approach using stable isotope tracers and flow modelling.*" Journal of Hydrology 180, pp. 31-53.
- TAYLOR, R. G. and HOWARD, K. W. F. (2000): "*A tectono-geomorphic model of the hydrogeology of deeply weathered crystalline rock: Evidence from Uganda.*" Hydrogeology Journal 8, pp. 279-294.
- THIERY, D. (2004): "*Plaquette de présentation du code de calcul GARDÉNIA du BRGM.*" Technical Report, BRGM.

- TIDJANI, E.-H., AFFATON, P., LOUIS, P. and SOCOHOU, A. (1997): "*Gravity characteristics of the Pan-African Orogen in Ghana, Togo and Benin (west Africa).*" *Journal of African Earth Sciences* 24(3), pp. 241-258.
- TRAVI, Y. (1993): "*Hydrogéologie et hydrochimie des aquifères du Sénégal – Hydrogéochimie du Fluor dans les eaux souterraines.*" University Louis Pasteur, CNRS, Strasbourg, France.
- UN-OHRLLS. (2007): "*List of Least Developed Countries.*" United Nations Office of the high representative for the least developed countries, landlocked developing countries and small island developing countries, from <http://www.un.org/special-rep/ohrlls/ldc/list.htm>.
- USDA-UNITED STATES DEPARTMENT OF AGRICULTURE (1954): "*Diagnosis and improvement of saline and alkali soils.*" Agriculture Handbook 60. Washington, USA.
- VARADO, N. (2004): "*Contribution au développement d'une modélisation hydrologique distribuée. Application au bassin versant de la Donga, au Bénin.*" Institut national polytechnique de Grenoble, 320 p., Grenoble, France.
- VOLLMERT, P., FINK, A. H. and BESLER, H. (2003): "'Ghana Dry Zone" und "Dahomey Gap": Ursachen für eine Niederschlagsanomalie im tropischen Westafrika." *Erde* 134(4), pp. 375-393.
- VON DER HEYDEN, C. J. (2004): "*The hydrology and hydrogeology of dambos: a review.*" *Progress in Physical Geography* Vol. 28, pp. 544-564.
- WANG, H. F. and ANDERSON, M. P. (1982): "*Introduction to Groundwater Modeling.*" 237 p., Academic Press Inc., San Diego, USA.
- WHO (2004): "*Guidelines for drinking-water quality.*" Geneva, Switzerland.
- WHITTOW, J. (1984): "*The Penguin Dictionary of Physical Geography.*" Penguin Books, London, UK.
- WORLD BANK (2005): "*African Water Development Report.*" World Bank, URL: (http://www.uneca.org/awich/African_Regional_Report/water_dvpt_report.htm). Washington, USA.
- WRIGHT, E. P. (1992): "*The hydrogeology of crystalline basement aquifers in Africa.*" in: *Hydrogeology of Crystalline Basement Aquifers in Africa.* Editors: E. P. WRIGHT and W. G. BURGESS, Geological Society Special Publication. 66, pp. 1-29.
- WRIGHT, E. P., HASTINGS, J. B., JONES, W. B. and WILLIAMS, H. R. (1985): "*Geology and Mineral Resources of West Africa.*" George Allen & Unwin Ltd., London, UK.
- WSP (2005): "*Towards a More Effective Operational Response: Arsenic Contamination of Groundwater in South and East Asian Countries. Volume I: Policy Report.*" Report No. 31303, World Bank, Washington, USA.
- WURZEL, P. (2001): "*Drilling Boreholes for Handpumps.*" SKAT, St. Gallen, Switzerland.
- ZOELLMANN, K. and AESCHBACH-HERTIG, W. (2001): "*Evaluation of environmental tracer data by the boxmodel approach.*" IHW-Institute of Hydromechanics and Water Resources Management, ETHZ, EAWAG, Zurich, Switzerland.
- ZOUMARO, K. and ANIKALIA, M. (1998): "*Etude de la forme des versants à partir de modèle numérique de terrain: Application à la Vallée de l'Ouémé.*" Departement de

References

Géographie et Aménagement du Territoire, Université Nationale du Bénin, Cotonou, Benin.

ZUPPI, G. M. (2005): "*Interconnection between crystalline and sedimentary aquifers in West Africa.*" UNESCO, G-WADI Project, URL: <http://www.gwadi.org/>.